Author/s:
Cheung, Pui Kwan

Title:
Irrigating urban green space as a cooling strategy – impacts on surface energy balance and microclimate

Date:
2023-08

Persistent Link:
https://hdl.handle.net/11343/340049

Irrigating urban green space as a cooling strategy – impacts on surface energy balance and microclimate

Pui Kwan CHEUNG

ORCID: 0000-0002-7774-9277

August 2023

School of Agriculture, Food and Ecosystem Sciences

Faculty of Science

The University of Melbourne

Submitted in total fulfilment for the degree of Doctor of Philosophy

Abstract

Urban green spaces are an important space for physical and social activities in cites. However, people's willingness to stay in urban green spaces will decrease with increasing air temperature in summer. It is necessary to find strategies to reduce air temperature in urban green spaces. Irrigating vegetation in urban green spaces is a promising cooling strategy. Irrigation can be a sustainable cooling strategy when non-potable water is collected for irrigation through stormwater harvesting and wastewater treatment. Yet, there is a lack of experimental evidence for the cooling effects of irrigating vegetation in urban green spaces. Also, little is known about how much environmental and management factors can influence the cooling effects of irrigation. This thesis identified and quantified the impacts of four environmental and management factors (background climate, daily irrigation amount, irrigation scheduling and weather) that influence the cooling effects of irrigation using field experiments and a computer model. A meta-analysis of the literature and a stepwise multiple linear regression was used to identify the background climate variables that significantly influenced the cooling effects of irrigation. The final regression model suggested that the cooling effect of irrigating vegetation in summer strengthened with increasing background air temperature and weakened with increasing rainfall. A field experiment was conducted in Melbourne, Australia to measure the impacts of irrigating turfgrass with three different irrigation amounts (2, 4 and 7 mm d^{-1}) on the surface energy balance and microclimate of a small green space (36 m^2). The differences in the impacts of the three different irrigation amounts were small because a large rainfall brought the soil moisture contents to the same level. Irrigation significantly reduced daytime air temperature and turf surface temperature, but it did not reduce human heat stress. The measured impacts of irrigation on the surface energy balance were small. Another field experiment was conducted in Melbourne, Australia to measure the impacts of three different irrigation schedules (single night-time, single daytime, and multiple daytime irrigation) on microclimate using the same amount of water (4 mm d^{-1}) in a small green space (36 m^2). The afternoon mean cooling effects of the multiple daytime irrigation on air temperature and turf surface temperature were significantly stronger than the single night-time and single daytime irrigation. The afternoon cooling effects were measured to strengthen with increasing air temperature, vapour pressure deficit and incoming shortwave radiation. Moreover, the data from this field experiment were used to assess the performance of an urban ecohydrological model, UT&C, in predicting the microclimate of unirrigated and irrigated turfgrass. UT&C was then used to predict the impacts of different daily irrigation amounts (2–30 mm d^{-1}) on the cooling effect of irrigation on air temperature. The cooling effect only strengthened significantly as irrigation amount increased from 2 to 4 mm d^{-1}. This thesis demonstrated that irrigating urban green spaces is

an effective strategy to reduce daytime air temperature and turf surface temperature in summer. However, more cooling strategies, e.g., shading, are necessary to reduce human heat stress in urban green spaces in summer.

Declaration

This is to certify that:

(i) the thesis comprises only their original work towards the Doctor of Philosophy except where indicated in the preface;

(ii) due acknowledgement has been made in the text to all other material used; and

(iii) the thesis is fewer than the maximum word limit in length, exclusive of tables, maps, bibliographies and appendices.

Pui Kwan Cheung

August 2023

Preface

The publication status and author contribution of each of the chapters of this thesis are as follows:

Chapter 1

Publication status:

Unpublished material not submitted for publication.

Author contribution:

I contributed solely to this chapter.

Chapter 2

Publication status:

Published by Environmental Research: Climate on 28 June 2022

Cheung, P.K., Nice, K.A., Livesley, S.J., 2022b. Irrigating urban green space for cooling benefits: the mechanisms and management considerations. Environ. Res. Clim. 1, 015001. https://doi.org/10.1088/2752-5295/ac6e7c

Author contribution:

Pui Kwan Cheung (90%): Conceptualisation, Methodology, Software, Formal analysis, Investigation, Data Curation, Writing – Original Draft, Writing – Review and Editing, Visualisation

Kerry Nice (3%): Writing – Review and Editing, Supervision

Stephen Livesley (7%): Writing – Review and Editing, Supervision, Project administration, Funding acquisition

Chapter 3

Publication status:

Published by Sustainable Cities and Society on 29 April 2021

Cheung, P.K., Livesley, S.J., Nice, K.A., 2021. Estimating the cooling potential of irrigating green spaces in 100 global cities with arid, temperate or continental climates. Sustain. Cities Soc. 71, 102974. https://doi.org/10.1016/j.scs.2021.102974

Author contribution:

Pui Kwan Cheung (90%): Conceptualisation, Methodology, Software, Formal analysis, Investigation, Data Curation, Writing – Original Draft, Writing – Review and Editing, Visualisation

Stephen Livesley (7%): Writing – Review and Editing, Supervision, Project administration, Funding acquisition

Kerry Nice (3%): Methodology, Writing – Review and Editing, Supervision

Chapter 4

Publication status:

Published by Urban Climate on 6 October 2022

Cheung, P.K., Jim, C.Y., Tapper, N., Nice, K.A., Livesley, S.J., 2022. Daytime irrigation leads to significantly cooler private backyards in summer. Urban Clim. 46, 101310. https://doi.org/10.1016/j.uclim.2022.101310

Author contribution:

Pui Kwan Cheung (88%): Conceptualisation, Methodology, Formal analysis, Investigation, Data Curation, Writing – Original Draft, Writing – Review & Editing, Visualisation.

Chi Yung Jim (1%): Resources, Writing – Review & Editing, Funding acquisition

Nigel Tapper (1%): Resources, Writing – Review & Editing, Funding acquisition

Kerry Nice (2%): Writing – Review and Editing, Supervision

Stephen Livesley (8%): Conceptualisation, Resources, Writing – Review & Editing, Supervision, Project administration, Funding acquisition

Chapter 5

Publication status:

Submitted to Landscape and Urban Planning on 16 November 2023. It is under review at the time of thesis submission.

Author contribution:

Pui Kwan Cheung (90%): Conceptualisation, Methodology, Software, Formal analysis, Investigation, Data Curation, Writing – Original Draft, Writing – Review and Editing, Visualisation

Kerry Nice (2%): Writing – Review and Editing, Supervision

Stephen Livesley (8%): Conceptualisation, Methodology, Resources, Writing – Review & Editing, Supervision, Project administration, Funding acquisition

Chapter 6

Publication status:

Submitted to Urban Climate on 16 June 2023. It is under review at the time of thesis submission.

Author contribution:

Pui Kwan Cheung (89%): Conceptualisation, Methodology, Software, Formal analysis, Investigation, Data Curation, Writing – Original Draft, Writing – Review and Editing, Visualisation

Naika Meili (5%): Methodology, Software, Investigation, Writing – Review and Editing

Kerry Nice (3%): Methodology, Writing – Review and Editing, Supervision

Stephen Livesley (3%): Writing – Review and Editing, Supervision, Project administration, Funding acquisition

No work in this thesis has been submitted for other qualifications. No work in this thesis was carried out prior to my enrolment in the degree. The only third-party editorial assistance provided in preparation of this thesis were the anonymous reviewers of the three published chapters (Chapters 2–5).

Research funding was provided by the Commonwealth of Australia through the Cooperative Research Centres program. My studies were supported by the Australian Government Research Training Program Scholarship, the Cooperative Research Centre for Water Sensitive Cities,

Madeleine Selwyn-Smith Memorial Scholarships and the Rowden White Scholarship. Kerry Nice was supported by NHMRC/UKRI grant (1194959). The work in Chapters 4 and 5 was additionally supported by the Research Matching Grant Scheme of the University Grants Council of Hong Kong. The work in Chapter 6 was additionally supported by National University of Singapore through the project 'Bridging scales from below: The role of heterogeneities in the global water and carbon budgets', Award No. 22- 3637- A0001.

Chapter 7

Publication status:

Unpublished material not submitted for publication.

Author contribution:

I contributed solely to this chapter.

Acknowledgements

To my supervisors, Stephen Livesley and Kerry Nice, thank you for the academic knowledge and skills that you have shared with me and the time that you spent on helping me to complete this thesis. What's more important is the exceptional personal qualities that you showed me. Steve, thank you for being professional, empathetic, and caring. Kerry, thank you for being generous, supportive, and easy-going. The consistent acts of kindness of both of you have strongly influenced me and encouraged me to do better.

To the staff members at Burnley Campus, Sascha Andrusiak, Rowan Berry, Andrew Smith and Lisa Wittick, thank you for helping me with my experiments in the field station and accommodating my requests and mistakes. I truly appreciate the generous support that you have provided me throughout my studies and the professionalism that you have demonstrated.

To my industry research partners, David Bergmann and Jamie Ewert, thank you for providing an opportunity for me to get involved in the research at Aquarevo. To my co-workers, Ninad Dharmadhikari and Kai James, thank you for working with me and making the experiments happen amid the lockdowns.

To my academic research partners, Professor CY Jim and Professor Nigel Tapper, thank you for overcoming many hassles and lending the instruments to support my experiments at Burnley. To another research partner, Dr Naika Meili, thank you for demonstrating a very high standard of research from which I have learned a lot.

To my fellow Burnley colleagues, thank you for broadening my horizons through sharing your cultures and perspectives with me.

To my friends whom I met at the University of Melbourne, Christie Lau, Jonas Chow, Kristy Chung and Junran Yang, thank you for your friendship during this amazing period of time in university.

To my beloved parents and sisters, thank you for your unconditional love and support throughout my life. What you do and say to me is always nourishing and heartwarming. You have nurtured a person who is healed by his childhood and family forever. To my niece, thank you for bringing simple happiness to our family and inspiring me to "see" the past and the future of our family through the present. To my partner Chloe, thank you for staying with me, making me a better and happier person and assuring me that my philosophy is important.

Tables of contents

List of tables

List of figures

Chapter 1 – Introduction

More than half of the world's population is living in urban areas (The World Bank, 2023). Urbanisation is characterised by the reduction in vegetated surfaces and the increase in impervious surfaces, as well as the changes in urban geometry and materials. These characteristics contribute to increase urban temperatures (Oke, 1982). The reduction of vegetation and the dominance of impervious surfaces substantially reduce soil moisture content and evapotranspiration in urban areas, leading to a reduction of latent heat flux and an increase in sensible heat flux. Urban canyons are a common type of urban geometry. Urban canyons allow multiple reflections of radiation to occur between the building surfaces, thus reducing the effectiveness of radiative cooling. The construction materials in urban areas often have a high thermal admittance, which increases the heat storage in urban areas. Global climate change can further increase urban air temperature (McCarthy et al., 2010). High urban air temperature can negatively impact cities and their inhabitants in different ways. High urban air temperature can directly increase electricity demand (Santamouris et al., 2015), increase elderly mortality and morbidity (Bunker et al., 2016), and increase the health impacts of air pollution (Anenberg et al., 2020). High urban air temperature can also undermine people's well-being by reducing their willingness to visit urban green spaces to engage in physical and social activities, particularly in summer (Cheung and Jim, 2018a).

There is clear evidence that people who visit urban green spaces more frequently have better physical (Twohig-Bennett and Jones, 2018) and mental health (Van den Berg et al., 2016). It is believed that the health benefits are delivered through people's engagement in physical and social activities in urban green spaces (Groenewegen et al., 2006). Therefore, it is important to ensure that urban green spaces are thermally comfortable for people to engage in different activities. Cooling strategies are needed to reduce the air temperature in urban green spaces in summer to ensure that the health benefits of urban green spaces can be delivered through people's active use of urban green spaces. Increasing the tree canopy cover in urban green spaces is an effective strategy to reduce air temperatures in urban green spaces (Cheung and Jim, 2019a; Li et al., 2021). However, tree planting may not be suitable for small urban green spaces and those focused on sports activities. Alternative cooling strategies are needed for these urban green spaces.

Irrigating vegetation is a promising cooling strategy for different types of urban green spaces because it can be applied at different spatial scales (Coutts et al., 2013; Livesley et al., 2021). Irrigating vegetation for cooling urban green spaces is different from irrigating vegetation for maintaining plant health. Irrigation for cooling should aim to increase or maximise evapotranspiration

processes, whereas irrigation for vegetation health should aim to meet but not exceed plant water requirements. The practical differences between the two are that irrigation for cooling may occur during the day to increase or maximise evaporation processes, whereas irrigation for vegetation tends to irrigate at night to minimise evaporation. Irrigating vegetation for cooling might suggest that a larger amount of water is required to maximise evapotranspiration, but this may not be necessary if timing and frequency (scheduling) of irrigation can achieve an increase in cooling benefit. Furthermore, irrigation can be a sustainable and feasible cooling strategy for urban green spaces when non-potable water is available for irrigation. Cities can collect non-potable water for irrigation through stormwater harvesting and wastewater treatment. These technologies and measures are increasingly being adopted in different parts of the world such as Australia (Wong, 2006) and the UK (Ashley et al., 2013).

Irrigation has been predicted to reduce air temperature in many modelling studies. Broadbent et al. (2018a) predicted that irrigating all pervious surfaces during a heatwave could reduce the daily mean air temperature by 2.3°C in Mawson Lake, Adelaide, Australia. Gao et al. (2020) predicted that irrigating all surfaces could reduce the summer mean air temperature by 0.5°C in metropolitan Sydney, Australia. Wang et al. (2019) predicted that irrigating all vegetated surfaces could reduce the summer mean air temperature by 2.0°C in the contiguous USA. However, there have also been modelling studies that predicted limited cooling effects from irrigation (Chen et al., 2017) or even a warming effect (Vahmani and Ban-Weiss, 2016). Such inconsistencies suggest that it is necessary to conduct a comprehensive literature review to understand the physical and energetic mechanisms of the cooling or warming effect of irrigation. This review will help us understand why and when irrigation is an effective cooling strategy for urban green spaces and why and when it is not. Moreover, there is evidence that background climate (Kueppers et al., 2007), seasonality and weather (Geerts, 2002), vegetation type (Ozdogan et al., 2010), irrigation time of day (Valmassoi et al., 2020) and irrigation amount (Broadbent et al., 2018a) can impact on the cooling effects of irrigation. It is important to consider these environmental and management factors when using irrigation as a cooling strategy for urban green spaces. In Chapter 2, I reviewed the cooling mechanisms of irrigating urban green spaces and discuss the management considerations.

Among the environmental and management factors that were identified to have impacts on the cooling effects of irrigation in Chapter 2, background climate plays a fundamental role because it influences the evaporative demand of the atmosphere and the precipitation inputs to the soils of a geographical region. For regions with a high evaporative demand and a low soil moisture level due to low rainfall, the impacts of irrigation should be larger because the extra soil moisture may

substantially increase evapotranspiration, which then modifies the microclimate. In contrast, for the regions with a low evaporative demand and a high soil moisture level due to high rainfall, the impacts of irrigation should be smaller because there is already enough soil moisture from rainfall to meet the evaporative demand of the atmosphere. Consequently, the summer mean air temperature reduction from irrigation can vary from 0.2°C in Eastern Europe to 1.0°C in northern India due to the differences in background climate (Thiery et al., 2017). Given that a number of agricultural and urban studies have reported the air temperature reductions from irrigation for a specific geographical location and time, it is possible to identify the empirical relationship between the air temperature reduction from irrigation and background climate. In Chapter 3, I conducted a meta-analysis of global irrigation studies to establish an empirical multiple linear regression model that can predict the mean summer air temperature reduction from irrigation under a range background mean air temperatures and rainfall amounts. The model was then used to predict the potential mean summer air temperature reduction from irrigation for one hundred cities around the world in 17 climate regions.

Most of the existing studies that have investigated the cooling effects of irrigating urban green spaces were modelling studies (Broadbent et al., 2018a; Gao et al., 2020; Valmassoi et al., 2020; Wang et al., 2019). There is a severe lack of empirical studies that measure the cooling effects of irrigating urban green spaces. One exception is an observational study conducted by Lam et al. (2020). Lam et al. (2020) measured the cooling effects of irrigation by comparing the air temperatures of the unirrigated and irrigated sites in an urban park in Melbourne, Australia. However, the authors stated that the results were likely influenced by the differences in ground cover, sky view factor, soil conditions and vegetation types between the paired irrigated and the unirrigated sites. Controlled experiments are needed to isolate and directly measure the cooling effects of irrigating urban green spaces. In Chapter 4, I designed and undertook a field experiment to measure the impacts of irrigating turfgrass on microclimate and surface energy balance in a small green space that mimics private backyards. Private green spaces are an important type of urban green space because they contribute to a substantial proportion of urban green spaces in many cities, such as >50% in Dunedin, New Zealand (Mathieu et al., 2007) and >30% in Brisbane, Australia (Rupprecht and Byrne, 2014). It is therefore important to study the cooling effects of irrigating small private urban green spaces. This experiment aimed to investigate how different irrigation amounts (2, 4 and 7 mm d^{-1}) influenced the cooling effects and how irrigating turfgrass changed the surface energy balance.

Apart from irrigation amount, irrigation scheduling is an important practical issue when using irrigation to cool urban green spaces. Irrigation scheduling can refer to the frequency of irrigation within a week or in a month, or the time of day when irrigation is applied. Irrigation scheduling is

defined as the time of day when irrigation is applied in this thesis unless otherwise specified. Irrigation traditionally is applied at night to reduce evaporation from canopy and soil surface because such evaporation does not contribute to plant water uptake (Playán et al., 2005). However, increased evaporation is beneficial when irrigation is used to cool urban green spaces because increased evaporation can reduce sensible heat flux and air temperature (Chen et al., 2018). Broadbent et al. (2018a) suggested that optimising irrigation scheduling could potentially strengthen the cooling effects of irrigation for certain periods of time in a day. Yang and Wang (2015) predicted that irrigating multiple times a day could strengthen the daily mean cooling effect of irrigation. Since people use urban green spaces frequently in the afternoon, it is important to investigate whether optimising irrigation scheduling can strengthen the cooling effects of irrigation without using more water. In Chapter 5, I designed and undertook another controlled and replicated field experiment to measure the impacts of three different irrigation schedules, namely single night-time, single daytime and multiple daytime irrigation. The impact I measured centred upon the afternoon (12:00–15:59) mean cooling effects of irrigating turfgrass in a small urban green space. The cooling effects were measured in air temperature, turf surface temperature, mean radiant temperature and universal thermal climate index. The three irrigation schedules used the same total amount of water (4 mm d^{-1}). Moreover, the relationships between the measured afternoon mean cooling effects of irrigating turfgrass and background weather conditions (air temperature, vapour pressure deficit, wind speed and incoming shortwave radiation) were investigated. The relationships can help understand under what weather conditions irrigating turfgrass is a more effective cooling strategy and under what weather conditions it is not.

During a heatwave, the daily mean air temperature reductions of irrigating urban green spaces have been predicted to increase from 0.5 to 2.3°C as simulated irrigation amounts increased from 5 to 30 mm d^{-1} (Broadbent et al., 2018a). However, it is unknown whether such relationship between the cooling effect and daily irrigation amount can hold under non-heatwave conditions. In Chapter 6, I used the experimental data from Chapter 5 to assess the performance of an ecohydrological model, UT&C (Urban Tethys-Chloris), in predicting the microclimate of irrigated and unirrigated turfgrass during summer months. After validating the performance of UT&C, I used it to predict the impacts of increasing irrigation amount (2–30 mm d^{-1}) on the daily, daytime and night-time mean cooling effects of irrigating turfgrass. The impacts of irrigating a reasonable amount (4 mm d^{-1}) on the surface energy balance and evapotranspiration processes were assessed using the model outputs. Such assessments are important to further understand the physical and energetic mechanisms of irrigation cooling effect and to identify the potential weaknesses of the model.

In Chapter 7, the final chapter of this thesis, I used the findings of the previous chapters to predict the potential cooling effect of irrigating urban green spaces during the 2009, 2013 and 2014 heatwaves in Melbourne using the historical background weather conditions. I discussed the contributions of the thesis to the advances in knowledge and suggested future research directions.

Chapter 2 – Irrigating urban greenspace for cooling benefits: the mechanisms and management considerations

A version of this chapter was published by Environmental Research: Climate on 28 June 2022

Cheung, P.K., Nice, K.A., Livesley, S.J., 2022. Irrigating urban green space for cooling benefits: the mechanisms and management considerations. Environ. Res. Clim. 1, 015001. https://doi.org/10.1088/2752-5295/ac6e7c

Abstract

Evapotranspiration is an important cooling mechanism in urban greenspace (UGS). Irrigating vegetated surfaces with potable water, collected stormwater or recycled sewage water has the potential to increase the cooling effect of UGS by increasing evapotranspiration. Such cooling effect may not always be strong because evapotranspiration is dependent on local and regional factors such as background climate, seasonality and vegetation type. When using irrigation for cooling, city managers also need to consider management issues such as irrigation water supply and amenity use of the UGS. This study aims to develop a theoretical framework that explains the physical and energetic mechanisms of irrigation cooling effect and a framework to assist city managers to make decision about the use of irrigation for urban cooling. This is achieved by reviewing the impacts of irrigation on local climate reported in the literature and identifying the environmental and management factors that influence irrigation cooling effect in warm seasons. The literature suggests that irrigation can potentially reduce daily maximum air temperature and ground surface temperature by approximately 2.5 and 4.9°C, respectively, depending on weather conditions and irrigation amount. Background climate is an important factor that influences the cooling potentials of irrigation. Cities with dry and warm climates have the highest cooling potentials from irrigation. The cooling potentials are also influenced by seasonality and weather, vegetation type, irrigation time of day and irrigation amount. Cities with a dry and warm season can consider using irrigation to mitigate urban heat within UGS because such climatic conditions can increase cooling potentials. To maximise irrigation cooling effect, cities with abundant irrigation water supply can use a soil moisture-controlled irrigation regime while those with limited supply can use a temperature-controlled regime. More studies are required to understand the cooling potentials of irrigating small, individual UGS.

2.1. Introduction

Urban greenspace (UGS) is an important landscape in cities because it offers a variety of ecosystem services (Derkzen et al., 2015; Livesley et al., 2016). One of the key ecosystem services that UGS provides is cooling effect in warm seasons (Masoudi et al., 2021). A systematic review study has shown that UGS is, on average, 0.94°C cooler in air temperature than its surrounding areas (Bowler et al., 2010). Shading and increased evapotranspiration are the two main cooling mechanisms of UGS (Oke et al., 1989; Tan et al., 2018). The vegetation canopy in UGS, particularly trees, is effective in reducing the amount of solar radiation reaching the ground surface (Konarska et al., 2014), and thereby reducing the air temperature within the UGS (Cheung and Jim, 2018b). Evapotranspirative cooling is also enhanced in UGS because of the presence of vegetation (Qiu et al., 2017) and the increase in infiltration and soil moisture storage from rainfall (Yang et al., 2015; Yao et al., 2015).

There are many factors that can influence the cooling potentials of UGS, such as its size, shape, vegetation composition, fraction of impervious surface and whether it is irrigated. The cooling potential of UGS generally increases with its size (Chang et al., 2007; Cheung and Jim, 2019a) and its irregularity in shape (Shah et al., 2021; Shih, 2017). Tree and shrub covers have higher cooling potentials than grass cover (Cheung and Jim, 2019b). A lower fraction of impervious surface is also conducive to higher cooling potentials of UGS (Qiu and Jia, 2020). The impact of irrigation on the cooling potentials of UGS is under-researched, but the existing evidence shows that the irrigated part of a UGS tend to be cooler than the unirrigated part because the extra soil moisture supplied by irrigation can support a stronger evapotranspirative cooling effect (Spronken-Smith and Oke, 1998). Irrigation thus offers an opportunity for unirrigated and under-irrigated UGS to increase their cooling potentials by increasing evapotranspiration.

The impact of irrigation on the microclimate of grass-covered areas in UGS is strong because evapotranspiration is the sole cooling mechanism in the absence of shading. Soil moisture status therefore has a direct impact on the microclimate because it supports evapotranspiration and the impact is particularly strong in the dry climate regions (Pearlmutter et al., 2007). The daytime surface temperature of the irrigated grass-covered area in a park in Vancouver, Canada, was only 16°C, whereas that of the unirrigated was 34°C (Spronken-Smith and Oke, 1998). Such cooling effect originates from the increase in latent heat flux and modifications of other surface energy fluxes and storage of the surface energy balance. Briefly, the addition of soil moisture through irrigation allows more available energy at the ground surface to be transformed into latent heat flux instead of sensible

heat flux, causing a reduction in air temperature and ground surface temperature (Spronken-Smith et al., 2000).

Irrigation has been principally used to support the growth and health of turfgrass in urban areas because the evapotranspiration from turfgrass in summer months often exceeds rainfall received (Awal et al., 2019; Litvak and Pataki, 2016; Nouri et al., 2013). The growth of urban vegetation can be further hampered by insufficient soil volume and excessive pavement (Jim, 2019), which limits their access to soil water. Therefore, irrigation is necessary to maintain a healthy and actively-transpiring layer of turfgrass. Moreover, other urban vegetation such as shrubs and trees may also need supplementary water irrigation to support their health (Connellan, 2002), particularly during heatwaves. Urban trees may lose up to 50% of their leaves during heatwaves (Sanusi and Livesley, 2020) due to high air temperature and low soil moisture content (Tyree et al., 1993). The loss of leaves in trees significantly reduces their cooling effects through shading and evapotranspiration. Irrigation may help urban trees to retain their leaves during heatwaves and thus enhancing their shade and transpiration cooling effects.

UGS irrigation has been proposed as an urban cooling strategy (Coutts et al., 2013; Daniel et al., 2018; Livesley et al., 2021). However, the physical and energetic mechanisms of such irrigation cooling effect have not been well-established with the support of the findings from the literature. It is important to develop a theoretical framework that provides the mechanistic basis of irrigation cooling effect by considering the storage and fluxes of the surface energy balance in order to justify the application of irrigation for urban cooling. Moreover, since irrigation cooling effect is dependent on evapotranspiration, its effectiveness is in turn dependent on other factors that influence evapotranspiration such as background climate, seasonality, vegetation type, irrigation time of day and soil moisture achieved (irrigation amount). It is necessary to consider these factors when making a decision about using UGS irrigation to mitigate urban heat in cities around the world. Decisions regarding UGS irrigation should also consider issues such as irrigation water supply and UGS characteristics such as soil properties, ecological values and amenity use.

This study aims to develop a theoretical framework that explains the physical and energy mechanism of irrigation cooling effect, and a decision framework that assists city managers to make decision about the use of irrigation for urban cooling. This is achieved by reviewing the impacts of irrigation on climate and surface energy balance reported in the literature and identifying the environmental and management factors that influence irrigation cooling effect in warm seasons. A comprehensive literature review was conducted to search for studies that can support the above-mentioned study aims. We began the search on Google Scholar (Google Scholar, 2020) using the

Boolean search terms: ('watering' OR 'irrigation') AND ('effect' OR 'impact') AND 'air temperature'). We screened the titles and abstracts of the first 1000 results sorted by relevance. Only peer-reviewed journal articles written in English language were included in this study. We identified 41 studies that provided relevant evidence to support the study aims (Tables 2.1 and 2.2). The selection criteria were that the study has reported the mean impacts of irrigation on air temperature over the study period and investigated the impacts of one of the environmental and management factors on irrigation cooling effect, namely background climate, seasonality, weather, vegetation type, irrigation time of day and daily irrigation amounts (Table 2.2). Section 2.2 will review the impacts of irrigation on soil moisture content, surface energy fluxes (ground heat flux, latent heat flux and sensible heat flux) and local climate (ground surface temperature, air temperature, vapour pressure and human thermal stress). Section 2.3 will construct theoretical framework about the impacts of irrigating urban green spaces on daytime and night-time microclimate. Section 2.4 will discuss the environmental and management factors that influence the cooling effect of irrigation. Five key factors were discussed, namely background climate, seasonality and weather, vegetation type, irrigation time of day and daily irrigation amounts. The duration of cooling effect after irrigation will also be discussed. After understanding the impacts of irrigation on local climate and the factors that influence those impacts, section 2.5 will develop a decision framework to assist city managers to decide whether or not to use UGS irrigation as an urban cooling strategy.

2.2. Impacts of irrigation on soil moisture content, surface energy fluxes and local climate

This section will review the impacts of irrigation on soil moisture, three surface energy fluxes (G, Q_E and Q_H), three climate variables (T_{sfc}, T_a and VP) and human thermal stress (Table 1). Understanding the impacts of irrigation on these variables are necessary for the development of the theoretical framework of irrigation cooling effect in section 3. Unless specified, we report the mean changes in these eight variables over the summer (northern hemisphere: June–August; southern hemisphere: December–February) because the findings are most relevant to UGS irrigation in summer when cooling effect is needed most.

Table 2.1. List of studies that reported the impacts of irrigation on daily mean soil moisture content, surface energy fluxes and local climate.

Variable	Impact	References
Soil moisture content	+	(Gao and Santamouris, 2019; Harding and Snyder, 2012; Kanamaru and Kanamitsu, 2008; Lobell et al., 2009; Yang et al., 2016; Yang and Wang, 2015; Zou et al., 2014)
Ground heat flux (into soil)	+	(Kanamaru and Kanamitsu, 2008; Vahmani and Ban-Weiss, 2016; Wang et al., 2019; Yang et al., 2016)
	Not specified	(Chen et al., 2017; Huber et al., 2014; Ozdogan et al., 2010)
Latent heat flux and sensible heat flux	+	(Adegoke et al., 2003; Broadbent et al., 2018a; Chen et al., 2018, 2017; Cook et al., 2015; Daniel et al., 2018; Gao et al., 2020; Harding and Snyder, 2012; Huber et al., 2014; Lobell et al., 2009; Ozdogan et al., 2010; Sacks et al., 2009; Sugimoto et al., 2019; Thiery et al., 2017; Vahmani and Hogue, 2015; Wang et al., 2019; Yang et al., 2016; Zou et al., 2014)
Ground surface temperature	–	(Boucher et al., 2004; Gao et al., 2020; Thiery et al., 2017; Vahmani and Ban-Weiss, 2016; Wang et al., 2019; Yang and Wang, 2015)
Air temperature	+	(Vahmani and Ban-Weiss, 2016)
	–	(Adegoke et al., 2003; Broadbent et al., 2019, 2018a; Chen et al., 2018; Cook et al., 2015; Gao et al., 2020; Geerts, 2002; Hancock et al., 2015; Harding and Snyder, 2012; Huber et al., 2014; Lobell et al., 2009; Puma and Cook, 2010; Sacks et al., 2009; Sorooshian et al., 2011; Thiery et al., 2017; Valmassoi et al., 2020; Wang et al., 2019; Wen and Jin, 2012; Yang et al., 2016, 2017; Yang and Wang, 2015; Zou et al., 2014)
	No change	(Chen et al., 2017; Kanamaru and Kanamitsu, 2008)
Vapour pressure	+	(Boucher et al., 2004; Chen et al., 2018; Geerts, 2002; Huber et al., 2014; Sorooshian et al., 2011; Yang et al., 2017)
Human thermal stress	–	(Broadbent et al., 2018a; Shashua-Bar et al., 2009; Yang and Wang, 2015)

2.2.1. Soil moisture content

Lobell et al. (2009) modelled the impacts of irrigation on climate in eight major irrigated regions in the world using the Community Atmosphere Model 3.3. They set the soil moisture to 40% (fraction of saturation point) every half an hour if the soil moisture dropped below 40%. The soil moisture in all eight regions increased except northeast China, which had a high initial soil moisture. The increase in soil moisture varied between 2.3% (fraction of saturation point) in Indo-Gangetic Plains to 20.7% (fraction of saturation point) in Aral Sea Basin. The differences reflected the variations in soil type and rainfall regime (consequently initial soil moisture) between the regions; a more significant change was detected in drier regions. Yang and Wang (2015) modelled the impact of

irrigation on the climate in mesic residential landscapes in Phoenix, USA. They applied 1.4 mm of irrigation to the top soil layer whenever the soil moisture dropped below 24% (v/v). The mean soil moisture increased from 10.7% (v/v) without irrigation to 27.6% (v/v) with irrigation. Other modelling studies have also predicted an increase in mean soil moisture with irrigation, ranging from 1.4% (v/v) (Harding and Snyder, 2012; Zou et al., 2014), 11.1% (v/v) (Kanamaru and Kanamitsu, 2008) to 17.1% (v/v) (Gao et al., 2020). None of the four observational or experimental studies identified in this review has reported the impacts of irrigation on soil moisture. It is difficult to make a meaningful comparison between studies because changes in soil moisture from irrigation is dependent on multiple factors, such as the interception loss from the vegetation canopy (in the case of sprinkler irrigation), soil type, initial soil moisture, atmospheric demand for evapotranspiration and irrigation amount. The differences in the impact of irrigation upon soil moisture reflect the variation in soil moisture conditions before irrigation, and unsurprisingly there are more significant changes (increase) in soil moisture in drier regions. This is very much related to the underlying soil type of a location and local rainfall inputs and potential evaporative outputs.

2.2.2. Ground heat flux (G)

All reviewed studies reported a net storage of heat into the ground, i.e. a positive G (Chen et al., 2017; Kanamaru and Kanamitsu, 2008; Wang et al., 2019). The common findings of these studies were that irrigation did not reverse the direction of mean G over the study period and the changes in magnitude were usually small (<5 W/m^2). However, it is still helpful to analyse the impacts of irrigation separately on daytime and nighttime G, as measures of daily mean G can hide significant and dynamic changes in the diurnal pattern of G. In two modeling studies (Kanamaru and Kanamitsu, 2008; Vahmani and Ban-Weiss, 2016), it was predicted that irrigation would increase soil thermal conductivity because of an increase in soil moisture, which thereby would increase storage (positive G) during the day and subsequent release (negative G) of that heat at night. Vahmani & Ban-Weiss (2016) also predicted from their model that this would lead to a significant increase in nighttime T_a, resulting in a net increase in daily mean T_a despite the important reduction in daytime T_a. Kanamaru & Kanamitsu (2008) also predicted from their modelling a similar diurnal variation in G , but they predicted a small reduction in daily mean T_a. The uncertainties in the predictions of G were attributed to the lack of detailed observational data regarding the response of soil thermal conductivity to the changes in soil moisture from irrigation (Kanamaru and Kanamitsu, 2008).

2.2.3. Latent heat flux (Q_E) and sensible heat flux (Q_H)

There is a general consensus in the literature that irrigating vegetated surfaces can lead to an increase in Q_E and a concurrent reduction in Q_H. Using the Regional Atmospheric Modelling System, Adegoke et al. (2003) simulated the effect of irrigation in Nebraska, USA, by keeping the upper 0.2 m of soil saturated. They estimated that mean Q_E would increase from 74.5 to 98.2 W/m^2, while Q_H would decrease from 86.9 to 79.8 W/m^2. Chen et al. (2017) initiated irrigation in their modelling study only when the root-zone soil moisture availability dropped below 50% during the growing season. The root-zone soil moisture availability was defined as the ratio of the difference between the current root-zone soil moisture and the wilting point and the difference between field capacity and wilting point. Simulated irrigation led to a daily mean increase in Q_E of 2.4 W/m^2 and a reduction in Q_H of 2.1 W/m^2. Broadbent et al. (2018a) studied a range of daily irrigation amounts from 5 up to 30 mm in their modelling study in a North Adelaide suburb. At 3 pm local time, the model predicted that with daily irrigation of 30 mm all the available energy was consumed in evapotranspiration ($Q^* = Q_E$) because of the nearly unlimited soil moisture supply. This evaporation from the land surface caused the T_{sfc} to drop below the T_a, resulting in a negative Q_H (–40 W/m^2).

This shift in the partitioning of surface energy fluxes is confirmed by a 12-year experimental study, which measured Q_E and Q_H over maize-soybean rotation fields using eddy-covariance flux tower systems in Nebraska, USA (Chen et al., 2018). They measured a mean increase in Q_E in irrigated maize fields of approximately 20 W/m^2 and a reduction in Q_H of 25 W/m^2. However, the changes in the partitioning of surface energy fluxes were more subdued in the soybean fields. As such, the measured cooling effect in terms of T_a was greater in the irrigated maize fields than in the irrigated soybean fields. This comparison between maize and soybean suggests that type of vegetation that is irrigated has an important impact on surface energy balance and the cooling effect of irrigation.

2.2.4. Ground surface temperature (T_{sfc})

Most modelling studies predicted a reduction in daily mean T_{sfc} with irrigation. Vahmani & Ban-Weiss (2016) modelled the climate impacts of irrigating xeric landscapes in Los Angeles, USA. Although they predicted an increase in daily mean T_a with irrigation, because of the increased release of ground heat storage at night, their model predicted a small reduction (0.2°C) in mean T_{sfc}. Kanamaru & Kanamitsu (2008) modelled the hourly differences in T_{sfc} between the irrigated and unirrigated crops in the California Central Valley, USA and noted that irrigation decreased the daily maximum T_{sfc} by 5.1°C at 3 pm, but increased the daily minimum T_{sfc} by 3.1°C at 5 am. A small daily mean reduction in T_{sfc} (0.5°C) was achieved despite the irrigation causing an extended warming

period (8 pm–6 am). Using an urban canopy model, Yang & Wang (2015) predicted a decrease of 4.6°C in the T_{sfc} of a mesic residential landscape in Phoenix, USA when applying a daily irrigation amount of 1.4 mm. Other regional modelling studies, using the Weather Research and Forecasting model, predicted that irrigation would lead to a reduction in mean daily T_{sfc} of between 1 and 2°C (Gao et al., 2020; Wang et al., 2019). Irrigation is likely to reduce daily mean and daytime T_{sfc} although nighttime T_{sfc} may increase due to the increased ground heat storage during the day and subsequent release at night.

2.2.5. Air temperature (T_a)

In terms of daily mean T_a, the vast majority of studies reported a cooling effect from irrigating vegetated surfaces. Broadbent et al. (2018a) modelled an increase in cooling effect from –0.5°C for 5 mm/day of irrigation to –2.3°C for 30 mm/day during a heatwave in Mawson Lake, North Adelaide, Australia. There was a diminishing cooling efficiency as the daily irrigation amount increased because the surface soil became saturated and the evapotranspiration rate was limited by the atmospheric demand. Chen et al. (2018) measured the cooling effect from irrigating a soybean field and from a maize field in Nebraska, USA. The cooling effect was much higher in the maize field (–0.43 °C) than the soybean field (–0.09 °C); the difference was confirmed by the contrast in surface energy fluxes between the two crops (see section 4.3). The authors explained the stronger cooling effect of the maize field by crop phenology such as plant height and LAI. In a recent observational study, the irrigation cooling effect measured in two urban parks in Melbourne, Australia was –2 to –1°C during a non-heatwave period, and the effect strengthened to –4 to –2°C during the heatwave period (Lam et al., 2020). However, the authors noted that the differences in surface type and other environmental characteristics between the irrigated and unirrigated sites were not controlled for, meaning that these uncontrolled factors might have contributed to the T_a differences in addition to irrigation.

Vahmani & Ban-Weiss (2016) used the Weather and Regional Forecasting model to predict that irrigation would lead to an increase in the daily mean T_a because of increased ground heat storage during the day; the storage would release at night, offsetting the smaller cooling benefit by day. Several other modelling studies have similarly predicted an increase in the daily minimum T_a, again as a result of stored heat releasing at night (Broadbent et al., 2018a; Kanamaru and Kanamitsu, 2008; Valmassoi et al., 2020). However, not all modelling studies have reported a nighttime warming in response to irrigation (Gao et al., 2020; Sorooshian et al., 2011).

The impact of irrigation on the daily maximum T_a is more consistent amongst modelling studies as most have predicted a reduction in the daily maximum T_a with irrigation (Gao et al., 2020;

Kanamaru and Kanamitsu, 2008; Sorooshian et al., 2011). The reduction in the daily maximum T_a seems to be associated with the magnitude of the daily maximum T_a. For example, Gao et al. (2020) predicted a small reduction of 0.4°C when the maximum T_a in the unirrigated scenario was 27.9°C, whereas Kanamaru and Kanamitsu (2008) modelled a larger reduction of 2.1°C when the maximum T_a was 34.6°C, and Sorooshian et al. (2011) modelled a 5.1°C reduction from irrigation when the maximum T_a was 38.0°C. Weather conditions are clearly an important factor in determining the strength of the cooling effect from irrigation (see detailed discussion in section 4.2).

2.2.6. Vapour pressure (VP) or humidity

As expected, research literature unanimously indicates there will be an increase in VP or other air humidity indices with irrigation. A controlled experiment in maize-soybean rotation fields in Nebraska, USA, measured irrigation increased the mean mixing ratio by 0.52 g/kg (~4%) over a 12-year study period (Chen et al., 2018). Geerts (2002) compared specific air humidity inside and outside of the Murrumbidgee-Coeambally-Murray irrigation area in Australia using historic data (1968–1996) from 28 weather stations. They observed that irrigation increased the mean specific humidity inside the irrigated areas by 0.9 g/kg. Similar humidity increases were predicted in other agricultural modelling studies (Sorooshian et al., 2011; Yang et al., 2017). For example, Harding & Snyder (2012) modelled the impacts of irrigation on climate in the Great Plains, USA by keeping soil moisture in the top 2 m at saturation. They predicted a 0.19 g/kg (~2%) rise in mixing ratio over the irrigated area.

2.2.7. Human thermal stress

Only a few studies have considered the impact of irrigation on human thermal stress. Broadbent et al. (2018a) modelled the impact of irrigation on human thermal stress in North Adelaide, Australia using the humidex index. Humidex integrates the effect of T_a and VP on human thermal stress into a single index. It is the dry T_a (with a negligible moisture content) at which its corresponding thermal stress level equates to that of a given combination of T_a and VP (Masterton and Richardson, 1979). The "comfortable" Humidex range is between 20 and 29°C, while the "varying degrees of discomfort" range is between 30 and 39°C. Their model predicted that irrigation reduced Humidex from 36.9 to 34.6°C at 3pm for a daily irrigation amount of 20 mm, suggesting a mitigation of heat stress on humans. They noted that the background humidity in North Adelaide was so low that the rise in humidity from irrigation would barely increase human heat stress. Yang & Wang (2015) modelled the impacts of irrigation on human thermal stress using the Index of Thermal Stress. The Index of Thermal Stress measures the rate of heat dissipation that the human body needs to achieve through sweating in order to maintain thermal equilibrium with the surrounding

environment (Givoni, 1963). An Index of Thermal Stress above 400 W indicates a "very hot" condition. They modelled that irrigation reduced the Index of Thermal Stress in all but one month of the year, and the greatest thermal stress reduction would be 32.5 W in June. In a controlled experiment, Shashua-Bar et al. (2011) measured the Index of Thermal Stress in an exposed area with irrigated grass to that in an exposed area with bare soil. The irrigation kept the thermal stress level in the lawn at "warm" for most of the day, whereas the "hot" and "very hot" levels persisted in the area with bare soil. However, this comparison did not only reflect the impact of irrigation because the surface type and albedo of the two sites were different.

2.3. Theoretical framework of irrigation cooling effect

In this section, we develop a theoretical framework to explain the physical and energetic mechanisms of irrigation cooling effect with the support of the findings in the previous section.

2.3.1. Surface energy balance

UGS irrigation has the potential to induce a cooling effect by modifying the urban surface energy balance. Assuming that the net horizontal advective heat flux and the anthropogenic heat flux are negligible, the urban surface energy balance for a grass-covered surface can be expressed as:

$$Q^* = Q_E + Q_H + \Delta Q_S (Wm^{-2}) \quad (1.1)$$

where Q^* is the net all-wave radiation, Q_E the latent heat flux, Q_H the sensible heat flux and ΔQ_S the net storage heat flux (Oke, 1988). The partitioning of Q^* into Q_E, Q_H and ΔQ_S is primarily dependent on surface type and soil moisture status (Williams and Torn, 2015). In the case of grass, soil moisture becomes the sole factor in the partitioning.

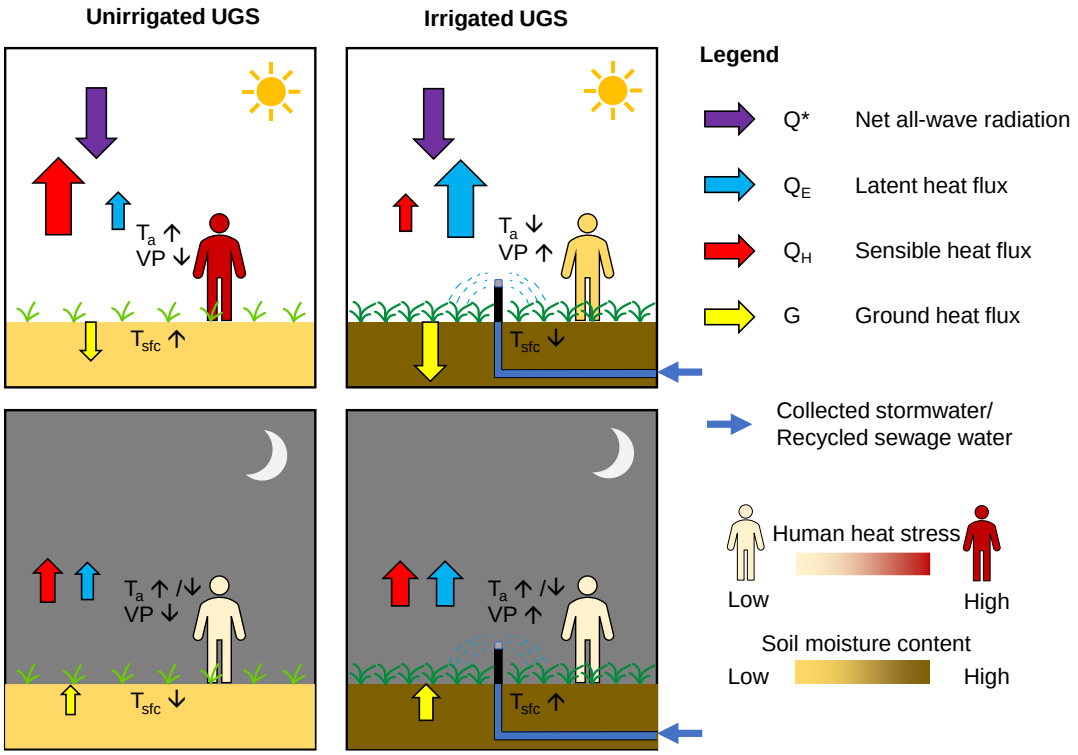

Fig. 2.1. A theoretical cooling mechanism of urban green space (UGS) irrigation based on the differences in surface energy fluxes between an unirrigated and an irrigated UGS in the daytime and nighttime in summer. The direction and relative strength of the energy fluxes are indicated by the coloured arrows. The black upward and downward arrows for the climate variables compare the magnitudes of the variables between the irrigated and unirrigated UGS at the same time of the day. In the daytime, UGS irrigation increases soil moisture content and evapotranspiration, which promotes latent heat flux (Q_E) and reduces sensible heat flux (Q_H). This in turn reduces air temperature (T_a), ground surface temperature (T_{sfc}) and human heat stress. The wetter soil in the irrigated UGS increases the downward ground heat flux (G) and ground heat storage. The increased evapotranspiration raises vapour pressure (VP), offsetting part of the cooling benefit. However, a net reduction in human heat stress is expected. In the nighttime, the higher soil moisture content in the irrigated UGS increases Q_E. The increased ground heat storage in the irrigated UGS increases upward G and T_{sfc}, which raises Q_H. The resultant impacts of irrigation on nighttime T_a and human thermal stress are unclear because the increased Q_E tends to reduce T_a and thermal stress while the increased G and Q_H tend to increase them.

The theoretical cooling mechanism of UGS irrigation is depicted in Fig. 2.1. The figure describes the differences in soil moisture, surface energy fluxes and some climate variables between an unirrigated and an irrigated UGS in the daytime and nighttime in summer. In the daytime, irrigation increases soil moisture and promotes evapotranspiration in the irrigated UGS (Chen et al., 2018). More energy is converted to Q_E and less to Q_H, resulting in a lower air temperature (T_a), surface temperature (T_{sfc}) and human thermal stress (Broadbent et al., 2018a). Downward G may slightly increase because a higher soil moisture is associated with a higher soil thermal conductivity, which increases the heat conduction into the soil (Kanamaru and Kanamitsu, 2008). However, G is usually

one order of magnitude smaller than Q_E and Q_H during the day (Spronken-Smith et al., 2000), making it less influential on the daytime T_a. Direct evaporation of water from the soil surface increases, leading to a lower T_{sfc} (Lobell et al., 2009). Irrigation may also support a lusher growth of grass, which further promotes Q_E by transpiration (Valmassoi et al., 2020). The enhanced evapotranspiration from the irrigated surface also raises vapour pressure (VP) (Sorooshian et al., 2011). In contrast, the unirrigated UGS lacks evapotranspiration and Q_E, causing a higher Q_H (Chen et al., 2018). The resultant effects are a higher T_a and T_{sfc}, but a lower VP (Gao et al., 2020). In the nighttime, Q_E and VP remain higher in the irrigated UGS than the unirrigated UGS because of the higher soil moisture (Valmassoi et al., 2020). The increased ground heat storage in the irrigated UGS from the daytime promotes the upward G at night, leading to a higher T_{sfc} and Q_H (Vahmani and Ban-Weiss, 2016). However, it is unclear whether the T_a and human thermal stress in the irrigated UGS are higher or lower than that in the unirrigated UGS because the increased Q_E tends to reduce T_a and thermal stress while the increased G and Q_H tend to increase them.

2.3.2. Human thermal stress

In addition to metabolic rate and clothing insulation, human thermal stress is determined by four climate variables, namely T_a, VP, mean radiant temperature and wind speed (Bröde et al., 2012; Fanger, 1970; Höppe, 1999). The theoretical cooling mechanism suggests that human thermal stress can be reduced by UGS irrigation (Fig. 2.2). The impacts of irrigation on human thermal stress begin with increasing soil moisture, which then modifies the partitioning of surface energy fluxes (Q_H, Q_E and G) by allowing more evapotranspiration. The increased evapotranspiration is generally associated with a smaller Q_H and a larger Q_E and G. The changes in these three energy fluxes are expected induce a reduction in T_{sfc} and T_a. The larger Q_E also inevitably increases VP. Eventually, the changes in T_{sfc}, T_a and VP affect human thermal stress. The lower T_a directly reduces human thermal stress, while the lower T_{sfc} reduces the stress by reducing the mean radiant temperature. The enhanced evapotranspiration from irrigation can increase VP and offset part of the cooling benefit, but irrigation is likely to cause a net reduction in thermal stress (Broadbent et al., 2018a). Different human thermal indices have been developed to integrate the effects of some of the four essential climatic variables e.g. Humidex (Masterton and Richardson, 1979), or all of them, e.g. Index of Thermal Stress (Givoni, 1963) and UTCI (Bröde et al., 2012). The impacts of irrigation on human thermal stress are best assessed by these thermal indices.

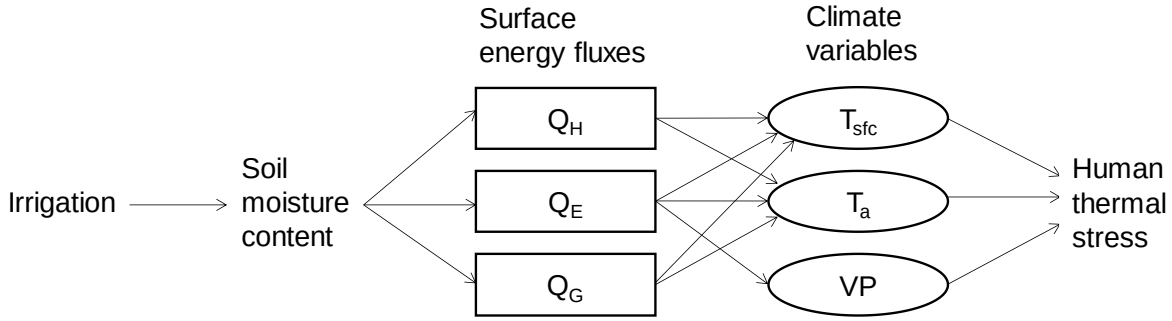

Fig. 2.2. The sequence of the impacts of irrigation. The impacts of irrigation begin with an increase in soil moisture content. The higher soil moisture modifies the partitioning of surface energy fluxes (sensible heat flux (Q_H), latent heat flux (Q_E) and ground heat flux (G)) by allowing more evapotranspiration. The increase in evapotranspiration generally leads to a smaller Q_H and a larger Q_E and G (see Section 2 for details). The changes in the three energy fluxes are expected to lead to a cooling in ground surface temperature (T_{sfc}) and air temperature (T_a). The increased Q_E is also associated with a higher VP. Human thermal stress is eventually affected by the changes in T_{sfc}, T_a and VP.

2.4. Environmental and management factors that influence irrigation cooling effect

This section will review the impacts of six environmental and management factors on irrigation cooling effect in terms of air temperature. The six factors include background climate, seasonality and weather, vegetation type, irrigation time of day, daily irrigation amount and duration of cooling after irrigation (Table 2.2). These factors are pertinent to the development of the decision framework for using UGS irrigation for urban cooling in section 2.5.

Table 2.2. List of studies that modelled or measured the impacts of environmental or management factors on irrigation cooling effect.

Factor	Irrigation cooling effect	Reference
Background climate	Stronger in warm and dry regions	(Cheung et al., 2021; Cook et al., 2015; Gao et al., 2020; Kueppers et al., 2007; Li et al., 2020; Lobell et al., 2009; Ozdogan et al., 2010; Puma and Cook, 2010; Sacks et al., 2009; Thiery et al., 2017; Wang et al., 2019)
Seasonality and weather	Stronger in the warm and dry seasons	(Bonfils and Lobell, 2007; Chen et al., 2018; Cook et al., 2015; Geerts, 2002; Kueppers et al., 2007; Li et al., 2020; Lobell et al., 2009; Lobell and Bonfils, 2008; Nocco et al., 2019; Ozdogan et al., 2010; Puma and Cook, 2010; Thiery et al., 2020, 2017; Wang et al., 2019; Yang et al., 2016; Yang and Wang, 2015; Zou et al., 2014)
	Stronger during heatwaves	(Gao et al., 2020; Lam et al., 2020)
Vegetation type	Stronger in maize than soybean	(Chen et al., 2018)
	Stronger in densely vegetated areas	(Lam et al., 2020)
	Weaker when vegetation types are classified in detail	(Ozdogan et al., 2010)
	Stronger in trees than grass	(Shashua-Bar et al., 2009)
Irrigation scheduling	No significant impact	(Broadbent et al., 2018a; Gao et al., 2020; Yang and Wang, 2015)
	Stronger when irrigation does not limit evapotranspiration	(Lobell et al., 2009; Puma and Cook, 2010)
	Significantly stronger when irrigated at noon than at night	(Sacks et al., 2009)
	Highly variable	(Valmassoi et al., 2020)
Daily irrigation amount	Stronger when irrigates more	(Daniel et al., 2018; Kanamaru and Kanamitsu, 2008; Nocco et al., 2019; Sorooshian et al., 2011; Zou et al., 2014)
	Stronger when irrigates more but additional cooling diminishes	(Broadbent et al., 2018a; Gober et al., 2010)
	Stronger when irrigates more but limited by atmospheric demand	(Lobell et al., 2009; Wang et al., 2019)
Duration of cooling after irrigation	A few hours after irrigation	(Lam et al., 2020)
	A few days after irrigation	(Chen et al., 2018)
	A few months after irrigation	(Sorooshian et al., 2011; Yang et al., 2016)

Note: not all reviewed studies are discussed in the text due to word limit.

2.4.1. Background climate

Background climate is the average weather conditions of a specific region over multiple decades. Both global (Sacks et al., 2009; Thiery et al., 2017) and regional (Gao et al., 2020) modelling studies have agreed that background T_a and rainfall are important controls of irrigation cooling effect.

From their global modelling results, Sacks et al. (2009) developed a simple linear relationship between irrigation cooling effect and daily irrigation amount separately for areas with a higher rainfall (>2.43 mm/day) and for those with a lower rainfall (≤2.43 mm/day). They predicted that, for a 1 mm/day increase in irrigation, the additional cooling effect in the drier areas was –0.7°C stronger than the wetter areas. Thiery et al. (2017) modelled the irrigation cooling effect in seven heavily irrigated regions in the world. Given a similar irrigation amount, they predicted a mean cooling effect of <–1°C in T_{sfc} in western North America and central North America in summer, and no cooling effect in Southeast Asia and East Asia. The main reason is that Western North America and central North America have a drier climate than Southeast Asia and East Asia. Irrigation in drier regions will induce a stronger evapotranspirative cooling effect because evapotranspiration is dependent on the availability of soil moisture (Koster et al., 2006). A similar conclusion was drawn by a regional modelling study (Gao et al., 2020). Their model predicted an increasing irrigation cooling effect from the coast towards the inland area in metropolitan Sydney, which coincided with the increasing background T_a gradient.

The quantitative relationship between irrigation cooling effect and background climate was established by a systematic review study (Cheung et al., 2021). Cheung et al. (2021) reviewed 17 studies that have reported the summertime mean irrigation cooling effect. They established a multiple linear regression model to predict irrigation cooling effect by background climate variables, namely T_a, rainfall, specific humidity, wind speed and net radiation. Only T_a and rainfall were the statistically significant variables that remained in the regression model after a stepwise elimination procedure. The model predicted that the irrigation cooling effect can strengthen by approximately –0.1°C for every 1°C increase in background mean T_a or 10 mm/month reduction in rainfall. In principle, this regression model corroborated with the findings in the literature because it suggested that background T_a and rainfall are the main factors that influence irrigation cooling effect.

2.4.2. Seasonality and weather

Notable seasonal variations in the magnitude of irrigation cooling effect have been reported by two modelling studies which applied a constant daily irrigation amount throughout the year. Lobell et al. (2009) modelled the monthly irrigation cooling effect in eight major irrigated regions in the northern hemisphere to be –5°C in the dry season, while the cooling effect was hardly noticeable in the wet season. Zou et al. (2014) modelled the monthly irrigation cooling effect in Haihe River Basin, China. They predicted a strengthening cooling effect from –2°C in April to –4°C in July as background T_a increased. They also predicted a warming effect up to 4°C in the winter months because of the constant irrigation throughout the year.

Day-to-day variations in irrigation cooling effect were also evident in an observational study in two urban parks in Melbourne, Australia (Lam et al., 2020). Compared to the non-heatwave period, the irrigation cooling effect in several lawn areas was –4 to –2°C stronger during heatwaves. Similar to background climate, warmer weather can increase irrigation cooling effect on a seasonal and daily basis because it provides more energy for evapotranspiration and increases vapour pressure deficit.

2.4.3. Vegetation type

In an experimental study, the daily mean irrigation cooling effect in maize fields (–0.43°C) in Nebraska, USA was significantly higher than that in soybean fields (–0.09°C) (Chen et al., 2018). The cooling effect from irrigation correlated with a decrease in sensible heat flux in the maize fields, whereas irrigation induced little change in sensible heat flux in the soybean fields. The difference in the cooling effect between maize and soybean may be attributed to their differences in plant height and leaf area index which affect the transport of heat. There is a paucity of studies that compare irrigation cooling effects among vegetation types, partly because the majority of the current land surface models do not account for different vegetation types (Ozdogan et al., 2010). One exception is a modelling study that compared the latent heat flux between a scenario where only one generic crop type was used and a scenario where the crop types where classified in detail (Ozdogan et al., 2010). The latent heat flux of the scenario with only one generic crop type was approximately 5 W/m^2 higher, indicating a stronger cooling effect.

Different vegetation types can influence irrigation cooling effect because of their differences in water demand and physical characteristics. For example, cool-season grasses generally have a higher crop factor (~0.65) than warm-season grasses (~0.25) (Handreck and Black, 2001). Trees and shrubs can have a crop factor >0.7 (Connellan, 2002). Crop factor is the proportion of water used by the plant in comparison to the water evaporated from a evaporation pan (Doorenbos and Pruitt, 1977). Cool-season grasses, trees and shrubs may therefore induce a stronger irrigation cooling effect than warm-season grasses with irrigation because they transpire more water per unit area.

Turfgrasses, shrubs and trees are common urban vegetation types that provide cooling benefits to UGS visitors by reducing air temperature. Their cooling effect is dependent upon their ability to transpire and shade (Rahman et al., 2019), as well as their impacts on aerodynamic roughness (Meili et al., 2021) and wind speed (Xing et al., 2019). In comparison tall shrubs and trees, turfgrasses do not provide overhead shading and therefore their cooling effect is mainly dependent upon their transpiration rate and albedo, which is further dependent upon their species, root system and plant area index. Short shrubs (<1 m) behave similarly to turfgrasses because they are not tall

enough to provide shade for humans or nearby dark impervious surfaces. Appropriate irrigation can support the growth and health of both turfgrasses and shrubs, increasing their plant area index. A vigorously-growing turfgrass can have a crop factor of 0.7, whereas a moderately-growing turfgrass may only have a crop factor of 0.25 (Handreck and Black, 2001), meaning that a vigorously-growing grass transpires more water per unit area and induces a stronger cooling effect. Turfgrasses and shrubs with a higher plant area index also have a higher albedo, which further reduces air temperature by reducing the amount of radiation absorbed and later released by the ground surface (Shiflett et al., 2017). The impacts of turfgrasses and short shrubs on aerodynamic roughness and wind speed are smaller than those of trees and therefore their cooling benefits may be easily diluted by near-surface turbulent mixing and advection (Spronken-Smith and Oke, 1998). Nevertheless, the advected cool air can benefit the urban areas downwind (Sugawara et al., 2016).

In the case of tall shrubs and trees, shading may contribute approximately 70% of their cooling effect and transpiration the rest 30% (Tan et al., 2018). Appropriate irrigation can support the growth and health of tall shrubs and trees, increasing their plant area index. Tall shrubs and trees with a higher plant area index can induce a stronger cooling effect from increasing overhead shading for humans and dark impervious surfaces, as well as increasing overall transpiration (de Abreu-Harbich et al., 2015; Sanusi et al., 2017). Moreover, the presence of tall shrubs and trees in UGS can reduce wind speed at the pedestrian level (Xing et al., 2019) and therefore retain the cool air within the UGS for longer. The impact of irrigation on the cooling effect of tall shrubs and trees are more complex than turfgrasses and short shrubs. Most urban green spaces have a combination of turfgrass areas with and without trees and shrubs, such that their impacts upon the energy balance and therefore cooling effects are complex. Urban green spaces will often contain vegetation with high and low transpiration rates, high and low leaf area indices, taller vegetation will shade lower vegetation and taller vegetation will change wind speed, aerodynamic roughness and turbulent exchange (Kent et al., 2017). More studies are required to understand the complex interactions between irrigation, plant area index and cooling effect of these common urban vegetation types.

2.4.4. Irrigation scheduling

Irrigation scheduling refers to the time in 24-h diurnal period when irrigation is applied. Only a limited number of studies have examined the impact of irrigation time. Broadbent et al. (2018a) modelled a negligible (<0.2°C) difference in the daily mean cooling effect between daytime (11 am–5 pm) and nighttime (11 pm–5 pm) irrigation in Mawson Lake, North Adelaide, Australia; however, the diurnal variation of the cooling effect was not reported. Valmassoi et al. (2020) modelled the diurnal variations in the irrigation cooling effect of nighttime (5 UTC), midday (12 UTC) and

afternoon (15 UTC) irrigation with sprinklers in Po Valley, Italy. The nighttime irrigation regime would induce a cooling effect of ≥–0.4°C after two hours from the starting time and it would have almost no impact on T_a in the rest of the day. The midday irrigation regime would induce a cooling effect of ≥–0.2°C at 15 UTC and a warming of a similar magnitude at night. The afternoon irrigation would induce a cooling effect of ≥–0.7°C which sustained for most of the time at night. Although the daily mean cooling effect was not explicitly reported, nighttime and afternoon irrigation seemed to induce a stronger daily mean cooling effect than midday irrigation.

2.4.5. Daily irrigation amount

Studies that modelled two levels of daily irrigation generally predicted an increase in cooling effect with increased irrigation amount (Kanamaru and Kanamitsu, 2008; Sorooshian et al., 2011; Zou et al., 2014). However, the results were mixed for studies that modelled the cooling effects from more than two levels of daily irrigation (Broadbent et al., 2018a; Lobell et al., 2009; Wang et al., 2019). In a global modelling study, Lobell et al. (2009) predicted that the cooling effect would be almost the same for keeping soil moistures at 30, 40 and 90% of saturation, because energy would become the greatest limiting factor upon evapotranspiration and latent heat flux, when soil moisture exceeds 30%. In a local-scale modelling study, however, daily irrigation amounts of 5, 15 and 30 mm/day would lead to mean daily cooling effects of –0.5, –1.5 to –2.3°C, respectively (Broadbent et al., 2018a). This local-scale model predicted a non-linear or 'diminishing return' in cooling effect with increasing daily irrigation amount. A direct comparison between these two studies is impossible because the equivalent daily irrigation amounts of keeping soil moisture at 30, 40 and 90% are unknown and dependent upon factors such as soil type, regional climate and vegetation type. This concept of diminishing cooling effect with increasing irrigation amount is supported by Wang et al. (2019), who modelled the irrigation cooling effects at four irrigation amounts in the contiguous USA. They predicted that the evapotranspiration and latent heat flux can be enhanced with large daily irrigation amounts only in the semi-arid and arid regions because of the large vapour pressure deficit in these regions, and only up to an amount of 10 mm/day. Background regional climate appears to be an important factor in determining how much cooling effect is possible with increasing daily irrigation amounts.

2.4.6. Duration of cooling after irrigation

Irrigation cooling effect can persist after irrigation stops as water continues to evaporate from the soil surface and plants continue to transpire. Experimental and observational studies have provided evidence that the cooling effect after irrigation can last for hours (Lam et al., 2020) and days

(Chen et al., 2018), while modelling studies predicted that it would last for months after continuous, daily irrigation in the warm season (Sorooshian et al., 2011; Yang et al., 2016). The cooling effect of evening and nighttime irrigation (8 pm–7 am) in Melbourne Gardens, Melbourne, Australia persisted for several hours into the morning (Lam et al., 2020). The cooling effect from irrigating maize fields in an experimental farmland in Nebraska, USA was <–0.5°C in the first six days after irrigation and was still evident (<–0.2°C) 11 days after irrigation (Chen et al., 2018).

The cooling effect of irrigation applied from May to August in the Central Valley, California, USA, was modelled (NCAR/Penn State MM5) to persist into September (–1.1°C) and October (–0.3°C) (Sorooshian et al., 2011). Yang et al. (2016) modelled the climate impacts of springtime (March-April-May) irrigation in the Huang-Huai-Hai Plain, China. The latent heat flux in the irrigated scenario was predicted to reduce significantly in the three months (June-July-August) after irrigation stopped, with only a minor reduction in T_a (0.1°C). Modelling studies reported a much longer duration of cooling after irrigation than experimental and observation studies mainly because they tracked the impacts of irrigation for a much longer period (a few months) after irrigation stopped. In comparison, the experimental study only measured the duration of cooling after irrigation up to 11 days because the irrigation was designed to applied every 4–11 days (Chen et al., 2018). The cooling effect might have lasted longer than 11 days, but the experimental design did not measure it.

2.5. Decision framework for using UGS irrigation for urban cooling at a local scale

To assist city managers and private property owners to make decisions about the use of UGS irrigation for local cooling, we present a three-stage decision support framework that steps through a sequence of practical issues (Fig. 2.3). Background climate is the first issue to consider because the cooling potential of UGS irrigation is higher in cities with a warm and dry season. Cities without a warm and dry season are unlikely to benefit greatly from UGS irrigation and should consider other cooling strategies or combination. If a city manager of a private property owner decides that UGS irrigation is suitable for their climate, the next issue to consider is irrigation water supply. The abundance of irrigation water is not restricted to potable water because bore water, recycled wastewater and stored stormwater are suitable for UGS irrigation too. Cities with an abundant water supply, preferably an alternative to potable water, can practice soil moisture-controlled irrigation throughout the warm, dry season, whereas those cities with a limited water supply can practice temperature-controlled irrigation to restrict irrigation to hotter days only. Under both irrigation-

control regimes, there are three major management issues to consider: soil properties, fauna and flora ecology and types of amenity use.

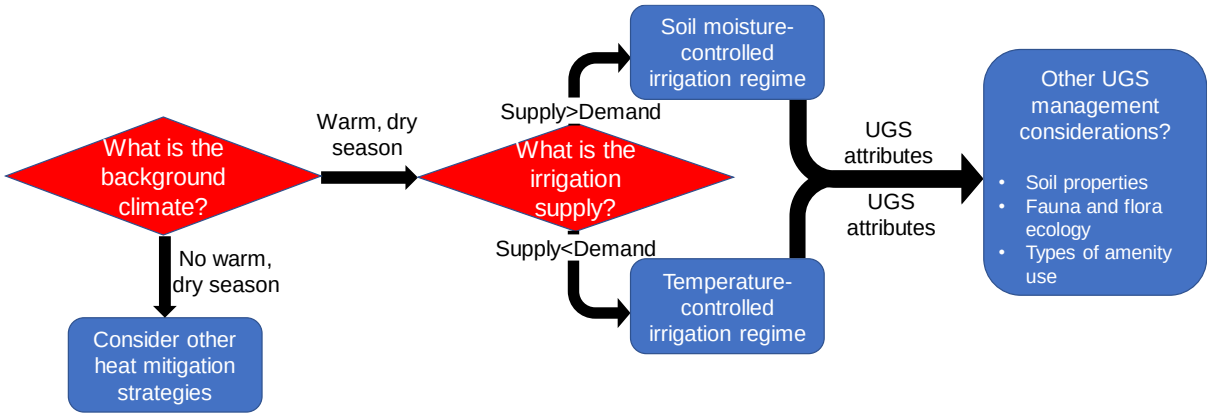

Fig. 2.3. A three-stage decision support framework for city managers and private property owners to decide whether or not to use UGS irrigation for cooling on a local scale. Background climate is the first issue to consider because the cooling potential of UGS irrigation is higher in cities with a warm and dry season; cities without a warm and dry season should consider other cooling strategies. If UGS irrigation is adopted, the next issue to consider is irrigation water supply. With the aim of maximising the cooling effect of UGS irrigation, cities with abundant irrigation water supply can practice a soil moisture-controlled irrigation regime, while those with limited irrigation water supply can practice a temperature-controlled irrigation regime. In both irrigation regimes, some management issues need to be considered: soil properties, fauna and flora ecology and types of amenity use.

2.5.1. Background climate

The background climate of a city, primarily background mean T_a and rainfall, determines whether UGS irrigation is an effective cooling strategy. A higher background T_a and lower rainfall will increase the cooling potential of irrigation, and vice versa. To demonstrate the impact of background climate we use the simple regression model developed by Cheung et al. (2021), to estimate the cooling potential of UGS irrigation in three global cities of contrasting climate: Hong Kong, Melbourne and Phoenix. This regression model predicts the cooling potential of UGS irrigation as the difference in daily mean T_a between an irrigated and an unirrigated UGS. The cooling potential of irrigation is presented for four seasonal periods: December–February (DJF), March–May (MAM), June–August (JJA) and September–November (SON) (Fig. 2.4).

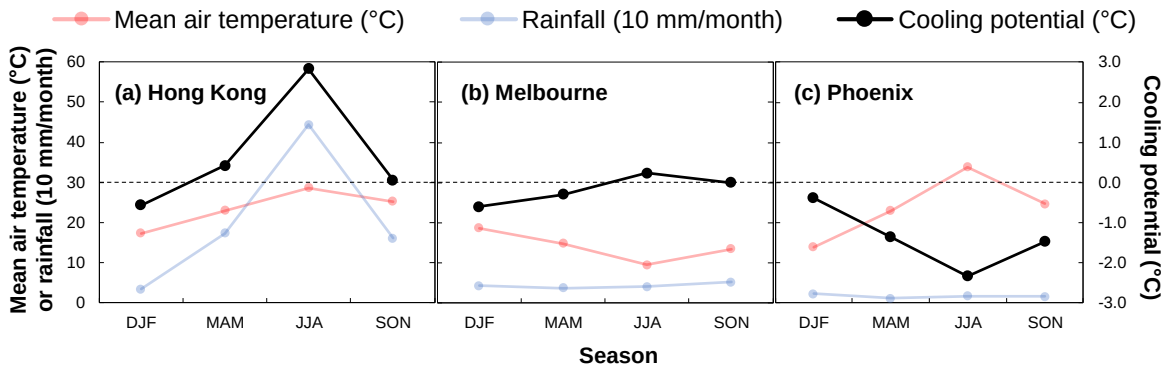

Fig. 2.4. The background mean air temperature, rainfall and cooling potential from irrigation in (a) Hong Kong, (b) Melbourne and (c) Phoenix, in December–February (DJF), March–May (MAM), June–August (JJA) and September–November (SON). The cooling potential is the difference between an irrigated and an unirrigated UGS in daily mean air temperature. A negative difference represents cooling and a positive one warming. The regression model in Cheung et al. (2021) is used to estimate the cooling potentials from the 30-year mean air temperature and rainfall. Data source: Hong Kong (Hong Kong Observatory, https://www.hko.gov.hk/en/index.html); Melbourne (Bureau of Meteorology, http://www.bom.gov.au/); Phoenix (National Oceanic and Atmospheric Administration, https://www.ncdc.noaa.gov/cdo-web/datatools/normals).

Hong Kong has a dry-winter humid subtropical climate (Köppen–Geiger climate classification: Cwa). It is a city without a warm and dry season (Fig. 2.3). The winter (DJF) in Hong Kong is dry (mean rainfall = 30 mm/month) but not warm (mean T_a = 17.3°C) (Fig. 2.4a); the other three seasons are warm (mean T_a>22.9°C) but not dry (mean rainfall >160 mm/month). As a result, the impact of UGS irrigation in the four seasons in Hong Kong is positive (warming) except in DJF (Fig. 2.4a). This warming is likely due to the increased soil thermal conductivity of wet soil after irrigation (Kanamaru and Kanamitsu, 2008). This leads to an increased ground heat storage during the day and released during the night, causing a substantial nighttime warming which outweighs the daytime cooling effect. Other urban cooling strategies such as urban greening and canopy shade (Cheung and Jim, 2018b), improving urban ventilation (Tan et al., 2017) and increasing albedo of impervious surfaces (Akbari et al., 2012) should be considered.

Melbourne has an oceanic climate (Köppen–Geiger climate classification: Cfb). It is a city with at least one warm and dry season (Fig. 2.3). The summer (JJA) in Melbourne is warm (mean T_a = 17.3°C) and dry (mean rainfall = 43 mm/month) (Fig. 2.4b). The estimated cooling potential of UGS irrigation under these summer climate conditions is –0.6°C, whereas the irrigation impact in the other three seasons is neutral. Since the cooling potential of irrigation in this simple model is the daily

mean difference in T_a the cooling effect during the middle of the day is likely to be <–0.6°C, suggesting that USG irrigation can be considered an effective cooling strategy to reduce daytime T_a.

Phoenix has an arid, hot desert climate (Köppen–Geiger climate classification: BWh). It is a city with more than one warm and dry season (Fig. 2.3). The background mean T_a and rainfall in MAM, JJA and SON are >23.0 °C and <18 mm/month, respectively (Fig. 2.4). Under such warm and dry climate conditions, the estimated cooling potential of UGS irrigation in these three warm, dry seasons are –1.4, –2.3 and –1.5 °C, respectively. UGS irrigation is a very effective cooling strategy for Phoenix.

As global climate change progresses, many cities are likely to become warmer with more variable rainfall patterns (Darmanto et al., 2019; Peck et al., 2012). Urban expansion is also likely to increase the intensity of urban heat islands because of reduced evapotranspiration and increased heat stored in urban structures and released as sensible heat (Argüeso et al., 2014). Thus, this decision framework may be used to consider the projected climate of a city to determine whether or when UGS irrigation will become an effective urban cooling strategy in the future.

2.5.2. Irrigation water supply and irrigation regimes

After determining the cooling potentials of UGS irrigation in a city based on its background climate, the next decision step is to consider irrigation water supply (Fig. 2.3). Although potable water remains the most common source of irrigation water supply in global cities, alternative water sources are being developed in many forward-thinking cities to support UGS irrigation and to reduce potable water consumption (Grant et al., 2012). Cities can increase their irrigation water supply by harvesting stormwater and roof water runoff (Hamlyn-Harris et al., 2018) and storing this in ponds or above-ground or below-ground (Livesley et al., 2021). Stormwater harvesting schemes in new developments in Melbourne, Australia can increase the city's non-potable water supply by seven times (9.8% of municipal water consumption) until 2050 (Environment and Natural Resources Committee, 2009). Irrigation water supply can also be enhanced by treating municipal sewage using conventional and advanced techniques (Leverenz et al., 2011). The majority of Israel's municipal sewage (73%) is treated and reused for agricultural irrigation (5% of national-wide water consumption) (Tal, 2006).

2.5.2.1. Soil moisture-controlled irrigation

For cities with abundant irrigation water supply which exceeds their water demand during warm and dry seasons, the soil moisture-controlled irrigation regime can be used to keep soil moisture high (Yang and Wang, 2015) to ensure that evapotranspiration is only limited by the atmospheric

demand and the transpiration rate of vegetation. Keeping the soil moisture at or just below field capacity of soil by irrigation is likely sufficient to ensure that evapotranspiration rate and Q_E are always at their maxima to achieve the strongest cooling effect. Field capacity is the soil moisture content when all macropores have emptied under gravity, whereas saturation is the moisture content when all pores (micro-, meso- and macro-) are filled with water. There are two ways to determine the amount of irrigation required to restore soil moisture to field capacity: (1) direct sensor measurement of soil moisture (Haley and Dukes, 2012), and (2) estimation from daily reference evapotranspiration data from the local meteorological bureau (Allen et al., 1998). Applying the estimated amount of irrigation during the day is likely to induce a stronger cooling effect than nighttime irrigation (Valmassoi et al., 2020), because the greater vapour pressure deficit during the day will promote direct evaporation as the irrigation water passes through the air, and a greater proportion of irrigation water can be evaporated from the surface of vegetation and the soil, before it infiltrates and contributes to soil moisture content.

2.5.2.2. Temperature-controlled irrigation regime

For cities with limited irrigation water supply which just meets their demand during warm and dry seasons, the temperature-controlled irrigation regime can be used to trigger irrigation when T_a, or other human thermal stress indices, exceeds a certain level, e.g. 30°C (Yang and Wang, 2015). As discussed in section 4.2, irrigation can induce a stronger cooling effect when the weather is warmer. A temperature-controlled irrigation regime can ensure that the limited water supply is only used when human heat stress is greatest. Irrigation may be applied whenever the human heat stress exceeds a certain threshold. This threshold to thermal stress can be determined by local questionnaire surveys within the UGS or the city itself (Cheung and Jim, 2019c; Lam and Lau, 2018).

2.5.3. Urban green space management considerations

2.5.3.1. Soil properties

Under both irrigation regimes, the field capacity of the soil needs to be considered to determine the irrigation amount and the frequency with which irrigation can be applied to support evapotranspiration without exceeding infiltration capacity and thereby surface ponding of water or excessive runoff. Direct soil moisture monitoring can prevent irrigation exceeding soil field capacity or the predefined level (Haley and Dukes, 2012) under both irrigation regimes. If the UGS is actively used for recreational or sports activities, soil compaction is an additional issue to be considered because the susceptibility of soils to compaction increases greatly at high soil moisture contents (Mosaddeghi et al., 2000), particularly for fine-textured soils (Kolka et al., 2012).

2.5.3.2. Fauna and flora ecology

Applying irrigation for cooling in UGS may keep the soil moisture at a relatively high level for an extended period of time, especially in the soil moisture-controlled irrigation regime. Wet soils may suppress the establishment and growth of the desired vegetation species in the UGS (Fay and Schultz, 2009; González-Muñoz et al., 2011) and promote the establishment of unwanted invasive species (Fay and Schultz, 2009). On the other hand, the cooling effect from UGS irrigation can reduce maximum T_a and provide cool refuge to vulnerable flora (McCarthy and Pataki, 2010) and fauna (Nowakowski et al., 2018; Tanner et al., 2017), especially during heatwaves. UGS managers and owners have to carefully weigh up the cooling effect against the potential ecological impacts (positive or negative) upon flora and fauna that use the UGS as habitat.

2.5.3.3. Types of amenity use

The soil moisture-controlled irrigation regime tends to maintain the soil moisture content in the UGS at a relatively high level, which can make recreational and sports activities difficult as the soils be more susceptible to compaction, and may lead to users getting wet from sitting or lying on the ground, or from direct water spray during daytime irrigation events. Moreover, the temperature-controlled irrigation regime may frequently interrupt the usage of the UGS on hot days because irrigation may be triggered multiple times. Similar to the management concerns in ecology, irrigation can reduce human heat stress in the UGS but at the same time cause inconvenience to UGS users.

2.6. Conclusion

Irrigation inarguably increases soil moisture content, which leads to an increase in daytime latent heat flux and a decrease in sensible heat flux. The resultant effect is a reduction in daytime T_a and T_{sfc}. However, the increase in soil moisture content also increases daytime ground heat storage, causing a greater release of heat from the soil at night and a possible nighttime warming effect in T_a and T_{sfc}. Overall, irrigation can reduce daily mean human thermal stress despite the increase in VP or humidity from evapotranspiration.

The cooling effect of UGS irrigation in T_a and T_{sfc} can be influenced by a number of environmental and management factors, with background climate being the most important factor. Dry and warm climates are most conducive to a strong irrigation cooling effect. Moreover, irrigation cooling effect is strongest in the warm season and on warm days. Vegetation type has a measurable impact on cooling effect but very few studies have examined this factor. Irrigation scheduling mainly

changes the diurnal temperature patterns and its impact on daily mean cooling effect remains unexplored. Increasing daily irrigation amount can strengthen cooling effect but a diminishing cooling impact can be expected as irrigation amount increases.

Based on the environmental and management factors that influence irrigation cooling effect, a three-stage decision framework was developed in this study to assist city managers and private property owners to make decisions about the use of UGS irrigation for local cooling. First, cities with a warm and dry season have a higher potential to use irrigation to mitigate urban heat on a local scale. Second, cities with abundant irrigation water supply can use a soil moisture-controlled irrigation regime to maximise the cooling effect and those with limited supply can use a temperature-controlled irrigation regime to achieve the same goal. Third, these two irrigation regimes can be adjusted for each UGS, taking into account its soil type, ecology and usage.

USG irrigation is an emerging urban cooling strategy and there remains many important knowledge gaps. We suggest that future studies should:

- Measure the cooling effect from irrigation in different climate regions and use the empirical data to validate the predictions from climate models.
- Model the cooling effect from irrigating a small, individual UGS instead of irrigating all the pervious surfaces in the whole city because the cooling effect from irrigation is likely to be highly localised (Coutts et al., 2013).
- Use more realistic irrigation schemes (Lobell et al., 2009) and more specific vegetation parameters (Ozdogan et al., 2010) to model the cooling effect from irrigation.
- Quantify the benefits of UGS irrigation in human thermal comfort using advanced thermal indices such as PET (Matzarakis et al., 1999), mPET (Lin et al., 2019) and UTCI (Bröde et al., 2012).

Chapter 3 – Estimating the cooling potential of irrigating green spaces in 100 global cities with arid, temperate or continental climates

A version of this chapter was published by Sustainable Cities and Society on 29 April 2021

Cheung, P.K., Livesley, S.J., Nice, K.A., 2021. Estimating the cooling potential of irrigating green spaces in 100 global cities with arid, temperate or continental climates. Sustain. Cities Soc. 71, 102974. https://doi.org/10.1016/j.scs.2021.102974

Abstract

Modern agricultural irrigation can produce extensive cooling that is strong enough to mask the current effect of global climate change. Irrigating urban green spaces therefore has the potential to mitigate heat stress in cities. However, the cooling potentials of irrigating urban green space in different climate regions of the world have never been estimated. Here we conducted a systematic literature review to determine air temperature reductions in past experimental, observational and modelling studies ($N = 17$). We developed an empirical model with the irrigation cooling effect as the dependent variable and background air temperature and rainfall of the study area as the independent variables. The model was subsequently used to estimate the cooling potential of irrigating green spaces in 100 global cities with arid, temperate and continental climates. We predict that 91 of the 100 cities will receive a cooling benefit from irrigating urban green space (mean = –1.09 °C), whereas the remaining nine cities will experience a slight warming effect (mean = +0.76 °C). The cooling potential of irrigating urban green space is greatest in arid cities (mean = –1.65 °C).

3.1. Introduction

The superimposing effect of global climate change (Matzarakis and Amelung, 2008), heatwaves (He et al., 2021) and urban heat islands (Tan et al., 2010) is expected to exacerbate heat stress in cities around the world and threaten human health (Basu and Samet, 2002). Heat stress in urban areas is stronger than rural areas because urban materials and morphology are conducive to heat accumulation (Oke, 1982) and the dominance of dry impervious surface favours the release of heat in the form of sensible heat over latent heat (Li et al., 2015). In response to the growing threat of heat stress, different strategies have been proposed to cool the urban environment (Ronchi et al., 2020; Santamouris et al., 2017), such as urban greening (Bowler et al., 2010; Coccolo et al., 2018), the use of reflective materials (Al-Obaidi et al., 2014; Santamouris et al., 2017), urban design for shading and ventilation (Arnfield, 1990; He et al., 2020; Unal Cilek and Cilek, 2021), and irrigating urban green space (Gao and Santamouris, 2019; Livesley et al., 2021).

Urban vegetation plays an important role in moderating urban climate. The cooling effect of urban vegetation is achieved mainly through the interception of solar radiation and evapotranspiration (Tan et al., 2018; Zheng et al., 2021). Urban greenery can be part of the city landscape such as parks and roadside trees; it can also be integrated into the exterior of the buildings, forming green roofs and green walls (Norton et al., 2015). Different forms of urban greenery can cool different parts of the city (Yang et al., 2021). Tree planting is a highly effective measure to mitigate heat stress in urban parks and open spaces (Rahman et al., 2020; Wu et al., 2019). Direct solar radiation is the key factor that contributes to outdoor heat stress, particular in tropical and subtropical regions (Emmanuel et al., 2007; Lin et al., 2010). A single tree with dense foliage can reduce the air temperature under its canopy by up to 2.1 °C in the humid subtropical climate (Cheung and Jim, 2018b). Urban parks can create a cool sanctuary from the heat stress in urban areas and they have the potential to cool their surrounding areas. A systematic literature review has showed that urban parks are on average 0.91 °C cooler than the surrounding built-up (Bowler et al., 2010). Under certain conditions, the cool air inside the parks can spill over to the surrounding areas, a phenomenon known as 'park cool island' effect (PCI) (Spronken-Smith and Oke, 1998). The PCI effect can extend to a distance about the same as the width of the park (Jauregui, 1990) at a notable magnitude (~ 1 °C in mean air temperature) (Doick et al., 2014).

The cooling effect of urban vegetation is heavily dependent on background climate (Yu et al., 2018) and irrigation (Spronken-Smith and Oke, 1998). Yu et al. (2018) compared the cooling effect of urban vegetation in ~~the~~ temperate monsoon climate and Mediterranean climates. The study found that the cooling effect of tree covered green spaces is positively correlated to background land surface

temperature in the temperate monsoon climate, whereas there is only a weak correlation in the Mediterranean climate. Moreover, a higher wind speed can enhance the cooling effect of trees in the Mediterranean climate but not in the temperate monsoon climate. A higher precipitation can increase the cooling effect of grass covered green spaces in both climate regions. The results suggest that background climate is an important factor to consider when designing urban vegetation for mitigating urban heat stress. Spronken-Smith and Oke (1998) investigated the thermal environment in the urban parks in Vancouver, Canada and Sacramento, US. They found that the surface temperature of irrigated grass (22–26 °C) was much lower than the dry grass (30–36 °C) within a park. In terms of air temperature, the daytime mean PCI of two parks with irrigated grass (2.2 °C) was somewhat stronger than those with unirrigated grass (1.4 °C). These studies indicated that irrigation has the potential to enhance the cooling effect of urban vegetation, particularly grass, and that the level of enhancement may be dependent on the background climate.

Irrigating urban green space for cooling is an emerging and promising heat mitigation strategy (Coutts et al., 2013; Livesley et al., 2021). In urban areas, the soil moisture can be limited on pervious surface because traditional stormwater infrastructure generally prioritise the quick removal of stormwater from cities to avoid flooding over soil infiltration. The high coverage of impervious surface also restricts the recharge of soil moisture in rainfall events, which forces more energy to be converted to sensible heat in the dry urban landscape. Urban irrigation can provide the moisture required for evapotranspiration and allow more energy to be converted to latent heat instead of sensible heat (Williams and Torn, 2015), thereby reducing air and surface temperatures, as well as heat stress. The cooling effect of irrigation is mainly achieved through direct evaporation from the vegetation and soil surface, and enhanced transpiration from vegetation, both leading to increased latent heat flux. This study will focus on the potentials of irrigating urban green spaces to cool cities and communities.

Although some urban studies have monitored the microclimate of irrigated urban green spaces (Potchter et al., 2006; Spronken-Smith and Oke, 1998), those studies did not focus on the measuring the cooling effect of irrigation. Irrigation has a long history of practice in agriculture. Insights can be borrowed from agricultural irrigation studies to understand the climate impacts of irrigating vegetated surfaces. On regional and global scales, the impacts of modern agricultural irrigation on near-surface air temperature have been extensively studied using observational data (Bonfils and Lobell, 2007; Shi et al., 2014; Yoshida et al., 2012) and climate models (Cook et al., 2011; Qian et al., 2013; Sacks et al., 2009). Irrigation has been estimated to reduce mean air temperature by up to 3 °C in certain parts of the world, such as northern India (Puma and Cook, 2010).

Globally, it has been estimated that the collective impact of current irrigation reduces mean air temperature by 0.21 °C (Cook et al., 2015). Although the reported magnitudes of cooling vary between different global climate models (Puma and Cook, 2010) and model sensitivity (Thiery et al., 2017), it is clear that the air temperature reduction is significant and can partially mask regional and global warming trends (Cook et al., 2015; Kueppers et al., 2007; Puma and Cook, 2010). In recent years, there has been more evidence that irrigating urban green spaces can induce a noticeable cooling effect. A modelling study has predicted that the mean daily air temperature can be reduced by up to 2.3 °C from irrigating all pervious surfaces in a suburb in Adelaide, Australia (Broadbent et al., 2018a). It was also estimated irrigating all urban green spaces can completely offset the urban heat island effect during the heatwaves in Paris, France (Daniel et al., 2018). Given that the cooling effect of irrigation is particularly strong within irrigated areas (Cook et al., 2015; Yang et al., 2016), it can be hypothesised that irrigating urban green spaces has the potential to mitigate urban heat stress in global cities.

Since the rate of evapotranspiration depends on the immediate meteorological conditions, when water availability is not limiting, the cooling effect of irrigation can change notably with the background climate of the region (Cook et al., 2015; Puma and Cook, 2010; Thiery et al., 2017). Therefore, it is necessary to examine the relationship between cooling magnitude and background climate before using irrigation for climate change adaptation. Although the concept of irrigation cooling effect has been discussed in several original research and review papers (Broadbent et al., 2018a; Coutts et al., 2013; Daniel et al., 2018; Gao et al., 2020; Gao and Santamouris, 2019), these studies did not consider the relationship between background climate and the potential cooling effect of irrigation. There have been few studies, either experimental, observational or modelling, specifically focused on the cooling impact of irrigating urban green space (Broadbent et al., 2018a; Chen et al., 2018). Since irrigation has been dominated by agriculture throughout the 20th century, studies that have assessed the cooling effect of irrigation globally, have only considered areas that have historically been irrigated for agriculture, and as such have not included major urban areas (Cook et al., 2011; Sacks et al., 2009; Thiery et al., 2017). Furthermore, studies that have quantified the cooling effect of irrigation in cities and regions have neglected the influence of background climate (Broadbent et al., 2018a; Kanamaru and Kanamitsu, 2008; Yang and Wang, 2015) as they mostly focused on a single climate region. These studies of irrigation in cities and regions have actually provided a unique opportunity for a retrospective analysis of the relationship between background climate and irrigation cooling effect. This study is believed to be the first to use a retrospective analysis to determine such a relationship.

In this study, we used a systematic review to identify regional, city-scale and experimental studies that report the difference in mean air temperature between irrigated and non-irrigated scenarios or sites. The magnitude of irrigation cooling in these studies was then related to background climate conditions of that region and for the study time period using a global historical climate database, the Global Land Data Assimilation System (GLDAS). From these data a simple, multiple-linear regression model was developed to predict irrigation cooling effect according to background climate conditions for arid, temperate and continental regions. The aims of this study are to: (1) develop a model from the relationships between background climate and the effect of irrigation on air temperature, and (2) use that model to assess the cooling potential of irrigating green spaces in arid, temperate and continental climate regions and 100 cities in these regions based on their background climate.

3.2. Systematic search for irrigation studies that report air temperature impacts

To collect the published data on the cooling effect of irrigating green spaces or other pervious surfaces, a literature search without time period limits was conducted with Google Scholar (Google Scholar, 2020) using the Boolean search terms: ('watering' OR 'irrigation') AND ('effect' OR 'impact') AND 'air temperature') (Fig. 3.1). The titles and abstracts of the first 1000 results sorted by relevance were screened to identify studies that measured or modeled near ground-level air temperature at irrigated and non-irrigated sites. Non peer-reviewed and non-English language journal articles were excluded. Also, global studies were excluded because the effect of a specific climate on irrigation cooling cannot be assessed. To allow a robust analysis of the relationship between irrigation-induced cooling effect and background climate, four additional inclusion criteria were applied : (1) the study area and time period were reported; (2) a non-irrigated site (control) was clearly identified and described; (3) the comparison between irrigated and non-irrigated sites did not involve a change in land cover or vegetation type; and (4) the impact of irrigation could be reported as a difference in mean air temperature over the whole study period (ΔT_{mean}). We further applied a non-parametric outlier test to remove studies that reported data that fell outside the range of the median ± 1.5 × the inter-quartile range (Jung et al., 2010). We identified 17 studies that met the above criteria ($N = 19$; one study with three study areas). We identified another 57 peer-reviewed irrigation studies that did not meet the four above-mentioned inclusion criteria and were excluded (Table S3.1).

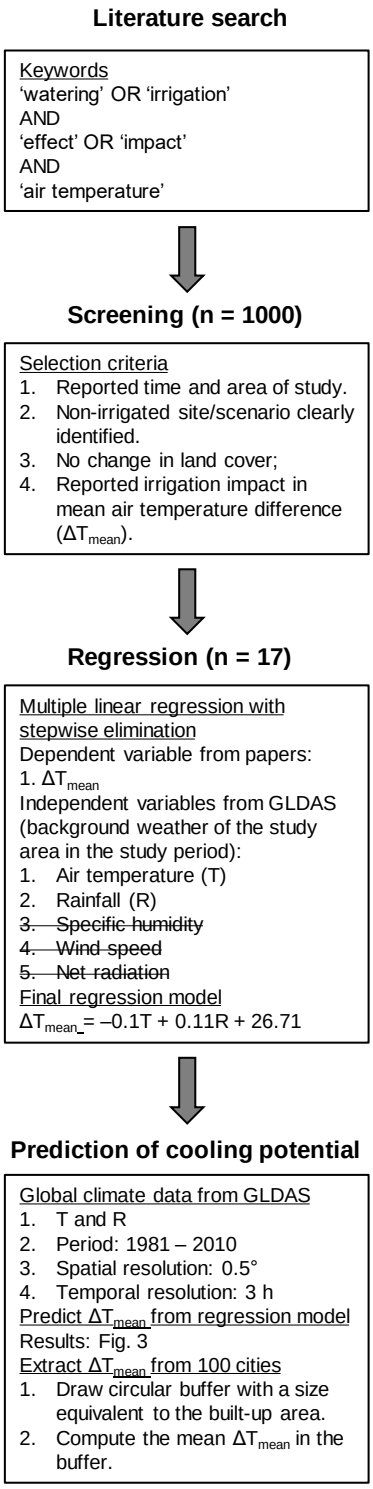

Fig. 3.1. Research procedures of this study. This study began with a literature search using Google Scholar. We screened 1000 papers and identified 17 of them that reported ΔT_{mean} and their study area and period. We then developed a regression model to predict ΔT_{mean} from background air temperature and rainfall. Finally, the cooling potential of irrigation was predicted for 100 global cities using the regression model.

3.3. Methods

3.3.1. Regression model of air temperature change and background climate conditions

To estimate the cooling potential of irrigating green space in cities in the three climate regions covered by the 17 study datasets (arid, temperate and continental), the relationship between ΔT_{mean} and background climate conditions was determined using stepwise multiple linear regression. The ΔT_{mean} was directly collected in some of the 17 studies, and in the others it was extracted from the Figs presented using ImageJ analysis (Schneider et al., 2012). If a study reported a monthly ΔT_{mean} in summer, then the mean background climate conditions of June, July and August (JJA) were used for studies in the northern hemisphere and the mean of December, January and February (DJF) for the southern hemisphere. Historical climate data were retrieved from GLDAS, developed by the National Aeronautics and Space Administration (NASA) and Atmospheric Administration (NOAA) (Rodell et al., 2004). GLDAS data was accessed through the Giovanni portal for the necessary spatial extent and time period of each of the 19 study sites. GLDAS provides gridded global climate data at a spatial resolution of 0.25 ° and a temporal resolution of 3 h. Five background climate conditions were extracted: mean near-surface air temperature, specific air humidity, wind speed, net radiation and rainfall data. These five meteorological variables can influence evapotranspiration within a vegetated landscape (Jung et al., 2010).

A multiple linear regression model was first constructed with the ΔT_{mean} data as dependent variable and the five background climate conditions as independent variables. A bi-directional stepwise elimination procedure was then applied to add or remove the independent variables one at a time from the full model until the Akaike Information Criterion (AIC) of the model was minimised (Hastie and Pregibon, 1992). AIC is a measure of the quality of a model and the best model is the one with the smallest AIC (Akaike, 1974). The above analysis was conducted in R Studio 1.3.959 (R Core Team, 2023).

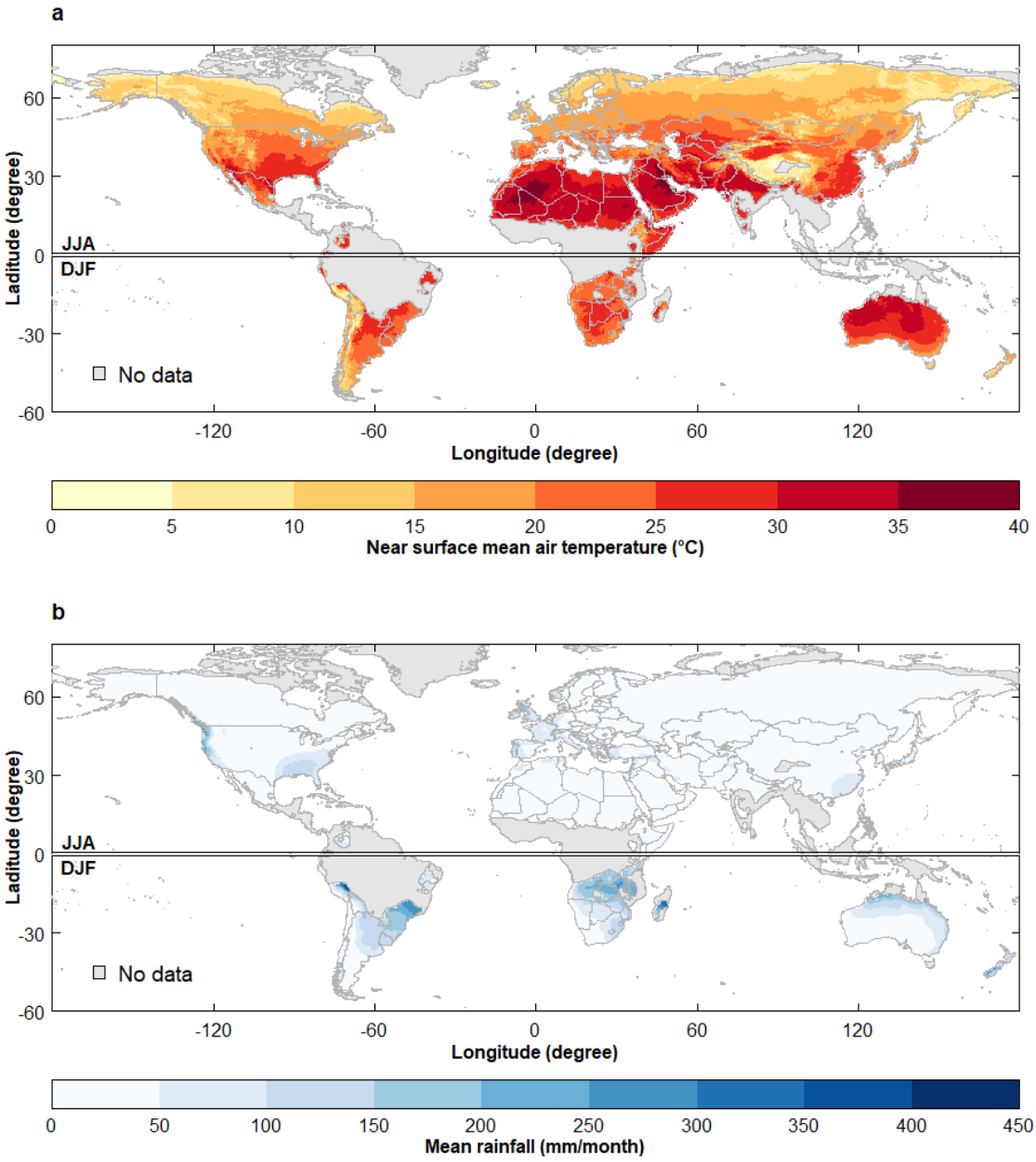

Fig. 3.2. 30-year (1981–2010) (a) near surface mean air temperature and (b) mean rainfall in JJA (northern hemisphere) and DJF (southern hemisphere). Tropical and Polar regions in the updated Köppen-Geiger climate classification are greyed out and denoted by 'No data'. Data were retrieved from the GLDAS (Rodell et al., 2004).

3.3.2. Predicting the potential cooling benefit of irrigating urban green space in 100 global cities

Using the regression model, a global map of estimated irrigation cooling potentials was produced based on the gridded 30-year (1981–2010) mean air temperature and rainfall data from the GLDAS (Rodell et al., 2004) (Fig. 3.2). The climate data in JJA and DJF were used for the northern

and southern hemispheres, respectively. The tropical and polar regions in the updated Köppen-Geiger climate classification were excluded because the 17 studies only covered the arid, temperate and continental climates. To estimate the irrigation cooling potentials in cities, 100 populous cities were selected from the arid, temperate and continental climates. The built-up areas of the cities were retrieved from Demographia (Demographia, 2020), local government statistics or satellite images. A circular buffer with a size equivalent to the built-up area was drawn around each city and the area-weighted ΔT_{mean} of that city was extracted from the global map. When the cooling or warming potential is mentioned in this study, negative values imply cooling and positive values imply warming.

3.4. Results

We have identified 17 studies that reported ΔT_{mean} in the literature (Table 3.1). We have a total of 19 cases because one of the studies reported the ΔT_{mean} in three study areas. The USA was the most common study area in terms of country (8 cases), followed by China (6 cases). The dataset covered arid (B), temperate (C) and continental (D) climate zones and nine sub-climate regions (BSk, BWh, BWk, Cfa, Csa, Cwa, Dfa and Dwa) in the updated Köppen-Geiger climate classification scheme (Fig. 3.3) (Peel et al., 2007). Four cases were experimental or observational studies and the rest were modelling studies. The models used in these studies included WRF, RegCM4, SCAM, SURFEX, RSM, NCAR/Penn STAT MM5 and RAMS. The study sites varied from highly homogenous experimental farmlands, complex city landscapes to large regional lands. Only seven studies reported irrigation rate, which ranged from 0.4 to 15 mm/day with a mean of 4.5 mm/day. The ΔT_{mean} reported in the 19 cases ranged from -2.67 °C (Yang and Wang, 2015) to 0.00 °C (Chen et al., 2017) with a mean of -0.77 °C.

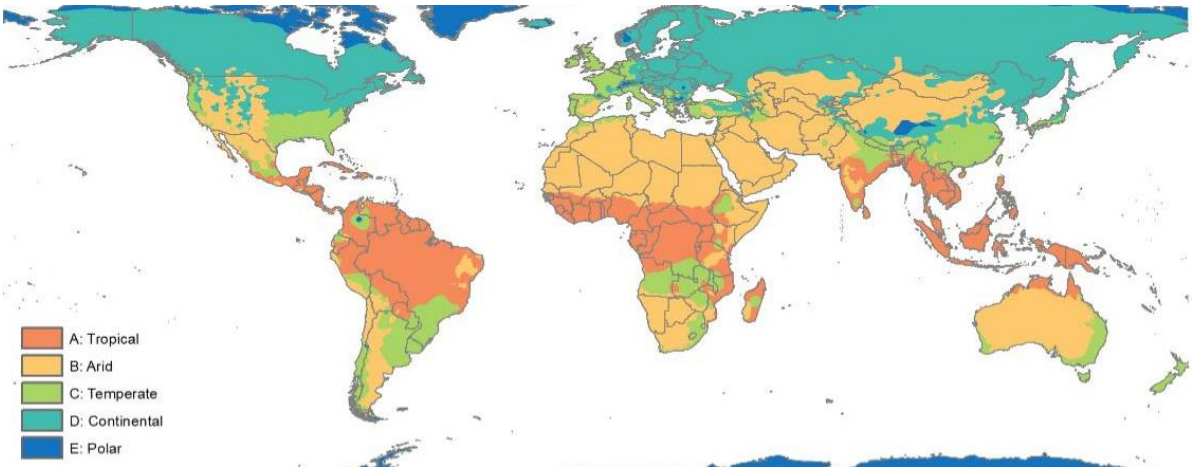

Fig. 3.3. Simplified Köppen-Geiger climate map of the world. Regions are grouped into five broad climate zones: A: Tropical, B: Arid, C: Temperate, D: Continental and E: Polar. Redrawn based on Peel et al. (2007).

The strongest multiple linear regression model contained the independent variables of air temperature and rainfall (Table 3.2), which explained 15.2% and 32.9% of the variability in ΔT_{mean}, respectively. This model was statistically significant (*F*-statistic: 7.397 on 2 and 16 DF, $p<0.01$, $R^2 =$ 48.0%). The model indicated that, for every 1 °C increase in background mean air temperature and a constant rainfall, ΔT_{mean} will decrease by 0.10 °C. Moreover, for every 10 mm/month increase in rainfall and a constant background mean air temperature, ΔT_{mean} will increase 0.11 °C. There did not appear to be any obvious trend according to whether data were sourced from experimental or modelling studies, or from arid, temperate or continental climate regions (Fig. 3.4). In other words, the research method and climate region did not directly determine ΔT_{mean}. However, ΔT_{mean} showed a decreasing trend with increasing mean air temperature (Fig. 3.4a) and an increasing trend with increasing rainfall (Fig. 3.4b).

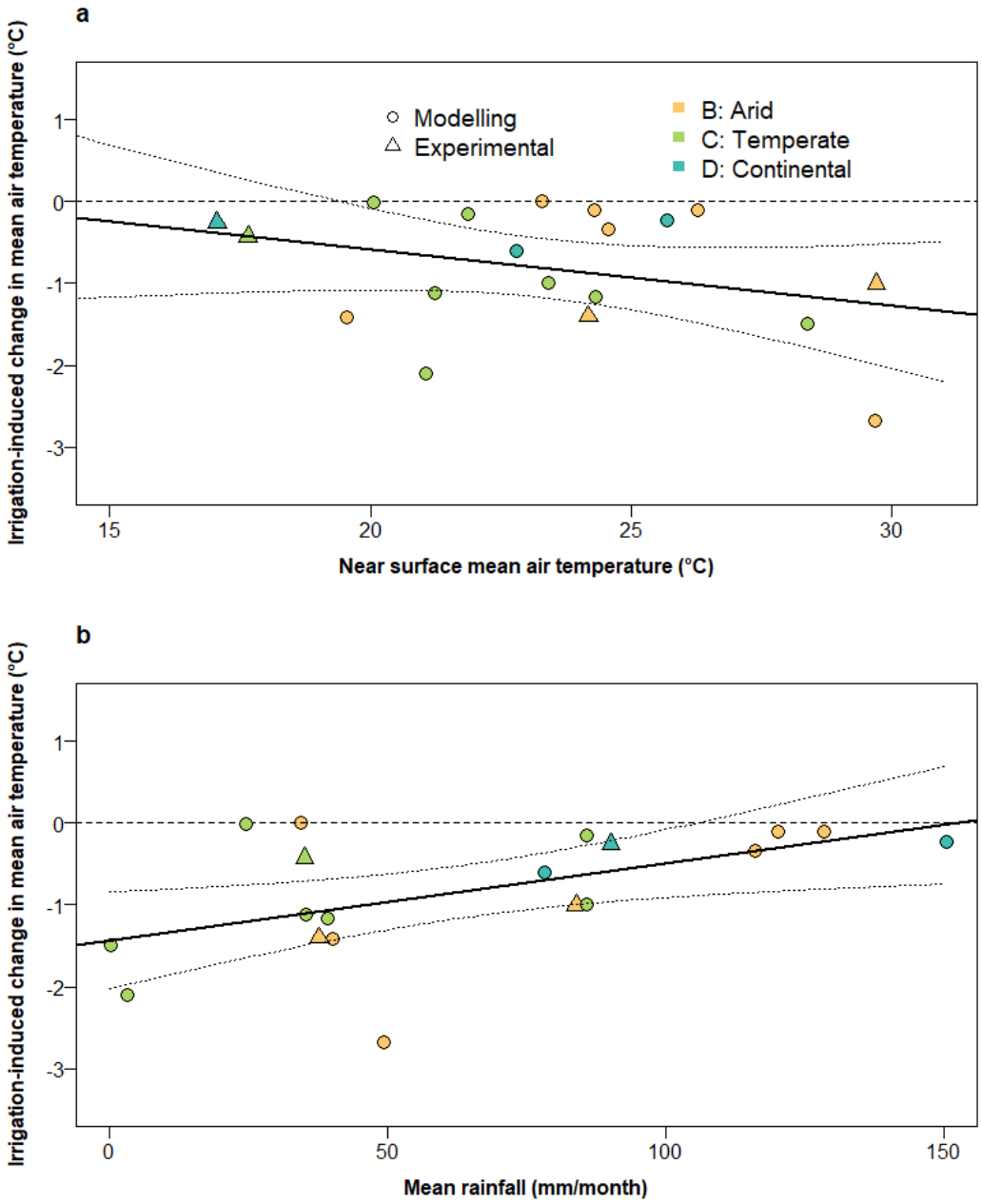

Fig. 3.4. Scatter plot of irrigation-induced change in mean air temperature against the (a) near surface mean air temperature, and (b) mean rainfall. Both variables are the means of the study period. The dataset consists of 17 studies (N = 19; one study with three study areas) that reported the irrigation-induced change in mean air temperature. The mean background air temperature and rainfall data are retrieved from the GLDAS (Rodell et al., 2004). The dotted lines surrounding the linear regression line represent the 95% confidence interval.

Table 3.1. Characteristics of the 17 studies (N = 19; one study with three study areas) that are included this study. The key inclusion criteria are that the study has reported the irrigation-induced change in mean air temperature and the comparison between the irrigated and non-irrigated sites did not involve a land cover or land use change (see Methods for detailed criteria).

Year	Location	Climate classification	Approach	Model	Environment	Irrigated surface	Irrigation rate (mm/day)	ΔT_{mean} (°C)	Citation
2017	Yellow River Basin, China	BSk	Modelling	WRF and Noah LSM	Regional scale	Crop	NA	–0.10	(Chen et al., 2017)
2002	Murrumbidgee-Coleambally-Murray Irrigation Areas, Australia	BSk	Observational	NA	Regional scale	Crop	NA	–1.40	(Geerts, 2002)
2014	Haihe River Basin, China	BSk	Modelling	RegCM4 and CLM	Regional scale	Crop	0.4	–0.34	(Zou et al., 2014)
2015	Gezira, Sudan	BWh	Observational	NA	Experimental farmland	NA	NA	–1.00	(Alter et al., 2015)
2015	Phoenix, USA	BWh	Modelling	UCM	City	Mesic	3.9	–2.67	(Yang and Wang, 2015)
2017	Yellow River Basin, China	BWk	Modelling	WRF and Noah LSM	Regional scale	Crop	NA	0.00	(Chen et al., 2017)
2012	Zhangye, China	BWk	Modelling	SCAM and CLM	City	Vegetation	NA	–1.42	(Wen and Jin, 2012)
2015	Toowoomba, Queensland, Australia	Cfa	Observational	NA	Experimental farmland	Crop	NA	–0.43	(Hancock et al., 2015)
2012	The Great Plains, USA	Cfa	Modelling	WRF and Noah LSM	Experimental farmland	Crop	NA	–0.16	(Harding and Snyder, 2012)
2014	The Great Plains, USA	Cfa	Modelling	WRF and Noah LSM	Experimental farmland	Crop	NA	–1.00	(Huber et al., 2014)
2020	Po Valley, Italy	Cfa	Modelling	WRF-ARW	Regional scale	Crop	5.7	–1.17	(Valmassoi et al., 2020)
2018	Mawson Lakes, Adelaide, Australia	Csa	Modelling	SURFEX (TEB-SBL, TEB-Veg)	City	Pervious surface	15.0	–1.50	(Broadbent et al., 2018b)
2008	California Central Valley, USA	Csa	Modelling	RSM and OSU	Regional scale	NA	NA	–0.02	(Kanamaru and Kanamitsu, 2008)
2011	California Central Valley, USA	Csa	Modelling	NCAR/Penn State MM5	Regional scale	NA	NA	–2.10	(Sorooshian et al., 2011)
2017	California Central Valley, USA	Csa	Modelling	WRF and Noah LSM	Regional scale	Crop	3.6	–1.11	(Yang et al., 2017)
2017	Yellow River Basin, China	Cwa	Modelling	WRF and Noah LSM	Regional scale	Crop	NA	–0.10	(Chen et al., 2017)
2003	Nebraska, USA	Dfa	Modelling	RAMS and LEAF-2	Regional scale	Crop	NA	–0.60	(Adegoke et al., 2003)
2018	Mead, Nebraska, USA	Dfa	Experimental	NA	Experimental farmland	Maize	2.6	–0.26	(Chen et al., 2018)
2016	Huang-Huai-Hai Plain, China	Dwa	Modelling	WRF and Noah LSM	Regional scale	Crop	0.4	–0.23	(Yang et al., 2016)

Table 3.2. Results of the stepwise multiple linear regression model on irrigated-induced change in mean air temperature.

Variable	Unit of comparison	Estimate	SE	*t*	*p*	R^2
(Intercept)	NA	26.71	11.46	2.3	<0.05	NA
Air temperature	1 °C	-0.10	0.04	-2.5	<0.05	15.2%
Rainfall	10 mm/month	0.11	0.03	3.4	<0.01	32.9%

F-statistic: 7.397 on 2 and 16 DF, $p<0.01$, $R^2 = 48.0\%$.

Note: The full model consists of five dependent variables of the background climate (air temperature, specific humidity, wind speed, net radiation and rainfall) with the irrigation-induced change in mean air temperature being the independent variable. Specific humidity, wind speed and net radiation are removed from the full model in the bi-directional stepwise elimination procedure to optimise the quality of the model.

The cooling potentials of irrigation are more apparent in the arid climate region than temperate and continental regions (Fig. 3.5). North Africa, the Middle East and north India have the highest irrigation cooling potentials (–3 to –2 °C), and these geographic areas have high mean air temperature (>30 °C) (Fig. 3.2a) and low rainfall (<50 mm/month) (Fig. 3.2b). An irrigation cooling potential between –2 and –1 °C is also predicted for central Asia, east and south China, mid-west and south-west USA, northern Mexico, southern Africa and southern and western Australia. These regions have moderate mean air temperature (15–30 °C) and low monthly rainfall (<50 mm). The majority of Europe, Russia, Canada, Argentina and east coast of Australia have an estimated cooling potential between –1 and 0 °C. Irrigation is predicted to cause warming of up to 3 °C along the east coast of North America, south Peru, southeast Brazil, Zambia, Madagascar, the UK, Tibet, and New Zealand. These regions have relatively high rainfall (> 100 mm) (Fig. 3.2b).

The majority of the 100 cities (91) are estimated to benefit from irrigation cooling of their urban green space (Table S3.2). Nine cities could potentially cool their urban green spaces by between –3.00 and –2.01 °C, 33 cities between –2.00 and –1.01 °C, and 49 cities between –1.00 and 0.00 °C. The three cities with the strongest estimated cooling benefit from irrigating urban green space are Kuwait (–2.60 °C), Doha (–2.55 °C) and Riyadh (–2.53 °C). The summer climate of these cities is very hot (mean air temperature > 35 °C) and dry (mean rainfall < 50 mm/month) (Fig. 3.2). The mean estimated cooling effect of irrigating urban green space in arid region cities ($N = 27$) is –1.65 °C, which is greater than that from irrigating urban green space in temperate region cities ($N = 49$, –0.50 °C) and continental region cities ($N = 23$, –0.97 °C) (Fig. 3.6).

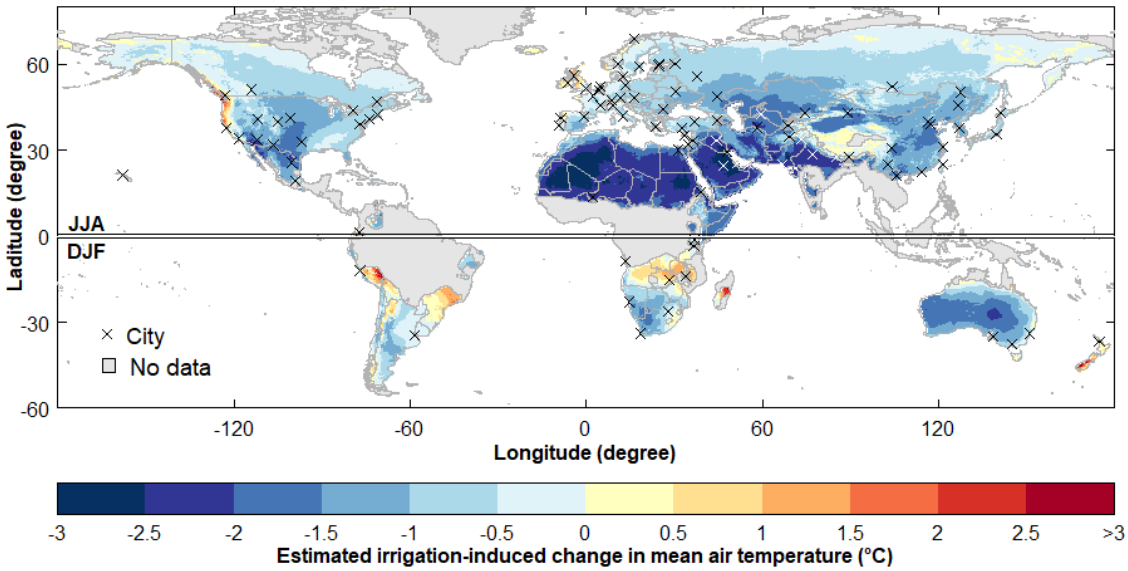

Fig. 3.5. Estimated irrigation-induced change in mean air temperature (ΔT_{mean}) in JJA (northern hemisphere) and DJF (southern hemisphere). ΔT_{mean} are calculated from the 30-year (1981–2010) near surface mean air temperature and rainfall (Fig. 3.2) using the regression model in Table 3.1. Tropical and polar regions in the updated Köppen-Geiger climate classification are greyed out and denoted by 'No data'. The locations of the 100 cities selected for further analysis (Tables S3.2) are marked by (×).

Urban green spaces in nine cities are predicted to experience a warming effect (mean = +0.76 °C) induced by irrigation (Table S3.2). The three cities with the strongest warming potentials from green space irrigation are Pasto (+1.47 °C), Vancouver (+1.41 °C) and Glasgow (+1.31 °C) and these cities have cool summer climates (air temperature: ~15 °C) with moderate rainfall (monthly rainfall: ~60 mm). Based on the estimated cooling potentials of the 100 cities, the three climate regions with the strongest irrigation cooling potential are BWh (-2.32 °C), BWk (-1.59 °C) and Dwa (-1.48 °C) (Table 3.3). The three climate regions with the weakest irrigation cooling potentials are Cfb (-0.10 °C), Csc (-0.02 °C) and Csb (+0.30°C).

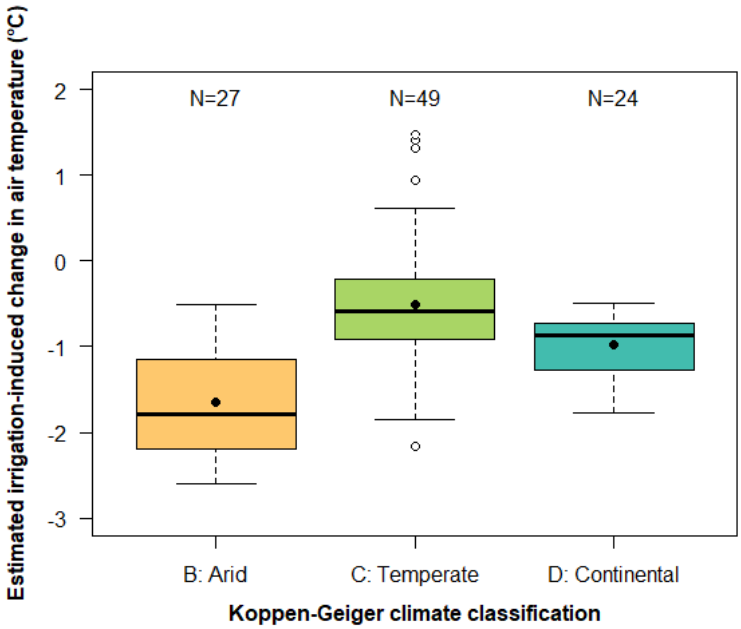

Fig. 3.6. Box-whisker plot of the estimated irrigation-induced change in mean air temperature of 100 global cities, grouped by three broad climate zones (B: Arid; C: Temperate; D: Continental). The black dots within the boxes indicate the mean.

Table 3.3. Estimated irrigation-induced change in mean air temperature of the 100 global cities by Köppen–Geiger climate classification.

Köppen–Geiger climate classification	N	Mean	SD	Min.	Max
BWh: Arid hot desert	8	–2.32	0.27	–2.60	–2.15
BWk: Arid cold desert	7	–1.59	0.51	–2.29	–1.25
Dwa: Hot–summer dry–winter continental	4	–1.48	0.19	–1.76	–1.39
BSh: Semi–arid hot steppe	6	–1.32	0.60	–2.16	–0.96
Dsa: Hot–dry summer continental	2	–1.20	0.29	–1.40	–1.10
BSk: Semi–arid cold steppe	6	–1.16	0.33	–1.78	–0.94
Cwa: Dry–winter humid subtropical	8	–1.04	1.16	–2.17	–0.79
Dfa: Hot–summer continental	6	–0.97	0.26	–1.38	–0.80
Dwb: Warm–summer dry–winter continental	3	–0.92	0.26	–1.14	–0.81
Dsb: Warm–dry summer continental	1	–0.82	NA	–0.82	–0.82
Cfa: Humid subtropical	9	–0.80	0.35	–1.33	–0.61
Csa: Mediterranean dry–hot summer	7	–0.73	0.31	–1.06	–0.51
Dfb: Warm–summer continental	8	–0.70	0.18	–1.01	–0.58
Cwb: Dry–winter subtropical highland	6	–0.62	0.32	–1.07	–0.50
Cfb: Oceanic	14	–0.10	0.70	–0.91	–0.05
Csc: Mediterranean dry–cold summer	1	–0.02	NA	–0.02	–0.02
Csb: Mediterranean dry–warm summer	4	+0.30	0.97	–0.90	0.68

3.5. Discussion

While the cooling effect of irrigation has been extensively researched from the perspective of global and regional climate change (Puma and Cook, 2010; Sugimoto et al., 2019; Thiery et al., 2017), the potential to use irrigation to mitigate heat stress in cities has yet to be evaluated in relation to the background climate of those cities. Four global studies have estimated the spatial variability of the cooling effect of agricultural irrigation (Cook et al., 2011; Puma and Cook, 2010; Sacks et al., 2009; Thiery et al., 2017) (Fig. 3.6). It is only possible to qualitatively compare the findings of these four global studies with our study, because they used complex climate models, whereas we used a simple regression model. In general, their findings corroborate our predictions in two irrigated regions. First, these four global studies indicate that north India and the Middle East have experienced the strongest cooling effect from agriculture irrigation (Fig. 4d in Sacks et al. (2009), Fig. 5 in Puma and Cook (2010), Fig. 6a in Cook et al. (2015) and Fig. 4a in Thiery et al. (2017)). Second, a weaker cooling effect from agriculture irrigation was predicted by these global studies for east China and the United States (same Figs as above). The consistency between our modelling results and those in the literature suggested that our simple model can broadly capture the impact of background climate on irrigation cooling effect. Compared to the more complex and mechanistic models used in the literature, an important advantage of our model is that it was simple enough to estimate the cooling potentials for arid, continental and temperate regions using only background air temperature and rainfall data. These two types of climate data are available in every global town and city.

Background air temperature and rainfall were the only climate variables that remained in our model, as specific humidity, wind speed and net radiation did not have a significant relationship with air temperature reduction in this dataset of 17 irrigation studies. A significant correlation between irrigation cooling effect and background air temperature was also confirmed in a recent modelling study (Gao et al., 2020). Our model is supported by classic hydrological theory about the constraints of evapotranspiration being a function of soil moisture and energy (Budyko, 1974; Koster et al., 2009; Seneviratne et al., 2010), with soil moisture being strongly linked to rainfall and air temperature being a strong component of vapour pressure deficit which provides the 'energy' for evapotranspiration.

Frequent visits to urban green space are known to be associated with better physical and psychological health (Maas et al., 2006a). Irrigating urban green spaces can improve the thermal comfort conditions, which may lead to a greater usage of the green spaces (Lin et al., 2013). However, the increase in humidity after irrigation may partially offset the air cooling benefit because a high humidity level can promote thermal discomfort (Ma et al., 2018). The overall effect of irrigation on thermal comfort is likely to also be heavily dependent on the background climate, for example the

negative effect of increased humidity may be less important in dry climate regions compared to moist ones. Although tree canopy shade in urban green spaces is likely to provide a stronger and more consistent cooling effect than intermittent irrigation, there are certain places in cities where tree planting is infeasible, such as sports fields and small backyards. Therefore, it is necessary to consider using irrigation for heat mitigation in these places. Moreover, a certain level of irrigation is sometimes required for maintaining a healthy tree canopy. The potentially synergy between tree canopy shade and irrigation in urban green spaces is worthy of future research attention.

As opposed to agriculture, in which irrigation is applied regularly to meet the growth requirement of crops, irrigation of urban green spaces to provide cooling is most needed when the heat stress is strong, particularly during heatwaves. The cooling potentials predicted in this study are only representative of the mean cooling in summer (JJA for northern hemisphere or DJF for southern hemisphere). The cooling benefits of urban green space irrigation during heatwaves are yet to be determined, but there is preliminary evidence that irrigation can induce an even stronger cooling benefit during heatwaves as compared to during non-heatwave periods (Gao et al., 2020). The landscape and surface characteristics of urban green spaces are often more complex than in agricultural landscapes as they can possess multiple vegetation layers, and as such the microclimatic response of irrigating urban green spaces may also be different. A well recognised cooling benefit provided by urban green spaces is the shade cast by urban trees as well as their transpiration, and irrigation or misting are likely to enhance these existing cooling benefits (Crum and Jenerette, 2017; Santamouris et al., 2018). An urban green space with turfgrass, shrubs and tall trees will have greater aerodynamic roughness and lower reflectance to shortwave radiation (Allen et al., 2005). The presence of trees in urban green space can provide a significant cooling effect because of shading (Brown et al., 2015; Shashua-Bar et al., 2009) and the increased surface roughness can enhance the convective cooling efficiency (Gunawardena et al., 2017). Nevertheless, irrigation of urban green spaces has been recognised as an important factor in mitigating urban heat stress and promoting the park cool island effect (Bowler et al., 2010; Crum and Jenerette, 2017; Ziter et al., 2019). Furthermore, since urban trees can experience significant leaf loss during a heatwave or drought (Sanusi and Livesley, 2020), leading to a reduced shading and cooling effect (Rahman et al., 2020), irrigating urban green space may create a synergistic cooling benefit by maintaining tree canopy cover and grass cover whilst promoting evapotranspiration cooling benefits of both.

The cooling and health benefits of green space irrigation are dependent on the available area of green space in these cities as well as the accessibility and ownership of those green spaces. The proportion of a city that is green space can vary from 11% in Birmingham, UK (Angold et al., 2006),

to 34% in Beijing, China (Yao et al., 2015) and to nearly 50% in Stockholm and some other European cities (Fuller and Gaston, 2009). The ownership of urban green space dictates the potential for irrigation and who the beneficiaries of the irrigation cooling benefits are likely to be. For example, the fraction of open space that is privately-owned in Hong Kong is 15% (Jim and Chan, 2016), while 60% of the green space in Brisbane, Australia, is private (Rupprecht and Byrne, 2014).

The cultural practice of irrigation also determines the feasibility of the promotion and expansion of green space irrigation. Although we predicted that the cooling benefits of green space irrigation would be the highest in arid cities, e.g. Kuwait, Doha and Riyadh, these cities are already irrigating many urban green spaces to support the survival of the vegetation in these arid cities. The cooling benefits from urban green space irrigation predicted by our model assume that these urban green spaces are not currently irrigated, which will apply to many cities in temperature and continental regions, as well as lower socio-economic cities in arid regions. Ultimately, the feasibility, benefits and costs of urban green space irrigation will depend on the actual conditions of individual cities. In a world with increasingly limited freshwater supply (Rodell et al., 2018) and a need to protect and conserve drinking water for potable uses only, integrated water management in modern cities can increase irrigation water supply through rainwater and stormwater collection, greywater use and recycling of sewage (Griggs, 2013; Howells et al., 2013; Wong and Brown, 2009). It was estimated that over 600 kL/year/ha of stormwater can be collected from a 42 % impervious catchment in Melbourne for a storage capacity of 20 kL/ha (Mitchell et al., 2007). The collected stormwater will allow an additional 0.16 mm/day of irrigation for the same area, assuming that the water is applied evenly across that area. The additional water may be enough to meet the water demand for all vegetated area because not all surfaces are vegetated and require irrigation.

If irrigation is infeasible due to limited water availability, other heat mitigation strategies, such as expanding the size of urban green spaces and changing the vegetation composition, may be considered. Xiao et al. (2018) measured the air temperature in small (< 4 ha) and large (> 10 ha) parks in a humid subtropical region (Köppen climate classification: Cfa) in China. They found that the cooling effect of large parks (3.32 °C) was much higher than the small ones (1.75 °C). Cheung and Jim (2019a) measured the air temperature impacts of three different types of vegetation (tree, shrub and grass) in a similar climate region (Cwa). They showed that an 50 % increase in tree cover can lead to a reduction in daytime mean air temperature by 0.4 °C, whereas the same increase in shrub cover can only lead to a 0.2 °C reduction and the impact of grass on air temperature is insignificant. However, similar to irrigating urban green space, the cooling potentials of these strategies are likely to be dependent on background climate. A recent review study showed that urban greening is more

effective in reducing air temperature in arid climate (monthly rainfall < 80 mm) than humid climate (monthly rainfall > 80 mm) (Lai et al., 2019). More studies are needed to compare the cooling effect of different strategies in different climate regions. Although our predictions of cooling effect using a simple model are somewhat consistent with the results from more complex earth system models, such simplification has several major limitations. First, we were unable to include irrigation rate as an independent variable in the model because only seven cases have reported their irrigation rates (Table 3.1). This severely restricts the implications of the model as we do not know how much water is required to achieve the predicted cooling potentials. We estimate that the required irrigation rate should be comparable to the median (3.6 mm/day) or mean (4.5 mm/day) of the seven reported irrigation rates in the dataset, assuming that the unreported irrigation rates followed a similar distribution as the reported ones. Second, the spatial and climatic coverage of the dataset were highly limited. All but four studies were undertaken in China or the United States (Table 3.1). The small variability of the dataset prevents us from predicting the cooling potential in the tropics, where cooling is much appreciated (Matzarakis and Amelung, 2008). The accuracy of the model is also uncertain due to the limited sample size (N = 19). Third, the linear assumption of this simple model may generate somewhat unrealistic predictions, particularly in regions with large amounts of rainfall. The model predicted that irrigation would produce a warming effect of over 2 °C in south Peru and Madagascar mainly because of their high rainfall (>200 mm/month). However, a global modelling study showed that historic irrigation in these regions did not induce a notable warming (<0.5 °C) in air temperature (Puma and Cook, 2010). It is unlikely that the addition of a few more millimeters of moisture through irrigation will result in a strong warming effect in these relatively wet climates.

3.6. Conclusion

We showed that background climate, namely air temperature and rainfall, had a strong impact on irrigation cooling potentials in arid, temperate and continental climates. The cooling potentials were greatest in the Middle East and north India; an apparent irrigation cooling effect was also plausible for most areas in Australia, China, Europe and the United States. The cooling potentials in arid climates were much higher than temperate and continental climates, because irrigation can unleash the huge evaporative cooling potentials in soils that are otherwise moisture-limited. Our model predicted that irrigation would help mitigate heat stress in green spaces in the majority cities in the arid, temperate and continental climates.

This study has assessed the impact of irrigation on air temperature in different climate regions. The results can be useful for identifying and prioritising urban heat mitigation strategies. In contrast to urban greening, the impact of irrigating urban green spaces on air temperature has rarely been

investigated explicitly (Broadbent et al., 2018a; Daniel et al., 2018; Yang and Wang, 2015). While urban greening strategies, particularly tree planting, are often limited by the availability of space (Jim and Chan, 2016), irrigation can enhance the cooling effect of existing urban green space in both the public and private realm. Sufficient irrigation is also beneficial for the health of urban vegetation and the sustained delivery of their ecosystem services. Although irrigation water supply may be restricted in the dry regions, innovative water sensitive urban design can be used to increase irrigation water supply by harvesting stormwater, with subsequent irrigation and redistribution to enhance soil moisture (Coutts et al., 2013). Such water sensitive urban designs can support cities to develop climate sensitive urban design (Oke et al., 2017) to mediate extreme urban climates in a warming world. However, more irrigation studies are required across those climate zones where few or no studies have been performed, to assess the cooling potentials of irrigating green spaces in cities across a wider range of climate zones more accurately. In addition, more city-scale studies are also needed to assess the irrigation cooling potentials of specific cities according to their urban configuration, climate and water supply.

3.7. Supplementary materials

Table S3.1. List of 57 excluded irrigation cooling studies and the exclusion reasons. DATE: study period was not reported. LCC: land cover change was involved along with irrigation such that the impact of irrigation cannot be isolated. LOMC: lack of a meaningful control. LTA: irrigation-induced change in mean air temperature (ΔT_{mean}) was not reported because the study focused on the long-term analysis of air temperature change between irrigated and non-irrigated areas. OTM: other air temperature measures were used, such as daily maximum air temperature difference (ΔT_{max}) and maximum instantaneous air temperature difference (ΔT_{imax}).

Reason	Air temperature measure used (for OTM studies)	Citation
DATE	NA	(Thompson et al., 1993)
LCC	NA	(Chase et al., 1999)
LCC	NA	(De Ridder & Gallée, 1998)
LCC	NA	(Jiang et al., 2014)
LCC	NA	(Jin & Miller, 2011)
LCC	NA	(Kueppers et al., 2007)
LCC	NA	(Kueppers et al., 2008)
LCC	NA	(Lobell, Bonfils, Kueppers, et al., 2008)
LCC	NA	(Marcella & Eltahir, 2014)
LCC	NA	(Mueller & Day, 2005)
LCC	NA	(Stohlgren et al., 1998)
LCC	NA	(Ter Maat et al., 2006)
LCC	NA	(Weare & Du, 2008)
LOMC	NA	(Fowler & State, 1974)
LOMC	NA	(Hobbs, 1973)
LOMC	NA	(Lakatos et al., 2010)
LOMC	NA	(Lakatos & Żyromski, 2012)
LOMC	NA	(Liu & Kang, 2006)
LOMC	NA	(Lomas & Mandel, 1973)
LOMC	NA	(Mahmood et al., 2006)
LOMC	NA	(Mahmood et al., 2013)
LOMC	NA	(Steiner et al., 1983)
LOMC	NA	(Wang et al., 2015)
OTM	ΔT/decade	(Biggs et al., 2008)
OTM	ΔT_{imax}	(Bonan, 2000)
OTM	ΔT/decade	(Bonfils & Lobell, 2007)
OTM	Daytime and nighttime ΔT_{imax}	(Broadbent et al., 2019)
OTM	ΔT/decade	(Chen & Jeong, 2018)
OTM	ΔT/decade	(Christy et al., 2006)
OTM	Daytime and nighttime ΔT_{imax}	(Daniel et al., 2018)
OTM	ΔT_{max}	(Dussi et al., 1997)
OTM	Unclear	(Evans et al., 1995)
OTM	Unclear	(Grossman-Clarke et al., 2010)
OTM	ΔT/decade	(Han & Yang, 2013)
OTM	ΔT_{max}	(Huang & Ullrich, 2016)

OTM	ΔT_{imax}	(Iglesias et al., 2002)
OTM	ΔT_{imax}	(Iglesias et al., 2005)
OTM	Unclear	(Kemp et al., 1974)
OTM	ΔT_{imax}	(Kohl & Wright, 1974)
OTM	Daytime ΔT	(Lawston et al., 2015)
OTM	ΔT/decade	(Lee et al., 2009)
OTM	ΔT_{imax}	(Lee et al., 2011)
OTM	ΔT_{max} and ΔT_{min}	(Lobell & Bonfils, 2008)
OTM	ΔT/decade	(Lobell, Bonfils, & Faurès, 2008)
OTM	ΔT_{imax}	(Nainanayake et al., 2008)
OTM	ΔT_{max}	(Nocco et al., 2019)
OTM	ΔT_{max}	(Parchomchuk & Meheriuk, 1996)
OTM	A range of ΔT	(Qian et al., 2013)
OTM	ΔT not reported	(Saeed et al., 2009)
OTM	ΔT/decade	(Shi et al., 2014)
OTM	ΔT_{max}	(Sridhar, 2013)
OTM	Mode of ΔT	(Sugimoto et al., 2019)
OTM	Daytime and nighttime instantaneous maximum ΔT	(Vahmani & Ban-Weiss, 2016)
OTM	ΔT_{max} and ΔT_{imax}	(Vahmani & Hogue, 2015)
OTM	ΔT/decade	(Yoshida et al., 2012)
OTM	Median ΔT	(Zhang et al., 2017)
OTM	ΔT/decade	(Zhu et al., 2012)

Table S3.2. Köppen–Geiger climate classification and the estimated irrigation-induced change in mean air temperature (ΔT_{mean}) of the 100 global cities.

Rank	City	Country/region	Köppen–Geiger climate classification	Estimated ΔT_{mean} (°C)
1	Kuwait	Kuwait	BWh	–2.60
2	Doha	Qatar	BWh	–2.55
3	Riyadh	Saudi Arabia	BWh	–2.53
4	Dubai	United Arab Emirates	BWh	–2.44
5	Baghdad	Iraq	BWh	–2.36
6	Turpan	China	BWk	–2.29
7	Karachi	Pakistan	BWh	–2.22
8	Delhi	India	Cwa	–2.17
9	Niamey	Niger	BSh	–2.16
10	Phoenix	United States of America	BWh	–1.96
11	Ashgabat	Turkmenistan	BWk	–1.91
12	Cairo	Egypt	BWh	–1.89
13	Hanoi	Vietnam	Cwa	–1.85
14	Nukus	Uzbekistan	BWk	–1.84
15	Monterrey	Mexico	BSh	–1.80
16	El Paso	United States of America	BWk	–1.79
17	Tianjin	China	BSk	–1.78
18	Beijing	China	Dwa	–1.76
19	Chengdu	China	Cwa	–1.65
20	Hong Kong	Hong Kong S.A.R.	Cwa	–1.48
21	Islamabad	Pakistan	Cwa	–1.45
22	Seoul	South Korea	Dwa	–1.41
23	Bishkek	Kyrgyzstan	Dsa	–1.40
24	North Platte	United States of America	Dwa	–1.40
25	Walvis Bay	Namibia	BWk	–1.39
26	Volgograd	Russia	Dfa	–1.38
27	Harbin	China	Dwa	–1.35
28	Dallas	United States of America	Cfa	–1.33
29	Yerevan	Armenia	BSh	–1.32
30	Luanda	Angola	BSh	–1.28
31	Shanghai	China	Cfa	–1.26
32	Kathmandu	Nepal	Cwa	–1.26
33	Bucharest	Romania	Dfa	–1.19
34	Zaragoza	Spain	BSk	–1.17
35	Denver	United States of America	BSk	–1.16
36	Heihe	China	Dwb	–1.14
37	Asmara	Eritrea	BSk	–1.13
38	Lima	Peru	BWk	–1.11
39	Kunming	China	Cwb	–1.07
40	Adelaide	Australia	Csa	–1.06
41	Dushanbe	Tajikistan	Csa	–1.02

42	Kiev	Ukraine	Dfb	–1.01
43	Salt Lake City	United States of America	Dsa	–1.00
44	Tokyo	Japan	Cfa	–1.00
45	Irkutsk	Russia	Dwb	–0.98
46	Washington, D.C.	United States of America	Cfa	–0.91
47	Vienna	Austria	Cfb	–0.91
48	Cape Town	South Africa	Csb	–0.90
49	Tel Aviv–Yafo	Israel	Csa	–0.89
50	Kabul	Afghanistan	BSk	–0.88
51	Toronto	Canada	Dfa	–0.88
52	Konya	Turkey	BSk	–0.87
53	Moscow	Russia	Dfb	–0.87
54	Mexico City	Mexico	Cwb	–0.86
55	Nicosia	Cyprus	BSh	–0.85
56	Rome	Italy	Csa	–0.85
57	Sapporo	Japan	Dfa	–0.84
58	Sivas	Turkey	Dsb	–0.82
59	Damascus	Syria	BWk	–0.81
60	New York	United States of America	Dfa	–0.78
61	Qu,bec	Canada	Dfb	–0.77
62	Boston	United States of America	Dfa	–0.74
63	St. Petersburg	Russia	Dfb	–0.72
64	Taipei	Taiwan	Cfa	–0.70
65	Milan	Italy	Cfa	–0.66
66	Athens	Greece	Csa	–0.66
67	Berlin	Germany	Cfb	–0.65
68	Calgary	Canada	Dwb	–0.63
69	Stockholm	Sweden	Dfb	–0.63
70	Lyon	France	Cfa	–0.61
71	Melbourne	Australia	Cfb	–0.60
72	Helsinki	Finland	Dfb	–0.59
73	Nairobi	Kenya	Cwb	–0.58
74	Arusha	Tanzania	Cwb	–0.57
75	Munich	Germany	Cfb	–0.57
76	Paris	France	Cfb	–0.55
77	Tallinn	Estonia	Dfb	–0.55
78	Honolulu	United States of America	BSh	–0.50
79	Oslo	Norway	Dfb	–0.49
80	Thimphu	Bhutan	Cwb	–0.48
81	Copenhagen	Denmark	Cfb	–0.45
82	Sydney	Australia	Cfa	–0.40
83	Los Angeles	United States of America	Csa	–0.37
84	Buenos Aires	Argentina	Cfa	–0.35
85	Lisbon	Portugal	Csa	–0.28
86	Zurich	Switzerland	Cfb	–0.24
87	Brussels	Belgium	Cfb	–0.23

88	Amsterdam	Netherlands	Cfb	–0.22
89	London	United Kingdom	Cfb	–0.21
90	Johannesburg	South Africa	Cwb	–0.16
91	Harstad	Norway	Csc	–0.02
92	Auckland	New Zealand	Cfb	+0.01
93	Porto	Portugal	Csb	+0.21
94	San Francisco	United States of America	Csb	+0.41
95	Dublin	Ireland	Cfb	+0.48
96	Lusaka	Zambia	Cwa	+0.61
97	Lilongwe	Malawi	Cwa	+0.95
98	Glasgow	United Kingdom	Cfb	+1.31
99	Vancouver	Canada	Cfb	+1.41
100	Pasto	Colombia	Csb	+1.47

Chapter 4 – Daytime irrigation leads to significantly cooler private backyards in summer

A version of this chapter was published by Urban Climate on 6 October 2022

Cheung, P.K., Jim, C.Y., Tapper, N., Nice, K.A., Livesley, S.J., 2022. Daytime irrigation leads to significantly cooler private backyards in summer. Urban Clim. 46, 101310. https://doi.org/10.1016/j.uclim.2022.101310

Abstract

Backyards play important roles for individual households because they provide a private and safe green space for social and environmental interactions, relaxation, gardening and children's activities. The use of backyards is highly dependent on their thermal conditions. Turf is a common surface type in backyards but unirrigated turf can be as warm as pavement, bringing thermal discomfort and discouraging people from using them. Under certain conditions, turf irrigation provides an opportunity to reduce thermal stress by increasing evapotranspiration. This study aims to measure the impacts of turf irrigation on microclimate in a backyard environment in the warm season in Melbourne, Australia. The experiment consisted of four 6 m × 6 m turf-covered plots. Daily irrigation was applied at four amounts: 0, 2, 4 and 7 mm for six weeks. In Week 6, the 4-mm irrigation reduced daytime soil temperature, turf surface temperature, air temperature and universal thermal climate index by 1.7, 2.3, 0.6 and 0.4°C, respectively. All daytime impacts were significant (p<0.05, t-test). Irrigation has the potential to significantly improve the thermal conditions of backyards in combination with the use of tree shade.

4.1. Introduction

4.1.1. Background

Urban green spaces offer a wide range of benefits to urban dwellers, such as climate regulation (Lin et al., 2016), noise reduction (Koprowska et al., 2018) and provision of space for physical and social activities (Jennings and Bamkole, 2019). Most studies have focused on public urban green spaces (Dewaelheyns et al., 2018). Private green spaces deserve more attention because they can constitute a large proportion of urban green space in many cities. For example, >30% in Brisbane, Australia (Rupprecht and Byrne, 2014), >35% in the UK cities (Loram et al., 2007) and >50% in Dunedin, New Zealand (Mathieu et al., 2007). Private greens spaces may be commercially owned and used by members of, or visitors to, that organisation; or they may small private residential green spaces used by individuals of a household. Private residential backyards have distinct roles for individual households because they provide a safe and enclosed green space for social gatherings, relaxation, gardening and children's activities (Hall, 2015).

The frequency of use of outdoor green spaces in summer is dependent upon the microclimate of the space (Cheung and Jim, 2018a). Intense summer heat can prevent people from using outdoor green spaces, including private backyards. In a turfed green space, the microclimate can be strongly influenced by soil moisture availability because it directly affects evapotranspiration. The daytime surface temperature of unirrigated turf can be as high as pavement, whereas that of irrigated turf in summer can be 10°C lower (Spronken-Smith and Oke, 1998) due principally to evapotranspiration. This highlights the potential role of turf irrigation in moderating the summer microclimate of private backyards to reduce air temperature and human heat stress.

Most studies in the literature used computer models to estimate the impact of irrigation on urban climate at a large spatial scale (Cheung et al., 2022b). Using the Weather Research and Forecasting model, Gao and Santamouris (2020) predicted that irrigating both vegetated and impervious surfaces in Metropolitan Sydney, Australia (~800 km^2) can reduce daily mean air temperature by 0.5°C. Using the SURFEX model, Broadbent et al. (2018a) predicted that irrigating all the vegetated surfaces in a suburb of Adelaide, Australia (~7 km^2) can reduce the daily mean air temperature by 2.3°C. Although other modelling studies also predicted a cooling effect from irrigation (Daniel et al., 2018; Li et al., 2015; Wang et al., 2019), there is a lack of experimental studies that directly measure the cooling benefits of irrigation. Moreover, most existing modelling studies have been undertaken at scales no more detailed than the city or regional scales. The impacts of small-scale irrigation on microclimate in the backyard environment are poorly understood. With the increasing availability of alternative

irrigation water supplies, such as collected stormwater and recycled grey water (Coutts et al., 2013), irrigating private green spaces offers a unique and sustainable opportunity to enhance the climate resilience and well-being of cities (Livesley et al., 2021; Tapper, 2021). Thus, it is important to understand the potential cooling benefits of irrigating small private green spaces.

In view of the lack of empirical evidence for the cooling potential of irrigation in cities, this study aims to measure the microclimatic impacts of turf irrigation in a field experiment. With the support of the literature, section 4.1.2 will present a theoretical framework that explains the key daytime and night-time processes induced by irrigating turf and the likely impacts on soil moisture, microclimate and surface energy fluxes. This study will test seven hypotheses derived from the theoretical framework.

4.1.2. Theoretical framework and study hypotheses

The theoretical framework underpinning this study is based upon literature and energy-balance understanding from irrigation studies in agricultural and urban landscapes. This theoretical framework represents the key daytime and night-time processes induced by irrigating turf and the likely impacts on soil moisture, microclimate and surface energy fluxes (Fig. 4.1). During the day, irrigated turf has a higher soil moisture content, which induces three simultaneous effects. First, evapotranspiration increases, which increases latent heat flux and reduces sensible heat flux (Chen et al., 2018; Gao et al., 2020). The change in energy partitioning reduces soil temperature, turf surface temperature and air temperature (Broadbent et al., 2018a) but increases vapour pressure (Harding and Snyder, 2012). The lower turf surface temperature reduces outgoing longwave radiation. Second, the albedo of irrigated turf is lower because of lusher grass and darker soils, causing a reduction in outgoing shortwave radiation (Roxy et al., 2010). Third, the wet soils have higher thermal conductivity and specific heat, causing an increase in downward soil heat flux and soil heat storage (Kanamaru and Kanamitsu, 2008). These changes in microclimate and surface energy fluxes cause a net reduction in UTCI (Daniel et al., 2018). During the night, in the absence of incoming solar radiation, the microclimate in a turf area is mainly determined by a strong radiative deficit and soil heat release (Kanamaru and Kanamitsu, 2008). Due to increased daytime storage, soil heat storage in an irrigated turf area is higher than that in an unirrigated area. At night-time, the warm soil releases more heat, i.e., an increase in heat flux out of the soils to raise turf surface temperature (Vahmani and Ban-Weiss, 2016). Higher turf surface temperature leads to a higher air temperature. These cascading changes in microclimate can cause a noticeable increase in UTCI in night-time.

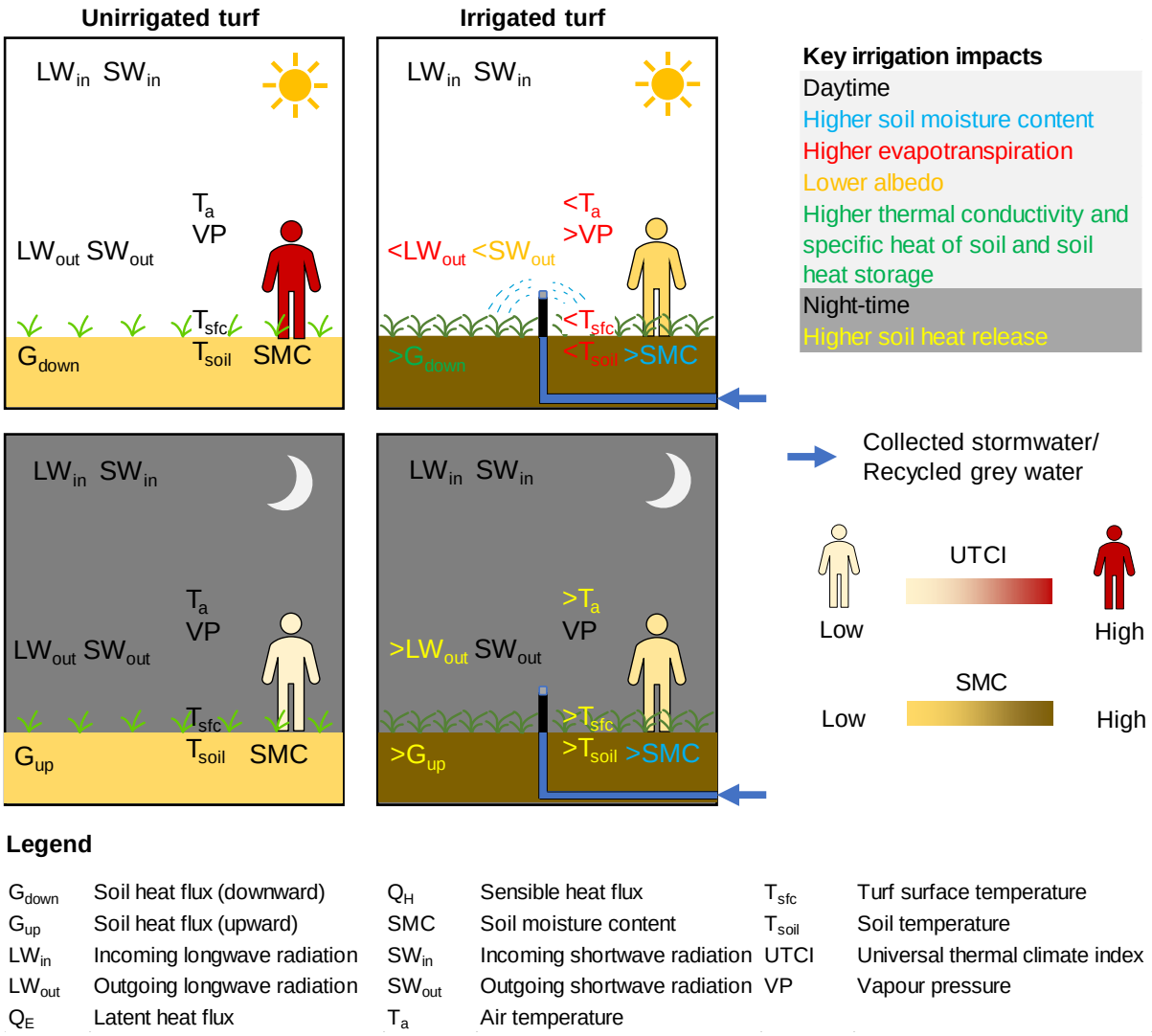

Legend

G_{down}	Soil heat flux (downward)	Q_H	Sensible heat flux	T_{sfc}	Turf surface temperature
G_{up}	Soil heat flux (upward)	SMC	Soil moisture content	T_{soil}	Soil temperature
LW_{in}	Incoming longwave radiation	SW_{in}	Incoming shortwave radiation	UTCI	Universal thermal climate index
LW_{out}	Outgoing longwave radiation	SW_{out}	Outgoing shortwave radiation	VP	Vapour pressure
Q_E	Latent heat flux	T_a	Air temperature		

Fig. 4.1. Theoretical framework describing the key daytime and night-time energetic processes that are induced by irrigating turf and the likely impacts on soil moisture, microclimate and surface energy fluxes. Changed font colour indicates irrigations impact on a key property or process such as soil moisture, microclimate or surface energy fluxes. The greater than and less than symbols indicate the direction of impact from irrigation. During the day, irrigating turf increases soil moisture content, which increases evapotranspiration and latent heat flux while reducing sensible heat flux. The increased evapotranspiration decreases soil temperature, turf surface temperature, outgoing longwave radiation and air temperature, but can increase vapour pressure. Due to irrigation, the lower albedo of wet soil surfaces and lusher grass reduces outgoing shortwave radiation. In contrast, the higher thermal conductivity and specific heat of moist soils increase downward soil heat flux and soil heat storage. These changes in microclimate cause a net reduction in UTCI. During the night, the irrigated turf has a higher soil temperature due to increased daytime heat storage to induce upward soil heat flux. More soil heat release leads to a higher turf surface temperature, and in turn, higher air temperature and UTCI.

This study will measure the microclimate in four 6 m × 6 m plots (one unirrigated and three irrigated at 2 mm/day, 4 mm/day and 7 mm/day). Based on the above theoretical framework, seven hypotheses will be tested in this study:

(i) Turf irrigation will induce daytime cooling effects in soil temperature, turf surface temperature, air temperature and UTCI;

(ii) The daytime cooling effect will strengthen with the increase in daily irrigation amount from 2 mm to 4 mm to 7 mm;

(iii) The daytime cooling effects are correlated with the differences in soil moisture content between the irrigated and the unirrigated plots;

(iv) Turf irrigation will induce night-time warming effects in soil temperature, turf surface temperature, air temperature and UTCI;

(v) The night-time warming effects will strengthen with the increase in daily irrigation amount from 2 mm to 4 mm to 7 mm;

(vi) The night-time warming effects are correlated with the difference in night-time upward soil heat flux between the irrigated and the unirrigated plots;

(vii) Irrigated plots will have a higher daytime latent heat flux and a lower sensible heat flux than the unirrigated plot, while the night-time latent heat flux and sensible heat flux will be similar in the four plots.

4.2. Methods and materials

4.2.1. Study area and climate

The study area was located at the Burnley Campus of the University of Melbourne, Australia. Melbourne has a temperate oceanic climate (Köppen climate classification: Cfb) (Peel et al., 2007). It has a warm and dry summer (Dec–Feb) with a mean daily maximum air temperature of approximately 26.2°C and a mean total rainfall of 155.3 mm (Bureau of Meteorology, 2023a). The highest air temperature ever recorded in Melbourne was 46.4°C during a heatwave in 2009 (Bureau of Meteorology, 2009). The intensity, frequency and duration of heatwaves in Australia have increased consistently in the past few decades (Trancoso et al., 2020). Melbourne is expected to experience sixteen days in a year with maximum air temperature >35°C in 2050, five days more than

the present (City of Melbourne, 2022). Irrigation is likely to be an effective cooling strategy because of Melbourne's warm and dry summer climate (Cheung et al., 2021). This study was conducted from January to March 2020 to measure the impacts of turf irrigation on the microclimate of a small enclosed private green space in Melbourne's summer. The mean reference crop evapotranspiration rate between January and March in Melbourne is approximately 4 mm/day (Bureau of Meteorology, 2023b).

4.2.2. Experimental design and irrigation system

The experiment in this study consisted of four 6 m × 6 m plots that are 2 m apart on a level surface (Fig. 4.2). The four plots received four different daily irrigation amounts, namely 0 mm (unirrigated), 2 mm, 4 mm and 7 mm. The three irrigation amounts represented a low, normal and high irrigation amounts relative to Melbourne's mean reference crop evapotranspiration (4 mm/day) in the same period. Each plot was surrounded by 1.8-m tall 70% shade cloth (SOLARSHADE^{TM}) to mimic a fenced backyard environment and reduce air mixing between the plots and the surrounding environment. The shade cloth did not shade the climate station in the plots. In each plot, irrigation was applied every day through one MP1000-360 (Hunter Rotator) at the centre and four MP1000-90 at the corners. The irrigation times of the 2-mm, 4-mm and 7-mm plots were 13:00−13:11, 13:12−13:35 and 13:36−14:23, respectively. The flow volumes were measured by Nymet flow sensors. The exact daily mean(±SD) irrigation amounts for the 2-mm, 4-mm and 7-mm plots were 2.3±0.0 mm, 4.2±0.1mm and 7.0±0.3mm, respectively. The MP Rotators created minimal mist during operation, and the water throw was adjusted to avoid hitting any sensors. In this way, the impacts of irrigation were only attributed to the direct evaporation of water droplets during irrigation and from the changes in evapotranspiration rate on the turf surface. Kikuyu (*Pennisetum clandestinum*) was the dominant grass species in the plots. The grass remained healthy and provided a complete cover of the plots in the course of the experiment. The grass was mowed every two weeks. The top soil (5−10 cm) of the site was sandy loam and the subsoil (50−55 cm) was sandy clay. The bulk density of the top soil and subsoil was 1.02 g/cm^3 and 1.58 g/cm^3, respectively. The pore volume of the top soil and subsoil was 61% and 40%, respectively. The soil was well-drained with an infiltration rate of approximately 650 mm/h.

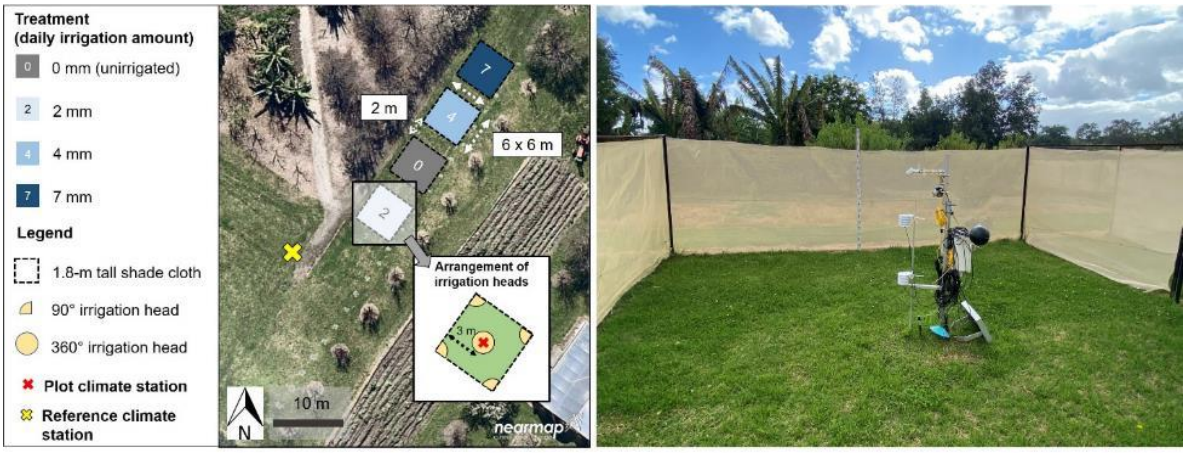

Fig. 4.2. An aerial photo showing the experimental site (Burnley Campus, the University of Melbourne) and the design of the experiment (left), and a ground photo showing one of the experimental plots (right). The experiment consisted of four 6 m × 6 m plots that received four different daily irrigation amounts: (1) 0 mm (unirrigated), (2) 2 mm, (3) 4 mm and (4) 7 mm. Each plot was surrounded by a 1.8-m tall 70% shade cloth (SOLARSHADE^{TM}) to mimic a backyard environment and reduce air mixing between the plots and with the surrounding environment. In each plot, irrigation was applied at the corners at 13:00 local time every day through one Hunter Rotator MP1000-360 at the centre and four Hunter Rotator MP1000-90. Kikuyu (*Pennisetum clandestinum*) was the dominant grass species. One climate station was installed at the centre of each plot and a reference climate station was installed approximately 8 m southwest of the 2-mm plot.

4.2.3. Soil and microclimate measurements

One climate station was installed at the centre of each plot (Fig. 4.2). Wind speed, black globe temperature, air temperature and vapour pressure were measured at 1.1 m above ground. Incoming and outgoing shortwave and longwave radiation and turf surface temperature were measured at 1.5 m above ground. Soil moisture content and soil temperature were measured at 0.02 m and 0.04 m below ground and soil heat flux 0.05 m below ground to monitor the near-surface response of soil variables to irrigation. The specifications of the instruments used in this study are listed in Table 1. A reference climate station was installed approximately 8 m southwest of the 2-mm plot (Fig. 4.2). Wind speed, wind direction and rainfall were measured at 2 m. Air temperature and water vapour pressure were measured at 0.6 m and 1.1 m. The difference between the reference climate station and the non-irrigated climate station was that the reference site was not enclosed by a shade cloth and the anemometer was installed at a height of 2 m above ground level. All variables were measured every 10 s, and the 1-min averages were logged.

All data analysis was performed in R Studio 2021.09.0 (R Core Team, 2023). UTCI was calculated using the "rBiometeo" package in R.

Table 4.1. Specifications of the instruments used in this study.

Location	Model and brand	Variable	Accuracy	Height/depth (m)
Plot	03101-L, Campbell Scientific	Wind speed	±0.5 m/s	1.1
	44031, Omega	Black globe temperature	±0.1°C @ 25°C	1.1
	ATMOS14, METER	Air temperature	±0.2 °C	0.6, 1.1
		Atmospheric pressure	±0.05 kPa @ 25°C	0.6, 1.1
		Vapour pressure	±0.05 kPa @ 25°C	0.6, 1.1
	CNR4, Kipp & Zonen	Incoming longwave radiation (4.5–42 μm)	<10% (daily total)	1.5
		Incoming shortwave radiation (0.3–2.8 μm)	<5% (daily total)	
		Outgoing longwave radiation (4.5–42 μm)	<10% (daily total)	
		Outgoing shortwave radiation (0.3–2.8 μm)	<5% (daily total)	
	CS650, Campbell Scientific	Soil moisture	±3%	–0.02, –0.04
		Soil temperature	±0.1°C	–0.02, –0.04
	HFP01, Huskeflux	Soil heat flux	±2%	–0.05
	SI-111-SS, Apogee	Turf surface temperature	±0.2°C (–10°C to +65°C)	1.5
Reference	05103, Campbell Scientific	Wind speed	±0.3 m/s	2
	03301, Campbell Scientific	Wind direction	±3%	2
	HMP155, Campbell Scientific	Air temperature	±(0.055+0.0057×T_a)	1.1
		Relative humidity	±1%	1.1
	TB4, Campbell Scientific	Rainfall	±2%	2

4.2.4. Bowen ratio-energy balance method

Latent heat flux and sensible heat flux were calculated using the Bowen ratio-energy balance method (Kustas et al., 1996). The Bowen ratio (β, -) is defined as:

$$\beta = \frac{Q_H}{Q_E} \tag{4.1}$$

where Q_E (W/m^2) latent heat flux (positive when water vapour pressure decreases with height) and Q_H (W/m^2) sensible heat flux (positive when air temperature decreases with height). The meanings of the variables used in this section are described in Table 4.2.

On a uniform surface and in the absence of advection, the energy fluxes can be expressed as:

$$R_n = G + Q_E + Q_H \tag{4.2}$$

where R_n (W/m^2) is the net radiation (positive downward), G (W/m^2) the surface soil heat flux (positive when conducted downward).

With Equation (4.1), Equation (4.2) can be rewritten as follows:

$$Q_E = \frac{R_n - G}{1 + \beta} \tag{4.3}$$

$$Q_H = \frac{\beta}{1 + \beta}(R_n - G) \tag{4.4}$$

Over an averaging period (60 min), the empirical relationships between latent heat flux and vertical water vapour pressure gradient, and between sensible heat flux and vertical air temperature gradient can be expressed as:

$$Q_E = \frac{-\rho_a c_p}{\gamma} k_v \frac{de}{dz} \tag{4.5}$$

$$Q_H = -\rho_a c_p k_h \frac{dT_a}{dz} \tag{4.6}$$

Under non-advective conditions, the exchange coefficient for water vapour (k_v, m^2/s) can be assumed to be equal to the exchange coefficient for sensible heat (k_h, m^2/s) such that:

$$\beta = \frac{Q_H}{Q_E} = \gamma \frac{d\,T_a/dz}{de/dz} = \gamma \frac{\Delta T_a}{\Delta e} \tag{4.7}$$

where $\gamma = c_p p/\epsilon L_v$ is the psychometric constant (kPa/°C). c_p is the specific heat of air at constant pressure (1.01 kJ/kg/°C), p the atmospheric pressure (kPa), ϵ (-) the ratio between the molecular weights of water vapour and air, and L_v the latent heat of vaporization (kJ/kg). $\Delta T_a = T_{a,0.6m} - T_{a,1.1m}$ and $\Delta e = e_{0.6m} - e_{1.1m}$ are the air temperature and water vapour pressure differences between the two measurement heights (0.6 and 1.1 m in this study), respectively.

By measuring the air temperature and water vapour pressure gradient, β can be obtained and substituted into Equations (4.3) and (4.4) to calculate latent heat flux and sensible heat flux.

Table 4.2. Symbol, unit and description of the variables used in the Bowen-ratio energy balance method.

Variable	Symbol	Unit	Description
Atmospheric pressure	p	kPa	Pressure caused by the gravitational force of the Earth on the air molecules within the atmosphere.
Bowen ratio	β	-	Ratio of the sensible heat flux density to the latent heat flux density.
Exchange coefficient for sensible heat	k_h	m^2/s	Rate of eddy diffusion for heat.
Exchange coefficient for water vapour	k_v	m^2/s	Rate of eddy diffusion for water vapour.
Latent heat flux density	Q_E	W/m^2	Heat release or absorbed by a system when it changes bewtween soild, liquid and gas states per unit area and time.
Latent heat of vapourisation of water	L_v	kJ/kg	Energy required to vapourise one mass unit of water.
Net radiation	R_n	W/m^2	The difference between all-wave incoming and outgoing radiant flux per unit area and time.
Psychometric constant	γ	kPa/°C	The ratio of specific heat of moist air at constant pressure to latent heat of vaporization of water.
Sensible heat flux density	Q_H	W/m^2	The heat energy able to be sensed that is released or absorbed by a system per unit area and time.
Specific heat of air	c_p	kJ/kg°C	Energy required to increase one mass unit of dry air by one degree Celcius at constant pressure.
Surface soil heat flux	G	W/m^2	Heat conducted into or out of the soil per unit area and time.

There are three inherent problems in the Bowen ratio-energy balance method (Perez et al., 1999). First, the estimates of latent heat flux and sensible heat flux are totally dependent upon the measurements of air temperature and water vapour pressure gradients (Equations 4.3, 4.4 and 4.7). The measurements can give incorrect signs to the fluxes when the fluxes change their signs during early morning and late afternoon, as well as during irrigation and precipitation. Second, the method fails when β is close to –1 because the denominators of Equations (4.3) and (4.4) will approach 0 and the calculated latent heat flux and sensible heat flux will lose their physical meanings. This situation usually happens during sunrise and sunset and precipitation when the direction of the air temperature gradient shifts to the opposite to that of the water vapour pressure gradient. Third, the Bowen ratio-

energy balance method gives inaccurate results when the air temperature and water vapour pressure differences are in the same order of magnitude as the resolution limits of the sensors. We followed the criteria described in Perez et al. (1999) to discard the latent heat flux and sensible heat flux data with any of the three problems.

4.2.4. Study period

The irrigation began on 2021-01-20. We used the data from the second to the sixth week (2021-01-27 to 2021-03-02, study period) for analysis because there were missing data in the first week (2021-01-20 to 2021-01-26). The mean air temperature over the study period was 19.4 °C, and there were eight days with a daily maximum air temperature ≥30.0 °C (Fig. 4.3a). The total rainfall in the study period was 58.8 mm. The mean relative humidity and wind speed over the study period were 63% and 0.49 m/s, respectively (Fig. 4.3b).

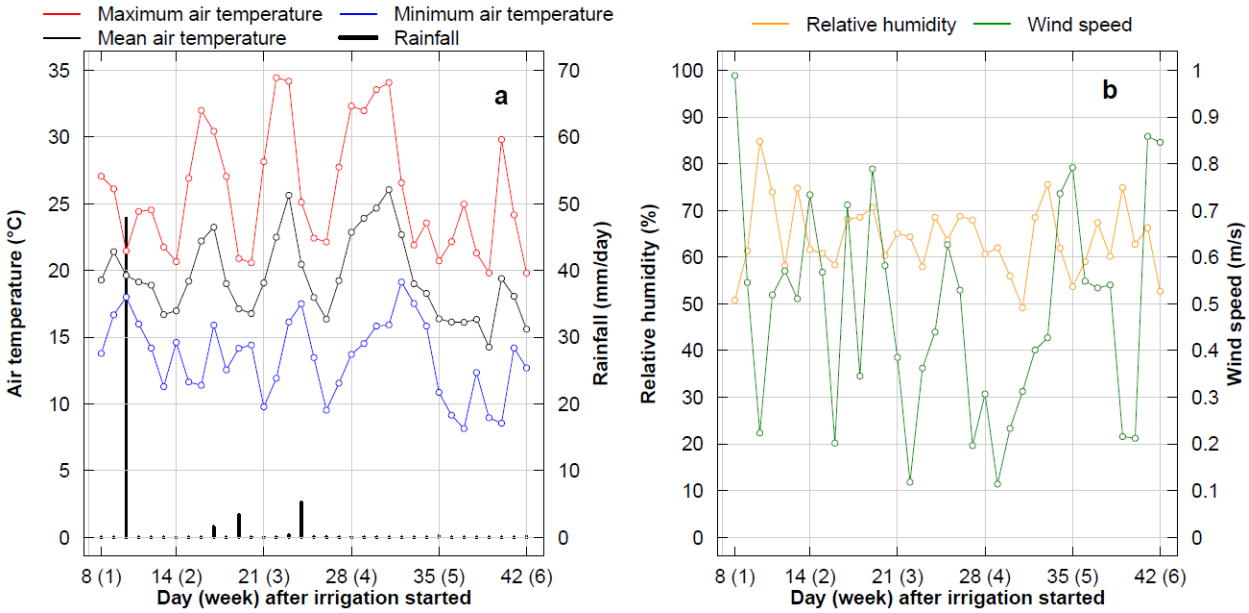

Fig. 4.3. Variations of (a) air temperature and rainfall, and (b) relative humidity and wind speed at the reference climate station in the study period. The study period is from the 8th to 42nd day (2nd to 6th week) after starting irrigation. The first seven days after irrigation started were excluded from the analysis because of incomplete data.

4.2.5. Definitions for daytime and night-time periods

Apart from measuring the impacts of irrigation on a daily mean basis, it is necessary to measure the daytime and night-time impacts separately because the impacts are controlled by different processes (Fig. 4.1). There are no universal definitions for daytime and night-time periods. Different

studies have different definitions according to their measurement periods, geographical locations and study purposes (Cheung and Jim, 2019c). This study observed sharp changes in various temperature metrics around 06:00 and 17:00 local time (Fig. 4.4a−d), which coincided with sharp changes in incoming shortwave radiation (Fig. 4.4e). The sharp changes in temperatures and incoming shortwave radiation were plausibly due to the shading from the trees next to the plots. It is necessary to avoid the above-mentioned periods in the daytime and night-time analyses. Considering the contrasting impacts of irrigation between the day and the night, as well as the potential shading effect from the trees, the daytime and night-time periods were defined as 10:00–15:59 and 21:00–04:59 local time, respectively.

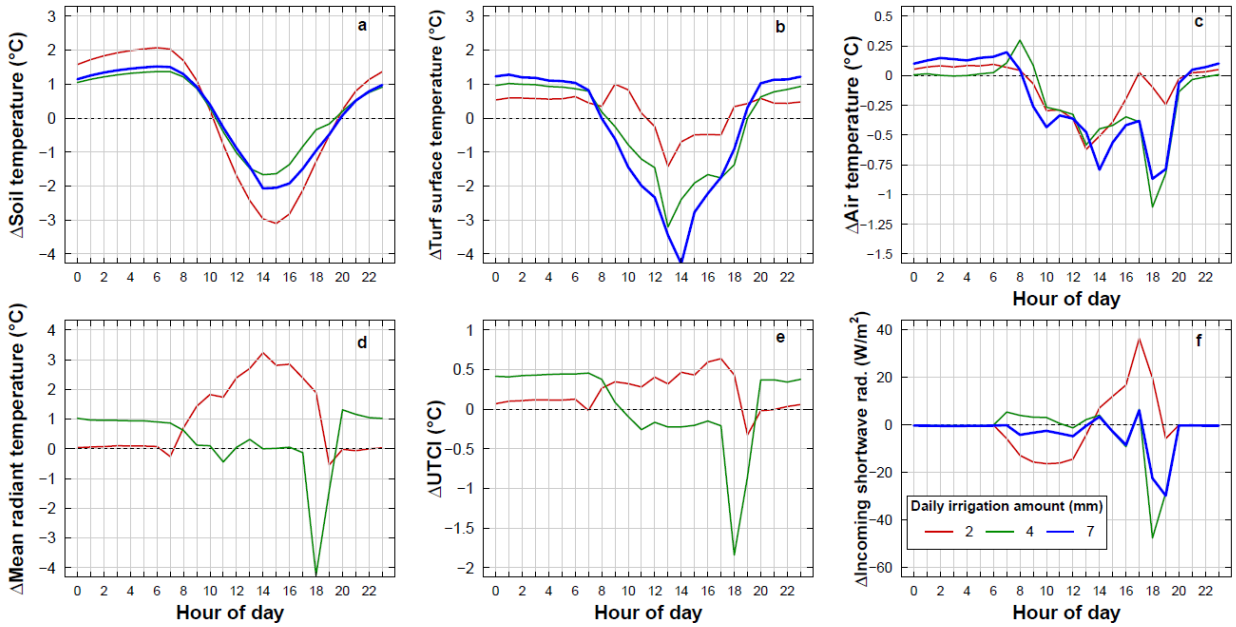

Fig. 4.4. Diurnal variations of the hourly mean differences between the irrigated plot and the unirrigated plot (Δ = irrigated – unirrigated) in (a) soil temperature, (b) turf surface temperature, (c) air temperature, (d) mean radiant temperature, (e) UTCI and (f) incoming shortwave radiation. Tree shade potentially impacted the incoming shortwave radiation received at the four plots at 06:00 and 17:00, causing sharp changes in various temperature metrics. Therefore, the daytime and night-time periods are defined as 10:00–16:00 and 21:00–05:00 local time, respectively. The mean radiant temperature and UTCI data in the 7-mm plot were missing due to instrument failure.

4.3. Results

4.3.1. Initial responses of soil moisture to irrigation

The initial soil moisture contents of the four plots ranged from 10% to 22% by volume (Fig. 4.5). Before irrigation began, the soil moisture contents of the four plots decreased gradually at a similar

rate. After four days of irrigation, the soil moisture contents in the 4-mm and 7-mm plots increased notably from approximately 20% to 35%, whereas the 2-mm plot remained rather stable at approximately 14%. The wetting-drying amplitudes were about 10% and 7% per annum for the 7 mm and 4 mm plots, respectively. In contrast, the 2 mm plot had considerably subdued fluctuations circumscribed at around 2%. The patterns indicated that more irrigation could bring more drawdown in the daily soil-moisture cycles. Meanwhile, the decreasing trend in soil moisture content in the unirrigated plot continued.

The 7.2-mm rainfall event on Day 6 and the 47.8-mm event on Day 9 promptly eliminated the differences in soil moisture content between the irrigated plots. The first low rainfall wetted the soil in the 2 mm plot notably more than the 0-mm, 4-mm and then 7-mm plots. The second high rainfall event wetted the 0-mm plot considerably, followed by the 2 mm and then 4 mm and 7 mm plots. From Day 10, the differences in soil moisture content between the unirrigated and irrigated plots enlarged quickly as the soils in the unirrigated plot dried up. Meanwhile, the diurnal soil moisture amplitudes of the irrigated plots stayed at ranges similar to the pre-rainfall period.

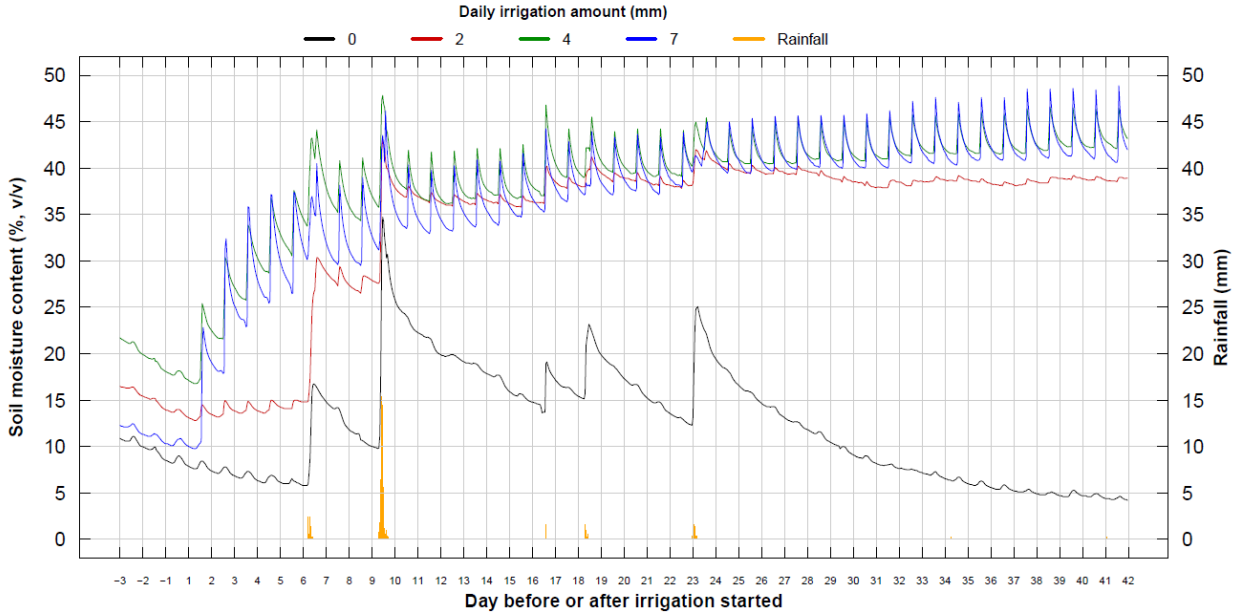

Fig. 4.5. Hourly variations in soil moisture content and rainfall from three days before irrigation started to 42 days after irrigation had begun in the four plots. The period between Day 8 and 42 was the study period. Before irrigation started, soil moisture content in all four plots decreased gradually at a similar rate. After irrigation started, the soil moisture content increased sharply in the 4-mm and 7-mm plots, whereas the soil moisture content in the 2-mm plot was maintained at the pre-irrigation level while the unirrigated plot continued the decreasing trend. The rainfall events on Days 6 and 9 increased the soil moisture content to ≥35% in the three irrigated plots and maintained above that level since then. From Day 10, the differences in soil moisture content between the unirrigated and the irrigated plots gradually increased as the soils in the unirrigated plot dried up.

4.3.2. Impacts of irrigation on daily mean soil moisture content, microclimate and soil heat flux

When the daily mean impacts of irrigation is considered, irrigation supplemented by rainfall significantly increased daily mean soil moisture content by >25% (p<0.05, t-test) in all three irrigated plots in the study period (Table 4.3). Irrigation also significantly reduced daily mean turf surface temperature, outgoing longwave radiation, air temperature and outgoing shortwave radiation (p<0.05, t-test) in most irrigated plots, but the reductions were small. Irrigation increased soil temperature, vapour pressure and UTCI by a small amount, and the significance of the impacts depended on irrigation amount. Irrigation significantly reduced soil heat flux in the 2-mm and 4-mm plots. Since the daytime and night-time impacts of irrigation are likely in opposite directions and the effects can be masked when the daily mean impacts are considered (Fig. 4.1), it is necessary to investigate the diurnal variation of the impacts.

Table 4.3. Impacts of irrigation on daily mean soil moisture content, soil heat flux and eight microclimate variables in the study period. The impact of irrigation is calculated as the difference between the irrigated and unirrigated plots (Δ = irrigated – unirrigated).

Variable	Unit	Daily irrigation amount (mm)					
		2		4		7	
		Mean	CI	Mean	CI	Mean	CI
Soil moisture content	%, v/v	**25.0**	22.6 to 27.3	**28.1**	25.6 to 30.7	**26.7**	23.8 to 29.7
Soil temperature	°C	0.2	0.0 to 0.3	**0.2**	0.1 to 0.4	**0.2**	0.1 to 0.3
Land surface temperature	°C	**0.2**	0.1 to 0.3	**–0.2**	–0.3 to –0.1	**–0.3**	–0.4 to –0.2
Outgoing longwave radiation	W/m^2	**–3.4**	–4.3 to –2.5	**–3.7**	–4.6 to –2.8	**–4.5**	–5.8 to –3.3
Air temperature	°C	**–0.1**	–0.1 to –0.1	**–0.2**	–0.2 to –0.2	**–0.2**	–0.2 to –0.1
Vapour pressure	kPa	**0.010**	0.007 to 0.013	0.002	–0.004 to 0.009	0.004	–0.003 to 0.012
Outgoing shortwave radiation	W/m^2	**2.3**	1.7 to 2.8	**–2.0**	–2.4 to –1.6	**–4.1**	–4.8 to –3.4
Soil heat flux	W/m^2	**–1.3**	–1.7 to –1.0	–0.9	–2.0 to 0.2	**–2.6**	–3.3 to –1.8
UTCI	°C	**0.2**	0.2 to 0.2	0.0	0.0 to 0.1	NA^	NA^

^Incomplete data due to sensor failure.

Note: Significant differences are bold (t–test, p<0.05); CI: confidence interval.

4.3.3. Impacts of irrigation on daytime/night-time soil moisture, soil heat flux and microclimate

4.3.3.1. Does irrigation induce daytime cooling effects?

All three levels of daily irrigation induced significant daytime cooling effects (p<0.05, t-test, indicated by open circles) in weekly mean soil temperature (Fig. 4.6a), turf surface temperature (Fig. 4.6b) and air temperature (Fig. 4.6c) for most of the weeks in the study period. The cooling effects in soil temperature, turf surface temperature and air temperature strengthened from Week 2 to Week 6, which coincided with the increasing soil moisture content (Fig. 4.6e). The impact of irrigation on UTCI was mixed (Fig. 4.6d). Although the cooling effects varied greatly from day to day (faint lines in Fig. 4.6), the strengthening cooling trends were consistent for all three irrigated plots and all four temperature metrics. After six weeks of daily 4-mm irrigation, soil temperature, turf surface temperature, air temperature and UTCI were 1.7, 2.3, 0.6 and 0.4°C cooler than the respective unirrigated plot (p<0.05, t-test).

In addition, irrigation significantly reduced outgoing longwave radiation by >6 W/m^2 (p<0.05, t-test) (Fig. 4.6f). Irrigation significantly increased outgoing shortwave radiation (Fig. 4.6g) in the 2-mm plot (p<0.05, t-test), but significantly reduced it in the 4-mm and 7-mm plots (p<0.05, t-test). Irrigation significantly reduced downward soil heat flux in the 2-mm plot (p<0.05, t-test) but significantly increased it in the 4-mm and 7-mm plot (p<0.05, t-test) (Fig. 4.6h). Except for the 2-mm plot, irrigation significantly reduced the vapour pressure by <0.03 kPa for most of the time in the study period (p<0.05, t-test) (Fig. 4.6i). However, this change was smaller than the sensor's accuracy (±0.05 kPa) (Table 4.3).

4.3.3.2. Do daytime cooling effects strengthen with irrigation amount?

The daytime cooling effects in soil temperature (Fig. 4.6a), air temperature (Fig. 4.6c) and UTCI (Fig. 4.6d) did not strengthen with increasing daily irrigation amount (p>0.05, ANOVA). In contrast, the cooling effect in turf surface temperature (Fig. 4.6b) strengthened significantly with daily irrigation amount (p<0.05, ANOVA). Daily irrigation amounts had a significant (p<0.05, ANOVA) but small impact on soil moisture content (<5%) (Fig. 4.6e) and vapour pressure deficit (<0.05 kPa) (Fig. 4.6i) in some of the weeks. Increasing daily irrigation amounts had no significant impact on outgoing longwave radiation (p>0.05, ANOVA) (Fig. 4.6f), but it significantly reduced incoming shortwave radiation (p<0.05, ANOVA) (Fig. 4.6g). Although the impacts of daily irrigation amount on soil heat flux were significant (p<0.05, ANOVA), the direction of its impact was unclear because the daily mean soil heat flux of the 7-mm plot was between the 2-mm and the 4-mm ones (Fig. 4.6h).

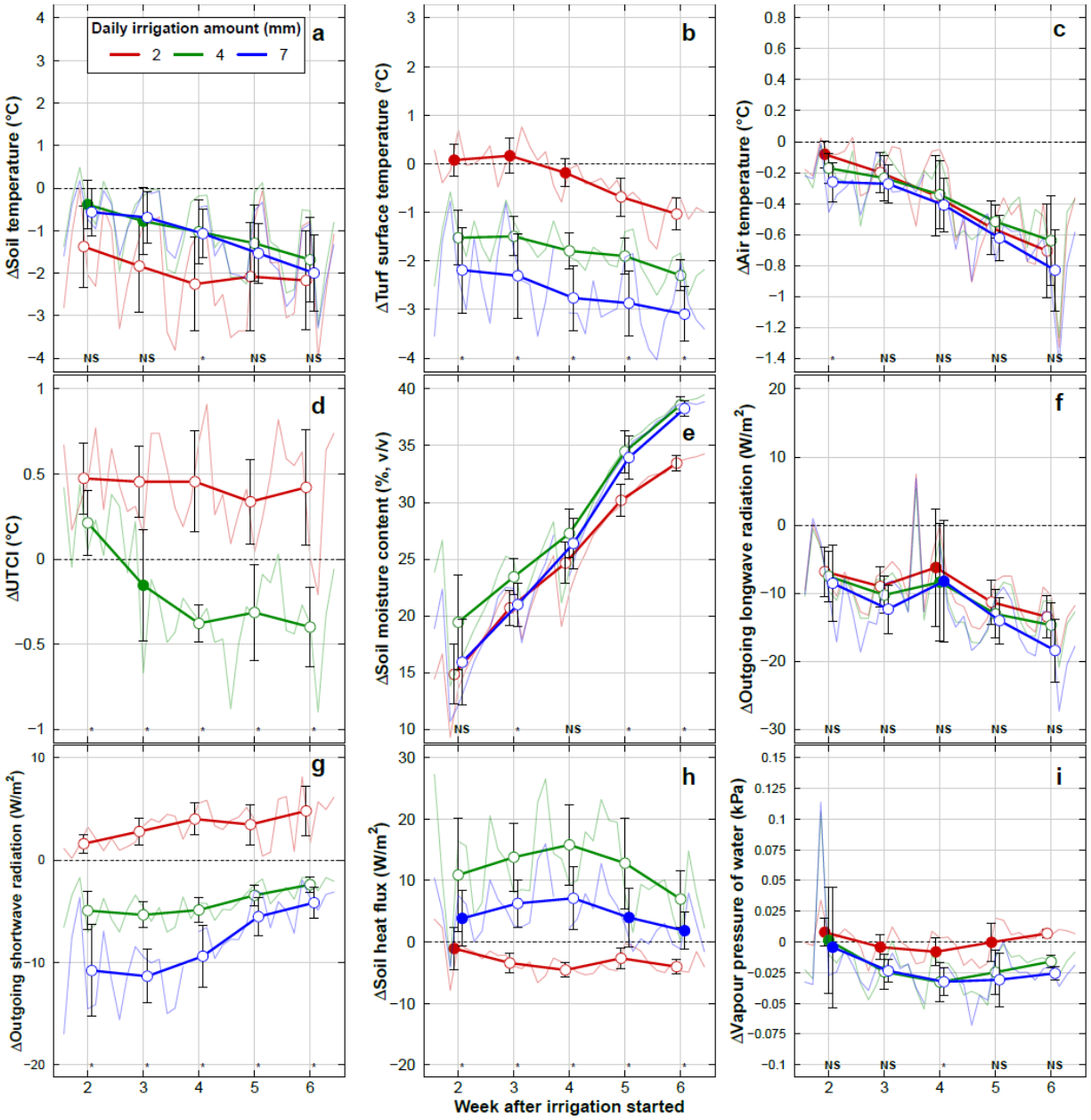

Fig. 4.6. Impacts of irrigation on daytime (10:00–16:00) mean (a) soil temperature, (b) turf surface temperature, (c) air temperature, (d) UTCI, (e) soil moisture content, (f) outgoing longwave radiation, (g) outgoing shortwave radiation (h) soil heat flux and (i) vapour pressure. The impact of irrigation is calculated as the difference between the irrigated and unirrigated plots (Δ = irrigated – unirrigated). The solid lines are the weekly means and the error bars are the 95% confidence intervals. The faint lines are the daily means. Open circles represent significant differences (p<0.05, t-test) in the weekly means between the irrigated and the unirrigated plots and closed circles represent insignificant differences. Significant differences (p<0.05, AONVA) in the weekly means between the three irrigated plots are represented by "*" and insignificant differences by "NS". The UTCI data of the 7-mm plot were missing due to sensor failure.

4.3.3.3. Do daytime cooling effects correlate with soil moisture difference?

The difference in soil moisture content between the irrigated and the unirrigated plots was significantly and negatively correlated with the differences in all four temperature metrics, namely soil temperature, turf surface temperature, air temperature and UTCI (p<0.05, t-test) (Fig. 4.7). In other words, as the difference in soil moisture content increased, the cooling effect became stronger (more negative differences in temperature). In particular, air temperature had the strongest correlation (R=0.7) with soil moisture content.

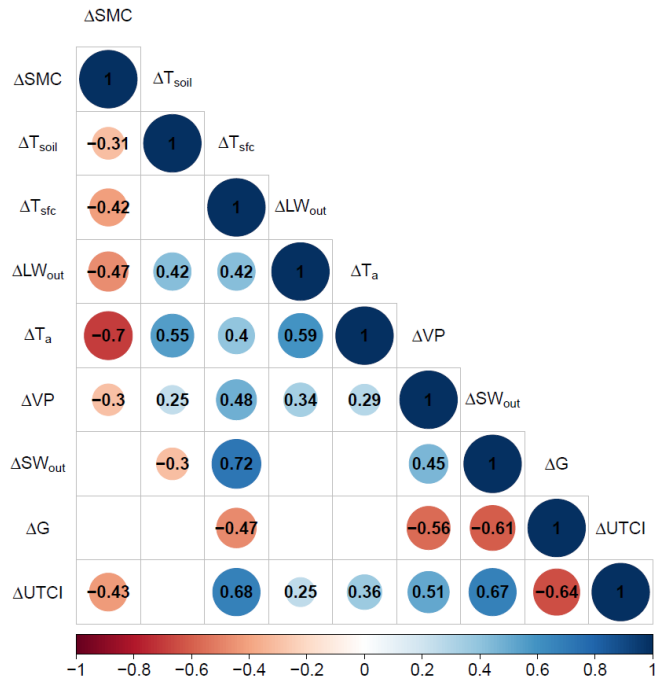

Fig. 4.7. A correlation matrix showing the Pearson's Correlation Coefficients between soil moisture content difference (ΔSMC), soil temperature difference (ΔT_{soil}), turf surface temperature difference (ΔT_{sfc}), outgoing longwave radiation difference (ΔLW_{out}), air temperature difference (ΔT_a), vapour pressure difference (ΔVP), outgoing shortwave radiation difference (ΔSW_{out}), soil heat flux difference (ΔG) and UTCI difference (ΔUTCI). The differences are the daytime (10:00–16:00) mean differences between the irrigated and unirrigated plots (Δ = irrigated – unirrigated). Data from all three irrigated plots are pooled. Only the statistically significant (p<0.05, t-test) correlations are shown.

4.3.3.4. Does irrigation induce night-time warming effects?

All three levels of daily irrigation induced a significant night-time warming effect (p<0.05, t-test) in weekly mean soil temperature (Fig. 4.8a), turf surface temperature (Fig. 4.8b) and UTCI (Fig. 4.8d) for most of the weeks in the study period. The warming effect in air temperature was small and not significant (p>0.05, t-test) (Fig. 4.8c). The warming effects in all four temperature metrics

strengthened from Week 2 to Week 6, which coincided with the increasing differences in soil moisture content between the irrigated and the unirrigated plots (Fig. 4.8e). After six weeks of daily 4-mm irrigation, soil temperature, turf surface temperature, air temperature and UTCI were 1.4, 1.3, 0.1 and 0.5 °C warmer than the respective non-irrigated plot (p<0.05, t-test, except for air temperature). The impacts of irrigation on outgoing longwave (Fig. 4.8f) and shortwave (Fig. 4.8g) radiation were small and not significant (p>0.05, t-test). Irrigation significantly increased upward soil heat flux by >6 W/m^2 in the 4-mm and the 7-mm plot (p<0.05, t-test), whereas the change in the 2-mm plot was not significant (p>0.05, t-test) (Fig. 4.8h). Most of the impacts on vapour pressure (Fig. 4.8i) were still below the accuracy of the sensor (±0.05 kPa) (Table 4.3).

4.3.3.5. Do night-time warming effects strengthen with irrigation amount?

Different daily irrigation amounts had a significant impact (p<0.05, ANOVA) on the night-time warming effects in soil temperature (Fig. 4.8a) and UTCI (Fig. 4.8d). However, the warming effect did not necessarily strengthen with increasing daily irrigation amount. The warming effect in the 2-mm plot was the strongest in soil temperature, contrary to UTCI. Daily irrigation amount had no significant impact (p>0.05, ANOVA) on the warming effects in turf surface temperature (Fig. 4.8b) and air temperature (Fig. 4.8d) for most of the weeks in the study period. It also had no significant impact (p>0.05, ANOVA) on soil moisture content (Fig. 4.8e), outgoing longwave radiation (Fig. 4.8f), outgoing shortwave radiation (Fig. 4.8g) and water vapour pressure (Fig. 4.8i). Different daily irrigation amounts had a significant impact (p<0.05, ANOVA) on night-time soil heat flux (Fig. 4.8h).

4.3.3.6. Do night-time warming effects correlate with night-time soil heat flux?

The difference in night-time soil heat flux between the irrigated and the unirrigated plots was significantly and positively correlated with the warming effects in all four temperature metrics, namely soil temperature, turf surface temperature, air temperature and UTCI (p<0.05, t-test) (Fig. 4.9). The difference in daytime soil heat flux between the irrigated and the unirrigated plots was significantly and negatively correlated with the night-time soil heat flux (p<0.05, t-test). It implied that more heat stored in the soils during the day would lead to more heat released from the soils at night.

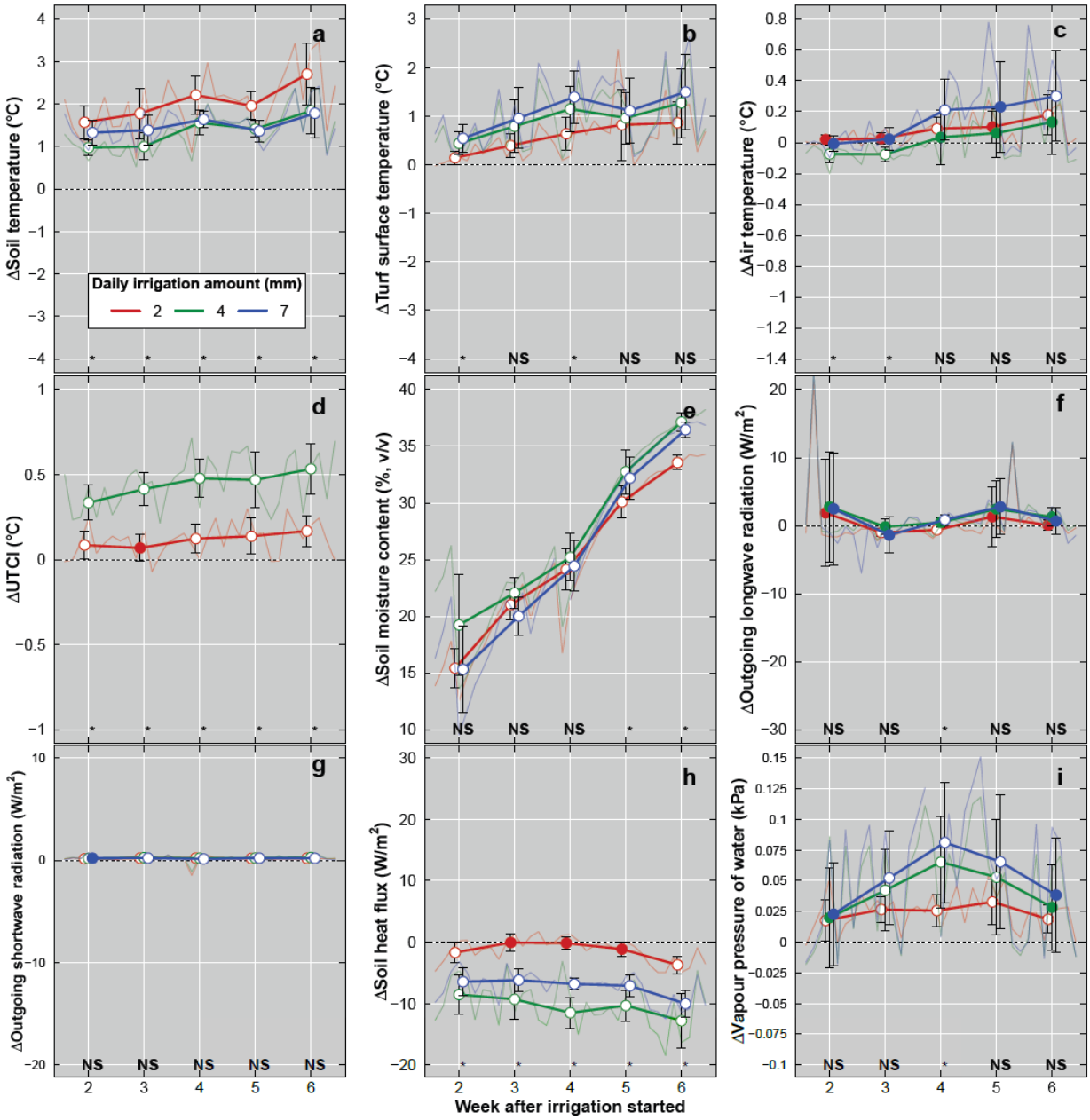

Fig. 4.8. Impacts of irrigation on night-time (21:00–05:00) mean (a) soil temperature, (b) turf surface temperature, (c) air temperature, (d) UTCI, (e) soil moisture content, (f) outgoing longwave radiation, (g) outgoing shortwave radiation (h) soil heat flux and (i) vapour pressure. The impact of irrigation is calculated as the difference between the irrigated and unirrigated plots (Δ = irrigated – unirrigated). The solid lines are the weekly means and the error bars are the 95% confidence intervals. The faint lines are the daily means. Open circles represent significant differences (p<0.05, t-test) in the weekly means between the irrigated and the unirrigated plots and closed circles represent insignificant differences. Significant differences (p<0.05, AONVA) in the weekly means between the three irrigated plots are represented by "*" and insignificant differences by "NS". The UTCI data of the 7-mm plot were missing due to sensor failure.

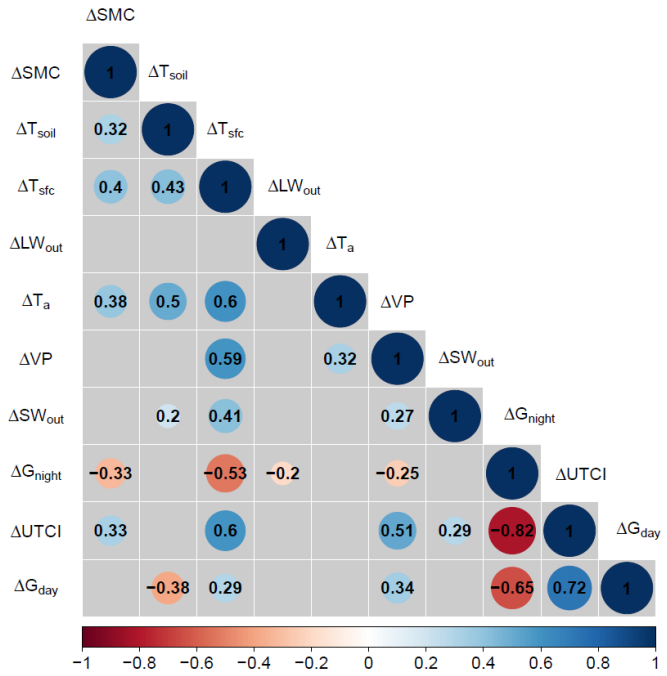

Fig. 4.9. A correlation matrix showing the Pearson's Correlation Coefficients between soil moisture content difference (ΔSMC), soil temperature difference (ΔT_{soil}), turf surface temperature difference (ΔT_{sfc}), outgoing longwave radiation difference (ΔLW_{out}), air temperature difference (ΔT_a), vapour pressure difference (ΔVP), outgoing shortwave radiation difference (ΔSW_{out}), night-time soil heat flux difference (ΔG_{night}), UTCI difference (ΔUTCI) and daytime soil heat flux difference (ΔG_{day}). Except specified, the differences are the night-time (21:00–05:00) mean differences between the irrigated and unirrigated plots (Δ = irrigated – unirrigated). Data from all three irrigated plots are pooled. Only the statistically significant (p<0.05) correlations are shown.

4.3.3.7. Does irrigation shift daytime and night-time latent and sensible heat fluxes?

The daytime latent heat flux of the unirrigated plot was always higher than that of the three irrigated plots (Fig. 4.10). A sharp increase in the latent heat flux was evident in the three irrigated plots after irrigation (13:00−14:00). This coincided with a sharp reduction in sensible heat flux. The sensible heat flux of the unirrigated plot was lower than the irrigated plots for most of the day. However, the differences in daytime latent heat flux and sensible heat flux between the irrigated plots and the unirrigated plot were not significant (p>0.05, Tukey HSD test), except for the latent heat flux between the 2-mm plot and the unirrigated plot. The daytime ratio of sensible heat flux to latent heat flux of the irrigated plots was 0.32, i.e., sensible heat was 32% that of latent heat.

The differences in night-time latent heat flux and sensible heat flux between the unirrigated and irrigated plots were not significant (p>0.05, Tukey HSD test), except that the latent heat flux of the 4-mm plot was significantly higher than the unirrigated plot (Δ=17 W/m^2).

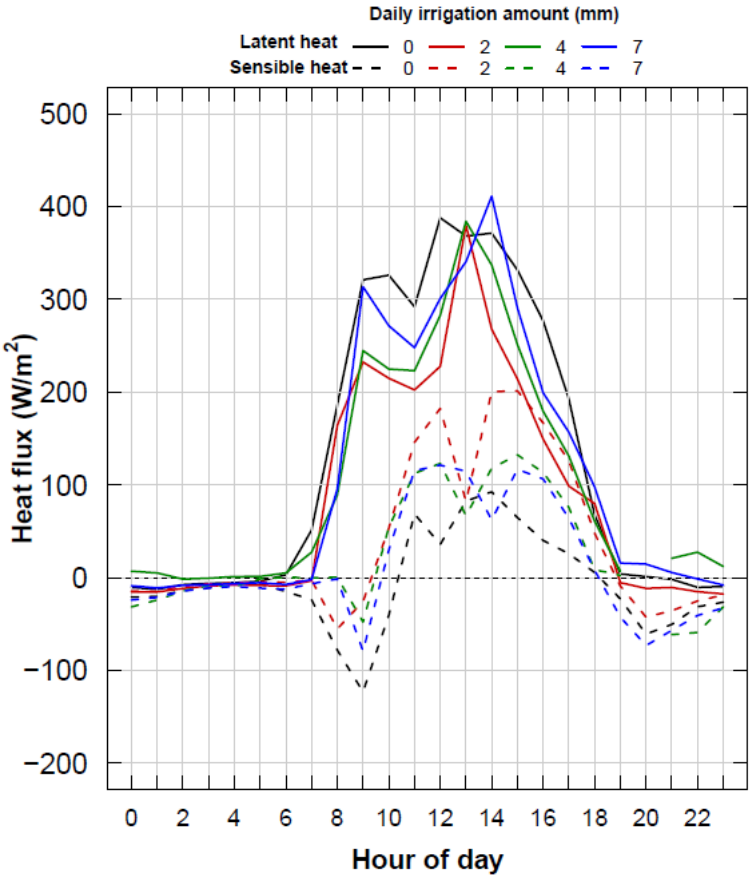

Fig. 4.10. Diurnal variations of the hourly mean latent heat flux and sensible heat flux.

4.4. Discussion

4.4.1. Impacts of irrigation on daytime microclimate

This field study showed that irrigating turf in a simulated backyard environment can significantly reduce daytime soil temperature, turf surface temperature and air temperature, but not UTCI. Modelling studies have predicted that irrigating vegetated surfaces over a large spatial scale could reduce daily mean soil temperature by 4.2°C (Gao et al., 2020), reduce daily mean surface temperature by 3.0°C (Wang et al., 2019) and reduce daily mean air temperature by 2.6°C (Broadbent et al., 2018a). UTCI has been included in some model predictions but was not explicitly reported (Daniel et al., 2018). Irrigation was predicted to reduce the humidex index by 2.3°C at 3 pm (Broadbent et al., 2018a) but the reduction was insufficient to improve thermal comfort because it takes at least a 5°C change in humidex in order to change the thermal comfort by one level on humidex's four-level scale (Masterton and Richardson, 1979). The predicted cooling effects from these modelling studies were all stronger than those measured in our field study. One possible

explanation is that these modelling studies simulated irrigation at a much higher daily amount (10–30 mm) than the 2 to 7 mm applied in our experiment. In addition, it is important to note that the analysis of the modelling studies was conducted at a much larger spatial scale (from city scale to national scale) than our experiment's. The background climate and weather conditions used in their simulations were also different. Therefore, the climate context and the methods of analysis or simulation must be taken into account when interpreting the potential cooling effects of irrigation of measurement or modelling studies.

Most modelling studies predict that the cooling effect of irrigation will strengthen as the daily irrigation amount increases. Broadbent et al. (2018a) predicted that the air temperature reductions from irrigating vegetated surfaces would strengthen from 0.5°C to 2.3°C as the daily irrigation amount increases from 5 mm to 30 mm. Similarly, Wang et al. (2019) predicted that the daily mean air temperature reductions from irrigating vegetated surfaces would strengthen from 0.5°C to 1.9°C as the daily irrigation amount increases from 4 mm to 13 mm. In our experiment, the relationship between the daily irrigation amount and cooling effect could not be directly measured because the differences in soil moisture contents of the three irrigated plots were small (<5%) throughout the study period, as a result of the 47.8-mm of rain on Day 9 which eliminated the difference in soil moisture content between the irrigated plots (Fig. 4.5). This event pushed all soil moisture contents to a high level, and reduced the irrigation treatment differences on soil moisture content (Fig. 4.6e).

Nevertheless, it is possible to infer the impacts of daily irrigation amount on the cooling effect because the cooling effect is strongly correlated with the difference in soil moisture content between the irrigated and the unirrigated plots (section 3.3.3). Based on the response of soil moisture content to irrigation before the rainfall event on Day 6, it is possible to infer that the soil moisture content in the 4-mm and 7-mm plots would have reached 35% on Day 10 without any rainfall (Fig. 4.5). Even if we increase the daily irrigation amount to 30 mm, the resulting soil moisture content trend will be the same as that of 4 mm after Day 10, meaning that the resulting cooling effect will also be the same. The almost linear increase in cooling benefit from increased irrigation up to 13 mm (Wang et al., 2019) or 30 mm (Broadbent et al., 2018a) is highly unlikely as soil moisture contents will reach saturation at moderate rates of irrigation in all but the sandiest of soils. We expect that the cooling effect will only strengthen when the daily irrigation amount increases at the lower range, possibly from 2 to 4 mm, because irrigating 2 mm daily was insufficient to bring soil moisture content up to 35% based on its trend before Day 6 (Fig. 4.5).

We observed a strengthening cooling effect from Week 2 to 6 (Fig. 4.6). This could be driven by either a further cooling of the irrigated plots or warming of the unirrigated plot over time. Since the

soil moisture contents of the irrigated plots had already reached the field capacity in Week 2 (Fig. 4.5), further cooling was impossible. Thus, the strengthening cooling effects were relative rather than absolute, driven by a warming of the unirrigated plot because the soils gradually dried up (Fig. 4.5) in the absence of major rainfall events after Week 1 (Fig. 4.3). The soil moisture contents of the irrigated plots were kept above 35% throughout the study period. It remains unknown whether a lower soil moisture content, e.g., 25%, can induce a similarly strong cooling effect as 35%. Future work should address this important question because the daily irrigation amount can be reduced to <2 mm if a 25% soil moisture content is sufficient to achieve the highest possible evapotranspiration and cooling effect. The daytime part of the theoretical framework (Fig. 4.1) is generally accurate, except that irrigation cannot reduce human thermal stress.

The results implied that the irrigated soils attained the field capacity early in the experiment and were maintained at field capacity by continual irrigation. The cyclical daily drawdown could be attributed mainly to evaporation plus some gravitational drainage of water held in larger pores. Closer to the field capacity of circa 35% soil moisture content which is the readily available water (RAW) zone, the adequate water supply can satisfy the evaporative needs of the turf to sustain the cooling effect at an optimal level. If soil moisture drops well below the field capacity point, entering the less available water (LAW) zone, the turfgrass could begin to experience moisture stress. In the circumstances, the turf cooling effect can be correspondingly trimmed. In the interest of water conservation, it will be helpful to find the interface between RAW and LAW, and adopt an irrigation rate that can keep the soil moisture content above it most of the time.

There were inconsistent results in UTCI (Fig. 4.6d), outgoing shortwave radiation (Fig. 4.6g) and soil heat flux (Fig. 4.6h) in the three irrigated plots, i.e., these variables increased in some of the irrigated plots and decreased in others increased these variables while other reduced them. There were probably inconsistencies in UTCI and outgoing shortwave radiation data because the changes were small in comparison to the accuracy of the sensors (Table 4.1). In particular, UTCI was calculated from air temperature, relative humidity, wind speed and mean radiant temperature; therefore, the uncertainties in the measurements of each of these variables have accumulated. The inconsistency in soil heat flux can be attributed to the high spatial variability of soil thermal properties (Usowicz et al., 1996). It is recommended that more soil heat flux plates should be installed to minimise the impacts of spatial variability on soil heat flux measurement (Sauer and Horton, 2005).

4.4.2. Impacts of irrigation on night-time microclimate

Irrigation induced a small night-time warming effect due to increased soil heat storage during the day and the subsequent release at night. The 4-mm daily irrigation increased night-time mean UTCI by 0.5°C, which is unlikely to cause any change in thermal stress because it takes at least a 6°C change in UTCI in order to shift thermal stress by one level on UTCI's 10-level thermal stress classification scale (Bröde et al., 2012). Despite the night-time warming, irrigation reduced daily mean air temperature. The impacts of irrigation on night-time temperatures are not as clear as on daytime (Cheung et al., 2022b). Some modelling studies reported a night-time cooling effect (Gao et al., 2020; Sorooshian et al., 2011), while others reported a night-time warming effect (Kanamaru and Kanamitsu, 2008; Vahmani and Ban-Weiss, 2016). Kanamaru and Kanamitsu (2008) predicted that irrigation in the California Central Valley, USA, will increase night-time minimal air temperature by 2.1°C, but irrigation has no impact on daily mean air temperature. They attributed night-time warming to the increased thermal conductivity in wet soil. Vahamani and Ban-Weiss (2016) predicted irrigation in Los Angeles, USA, will increase night-time minimum air temperature by 2.1°C and daily mean air temperature by 0.9°C. Similarly, they attributed the warming to increased heat flux into the soil. In an experimental study in Nebraska, USA, irrigating maize reduced night-time minimum air temperature by approximately 0.5°C whereas irrigating soybean had mixed impacts on it (Chen et al., 2018). Vegetation type is likely to influence the impacts of irrigation on daytime and night-time microclimate but few studies have directly compared the responses of different types of vegetation to irrigation.

4.4.3. Impacts of irrigation on latent and sensible heat fluxes

The daytime latent heat flux of the irrigated plots was not significantly different from the unirrigated plot, except for the 2-mm plot. This finding was somewhat inconsistent with the cooling effects observed in the irrigated plots. The Bowen ratio-energy balance method has been successfully used to monitor the latent heat flux and sensible heat flux of contrasting landscapes (Cellier and Olioso, 1993) or a single landscape (Todd et al., 2000). Since the microclimatic differences between the irrigated and the unirrigated plots were somewhat small, the differences in latent heat flux and sensible heat flux were likely to be small too. In fact, the daytime and night-time differences in latent heat flux and sensible heat flux between the irrigated and the unirrigated plots were mostly not significant. As the measurement error of the instruments can accumulate, propagate and enlarge through the calculation procedures, the Bowen ratio-energy balance method may not be accurate

enough to differentiate the small differences in heat fluxes between the sites in this experiment. However, this method could capture the sharp increase in latent heat flux and the concurrent sharp reduction in sensible heat flux in a short period after irrigation (Fig. 4.10).

4.4.4. Irrigation as an urban cooling strategy

Rainwater collection and grey-water recycling systems have become more readily available as part of water-sensitive urban design in old and new residential development in Australia and other parts of the world (Cook et al., 2018). They can provide a sustainable water source to support active irrigation for urban cooling in private green spaces. Under the simulated backyard conditions in this field study, irrigation reduces daytime air temperature to a measurable extent. Since the frequency with which outdoor spaces are used or visited depends upon the microclimate of that space (Cheung and Jim, 2018a; Lin et al., 2013), daytime irrigation can encourage the use of backyards. In principle, irrigation can also increase the evapotranspiration and cooling effect of other vegetated areas such as lawns in public green spaces and treed street canyons. Irrigation has the potential to cool these urban environments and encourage their use. In terms of daytime mean air temperature, the 0.6°C reduction in from turf irrigation (cf. section 3.3.1) is a significant reduction for Melbourne compared to other cooling strategies such as tree planting. Daytime air temperature in a treed street canyon in Melbourne was only 0.2°C lower than an open street canyon (Coutts et al., 2016). In another observational study, the daytime mean air temperature directly below a tree was 0.7–1.5°C lower than that without tree shade (Sanusi et al., 2017). However, it is difficult to predict the cooling magnitude of irrigating other vegetation in public green spaces and street canyons because the cooling magnitude is dependent upon plant phenology such as microclimatic conditions (Cheung et al., 2022b), height and leaf area index (Chen et al., 2018), wind speed (Lam et al., 2020) and soil types (Kanamaru and Kanamitsu, 2008). More studies are needed to assess the cooling potentials of irrigation in different urban environments with different vegetation types.

Although irrigation significantly reduced UTCI by 0.4°C in the 4-mm plot, the reduction was marginal in terms of thermal stress, because it takes a 6°C reduction to reduce heat stress by one level on UTCI's 10-level thermal stress classification scale (Bröde et al., 2012). Mean radiant temperature and incoming shortwave radiation are usually the most important climate variables influencing UTCI in the outdoor environment (Krüger et al., 2014). Irrigation has minimal impacts on UTCI because our experiment showed that it cannot reduce mean radiant temperature and incoming shortwave radiation (Fig. 4). Tree shade remains critically important for improving outdoor thermal comfort,

particularly for trees with a high plant area index (de Abreu-Harbich et al., 2015). Urban trees may lose up to half of their leaves during heatwaves, thus undermining their cooling effects (Sanusi and Livesley, 2020). The foliage loss is likely due to high air temperature and aggravated by low soil moisture content (Tyree et al., 1993). Although irrigation cannot directly reduce incoming shortwave radiation, it may help alleviate water stress in urban trees and increase their foliage density. More research is needed to examine the interaction between irrigation and the cooling effects of trees.

Identifying the optimal daily irrigation amount that maximises the cooling effect is one of the key questions regarding the use of irrigation for urban cooling. As mentioned in section 4.4.1, when the soil is at field capacity, evapotranspiration and the associated cooling effect will reach their maximum level. Further increase in daily irrigation will not strengthen the cooling effect because evapotranspiration will be limited by atmospheric demand but not soil moisture availability. For cities with a warm and dry climate and assuming that the soil moisture content is at field capacity, the optimal daily irrigation amount that maximises the cooling effect will be the amount that fully compensates the evapotranspiration extraction in the previous day. Evapotranspiration rate can be estimated using the FAO Penman-Monteith equation with the measurements of several climate variables (Allen et al., 1998). The maximum daily effect from turf irrigation in Melbourne is approximately 0.2°C (Table 4.3), whereas daytime mean cooling may be up to 0.8°C (Fig. 4.6c). These irrigation cooling potentials are likely to increase if the climate becomes warmer and drier in the future. Since evapotranspiration is highly dependent on background climate conditions (Seneviratne et al., 2010), the results of this study are only representative of Melbourne and regions with similar summer climate conditions. A systematic review suggested that the magnitude of irrigation cooling effect is positively correlated with mean air temperature and negatively correlated with rainfall (Cheung et al., 2021), meaning that irrigation will induce a stronger cooling effect in warmer and drier regions. The optimal daily irrigation amount is likely to vary with background climate conditions but maintaining soil moisture content at field capacity remains the key to maximise irrigation cooling effect while minimising water consumption.

4.4.5. Suggestions for future studies

From a broader perspective, more experimental and observational studies are required to gather empirical data about the microclimate impacts of irrigating vegetation because much of the current understanding comes from modelling studies (Cheung et al., 2022b). The empirical data can serve two major purposes. First, they can provide a quick and realistic assessment of the potential

cooling effect from irrigation for a specific location. Since background climate can strongly influence the strength of irrigation cooling effect (Cheung et al., 2021; Thiery et al., 2017), the findings from this study are only applicable to regions with a similar climate to Melbourne. Second, the empirical data is important for validating and improving mechanistic models. As we have mentioned in section 4.4.1, some of the model predictions for irrigation cooling effect are not in line with our measurements. Comprehensive microclimate and soil moisture and thermal data are required to identify the specific processes and parameters that need to be improved in urban climate models.

From the perspective of using irrigation to cool green spaces, more studies are required to understand the impacts of vegetation response from irrigation, irrigation time of day and daily irrigation amount on the strength of the cooling effect. Since irrigation may promote the growth of vegetation, it may create a synergistic cooling effect with the vegetation from the extra shading and increased transpiration due to the increase in leaf area index. The interaction between irrigation and plant growth is poorly represented in computer models (Ozdogan et al., 2010) and has rarely been examined in empirical studies. Irrigation time of day can directly impact the cooling benefits experienced by the green space users because the cooling effect will be the strongest immediately after irrigation (Fig. 4.4). More studies are needed to examine how irrigation time of day changes the daytime mean and instantaneous cooling effects of irrigation. In this study, we estimate that the daytime mean cooling effect in Melbourne can strengthen as daily irrigation amount increases from 2 to 4 mm. However, this range is likely to vary between climate regions and seasons. Climate-specific studies are required to provide guidance for optimising irrigation amount in different regions.

4.5. Conclusions

This study measured the impacts of turf irrigation on daytime and night-time microclimate and surface energy balance in a backyard environment during summer in Melbourne. Under the warm summer climatic conditions of Melbourne and in a backyard environment, turf irrigation (> 2mm/day) can induce a strong daytime cooling effect in soil temperature, turf surface temperature and air temperature, but it cannot significantly reduce daytime human thermal stress (Hypothesis (i) is partially accepted). The increase in daily irrigation amounts from 2, 4 to 7 mm did not induce a stronger cooling effect because a large rainfall event eliminated the differences in soil moisture content between these three treatments (Hypothesis (ii) could not be tested properly). The strength of the daytime cooling effect is highly correlated with the difference in soil moisture content between the irrigated and the unirrigated spaces (Hypothesis (iii) is accepted).

Turf irrigation (>2 mm/day) can induce a weak night-time warming effect in soil temperature and turf surface temperature, but the impacts on night-time air temperature and human thermal stress were minimal (Hypothesis (iv) is partially accepted). The increase in daily irrigation amounts did not have an impact on night-time warming effect for the same above-mentioned reason (Hypothsis (v) could not be tested properly). The difference in night-time soil heat flux between the irrigated and the unirrigated plots was significantly and positively correlated with the warming effects (Hypothsis (vi) is accepted). There were no significant differences in daytime and nigh-time latent and sensible heat fluxes between the irrigated and unirrigated plots (Hypothesis (vii) is partially accepted).

Chapter 5 – Short and frequent daytime irrigation increases the cooling benefits of urban green space irrigation without using more water

A version of this chapter was submitted to Landscape and Urban Planning on 16 November 2023. It is under review at the time of thesis submission.

Abstract

The increasing heat stress in cities due to climate change and urbanisation can prevent people from using urban green spaces. Irrigating vegetation is a promising strategy to cool urban green spaces in summer. Irrigation scheduling, such as daytime vs night-time irrigation and the frequency of irrigation in a day, can influence the cooling benefit of irrigation. This study aimed to investigate whether irrigation scheduling can be optimised to increase the cooling benefit and determine how the cooling benefit changes with weather conditions. A field experiment with twelve identical turfgrass plots (three replicates × four irrigation treatments) was set up to measure the afternoon cooling benefits of irrigation. The four treatments included: unirrigated (U0), 4 mm irrigated at 01:00 am (N1), 4 mm irrigated at 13:00 pm (D1), and 1 mm irrigated at 12:00, 13:24, 14:00 and 15:00 pm (D4). The three irrigated treatments (N1, D1 and D4) received the same amount of water (4 mm d^{-1}). The cooling benefit was defined as the air temperature difference measured at 1.1 m above the turfgrass between the irrigated and unirrigated treatments. The afternoon (12:00–15:59) mean cooling benefit of D4 –0.93°C which was significantly stronger than the air temperature cooling benefit of N1 (–0.66°C) and D1 (–0.51°C). Interestingly, there was no significant difference in the cooling benefit of irrigating through one event at night (N1) or by day (D1). Regardless of irrigation scheduling, the afternoon mean cooling benefits of irrigation were greater for days when background air temperature, vapour pressure deficit and incoming shortwave radiation were higher The findings suggested that irrigation scheduling can be optimised to increase the cooling benefit of urban green space irrigation without increasing overall water use.

5.1. Introduction

Urban green spaces are an important part of a city because they offer a number of ecosystem services to urban dwellers such as noise pollution reduction (Koprowska et al., 2018), air purification (Wu and Chen, 2023) and human health benefits (Lee and Maheswaran, 2011). The perceived general health (Maas et al., 2006b) and mental health (van den Berg et al., 2015) of urban residents are positively associated with the proximity of urban green spaces to their homes. Good proximity of urban green spaces encourages people to engage in physical and social activities and these activities are related to better physiological health and well-being (Markevych et al., 2017). Providing a safe space for physical and social activities is increasingly being recognised as one of the most important roles of urban green spaces (Lachowycz and Jones, 2013).

Nevertheless, the presence and good proximity of urban green spaces does not necessarily equate to the use of those urban green spaces by local residents. The use of urban green space is highly dependent on the quality of the space (Giles-Corti et al., 2005). Thermal comfort is an important aspect of urban green space quality. Urban green spaces with dry soil (Spronken-Smith and Oke, 1998) or sparse and unhealthy vegetation (Shashua-Bar and Hoffman, 2000; Speak et al., 2013) can have a high air temperature. High air temperature can reduce people's willingness to use urban green spaces (Cheung and Jim, 2018a), thereby undermining the health benefits that urban green spaces can deliver. As summer air temperature is expected to increase in many parts of the world due to climate change (Matzarakis and Amelung, 2008), cooling strategies are needed for urban green spaces to maintain their functionality and high use by local residents.

Irrigating vegetation has been proposed as a sustainable and effective cooling strategy to reduce air temperatures in urban green spaces and other parts of a city (Coutts et al., 2013; Livesley et al., 2021). Irrigation can be a sustainable cooling strategy when non-potable water is used for irrigating urban vegetation. Non-potable water can be collected and retained in the city through stormwater harvesting and wastewater treatment (Wong, 2006). The effectiveness of irrigating vegetation as an urban cooling strategy has been investigated in some modelling studies (Gao et al., 2020; Wang et al., 2019). Gao et al. (2020) used the Weather Research and Foresting model to predict that irrigating all ground surfaces in Metropolitan Sydney, Australia during a heatwave would reduce daily mean air temperature by approximately 0.5°C. Wang et al. (2019) used the Weather Research and Forecasting model to predict that irrigating all vegetated surfaces in the urban areas of the contiguous US in summer would reduce daily mean air temperature by 1.8°C. There is also some empirical evidence that the irrigating vegetation in urban green spaces can reduce air temperature (Cheung et al., 2022a;

Lam et al., 2020). Such cooling effects of irrigating vegetation are induced by an increase in latent heat flux from increased evapotranspiration (Chen et al., 2018).

Since urban green spaces are frequently used in the afternoon, it is important to investigate whether optimising irrigation scheduling can increase evapotranspiration and strengthen the cooling effect in the afternoon. Daytime and night-time are two contrasting irrigation schedules that can be considered. When irrigation is used solely to maintain plant health, daytime irrigation is avoided because evaporation occurs more quickly during the day (Burt et al., 2005) and this does not directly improve plant growth. However, if irrigation was to be used primarily to cool urban green spaces, then daytime irrigation may be desirable because evaporation occurs more quickly during the day, which can potentially strengthen the cooling effect during and immediately after irrigation (Chen et al., 2018). Broadbent et al. (2018a) suggested that irrigation scheduling could be optimised to potentially strengthen the cooling effects but using the same amount of irrigation water.

Weather conditions can have a strong influence on the cooling effects that result from irrigating urban green spaces. Studies have reported a stronger cooling effect of irrigation during a heatwave than during non-heatwave conditions, again due to the higher rates of evapotranspiration (Gao et al., 2020; Lam et al., 2020). When soil water availability is not limiting, the rate of evapotranspiration from a turfed soil surface is dependent on the background air temperature, vapour pressure deficit, wind speed and solar radiation (Allen et al., 1998). High air temperature and solar radiation provide more energy for water to be evaporated while high vapour pressure deficit and wind speed reduce the resistance for that water vapour to diffuse from the evaporating surface (Burt et al., 2005). Although it is clear that the cooling effect from irrigation is stronger in warmer seasons (Wang et al., 2019; Yang and Wang, 2015), little is known about the impacts of different weather conditions on the cooling effects from irrigation within a summer season. It is important to understand how different weather conditions can make irrigating urban green spaces a more effective, or less effective, cooling strategy to inform irrigation management.

In this study, we used a replicated field experiment to measure the impacts of irrigation scheduling and weather conditions on the afternoon (12:00–15:59) mean cooling effect of irrigating a small turfed green space. The experiment consisted of four treatments: unirrigated (U0), 4 mm irrigated at 01:00 am (N1), 4 mm irrigated at 13:00 pm (D1), and 1 mm irrigated at 12:00, 13:24, 14:00 and 15:00 pm (D4). The three irrigation treatments were irrigated at different times of the day, but they received the same daily total irrigation amount. We defined the cooling effects of irrigation as the difference between the irrigated and unirrigated treatments (Δ = irrigated – unirrigated). We used air temperature,

turf surface temperature, mean radiant temperature and universal thermal climate index (UTCI) to quantify the cooling effects. We tested the following three hypotheses:

(1) all three irrigation treatments would induce significant afternoon (12:00–15:59) mean cooling effects;

(2) the strongest afternoon (12:00–15:59) mean cooling effect would be irrigating four times in the afternoon (D4), and the least significant would be irrigating once at night (N1);

(3) the afternoon (12:00–15:59) mean cooling effects of irrigating turf would be significantly and positively associated with background air temperature, vapour pressure deficit, wind speed and incoming shortwave radiation.

This is study is unique because it directly measures the cooling effect of irrigating turfgrass in a replicated experiment, which provides empirical evidence to help optimise irrigation scheduling as a strategy to cool urban green spaces and the urban landscape more broadly.

5.2. Methods and materials

5.2.1. Study area and climate

This study was conducted at the Burnley Campus of the University of Melbourne, Australia. The elevation of the study area was 13 m above mean sea level. This area is classified as Local Climate Zone B (scattered trees) (Demuzere et al., 2022) under the local climate zone classification system (Stewart and Oke, 2012). Melbourne (–37.8, 145.0) has a temperate oceanic climate (Köppen climate classification: Cfb). The summer of Melbourne is dry. The mean monthly total rainfall of summer (December–February) is only 51.8 mm. The dry summer climate of Melbourne is conducive to a strong cooling effect of irrigating urban green spaces (Cheung et al., 2022b). The summer of Melbourne is also characterised by a large difference between daytime and night-time air temperatures. The mean daily maximum air temperature of summer (December–February) is 26.2°C and the minimum is 15.6°C (Bureau of Meteorology, 2023a). A large difference between daytime and night-time air temperatures provides an opportunity to strengthen the cooling effect of irrigation by optimising the irrigation schedule.

5.2.2. Experimental design

The field experiment consisted of twelve identical plots (four treatments × three replicates). Each plot had a footprint of 36 m^2 (6 m × 6 m) and was enclosed by a 1.8-m 70% shade cloth (SOLARSHADE™) to reduce air mixing between the plots and the surrounding (Fig. 5.1). The

surface of the plot was turfgrass and the dominant species was Kikuyu (*Pennisetum clandestinum*). The turfgrass was mowed every two weeks to approximately 0.05 m tall. The top soil (5–10 cm) of the site was sandy loam and the subsoil (50–55 cm) was sandy clay. The pore volume of the top soil and subsoil was 61% and 40%, respectively. The bulk density of the top soil and subsoil was 1.02 g cm^{-3} and 1.58 g cm^{-3}, respectively. The soil was well-drained with an infiltration rate of approximately 650 mm/h. A climate station was installed at the centre of each plot to continuously measure air temperature, vapour pressure, black globe temperature, wind speed and soil moisture. Incoming and outgoing shortwave and longwave radiation and turf surface temperature were measured in one of the three replicates. A reference climate station was installed within 50 m of the plots to provide background air temperature, relative humidity, wind speed and rainfall. The specifications of the instruments and their installation height/depth are provided in Table 5.1. All climate and soil variables were measured every 10 seconds and the 1-minute average was logged.

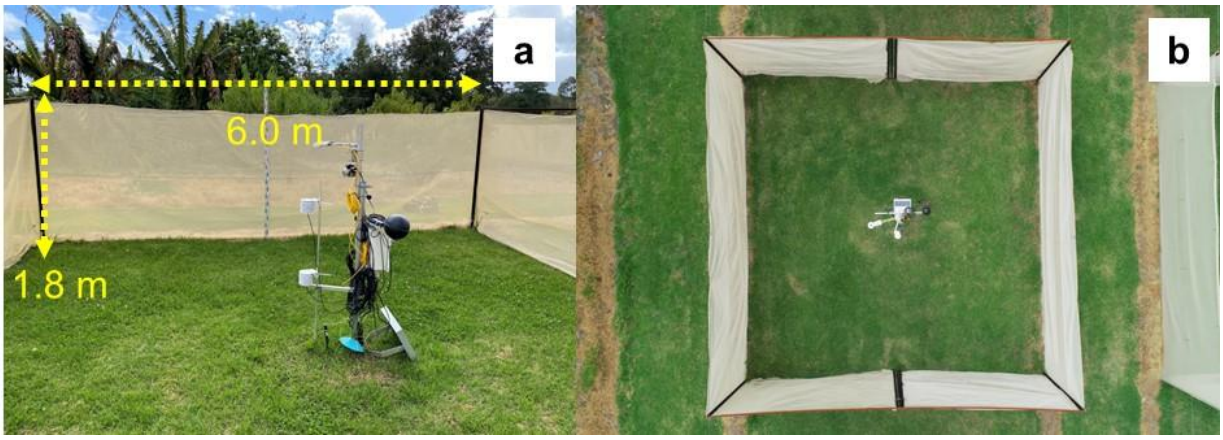

Fig. 5.1. (a) Ground view and (b) bird-eye view of a plot. The experiment consisted of twelve identical plots (four treatments × three replicates). The four treatments were: unirrigated (U0), irrigated at 01:00 (N1), irrigated at 13:00 (D1), irrigated at 12:00, 13:24, 14:00 and 15:00 (D4). The daily total irrigation amount of the three irrigated plots was the same except that they were irrigated at different times of the day. Each plot was 6 m × 6 m and was enclosed by 1.8-m tall 70% shade cloth (SOLARSHADE™). A climate station was installed at the centre of each plot, measuring soil temperature (–0.05 m), soil moisture content (–0.05 m), air temperature (1.1 m), vapour pressure (1.1 m), turf surface temperature (1.5 m), and incoming and outgoing shortwave and longwave radiation (1.5 m). A reference climate station was installed at the centre of the experimental site, measuring air temperature (1.1 m), vapour pressure (1.1 m), rainfall (2.0 m) and wind speed (2.0 m).

Table 5.1. Specifications of the microclimate and soil instruments used in this study and their installation height/depth.

Location	Model and brand	Variable	Accuracy	Height/depth (m)
Plot	03101-L, Campbell Scientific	Wind speed	±0.5 m/s	1.1
	44031, Omega	Black globe temperature	±0.1°C @ 25°C	1.1
	ATMOS14, METER	Air temperature	±0.2 °C	1.1
		Vapour pressure of water	±0.05 kPa @ 25°C	1.1
	CNR4, Kipp & Zonen	Incoming longwave radiation (4.5–42 μm)	<10% (daily total)	1.5
		Incoming shortwave radiation (300–2800 nm)	<5% (daily total)	
		Outgoing longwave radiation (4.5–42 μm)	<10% (daily total)	
		Outgoing shortwave radiation (300–2800 nm)	<5% (daily total)	
	CS650, Campbell Scientific	Soil moisture	±3%	–0.05
	SI-111, Apogee	Turf surface temperature	±0.2°C (−10°C to +65°C)	1.5
Reference	S-RGB-M002, Onset HOBO	Rainfall	±1%	2
	S-THB-M002, Onset HOBO	Air temperature	±0.2 °C at 25°C	1.1
		Relative humidity	±2.5% (10–90%)	1.1
	S-WCA-M003, Onset HOBO	Wind speed	±0.5 m/s (<17 m/s)	2

The four treatments of the experiment included: unirrigated (U0), irrigated from 01:00–01:23 (N1), irrigated from 13:00–13:23 (D1), and irrigated from 12:00–12:07, 13:48–13:55, 14:00–14:07 and 15:00–15:07 (D4). N1, D1 and D4 were irrigated at different times of the day but their daily total irrigation amount was the same, i.e., 2 mm. D4 was irrigated four times per day with 0.5 mm each time. The daily total irrigation amount was increased to 4 mm in the last 26 days of the study period. Four Hunter MP1000–90 Rotator nozzles and one Hunter MP1000–360 Rotator nozzle were installed at the four corners and the centre of each plot, respectively. The five nozzles in a plot were operated at 280 kPa, delivering 4 mm of water in approximately 24 minutes. The Hunter MP Rotator nozzles irrigate by creating multiple water streams (Hunter, 2023) while traditional impact sprinklers irrigate by creating fine droplets of water (Jiang et al., 2021). The Hunter MP Rotator nozzles were chosen for this experiment because it would not create fine droplets of water that rest on and affect the temperature and humidity sensors. The nozzles were also carefully adjusted such that the water streams would not hit the climate station.

5.2.3. Weather conditions of the study period

The study was conducted from 2023-01-18 to 2023-03-06. The irrigated plots were irrigated daily in this period. The total rainfall in this period was 120.4 mm and the mean air temperature was 21.6°C (Fig. 5.2). There were seven days when daily maximum air temperature ≥ 35.0°C. The differences between daily minimum and maximum air temperatures were generally ≥ 10.0°C. The daily mean vapour pressure was 0.94 kPa with a range between 0.19 and 1.92 kPa. The daily mean wind speed was 0.33 m s^{-1} with range between 0.00 and 0.33 m s^{-1}. The daily mean incoming shortwave radiation was 254 W m^{-2} with a range between 89 and 377 W m^{-2}.

5.2.4. Data analysis

Six dependent variables were analysis in this study: soil moisture content, air temperature, vapour pressure, turf surface temperature, mean radiant temperature and UTCI. Soil moisture content, air temperature, vapour pressure and turf surface temperature were directly measured. Mean radiant temperature was calculated from air temperature, black globe temperature and wind speed measurements, according to ISO 7726 (1998). UTCI was calculated using the 'rBiometeo' package in R Studio 4.1.1 (R Core Team, 2023). UTCI is a thermal index that integrates the impacts of air temperature, vapour pressure, mean radiant temperature and wind speed on human thermal stress (Bröde et al., 2012). UTCI is measured in °C and can be classified into one of the ten UTCI thermal stress categories from 'extreme cold stress' and 'extreme heat stress'.

The average diurnal cycles of the three replicated plots were similar for all four irrigation treatments and all analysed variables except there were ~5°C differences in mean radiant temperature between the replicates in U0, D1 and D4 from 10:00 to 16:59 (Fig. S5.1). Black globe temperature is commonly used to estimate mean radiant temperature in outdoor thermal comfort research (Guo et al., 2020). Using black globe temperature to estimate mean radiant temperature in the outdoor environment is known to have a larger uncertainty than the radiation integral method because wind speed is involved in the estimation to account for free convection and wind speed is inherently variable in time and space (Teitelbaum et al., 2020). To reduce the impacts of the uncertainties of measurements on the results, the mean of the three replicated plots was used in the analysis for all variables.

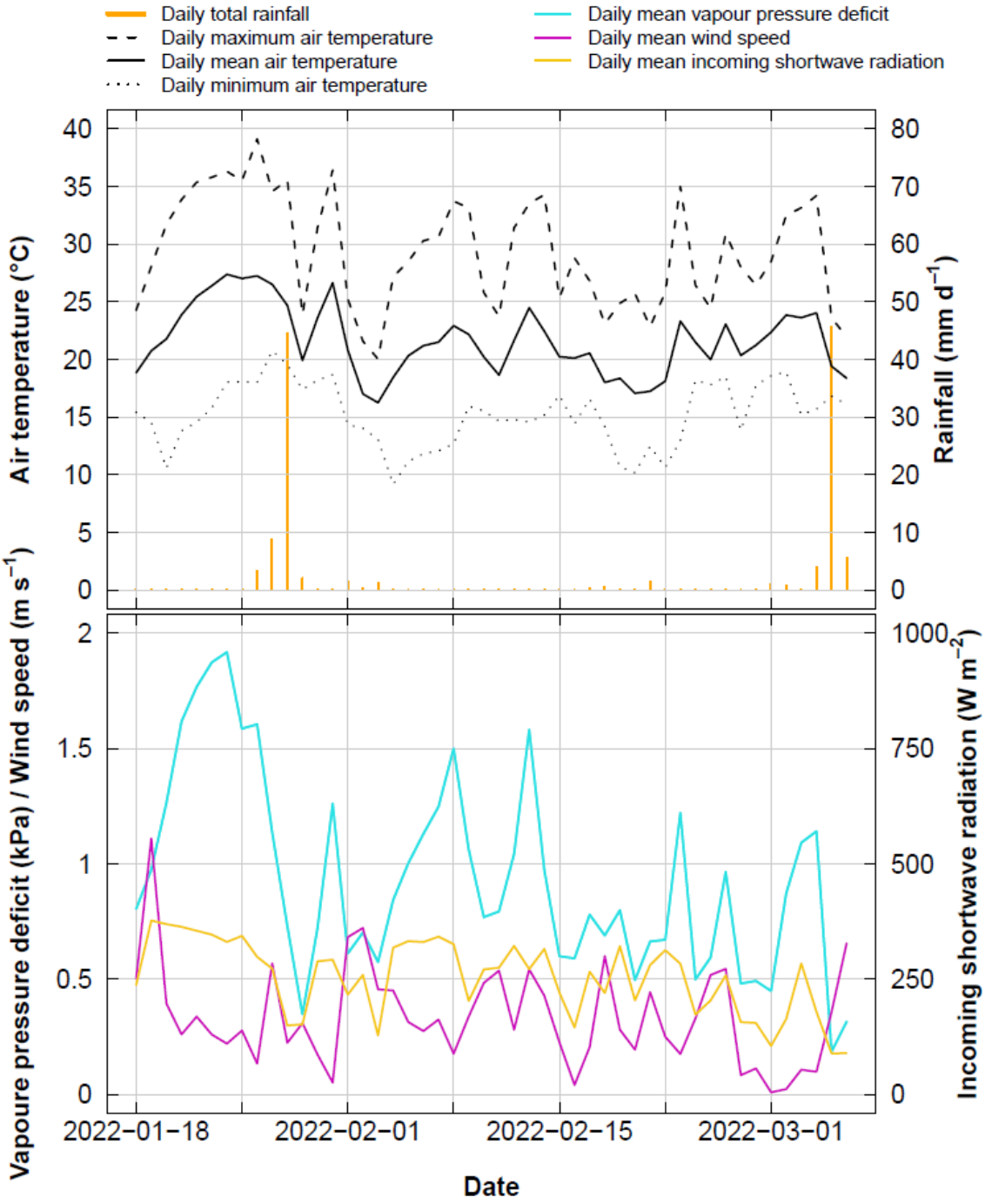

Fig. 5.2. Daily total rainfall, daily maximum, mean and minimum air temperatures, daily mean vapour pressure deficit, daily mean wind speed and daily mean incoming shortwave radiation of the study period (2022-01-18 to 2022-03-06).

To investigate the impacts of irrigation scheduling on the afternoon (12:00–15:59) cooling effects, the 1-minute average cycle between 10:00 and 15:59 of the study period was plotted for all

three irrigated treatments and the one unirrigated treatment. The plotted variables included soil moisture content, air temperature, vapour pressure, turf surface temperature, mean radiant temperature and UTCI. In a separate figure, the cooling effect of each irrigated treatment in the same cycle was plotted. The cooling effect was defined as the differences between the irrigated treatment and the unirrigated treatment (Δ = irrigated – unirrigated). The afternoon (12:00–15:59) mean cooling effects were computed for each irrigated treatment. Tukey's Honest Significance Difference test was used to assess the significance of differences between the three irrigated treatments in their afternoon (12:00–15:59) mean cooling effects.

To investigate the relationship between the cooling effects of irrigation and weather conditions, the daily afternoon (12:00–15:59) mean cooling effects (air temperature and turf surface temperature) were plotted against the daily afternoon (12:00–15:59) mean weather conditions (air temperature, vapour pressure deficit, wind speed, and incoming shortwave radiation). Only the cooling effects on air temperature and turf surface temperature were analysed because irrigation did not consistently reduce mean radiant temperature and UTCI. After initial examination of the graphs, both the cooling effects on air temperature and turf surface temperature were linearly correlated with the background air temperature, vapour pressure deficit and incoming shortwave radiation while they were correlated with background wind speed in an inverted bell curve shape. Linear and Gaussian models were established if the estimates of the models were statistically significantly. The linear model takes the following form:

$$y = mx + c \tag{1}$$

where y is the afternoon (12:00–15:59) mean cooling effect, x the afternoon (12:00–15:59) mean weather conditions (air temperature, vapour pressure deficit, wind speed, or incoming shortwave radiation), m the slope of the model, and c the intercept of the model.

The Gaussian model with parametric extension takes the following form:

$$y = aexp\left(\frac{-(x-b)^2}{2c^2}\right) \tag{2}$$

where y is the afternoon (12:00–15:59) mean cooling effect, x the background weather conditions, a the height of the curve's peak, b the position of the centre of the peak a c the width of the bell curve.

The coefficient of determination (R^2) was computed for the linear models but not the Gaussian models because its meaning in linear regression does not hold when used in non-linear regression (Kvålseth, 1985). In linear regression, R^2 is the proportion of variance explained by the regression model (Nagelkerke, 1991).

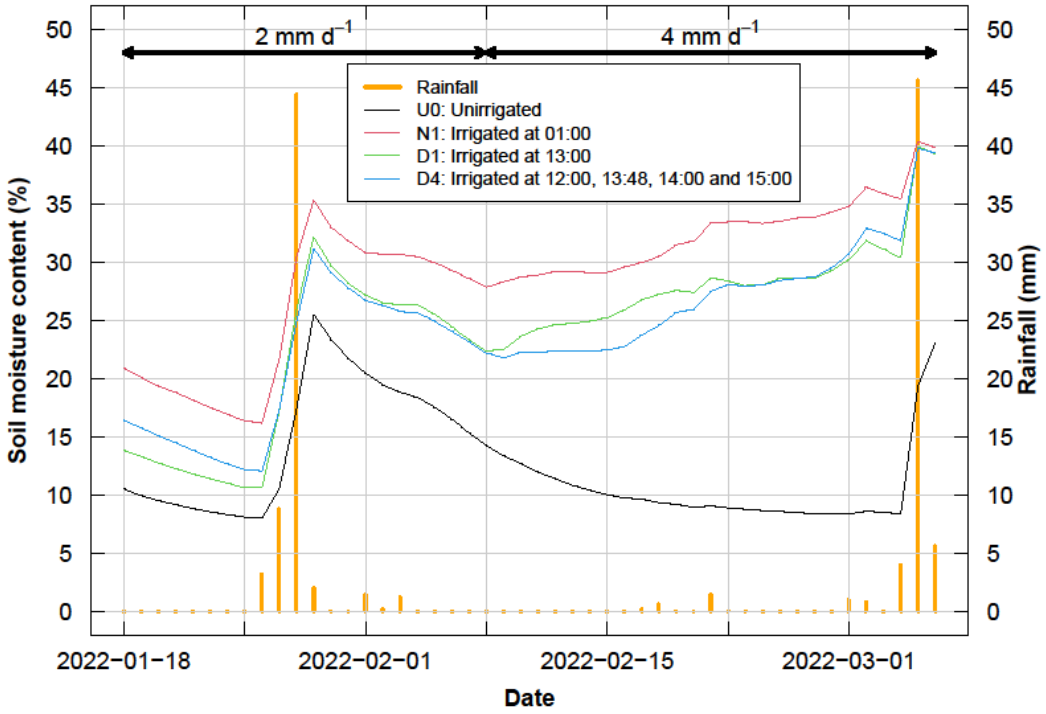

Fig. 5.3. Changes in daily mean soil moisture content of plot U0 (unirrigated), plot N1 (irrigated 2 or 4 mm d^{-1} at 01:00), plot D1 (irrigated 2 or 4 mm^{-1} at 13:00) and plot D4 (irrigated 0.5 or 1 mm at 12:00, 13:48, 14:00 and 15:00 = 2 or 4 mm d^{-1}), and rainfall at the reference climate station. Each plot had three replicates and the mean of the three replicates was used.

5.3. Results

5.3.1. Changes in soil moisture content in the study period

The soil moisture contents of plots N1, D1 and D4 were always higher than plot U0 throughout the study period (Fig. 5.3). When the irrigation amount was 2 mm d^{-1}, the soil moisture contents of plots N1, D1 and D4 were 5–10% higher than plot U0. When the irrigation amount increased to 4 mm d^{-1}, the difference increased to as much as 25 %.

5.3.2. Impacts of irrigation scheduling on afternoon mean soil moisture content and cooling effects

From 10:00 to 15:59, the soil moisture contents of all four plots (Fig. 5.4a–c) were stable, except it increased in D1 during irrigation. The air temperature of U0 was always higher than those of N1, D1 and D4 (Fig. 5.4d–f). The air temperatures of N1, D1 and D4 were similar except that it reduced in D1 and D4 during and immediately after irrigation. The vapour pressures of U0, N1 and D1 were similar except for a slight increase during irrigation in D1 (Fig. 5.4g–i). The turf surface temperature of U0 was always higher than N1, D1 and D4 (Fig. 5.4j–l). The turf surface temperature of N1, D1 and D4 were similar except for a slight reduction during and immediately after irrigation in D1 and D4. The mean radiant temperature of N1 and D4 were higher than U0 and D1 (Fig. 5.4m–o). The mean radiant temperatures of D1 and D4 were unaffected by irrigation and that of N1 only responded to weather changes in this period (10:00–15:59) because it was irrigated at night. The UTCI of all four plots were similar (Fig. 5.4p–r). The UTCI of D1 and D4 were unaffected by irrigation and that of N1 only responded to weather changes in this period (10:00–15:59) because it was irrigated at night.

The afternoon (12:00–15:59) mean impacts of all three irrigation treatments (N1, D1 and D4) on all analysed variables (soil moisture content, air temperature, vapour pressure, turf surface temperature, mean radiant temperature and UTCI) were statistically significant ($p < 0.05$) (Fig. 5.5), except for the UTCI of N1 (Fig. 5.5p). The afternoon (12:00–15:59) mean impacts of N1 on soil moisture content (16.93%) was significantly larger ($p < 0.05$) than D1 (12.51%) and D4 (11.84%) (Fig. 5.5a–c). The afternoon (12:00–15:59) mean cooling effect of D4 in air temperature (–0.93°C) was significantly larger ($p < 0.05$) than N1 (–0.66°C) and D1 (–0.51°C) (Fig. 5.5d–f). The afternoon (12:00–15:59) mean impacts of N1, D1 and D4 on vapour pressure were small (<0.01 kPa) (Fig. 5.5g–i). The afternoon (12:00–15:59) mean cooling effect of D4 for turf surface temperature (–4.91°C) was significantly larger ($p < 0.05$) than N1 (–3.38°C) and D1 (–4.03°C) (Fig. 5.5j–l). The afternoon (12:00–15:59) mean impacts of D4 on mean radian temperature (<1.5°C) were significantly larger ($p < 0.05$) than N1 (1.32°C) and D1 (–0.59°C) (Fig. 5.5m–o). The afternoon (12:00–15:59) mean impacts of N1, D1 and D4 on UTCI were significantly different ($p < 0.05$) from each other but the impacts were small (<0.5°C) (Fig. 5.5p–r).

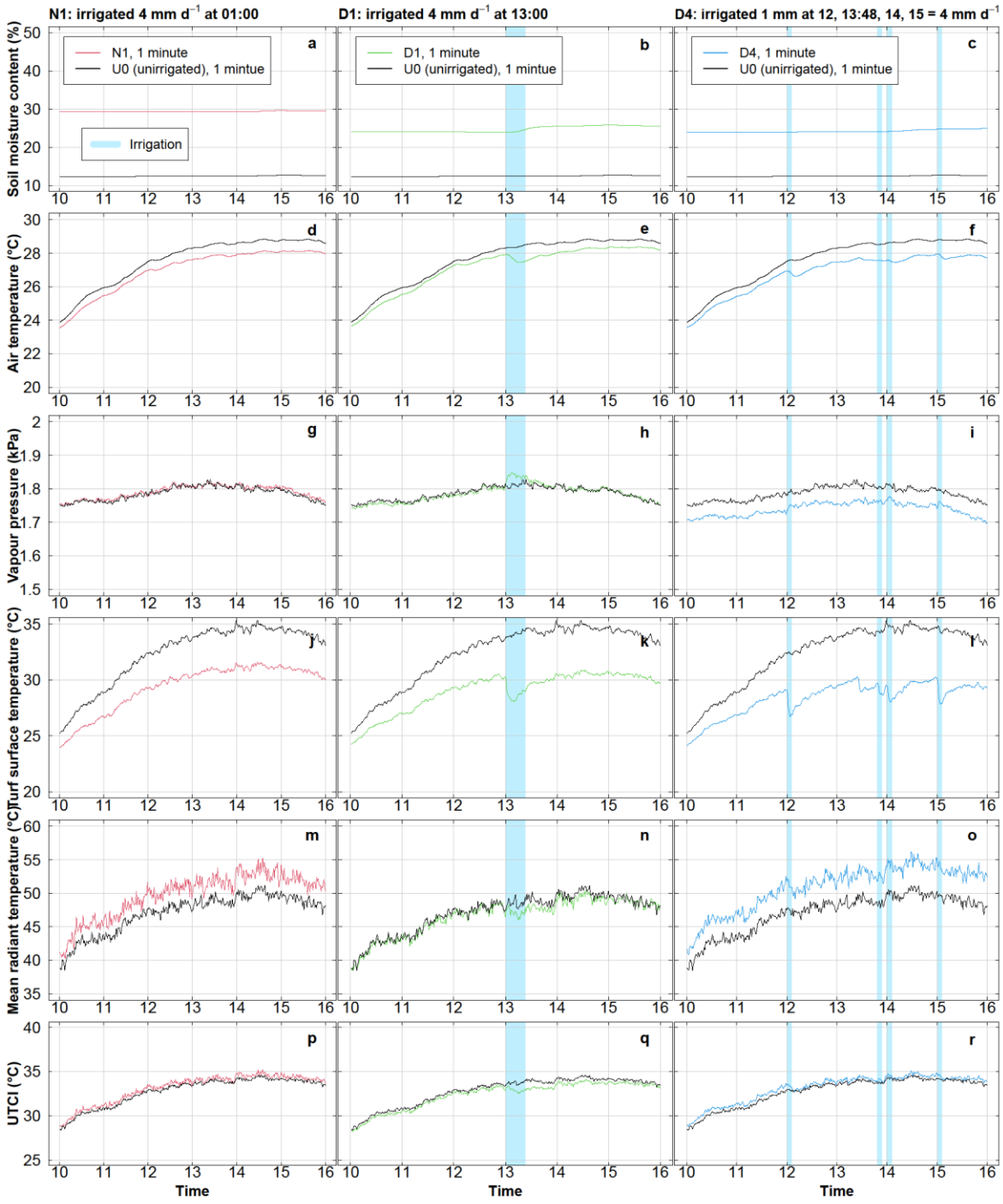

Fig. 5.4. Average cycles (1-minute) of soil moisture content, air temperature, vapour pressure, turf surface temperature, mean radiant temperature and universal thermal climate index (UTCI) of plot U0 (unirrigated), plot N1 (irrigated 4 mm d^{-1} at 01:00), plot D1 (irrigated 4 mm d^{-1} at 13:00), plot D4 (irrigated 1.0 mm at 12:00, 13:48, 14:00 and 15:00 = 4 mm d^{-1}) from 10:00 to 15:59.

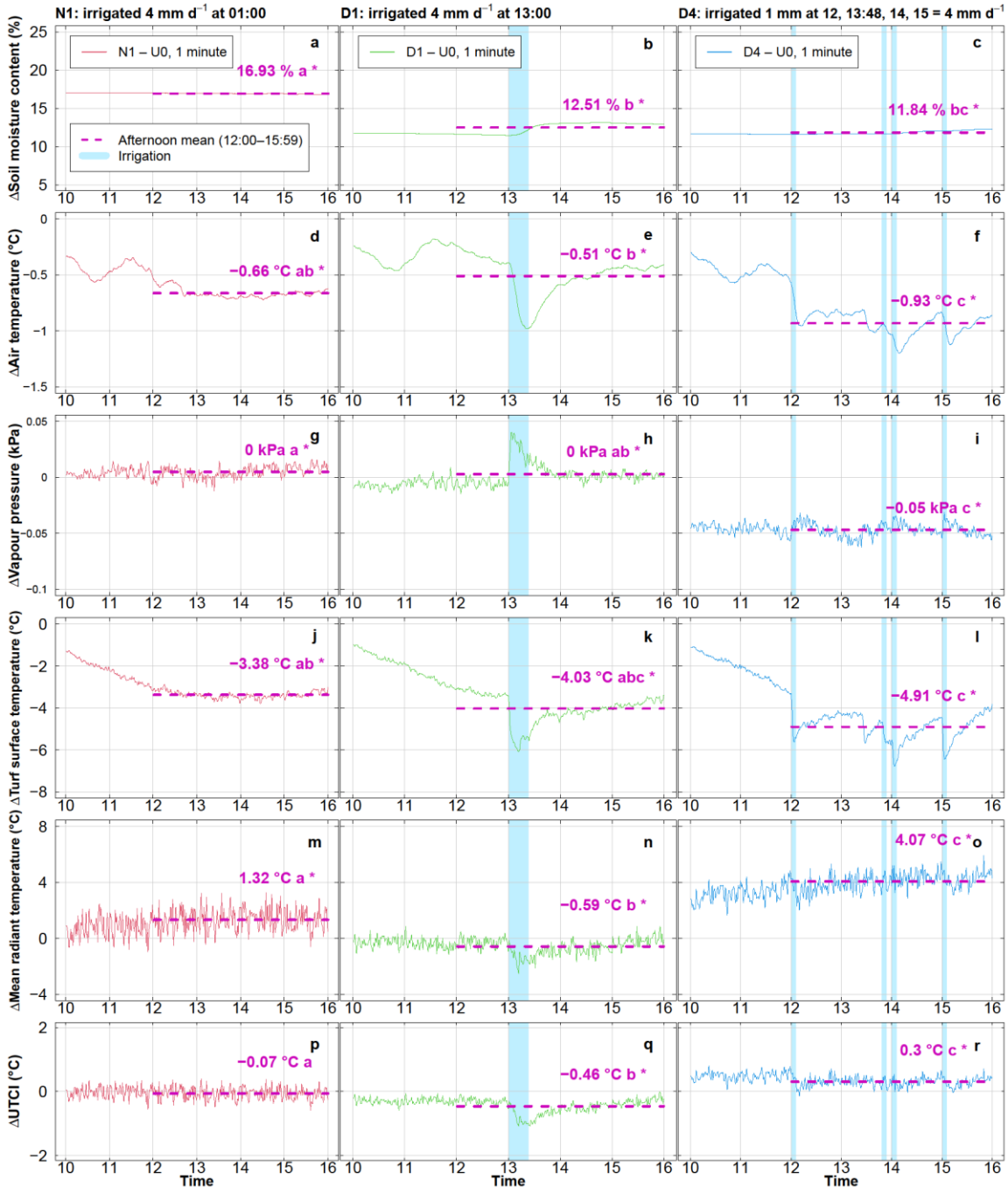

Fig. 5.5. Average impacts (1-minute) of irrigation on soil moisture content, air temperature, vapour pressure, turf surface temperature, mean radiant temperature and universal thermal climate index (UTCI) for plot N1 (irrigated 4 mm d^{-1} at 01:00), plot D1 (irrigated 4 mm d^{-1} at 13:00) and plot D4 (irrigated 0.5 mm d^{-1} at 12:00, 13:48, 14:00 and 15:00, respectively) from 10:00 to 15:59. The impacts were measured as the differences between the irrigated and unirrigated plots (Δ = irrigated – unirrigated). The horizontal dashed lines represent the afternoon (12:00–15:59) mean impacts. The letters, 'a', 'b' and 'c', indicate the significance of differences between the three irrigated plots in their afternoon (12:00–15:59) mean cooling effects. The pairs that do not have the same letter are significantly different from each other ($p < 0.05$, Tukey's Honesty Significant Difference test). The

presence of the symbol, '*', indicates that the afternoon (12:00–15:59) mean cooling effect is significant ($p < 0.05$, *t* test).

5.3.3. Relationships between afternoon mean cooling effects and weather conditions

The afternoon (12:00–15:59) mean air temperature cooling effects of irrigation strengthened with increasing background air temperature, vapour pressure deficit and incoming shortwave radiation for all three irrigation treatments (Fig. 5.6a, 5.6b and 5.6d). For every 1°C increase in background air temperature, the cooling effects from irrigation strengthened by 0.03, 0.03 and 0.04°C for N1, D1 and D4, respectively. For every 1 kPa increase in background vapour pressure deficit, the cooling effect strengthened by 0.17, 0.15 and 0.23°C for N1, D1 and D4, respectively. For every 1 W m^{-2} increase in background incoming shortwave radiation, the cooling effect strengthened by 0.001°C for N1, D1 and D4. The afternoon (12:00–15:59) mean air temperature cooling effects from irrigation changed with wind speed in an inverted bell curve shape for all irrigation treatments (Fig. 5.6d). The cooling effects strengthened when wind speed increased from 0 and peaked at 0.52 m s^{-1} for N1, 0.45 m s^{-1} for D1 and 0.52 m s^{-1} for D4. The cooling effects weakened as wind speed increased beyond these peaks.

The afternoon (12:00–15:59) mean turf surface temperature cooling effects of irrigation strengthened with increasing background air temperature, vapour pressure deficit and incoming solar radiation (Fig. 5.7a, 5.7b and 5.7d). For every 1°C increase in background air temperature, the cooling effects from irrigation strengthened by 0.38, 0.35, 0.30°C for N1, D1 and D4, respectively. For every 1 kPa increase in background vapour pressure deficit, the cooling effects from irrigation strengthened by 2.17, 2.09 and 1.84°C for N1, D1 and D4, respectively. For every 1 W m^{-2} increase in background incoming shortwave radiation, the cooling effects from irrigation strengthened by 0.01°C for N1, D1 and D4. The afternoon (12:00–15:59) mean turf surface temperature cooling effects of irrigation only strengthened with increasing background wind speed for N1 (Fig. 5.7c). The cooling effects from irrigation strengthened when wind speed increased from 0 and peaked at 0.49 m s^{-1}.

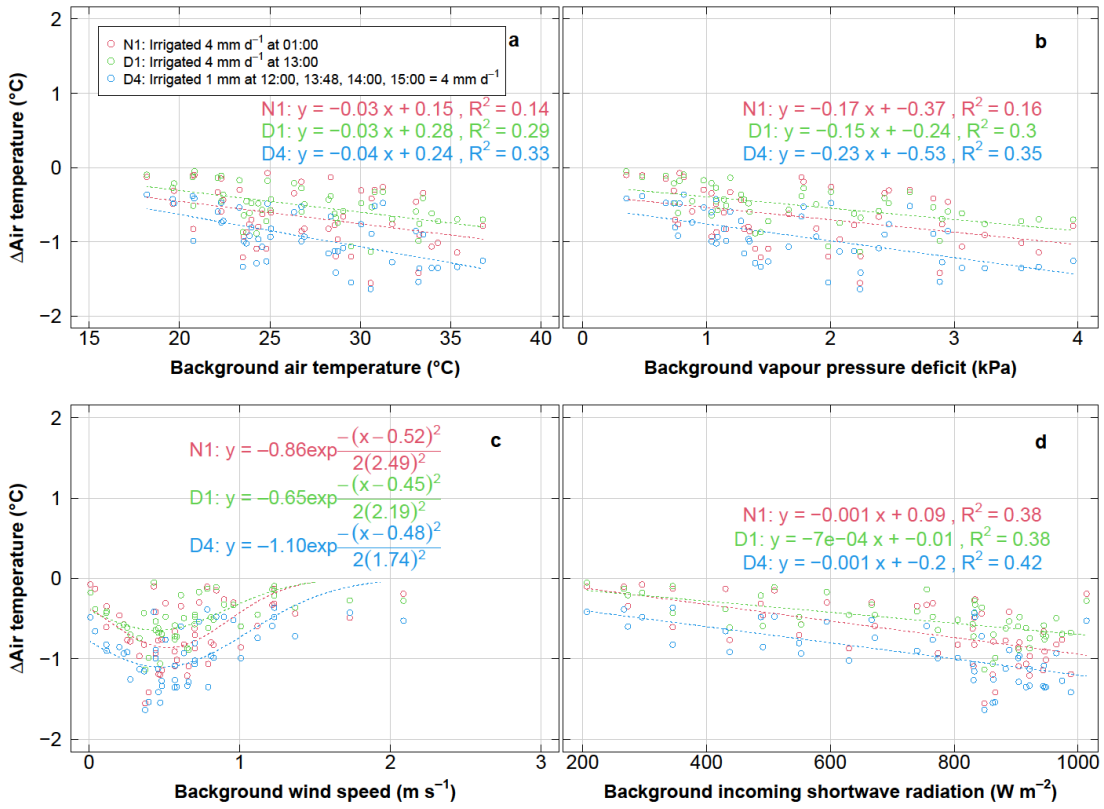

Fig. 5.6. Scatter plots of the afternoon (12:00–15:59) mean cooling effect of irrigation (Δ = irrigated – unirrigated) in air temperature against background (a) air temperature, (b) vapour pressure deficit, (c) wind speed and (d) incoming shortwave radiation. Linear regression models were used for background air temperature, vapour pressure and incoming shortwave radiation, and Gaussian regression models for wind speed. Only the models with a significant slope/parameter estimate were plotted.

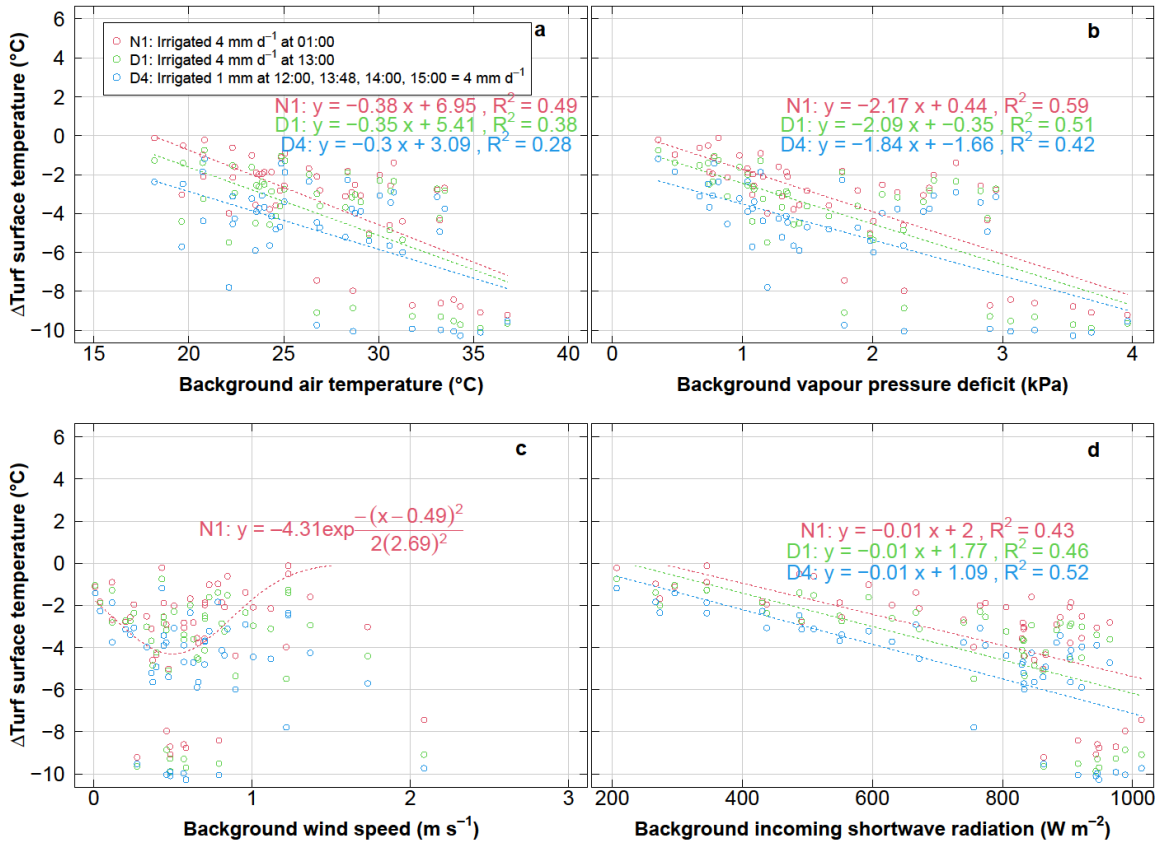

Fig. 5.7. Scatter plots of the afternoon (12:00–15:59) mean cooling effect of irrigation (Δ = irrigated – unirrigated) in turf surface temperature against background (a) air temperature, (b) vapour pressure deficit, (c) wind speed and (d) incoming shortwave radiation. Linear regression models were used for background air temperature, vapour pressure and incoming shortwave radiation, and Gaussian regression models for wind speed. Only the models with a significant slope/parameter estimate were plotted.

5.4. Discussion

5.4.1. Impacts of irrigation time on afternoon mean soil moisture content and cooling effects

All three irrigation treatments induced significant and strong afternoon (12:00–15:59) mean cooling effects on air temperature and turf surface temperature, whereas the cooling effects on mean radiant temperature and UTCI were inconsistent and weak. This means that our results partially support Hypothesis 1 as measured cooling benefits from irrigation were evident for air temperature and turf surface temperature only. Gao et al. (2020) modelled that the strongest cooling effects of night-time irrigation on air temperature (–0.6°C) and surface temperature (–2.7°C) would occur at 13:00 local time. Their model predictions are comparable to our measurements. The cooling effects of the night-time irrigation on air temperature and turf surface temperature in our study also reached

their strongest at approximately 13:00 and maintained at the same levels for the rest of the afternoon. Such cooling effects were driven by the increase in evapotranspiration due to increased soil moisture content (Chen et al., 2018). The increased evapotranspiration increases the latent heat flux and reduces sensible heat flux, leading to the reductions in air temperature and turf surface temperature.

The afternoon (12:00–15:59) air temperature reduction from irrigating 4 mm through four separate 1 mm events (D4) was significantly stronger than applying all 4 mm in one irrigation event (N1 and D1). However, the air temperature cooling benefits of irrigating 4 mm at night (N1) were not significantly different from those when irrigating by day (D4). These results again provide partial support for Hypothesis 2 that greatest cooling benefit would be derived from irrigation scheduling that applies small amounts of water (1 mm) on multiple occasions (four) during the day, and least cooling benefit would be derived from irrigating the same amount through one irrigation event at night. This finding supports the suggestion of Broadbent et al. (2018a) that optimising irrigation scheduling can strengthen the cooling effects of irrigation in certain periods of time using the same irrigation amount.

The differences between the irrigation treatments in their afternoon cooling effects can be explained by their differences in evapotranspiration processes in the afternoon (Fig. 5.8). For the unirrigated treatment, soil evaporation and transpiration were the only two evapotranspiration processes in the afternoon (Fig. 5.8a). Since the unirrigated treatment has the lowest soil moisture content among the four treatments, it had the smallest soil evaporation, transpiration and evapotranspiration. Consequently, the unirrigated treatment had the highest afternoon air temperature among the four treatments. For the single night-time irrigation treatment, soil evaporation and transpiration were also the only two evapotranspiration processes in the afternoon (Fig. 5.8b). Since it had a higher soil moisture content than the unirrigated treatment, it had a higher soil evaporation, transpiration and evapotranspiration. Consequently, the single night-time irrigation treatment had a significantly lower afternoon air temperature compared to the unirrigated treatment. For the single midday irrigation treatment, its soil moisture content was similar to the single night-time irrigation treatment because daily total irrigation amount was the same. In comparison to the single night-time irrigation, the single midday irrigation introduced two extra evaporation processes in the afternoon, namely droplet evaporation and canopy evaporation (Fig. 5.8c). Droplet evaporation is the evaporation that occurs when water droplets pass through the air before impact. Droplet evaporation is usually small (~1% of irrigation amount) when the irrigation amount is high (≥25 mm) (Thompson et al., 1997). Canopy evaporation is the evaporation of water stored on the canopy surface. Canopy evaporation can account for >80% of afternoon (12:00–15:59) evapotranspiration for a corn field that

is irrigated by sprinkler during the day (Thompson et al., 1993). However, the afternoon cooling effects of the single midday irrigation and single night-time irrigation treatments on air temperature were not significantly different. It was likely because the afternoon soil evaporation and transpiration in the single midday irrigation were suppressed by the irrigation itself because of the humidification of the environment (Tolk et al., 1995). Consequently, the increase in afternoon canopy evaporation from the midday irrigation might be offset by the reduction in soil evaporation and transpiration.

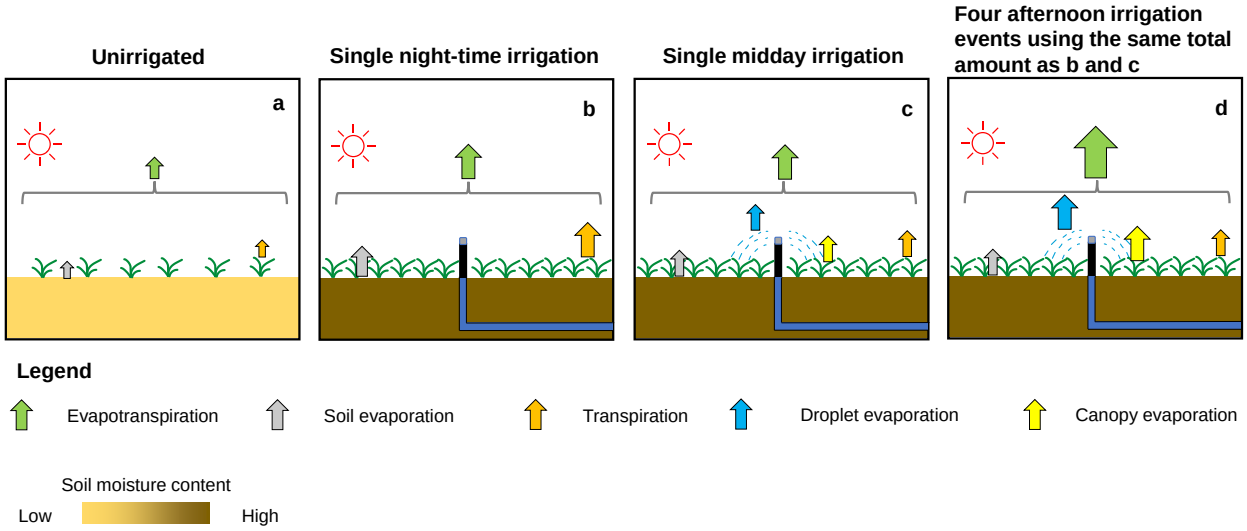

Fig. 5.8. A conceptual diagram that explains the impact of different irrigation schedules on evapotranspiration processes in turfgrass in the afternoon. In (a), when the turfgrass is unirrigated, the evapotranspiration consists of a small amount of soil evaporation and transpiration. In (b), when the turfgrass is subject to a single night-time irrigation, the evapotranspiration consists of a larger amount of soil evaporation and transpiration. In (c), when the turfgrass is subject to a single midday irrigation, the evapotranspiration consists of soil evaporation, transpiration, droplet evaporation and canopy evaporation. In (d), when the turfgrass is subject to four afternoon irrigation events, the total evapotranspiration increases due to an increase in droplet evaporation and canopy evaporation.

For the multiple afternoon irrigation treatment, the multiple irrigation events were likely to increase the droplet evaporation and canopy evaporation compared to the single midday irrigation, causing a significantly higher afternoon evapotranspiration (Fig. 5.8d) and significantly lower afternoon air temperature. Droplet evaporation and canopy evaporation increase notably if the irrigation is short and frequent, causing near total water evaporation, either in the air or on the canopy surface, before reaching the soil (Burt et al., 2005). There are two reasons for that. First, the vapour pressure deficit can increase quickly and return to the pre-irrigation level after one short irrigation event, leading to a relatively dry environment that is conducive to droplet evaporation and canopy evaporation for the next irrigation (Tolk et al., 1995). Second, the short irrigation events increase the

total canopy evaporation by only depositing a small amount of water onto the canopy in each irrigation event, thereby limiting the amount of water dripping from the canopy onto the soil surface. This was reflected in the smaller increase in soil moisture content in the multiple afternoon irrigation treatment (0.2%, Fig. 5.4c) than the single midday irrigation treatment (0.8%, Fig. 5.4b) from the morning (10:00–11:59) to the afternoon (12:00–15:59). The wet turfgrass canopy in the multiple afternoon irrigation treatment after the first irrigation at 12:00 was likely to dry within 30 minutes (Burt et al., 2005), allowing the canopy to store and evaporate more water in the next irrigation event. Similar to the single midday irrigation treatment, the repeated wetting of turfgrass canopy in the multiple afternoon irrigation treatment was likely to suppress transpiration and soil evaporation because of the humidification of the environment. However, the air temperature data suggested that the afternoon total evapotranspiration was significantly higher in the multiple afternoon irrigation treatment than the single midday irrigation treatment. Air temperature has been demonstrated to reflect the evapotranspiration of vegetation before, during and after irrigation accurately (Thompson et al., 1993).

The evapotranspiration processes in Fig. 8 can change notably irrigation type. The irrigation nozzles (Hunter MP-1000 rotators) used in this study were different from traditional impact sprinklers because the MP-1000 rotators deliver water in multiple rotating streams instead of water droplets. The droplet evaporation in this study would have been higher if an traditional impact sprinklers were used because they would create smaller droplets than are more conducive to evaporation (Thompson et al., 1993).

The cooling effects of irrigation on human thermal comfort were less clear in the literature. Broadbent et al. (2018a) modelled that the cooling effect of continuous (24-hour) sprinkler irrigation would improve human thermal comfort by –2.3°C at 15:00 pm in the afternoon. However, Broadbent et al. (2018) estimated this using the humidex index which does not account for the effect of mean radiant temperature, the most important microclimate variable that influences human thermal comfort (Thorsson et al., 2007). UTCI is a more comprehensive index of human thermal comfort because it integrates all relevant microclimate variables, namely air temperature, relative humidity, wind speed and mean radiant temperature (Bröde et al., 2012). The most important driver of daytime mean radiant temperature and therefore human thermal comfort is incoming and lateral shortwave radiation (Cheung and Jim, 2018b; Middel and Krayenhoff, 2019). Although a lower turf surface temperature may lead to a lower mean radiant temperature and UTCI due to a reduced emission of longwave radiation from the surface, the reduction in turf surface temperature in this study seemed to be insufficient to influence mean radiant temperature and UTCI in the afternoon. Since irrigation alone

cannot reduce incoming and lateral shortwave radiation, additional cooling strategies, such as overhead tree canopy shading and green walls, will help to reduce incoming and lateral shortwave radiation and improve human thermal comfort.

5.4.2. Relationships between afternoon mean cooling effects and weather conditions

In this study, the afternoon (12:00–15:59) mean cooling effects of irrigating turfgrass on air temperature and turf surface temperature were significantly and positively correlated with background air temperature, vapour pressure deficit and incoming shortwave radiation, but not wind speed. The results provide partial support for Hypothesis 3 that the cooling effects would significantly correlate with all four weather variables. Our findings were consistent with Vivoni et al. (2020)'s findings, which showed a significant linear correlation between daily total evapotranspiration and daily mean air temperature ($R^2 = 0.79$) and incoming shortwave radiation ($R^2 = 0.82$) in an irrigated turfgrass. With almost unlimited soil moisture supply throughout the year (soil moisture content ≥ 40%), they measured a much higher evapotranspiration in summer (6–8 mm d^{-1}) than in winter (1–3 mm d^{-1}), suggesting that the evapotranspiration in a well-irrigated turfgrass was limited and controlled by available energy. The cooling effects of irrigating turfgrass were correlated with background air temperature and incoming shortwave radiation because they were the main sources of energy to support evapotranspiration, i.e. the cooling effects (Spronken-Smith et al., 2000). Studies that measured or modelled the cooling effects of irrigating vegetation provided more direct evidence for the correlation between the cooling effects and available energy. Lam et al. (2020) measured that the air temperature cooling effect of irrigating an urban green space in Melbourne, Australia was stronger during heatwaves (–4 to –2°C) than non-heatwave periods (–1.0 to –0.5°C). Gao et al. (2020) modelled similar results for irrigating all pervious surface in Metropolitan Sydney. In a previous study, we used a meta-analysis of published studies to develop a linear regression model between the air temperature cooling effects of irrigating vegetation and background air temperature (Cheung et al., 2021). The model predicted that the daily mean cooling effects on air temperature would strengthen by 0.1°C for every 1°C increase in background mean air temperature. The effect estimate (0.1°C $°C^{-1}$) was three times higher than that in this study (0.03°C $°C^{-1}$). Although direct comparison of the magnitude between the two effect estimates is not meaningful because of the obvious differences in methods, both studies agree that the cooling effects of irrigating vegetation are stronger on warmer days or in warmer climate regions.

The afternoon (12:00–15:59) mean cooling effects of irrigating turfgrass on air temperature and turf surface temperature were significantly correlated with background vapour pressure deficit (Fig. 5.6 and 5.7). Vapour pressure deficit is the atmospheric demand for water (Seneviratne et al.,

2010). Under unlimited soil moisture supply, evapotranspiration of turfgrass increases with vapour pressure deficit (Allen et al., 2005). Although transpiration may be suppressed by a high vapour pressure deficit because of stomatal closure (McAdam and Brodribb, 2015), transpiration only accounts for <20% of the total evapotranspiration in irrigated vegetation while soil evaporation and canopy evaporation account for >80% (Thompson et al., 1993). Since our turfgrass plots were well-irrigated (Fig. 5.3), increased vapour pressure deficit could lead to increased evapotranspiration and stronger cooling effects.

The afternoon (12:00–15:59) mean cooling effects of irrigating turfgrass on air temperature were significantly correlated with background wind speed in an inverted bell curve shape (Fig. 6 and 7). A high wind speed reduces the aerodynamic resistance of heat and vapour transfer from the evaporating surface to the air above the canopy, increasing evapotranspiration (Allen et al., 1998). A high wind speed also increases the vapour pressure deficit of the irrigated area if the surrounding surfaces are unirrigated, which in turn increases evapotranspiration. Our data showed that the cooling effects on air temperature reduced when wind speed was > 0.5 m s^{-1}. Since the irrigated plots were small (6 m × 6 m), it was likely that the cool air inside the irrigated plots dissipated and being replaced by the warm air from the surrounding unirrigated surfaces as wind speed increased. Playán et al. (2005) measured a short (a few minutes) cooling effect from irrigating a small area of bare soil (15 m × 15 m) under a wind speed of approximately 4 m s^{-1}. In contrast, Thompson et al. (1993) measured a longer (20 minutes) cooling effect from irrigating a larger area of corn (82 m × 165 m) under a wind speed of approximately 6 m s^{-1}. As the size of the irrigated area increases, the spatial scale of the impacts of urban green space irrigation on urban climate will resemble that of agricultural irrigation. Large-scale agricultural irrigation is capable of influencing regional and global climate (Cook et al., 2015; Lobell et al., 2008b; Thiery et al., 2020). When a larger urban green space is irrigated, we expect that the cooling effect at the centre of the urban green space would not be weakened by the surrounding unirrigated surfaces and high wind speeds. Instead, the cooling effects of irrigating a large urban green space will benefit the urban areas downwind (Spronken-Smith and Oke, 1998) and upwind (Vivoni et al., 2020) through advection.

5.4.3. Practical implications for using irrigation to cool urban green spaces

When irrigation is used solely to maintain plant health, daytime irrigation is often undesirable because it is less water-efficient as it increases evaporation losses which do not contribute to plant uptake (Urrego-Pereira et al., 2013). In contrast, this study showed that when irrigation is used to

prioritise the cooling of urban green spaces, daytime irrigation is desirable because it increases evaporation losses which directly contribute to significantly stronger cooling effects. Multiple short daytime irrigations are ideal for maximising the daytime mean cooling effects, in comparison to a single long daytime irrigation that uses the same amount of water. Yang and Wang (2015) reached a similar conclusion from their modelling study that predicted a stronger daily mean cooling effect by irrigating multiple times a day when soil temperature exceeded a certain threshold than irrigating once a day at a fixed time. The time between two short irrigations should be at least 0.5 hour because the intercepted water on the canopy takes 0.5–2.0 hours to dry during the day, depending on the plant species and weather conditions (Burt et al., 2005).

The significant correlations between irrigation cooling effects and weather conditions have important implications for scheduling irrigation, particularly when irrigation water supply is limited. When irrigation water supply is limited, irrigation can be applied to urban green spaces on a warmer day to obtain stronger cooling benefits. For example, the afternoon (12:00–15:59) mean cooling effect on air temperature is predicted to be –1.0°C when the background mean air temperature was 35°C, whereas it is only –0.6°C when the background mean air temperature was 25°C (Fig. 5.6). When irrigation water supply is abundant, irrigation can be applied on a daily basis throughout summer months. The total daily irrigation amount should not exceed the crop evapotranspiration given by the FAO-56 equation (Allen et al., 1998) unless the irrigation also aims to increase soil moisture content and issues of pedestrian access, wet ground and soil compaction are not of concern. The FAO-56 equation estimates the daily total crop evapotranspiration for a given crop under a given set of weather conditions when soil moisture is unlimited. This estimate is the maximum possible daily total crop evapotranspiration regardless of the daily total irrigation amount. In other words, the cooling effects of irrigation will not strengthen even if the daily total irrigation amount exceeds the estimated crop evapotranspiration.

It is crucial to establish alternative water supplies to support irrigation when irrigation is used to prioritise the cooling of urban green spaces, particularly in dry climate regions. Dry climate regions will benefit from a stronger irrigation cooling effect than wetter regions (Cheung et al., 2021), but there is also likely to be a greater demand on local freshwater resources. Water sensitive urban designs offer an opportunity for cities in the dry climate regions to collect non-portable water to support urban green space irrigation. Water sensitive urban designs are the approaches and technologies that collect and retain fit-for-purpose water in the urban areas to meet different needs (Coutts et al., 2013). Stormwater harvesting and wastewater treatment are two important approaches to collecting non-portable water for irrigating urban green spaces (Wong, 2006).

5.5. Conclusion

The afternoon mean (12:00–15:59) cooling effects of irrigating an urban green space at three different times of the day with the same daily total irrigation amount were measured in this study. All three irrigation time treatments induced significant and strong afternoon mean cooling effects on air temperature and turf surface temperature. The single night-time (N1) and single midday (D1) irrigation treatments induced similar afternoon mean cooling effects, while the multiple daytime (D4) irrigation treatment induced significantly stronger afternoon mean cooling effects than N1 and D1. The results suggested that applying short irrigation for multiple times during the day can increase the cooling benefits of irrigation without using more water.

The correlations between the afternoon mean (12:00–15:59) cooling effects of irrigation and background weather conditions were determined. The afternoon mean cooling effects on air temperature and turf surface temperature strengthened linearly with background afternoon mean air temperature, vapour pressure deficit and incoming solar radiation. The afternoon mean cooling effects strengthened with background afternoon mean wind speed from 0.0 to 0.5 m s^{-1} and weakened as wind speed increased beyond 0.5 m s^{-1}. The results suggested that, when irrigation water supply is limited, irrigation can be prioritised to warmer days to obtain stronger cooling benefits.

5.6. Supplementary materials

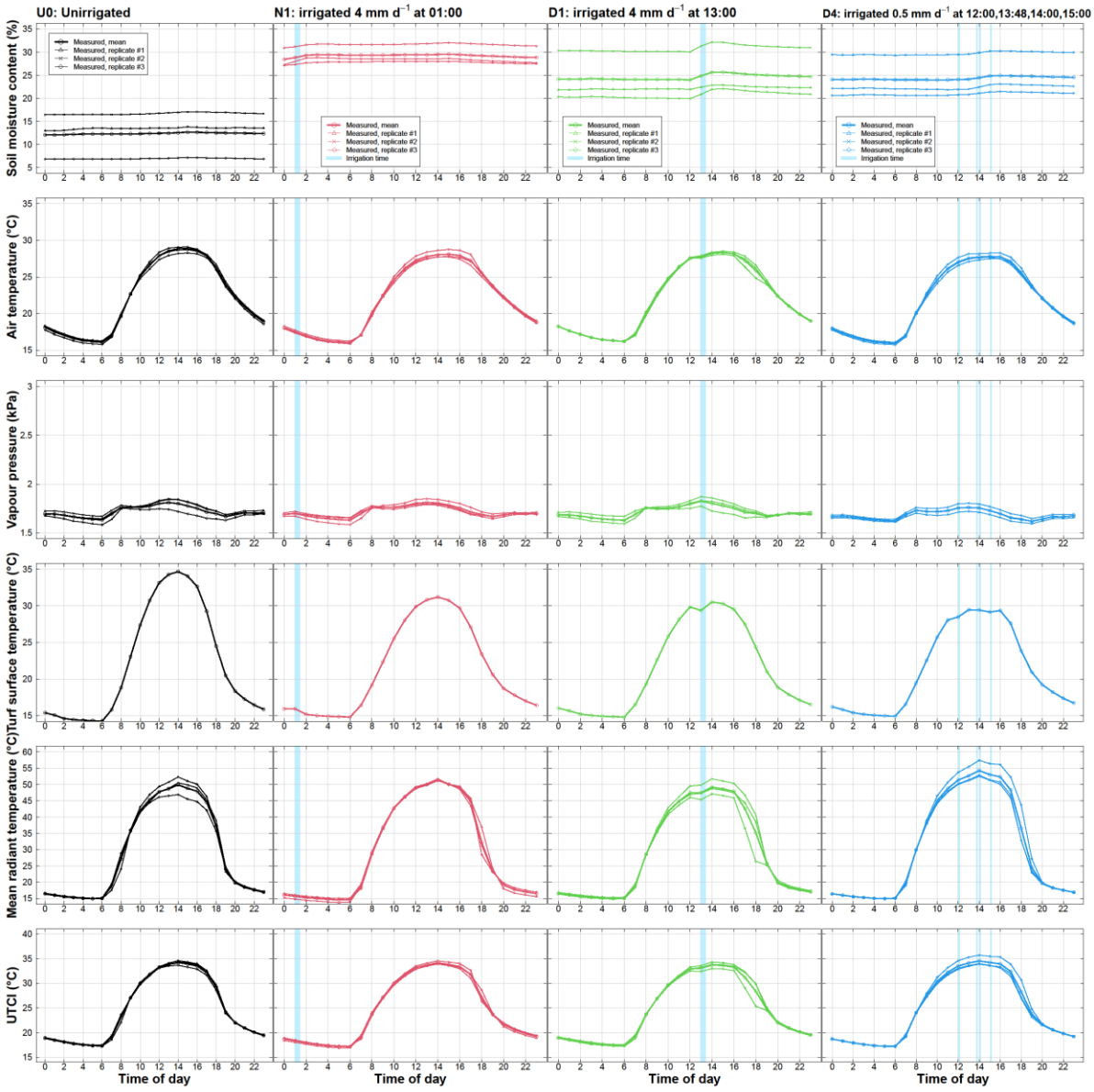

Fig. S5.1. Average diurnal cycles of the three replicated plots for each variable and irrigation treatment.

Chapter 6 – Identifying the mechanisms by which irrigation can cool urban green spaces in summer

A version of this chapter was submitted to Urban Climate on 16 June 2023. It is under review at the time of thesis submission.

Abstract

High temperatures in summer can prevent people from using urban green spaces. Irrigating urban green spaces is a promising strategy to reduce temperatures. This study uses an urban ecohydrological model, Urban Tethys-Chloris (UT&C), to identify proportional contribution of different irrigation cooling mechanisms and quantify the impacts of different irrigation amounts (from 2 to 30 mm d^{-1}) on the cooling effect. A field experiment was conducted in Melbourne, Australia to provide empirical data to calibrate and then assess UT&C simulation performance. The field experiment consisted of six identical turfgrass plots (three with irrigation and three without). UT&C was accurate modelling the soil moisture content and air temperature of the irrigated and unirrigated plots. Then, we used UT&C to partition the contribution of different irrigation cooling mechanisms. UT&C predicted that irrigation increased the evaporation from canopy interception and soil surface by 0.2 and 0.6 mm d^{-1}, respectively. With regards to the impacts of irrigation amounts, UT&C predicted the daytime (10:00–16:59) mean air temperature reductions would increase from 0.2 to 0.4°C when the irrigation amount increased from 2 to 4 mm d^{-1}. However, increasing the irrigation amount beyond 4 mm d^{-1} would not significantly increase the cooling benefits.

6.1. Introduction

Urban green spaces are an important space for physical and social activities in a city. The use of urban green spaces is strongly dependent on the thermal conditions of the space (Cheung and Jim, 2018a). High temperatures in summer can prevent people from using urban green spaces (Hao et al., 2023). Various mitigation strategies have been proposed to reduce the air temperature of urban green spaces in summer and these strategies can be divided into four major types (Lai et al., 2019): provision of shade, addition of vegetation, modification of surface reflectivity and water-based cooling. While the first three strategies have been widely studied in the past few decades (Santamouris et al., 2017), water-based cooling has received much less attention.

Irrigating urban green spaces is a promising water-based cooling strategy for cities (Coutts et al., 2013; Livesley et al., 2021). To make such a strategy acceptable it is important to make use of alternative water sources (e.g., stormwater harvesting, recycled waste water) so that cooling is not promoted at a cost to potable water resources. Stormwater harvest has been demonstrated to be effective in water saving, particularly in the dry regions (Zhang et al., 2023). A modelling study predicted that irrigating all vegetated surfaces in the metropolitan region of Sydney, Australia could reduce daily mean air temperature by 0.5°C during a heatwave (Gao et al., 2020). However, under normal summer conditions, irrigating turf has been measured to reduce daytime mean air temperature in small urban green spaces by only 0.6°C in Melbourne, Australia (Cheung et al., 2022a). The cooling effect of irrigation can be best understood and explained by analysing the surface energy balance. On a homogenous turf surface, the energy balance can be expressed as:

$$Q \quad + Q_f = Q_E + Q_H + \Delta Q_S (Wm^{-2}) \tag{6.1}$$

where Q^* is the all-wave net radiation [W m^{-2}], Q_f anthropogenic heat flux [W m^{-2}], Q_E the latent heat flux [W m^{-2}], Q_H the sensible heat flux [W m^{-2}] and ΔQ_S the net storage heat flux [W m^{-2}] (Oke, 1988). Most modelling studies predicted that irrigation would reduce air temperature as a result of a reduction in sensible heat flux and an increase in latent heat flux through evapotranspiration (Gao et al., 2020; Wang et al., 2019). Evapotranspiration can be partitioned into evaporation from wet surfaces and transpiration (Kool et al., 2014). For a surface covered by grass, evaporation can occur for water on the grass canopy, ponded surface water or soil water evaporated through the soil surface (Meili et al., 2020). The proportional contribution of these evaporation and transpiration processes to an increase in latent heat flux when irrigating urban green spaces has not been adequately simulated.

This is because many urban canopy models over-simplify plant physiological processes and sometimes omit some interactions between vegetation and hydrology (Meili et al., 2020). Partitioning evapotranspiration into its constituent evaporation and transpiration processes is important to understand the mechanism of irrigation cooling effect and predict the magnitude of the cooling effect.

Irrigation amount is a key factor that influences the level of cooling benefit of irrigating urban green spaces (Cheung et al., 2022b). As opposed to agricultural irrigation which aims to maximise plant water use efficiency (Zhang et al., 2022), urban green space irrigation can be used to maximise the cooling benefits in these green spaces in addition to meeting plant water requirements A modelling study in Adelaide, Australia predicted that the relationship between daily mean air temperature reduction and irrigation amount was almost linear, providing 0.5°C from 5 mm d^{-1} up to 1.8°C cooling from 15 mm d^{-1} during a heatwave (Broadbent et al., 2018a). The same study predicted that additional cooling benefits from increasing irrigation above 15 mm d^{-1} were negligible as evapotranspiration was no longer limited by the supply of soil moisture, but rather the evaporative demand of the atmosphere, i.e., weather conditions. Most studies have focused on the cooling benefits of irrigation during heatwaves (Broadbent et al., 2018a; Daniel et al., 2018; Gao et al., 2020), the impacts of different daily irrigation amounts on the cooling benefits of irrigation in normal summer conditions are not well understood. Since the maximum cooling benefit that can be achieved with a reasonable irrigation amount can vary with background climate and weather conditions (Cheung et al., 2022b), it is important to understand impacts of daily irrigation amount on the cooling benefits of irrigation to inform the management of urban green spaces for optimal cooling.

In this study, a replicated field experiment was first set up to measure the impacts irrigating 36 m^2 plots of turf with different amounts of water on microclimate, soil moisture content and soil temperature for two consecutive summers in Melbourne, Australia. The experimental data were used to test and evaluate the performance of a mechanistic urban ecohydrological model, UT&C (Meili et al., 2020). UT&C was subsequently used to model the impacts of irrigating turf on surface energy balance and evapotranspiration processes, as well as the impacts of different daily irrigation amounts on irrigation cooling benefits in normal summer conditions. This study is unique because a replicated experiment with controlled treatments was conducted to disentangle certain contributory factors and mechanisms of irrigation cooling effect. Both above- and below-ground observations were made in the experiment to evaluate the performance of UT&C comprehensively. This study can contribute to the development of climate adaptation strategies for cities because it directly measured and assessed the cooling benefits of a promising cooling strategy.

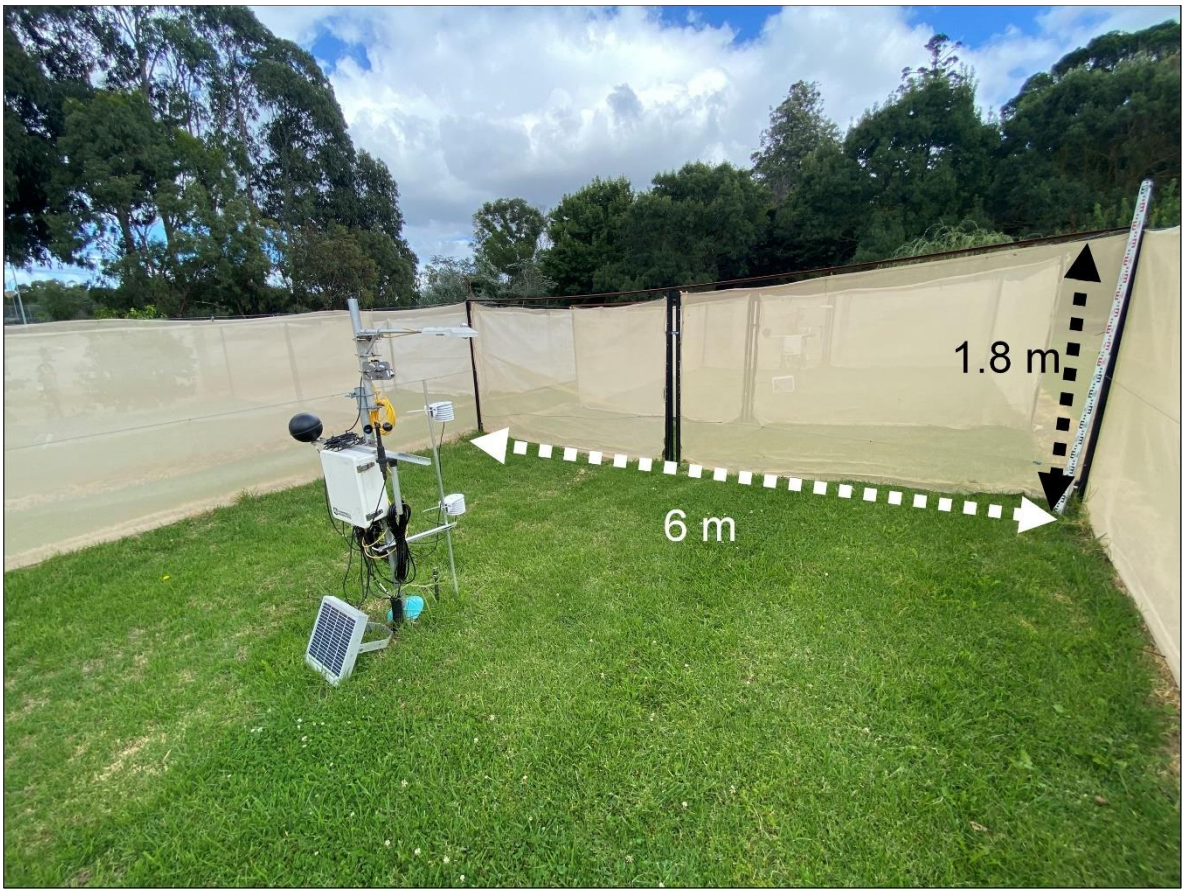

Fig. 6.1. Six identical plots (6×6 m) were set up at the Burnley Campus of the University of Melbourne. Three were unirrigated and three received 4 mm of irrigation at 13:00 every day. Each plot was surrounded by 1.8-m tall 70% shade cloth (SOLARSHADE™) and a climate station was installed at the centre of each plot to continuously monitor the microclimate, soil temperature and soil moisture content.

6.2. Methods and materials

6.2.1. Experiment to measure impacts of irrigating turf on microclimate and soil temperature

A field experiment was set up at the Burnley Campus of the University of Melbourne, Australia (–37.8, 145.0) to collect testing and model evaluation data. The site is classified as Local Climate Zone B (scattered trees) (Demuzere et al., 2022) under the local climate zone classification system (Stewart and Oke, 2012). The experiment consisted of six identical plots (6×6 m, 36 m^2). Three of the plots were irrigated 13:00 local time every day and the remaining three were unirrigated. In each plot, four 90° Hunter Rotator nozzles (MP-1000) were installed at the corners and one 360° nozzle at the centre to deliver the irrigation. Since a climate station was installed at the centre of each plot, the nozzles were carefully adjusted such that the water did not hit the sensors of the climate

station (Fig. 6.1). The irrigation volumes were measured by Nymet flow sensors. A 1.8 m tall 70% shade cloth (SOLARSHADE™) was used to enclose the plots to reduce air mixing between the plots and the environment (Fig. 6.1). The plot ground surface was covered by turfgrass, which was mowed to approximately 50 mm tall every two weeks. The dominant grass species was Kikuyu (*Pennisetum Clandestinum*). The top soil (5–10 cm) was sandy loam (sand:silt:clay = 0.7:0.2:0.1) and the subsoil (50–55 cm) was sandy clay (sand:silt:clay = 0.5:0.1:0.4). The organic matter content of the soil was approximately 0.06 (6 %).

In each plot, air temperature, vapour pressure, and wind speed were continuously measured at a height of 1.1 m above the ground and soil moisture content and soil temperature continuously measured at a soil depth of 0.05 m. In one irrigated and one unirrigated plot, incoming and outgoing longwave and shortwave radiation and turf surface temperature were also measured. A reference climate station was located within 30 m of these six experimental plots to provide reference climate conditions and forcing data for the model. All variables were measured every 10 seconds and 1 minute averages were logged. The measurement heights and specifications of the climate and soil instruments were listed in Table 6.1. The model testing data set (2021-01-21 to 2021-03-02, 41 days) consisted of one irrigated (4 mm d^{-1}) and one unirrigated plot. The model evaluation data set (2022-01-28 to 2022-03-06, 38 days) consisted of three irrigated and three unirrigated plots; the irrigated plots received 2 mm d^{-1} from 2022-01-28 to 2022-02-08 and 4 mm $d^{-1}$from 2022-02-09 to 2022-03-06. The model testing data set was used to identify the optimal levels of six important parameters for the study site (explained in section 6.2.3) and the model evaluation data set was used to evaluate the model performance (explained in section 6.2.4).

Melbourne has a temperate oceanic climate (Köppen climate classification: Cfb). The summer (Dec–Feb) of Melbourne is warm and dry. The mean summer air temperature is 26.2°C and the mean summer rainfall is 155.3 mm (Bureau of Meteorology, 2023a). In the model testing period, the mean air temperature was 20.0°C and the total rainfall was 66 mm (Fig. S6.1). There were eight days with maximum air temperature >30.0°C. In the model evaluation period, the mean air temperature was 21.6°C and the total rainfall was 120.4 mm (Fig. 6.2). There were 23 days with maximum air temperature >30.0°C.

Table 6.1. Specifications of the climate and soil instruments.

Location	Model and brand	Variable	Accuracy	Height/depth (m)
Reference	ATMOS14, METER	Air temperature	±0.2°C	1.1
		Vapour pressure	±1.5% @ 25°C	1.1
	CNR4, Kipp & Zonen	Incoming longwave radiation (4.5–42 µm)	<10% (daily total)	1.5
		Incoming shortwave radiation (300–2800 nm)	<5% (daily total)	
		Outgoing longwave radiation (4.5–42 µm)	<10% (daily total)	
		Outgoing shortwave radiation (300–2800 nm)	<5% (daily total)	
	CS650, Campbell Scientific	Soil moisture content	±3%	–0.05
		Soil temperature	±1°C	
	SI-111, Apogee	Turf surface temperature	±0.2°C (−10°C to +65°C)	1.5
	05103, Campbell Scientific	Wind speed	±0.3 m/s	2.0
	HMP155, Campbell Scientific	Air temperature	±(0.055+0.0057×air temperature)	2.0
		Relative humidity	±1%	2.0
	TB4, Campbell Scientific	Rainfall	±2%	2.0

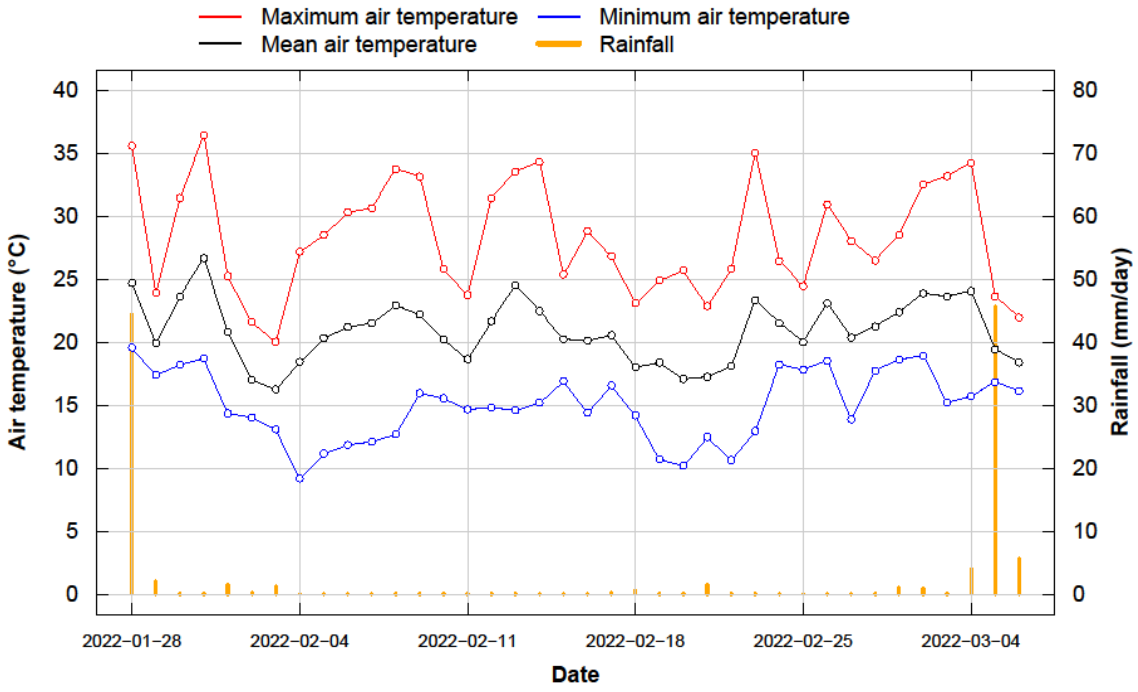

Fig. 6.2. Daily minimum, mean and maximum air temperatures and rainfall of the model evaluation period (2022-01-28 to 2022-03-06, 38 days).

6.2.2. Model description

Urban Tethy-Chloris (UT&C) is mechanistic model that combines an urban canyon scheme and an ecohydrological model (Meili et al., 2020). UT&C solves the energy and water budgets on a neighbourhood scale. The simulation space of UT&C is a two-dimensional infinite urban canyon the edges of which are defined by building height and canyon width. The ground surface can be a combination of vegetated (grass), bare soil or impervious fractions. UT&C can simulate the structural, optical, interception and physiological properties separately for grass and/or trees. Transpiration of grass (and/or trees) is calculated based on meteorological conditions, soil moisture accessed by roots and plant photosynthetic activity (Meili et al., 2020).

UT&C can partition rainfall or sprinkler irrigation into canopy interception and throughfall on to soil surface. The fraction of water intercepted by plant canopy is calculated following the Rutter model (Fatichi et al., 2012; Rutter et al., 1971). The plant canopy is further divided into a wet and a dry fraction (Deardorff, 1978). Transpiration only occurs on the dry fraction while evaporation occurs on the wet fraction. If rainfall or irrigation exceeds the infiltration rate of the soil, ponded surface water is formed which eventually evaporates. Evaporation also occurs from the soil surface below the plant canopy. Effectively, in the absence of trees, UT&C partitions evapotranspiration into four processes, namely evaporation from grass canopy interception, evaporation from soil surface, evaporation from ponding surface water and transpiration of grass. UT&C can simulate sprinkler irrigation (irrigate onto the plant canopy) or drip irrigation (irrigation onto the ground surface) in each time step. UT&C is suitable for our irrigation simulation study because it allows irrigation to be applied onto the plant canopy surface, at a precise time and a precise amount, includes detailed representations of the interactions between vegetation and hydrology, and enables partitioning of evapotranspiration.

UT&C calculates a) air temperature and vapour pressure at 2 m above ground, b) turf surface temperature and c) soil temperature by solving the urban energy (Equation 6.1) and water (Equation 6.2) budgets:

$$P + Ir = R + E + Lk + \Delta S (kgm^{-2}s^{-1}) \quad (6.2)$$

where P is the rainfall [kg m^{-2} s^{-1}], Ir the irrigation [kg m^{-2} s^{-1}], R the surface runoff [kg m^{-2} s^{-1}], E the evapotranspiration [kg m^{-2} s^{-1}], Lk the deep drainage [kg m^{-2} s^{-1}] and ΔS the change in soil water storage [kg m^{-2} s^{-1}]. A detailed model description can be found in Meili et al. (2020).

6.2.3. Model set up for this irrigation study

For our UT&C simulations we set up a shallow canyon (width = 50 m; building height = 5 m) with grass-covered ground surface to mimic the open vegetated area of the experimental plots (Table S6.1). The height of the grass was set to 0.1 m which was the average height of the grass during the experiments (Table S6.2). We used the optical and physiological parameters for grass from Meili et al. (2020), such as canopy light extinction coefficient, root length index, soil water potential at 50% stomatal closure and canopy nitrogen decay coefficient. We also used the soil, interception and runoff parameters from (Meili et al., 2020), such as hydraulic conductivity and maximum interception capacity (Table S6.3). Anthropogenic heat input was assumed to be zero for the site (Table S6.4). We identified six important parameters that were highly site-specific and tested them to determine the optimal parameter settings to simulate our experiment site. The six parameters are: (i) initial soil moisture content at the start of the simulation, (ii) the depth below which soil moisture content is kept at a fixed value (here at field capacity) [mm], (iii) ground soil composition (i.e. fraction of sand, clay and organic material) [–], (iv) empirical coefficient governing stomatal closure as a function of vapour pressure deficit [Pa], (v) root depth (95^{th} percentile) [mm], and (vi) maximum rubisco capacity at 25°C at the leaf scale [μmol CO_2 m^{-2} s^{-1}). Four levels of each parameter were used to run the model with the forcing data of the model testing period (2021-01-21 to 2021-03-02, 41 days). Root mean square errors were calculated between the hourly mean modelled air temperature difference between the irrigated and unirrigated scenarios and the measured air temperature differences between the irrigated and unirrigated plots. The level that resulted in the smallest root mean square error (Table S6.5) was used in the model evaluation (section 6.3.1) and subsequent analysis of the impacts of irrigation on surface energy balance (section 6.3.2) and the impacts of daily irrigation amounts on cooling benefits (section 6.3.3).

We used hourly meteorological data to force the model. Rainfall and incoming shortwave radiation were directly measured at the site (Table 6.1). The measured data at the reference climate station (Fig. 6.1) and the ERA5 reanalysis data (1000 hPa) (Hersbach et al., 2020) were interpolated to obtain the air temperature and relative humidity at 80 m above sea level, i.e. the atmospheric reference height of the model. Wind speed was extrapolated from the measurements at the reference

climate station using the logarithmic wind profile (Mahat et al., 2013). The zero-plane displacement height and momentum roughness length of the canyon were calculated following Kent et al. (2017) and Macdonald et al. (Macdonald et al., 1998). Atmospheric pressure was calculated according to Portland State Aerospace Society (2004). Two different sets of forcing data were used, one for the model testing period (2021-01-21 to 2021-03-02, 41 days) and one for the model evaluation period (2022-01-28 to 2022-03-06, 38 days). Sprinkler irrigation was applied daily at 13:00 local time and the irrigation amount was the same as the experiment, i.e., 4 mm d^{-1} for the model testing period, and 2 mm d^{-1} (2022-01-28 to 2022-02-08) and 4 mm d^{-1} (2022-02-09 to 2022-03-06) for the model evaluation period.

6.2.4. Model evaluation

The UT&C model was evaluated qualitatively by comparing average diurnal cycles, times series and scatter plots of the modelled output variables to those measured. The UT&C model was also evaluated quantitatively using metrics of coefficient of determination (R^2), mean bias error (MBE), and root mean square error (RMSE). The evaluated model output variables included air temperature (2 m), vapour pressure (2 m), turf surface temperature and soil temperature (depth = 0–0.1 m). The evaluation was done separately for the irrigated scenario, unirrigated scenario and the difference between the two (irrigated–unirrigated). Since the impacts of irrigation on microclimate and soil temperature were distinctly different in the day and at night, the evaluation was also done separately for daytime (10:00–16:59) and night-time (21:00–05:59) periods where applicable. The model evaluation period was from 2022-01-28 to 2022-03-06 (38 days).

There were anomalies in the modelled night-time data in the model evaluation period. The anomalies were due to the failure of the energy balance to converge when the model tried to solve a non-linear equation with multiple variables (Fig. S6.4 and Fig. S6.5). We excluded the affected periods in the subsequent analysis (31 out of 912 hours in section 6.3.2 and 56 out of 912 hours in section 6.3.3).

6.2.5. Modelling the impacts of irrigating turf on surface energy balance and evapotranspiration processes

The model outputs of latent heat flux, sensible heat flux and soil heat flux of the irrigated and unirrigated scenarios were examined in an average diurnal cycle to understand the impacts of irrigating turf on the surface energy balance. The model outputs also partition evapotranspiration into four processes, namely 1) evaporation from canopy interception, 2) evaporation from soil surface, 3)

evaporation from ponding surface water, and 4) transpiration. The average diurnal cycle of these processes was examined, and their daily means were calculated and compared in a table.

6.2.6. Modelling the impacts of different daily irrigation amounts on cooling benefits

In a separate simulation, the model was used to predict the impacts of different daily irrigation amounts, namely 2, 4, 6, 8, 15 and 30 mm, on the cooling benefits provided under non-heatwave summer conditions. Sprinkler irrigation was applied daily at 13:00 local time for all six irrigation amounts. The predictions were made using the forcing data of the model evaluation period (2022-01-28 to 2022-03-06, 38 days). The cooling benefits were calculated as the differences in air, turf surface and soil temperatures and air vapour pressure between the irrigated and unirrigated scenarios (Δ = irrigated–unirrigated). The mean daily daytime (10:00–16:59) and night-time (21:00–05:59) cooling benefits and their 95% confidence intervals were calculated and compared in plots showing the means and error bars.

The workflow of this study is summarised in Fig. 6.3.

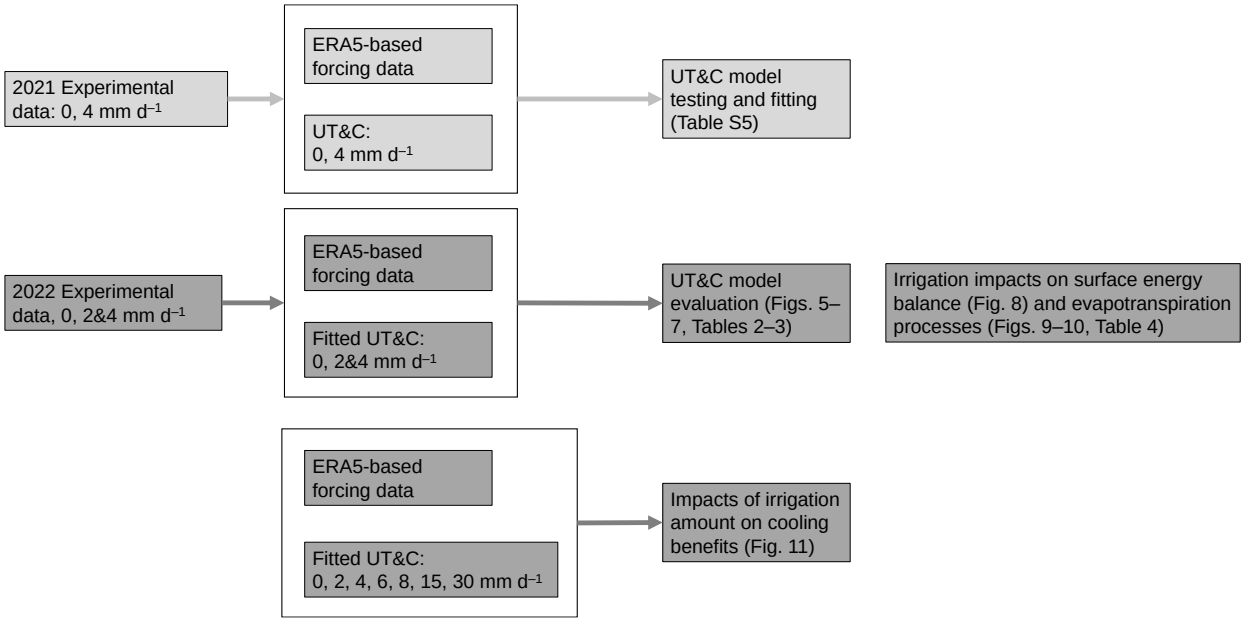

Fig. 6.3. Workflow of this study. The 2021 experimental data were used to test the UT&C model and identify the best-fit parameters, which were used in subsequent simulations of 2022. The 2022 experimental data were used for model evaluation for air temperature, vapour pressure, turf surface temperature and soil temperature. From the model evaluation dataset, the irrigation impacts on surface energy balance and evapotranspiration processes were examined. In a separate simulation using the 2022's forcing data, we examined the impacts of different irrigation amounts on cooling benefits.

6.3. Results

6.3.1. Model evaluation

UT&C predicted the soil moisture content of the irrigated and unirrigated plots well, except after large rainfall events, namely 2022-01-28 (44.4 mm) and 2022-03-05 (45.6 mm) (Fig. 6.4). Small rainfall events, e.g., 2022-02-18 (0.6 mm), were registered in the modelled soil moisture content at a depth of 0.05 m, but not measured by the soil moisture sensors at the same depth. The soil moisture content of the irrigated and unirrigated plots (scenarios) decreased during the 2-mm irrigation period. The soil moisture content of the irrigated plot (scenario) increased during the 4-mm irrigation period up to a maximum soil moisture content of 35 %.

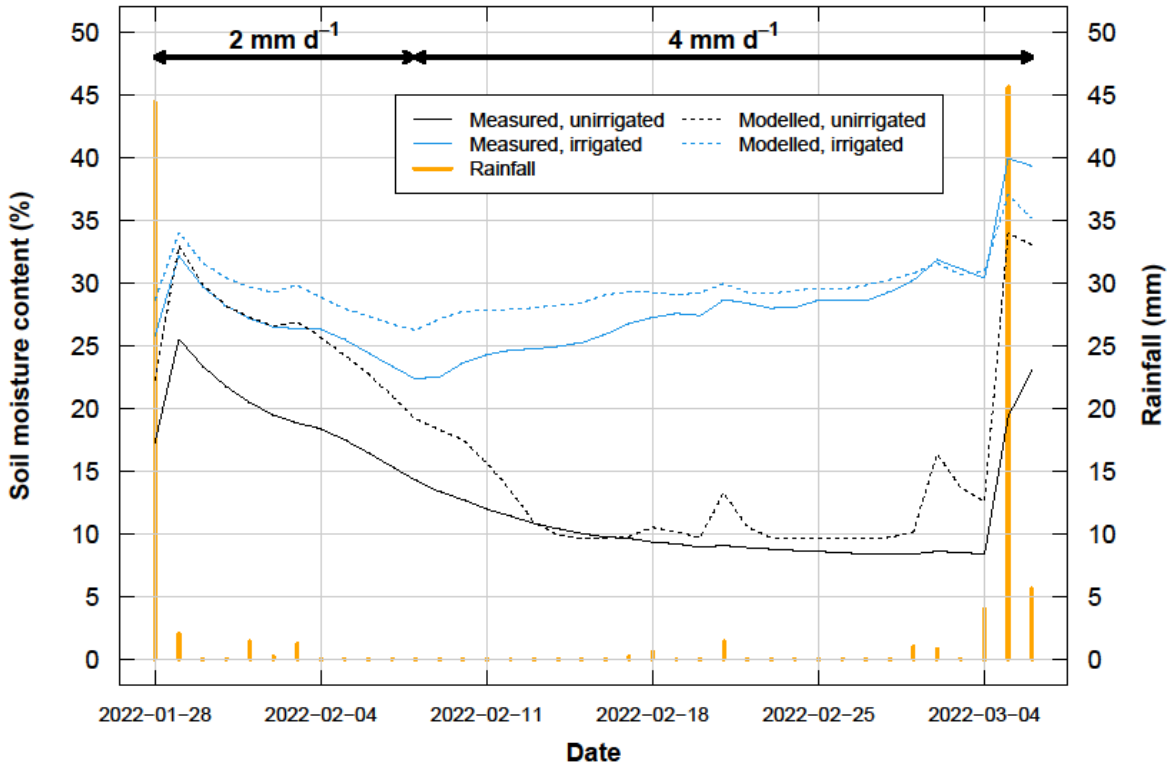

Fig. 6.4. Comparison of modelled (first soil layer, 0–0.10 m below ground) and measured (0.05 m below ground) daily mean soil moisture content in the model evaluation period (2022-01-28 to 2022-03-06, 38 days). The turf was irrigated 2 mm d^{-1} from 2022-01-28 to 2022-02-07 and 4 mm d^{-1} from 2022-02-08 to 2022-03-06 at 13:00 local time. In the experiment, the 2-mm irrigation occurred from 13:00 to 13:11, and the 4-mm occurred from 13:00 to 13:23. In the simulation, both 2 and 4 mm were applied to the 13:00–13:59 time step.

The measured air temperatures, vapour pressures and soil temperatures of the three unirrigated plots (Fig. S6.2) and the three unirrigated plots (Fig. S6.3) were similar. Therefore, the

mean and standard error of the three replicates were used to compare against the modelled results (Fig. 6.5 and Fig. 6.6).

UT&C predicted the average diurnal cycle of air temperature of the irrigated plot well (Fig. 6.5a). However, the sharp reduction of air temperature measured at 13:00 due to irrigation was not captured by the model (Fig. 6.5a). Both the modelled daytime (10:00–16:59) (Fig. 6.5b) and night-time (21:00–05:59) (Fig. 6.5c) mean air temperatures closely followed the measured ones. The modelled and measured air temperature were highly correlated in the daytime period (R^2=0.93) and moderately correlated in the night-time period (R^2=0.69) (Fig. 6.4 and Table 6.2). The daytime (night-time) mean bias error and root mean square error of air temperature were -1.7°C (-1.2°C) and 2.1°C (2.1°C), respectively. UT&C over-predicted the vapour pressure of the irrigated plot throughout the day (Fig. 6.5e–h). The modelled and measured vapour pressure were moderately correlated in the daytime (R^2=0.73) and night-time (R^2=0.45) periods (Table 6.2). The daytime (night-time) mean bias error and root mean square error of vapour pressure were 0.4 kPa (0.2 kPa) and 0.5 kPa (0.3 kPa), respectively. UT&C predicted the turf surface temperature of the irrigated plot well (Fig. 6.5g–l). However, the sharp reduction at 13:00 due to irrigation was only captured by the measurement but not the model (Fig. 6.5g). The modelled and measured turf surface temperature were more highly correlated in the daytime period (R^2=0.89) than night-time period (R^2=0.60) (Table 6.3). The daytime (night-time) mean bias error and root mean square error of turf surface temperature were -1.0°C (0.9°C) and 1.7°C (2.2°C), respectively. UT&C under-predicted the soil temperature of the irrigated plot, particularly during the night-time (Fig. 6.5m–p). The modelled and measured soil temperature were moderately correlated for both daytime (R^2=0.70) and night-time (R^2=0.72) periods (Table 6.2). The daytime (night-time) mean bias error and root mean square error of soil temperature were -2.0°C (-5.2°C) and 2.6°C (5.4°C), respectively.

The performance of UT&C in predicting air temperature (Fig. 6.6a–d), vapour pressure (Fig. 6.6e–h) and soil temperature (Fig. 6.6m–p) of the unirrigated plot was similar to that of the irrigated plot (Fig. 6.5). However, UT&C under-predicted the daytime (10:00–16:59) and over-predicted the nigh-time (21:00–05:59) turf surface temperatures of the unirrigated scenario to a larger extent (Fig. 6.6g–l and Table 6.2).

Table 6.2. The performance of UT&C in predicting the daytime (10:00–16:59) and night-time (21:00–05:59) hourly mean air temperature, vapour pressure, turf surface temperature and soil temperature of the irrigated scenario and unirrigated scenario, as well as the differences between the irrigated and unirrigated scenarios. The model performance is evaluated by coefficient of determination (R^2), mean bias error (MBE) and root mean square error (RMSE). The evaluation period was from 2022-01-28 to 2022-03-06 (912 hours).

			Daytime (10:00–16:59)			Night-time (21:00–05:59)		
	Variable	Unit	R^2	MBE	RMSE	R^2	MBE	RMSE
Irrigated	Air temperature	°C	0.93	-1.7	2.1	0.69	-1.2	2.1
	Vapour pressure	kPa	0.73	0.4	0.5	0.45	0.2	0.3
	Turf surface temperature	°C	0.89	-1.0	1.7	0.60	0.9	2.2
	Soil temperature	°C	0.70	-2.0	2.6	0.72	-5.2	5.4
Unirrigated	Air temperature	°C	0.92	-2.1	2.5	0.68	-1.1	2.1
	Vapour pressure	kPa	0.73	0.4	0.5	0.45	0.2	0.3
	Turf surface temperature	°C	0.88	-3.2	3.7	0.54	1.4	2.7
	Soil temperature	°C	0.66	-1.5	2.4	0.60	-4.9	5.1
Irrigated–Unirrigated	Air temperature	°C	0.29	0.1	0.3	0.01	-0.2	1.1
	Vapour pressure	kPa	0.12	0.1	0.1	0.00	0.0	0.2
	Turf surface temperature	°C	0.19	1.5	2.0	0.03	-0.6	1.5
	Soil temperature	°C	0.08	-0.9	1.0	0.09	-0.6	1.0

Regarding the differences between the irrigated and unirrigated turf, i.e., the impacts of irrigation, UT&C predicted the reduction in daytime (10:00–16:59) air temperature well (Fig. 6.7a–b). Both the modelled and measured reductions in daytime mean air temperature were –0.3°C and –0.4°C, respectively (Table 6.3). UT&C predicted no impact on night-time (21:00–05:59) air temperature by irrigation, while we measured a small increase in night-time air temperature (Fig. 6.7a and 6.7c) (Table 6.3). UT&C predicted an increase in both daytime and night-time vapour pressure by irrigation, while we measured almost no impact on vapour pressure (Fig. 6.7e–h) (Table 6.3). UT&C predicted a small reduction in daytime mean turf surface temperature (–0.8°C), while we measured a large reduction (–2.3°C) (Fig. 6.7g) (Table 6.3). UT&C predicted the diurnal variation of soil temperature well (Fig. 6.7m). The mean bias error and root mean square error of daytime air temperature were 0.1°C and 0.3°C, respectively (Table 6.2), which were in the same order of magnitude of the modelled (–0.3°C) and measured (–0.4°C) reductions in daytime mean air temperature (Table 6.3), and the same applied to daytime turf surface temperature.

Table 6.3. The measured and modelled impacts of irrigating turf on daytime (10:00–16:59) and night-time (21:00–05:59) mean air temperature, vapour pressure, turf surface temperature and soil temperature.

		Daytime (10:00–16:59)		Night-time (21:00–05:59)	
Variable	Unit	Modelled	Measured	Modelled	Measured
Air temperature	°C	**-0.3**	**-0.4**	0.0	**0.1**
Vapour pressure	kPa	**0.05**	0.00	**0.04**	**-0.01**
Turf surface temperature	°C	**-0.7**	**-2.3**	0.0	**0.6**
Soil temperature	°C	**-0.5**	**0.4**	**-0.2**	**0.3**

Significant impacts ($p<0.05$, *t*-test) are in bold.

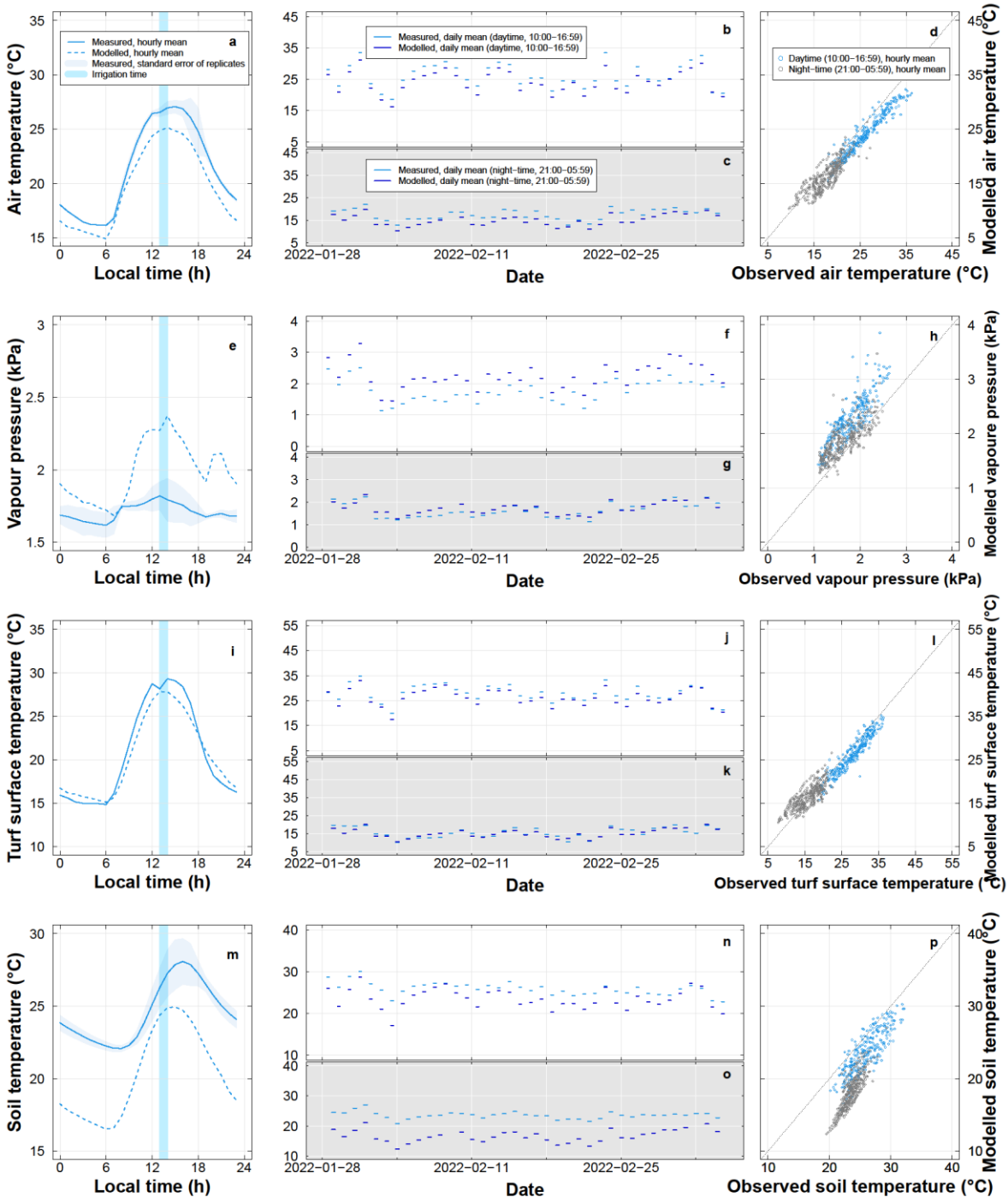

Fig. 6.5. Model evaluation that compared the modelled and the measured (a–c) air temperature, (d–f) vapour pressure (g–i) turf surface temperature, (j–l) soil temperature of the irrigated scenario (plot). The modelled and measured data were compared in terms of their average diurnal cycles (left column), daytime and night-time daily means (middle column) and scatter plot of hourly means (right column). In the middle column, the broken lines were a time series split into daytime (10:00–16:59, white panels) and night-time (21:00–05:59, grey panels). The model evaluation period was from 2022-01-28 to 2022-03-06.

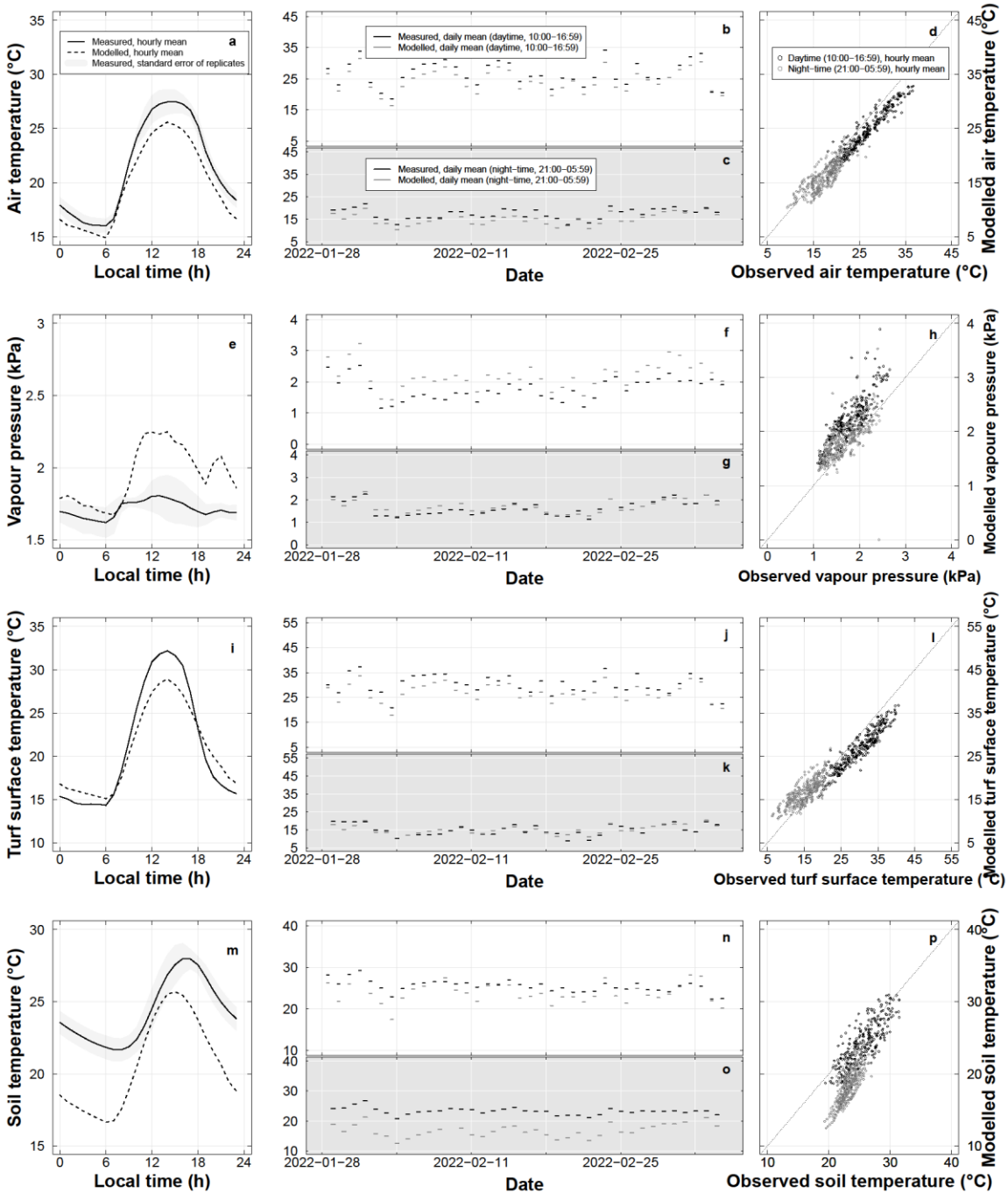

Fig. 6.6. Model evaluation that compared the modelled and the measured (a–c) air temperature, (d–f) vapour pressure (g–i) turf surface temperature, (j–l) soil temperature of the unirrigated scenario (plot). The modelled and measured data were compared in terms of their average diurnal cycles (left column), daytime and night-time daily means (middle column) and scatter plot of hourly means (right column). In the middle column, the broken lines were a time series split into daytime (10:00–16:59, white panels) and night-time (21:00–05:59, grey panels). The model evaluation period was from 2022-01-28 to 2022-03-06.

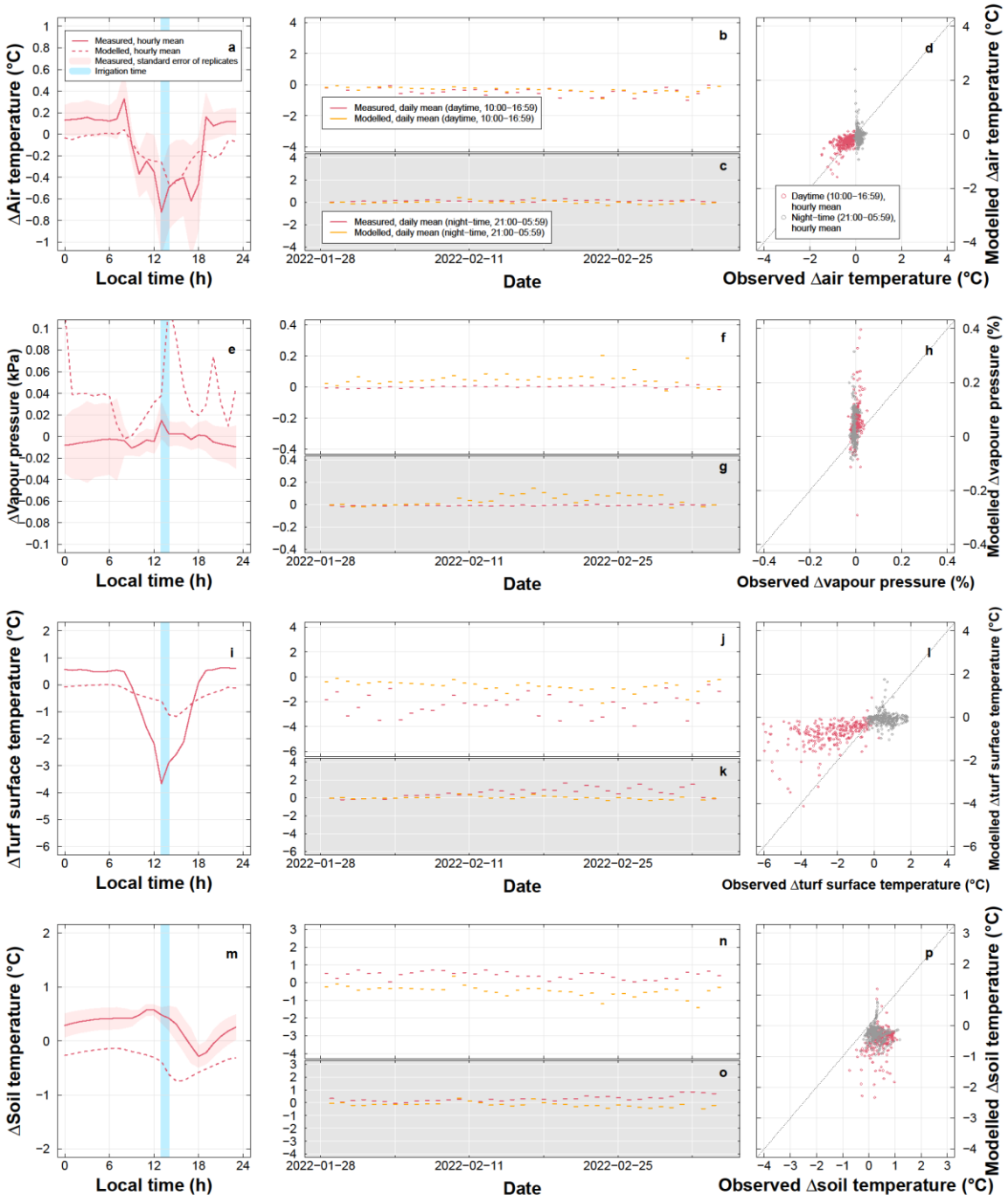

Fig. 6.7. Model evaluation that compared the modelled differences between the irrigated and unirrigated scenarios (Δ = irrigated – unirrigated) and the measured differences between the irrigated and unirrigated plots in (a–c) air temperature, (d–f) vapour pressure (g–i) turf surface temperature, (j–l) soil temperature. The modelled and measured data were compared in terms of their average diurnal cycles (left column), daytime and night-time daily means (middle column) and scatter plot of hourly means (right column). In the middle column, the broken lines were a time series split into daytime (10:00–16:59, white panels) and night-time (21:00–05:59, grey panels). The model evaluation period was from 2022-01-28 to 2022-03-06.

6.3.2. Modelling the impacts of irrigating turf on surface energy balance and evapotranspiration processes

UT&C predicted that irrigation increased latent heat flux and reduce sensible heat flux and ground heat flux (less energy flowing into the ground) from approximately 12:00 to 16:59 local time (Fig. 6.8). At 14:00, irrigation increased latent heat flux by 42.5 W m^{-2} and reduced sensible heat flux and ground heat flux by 13.8 W m^{-2} and 22.0 W m^{-2}, respectively. Irrigation did not change the latent heat flux, sensible heat flux and ground heat flux from 20:00 to 09:59.

UT&C predicted that irrigation increased the daily total evaporation from canopy interception and soil surface by 0.2 and 0.6 mm d^{-1}, respectively (Table 6.4). Irrigation reduced the daily total transpiration by 0.6 mm d^{-1}. These changes occurred primarily in the two hours after irrigation (13:00–14:59 local time) (Fig. 6.9). Irrigation had no impact on the daily total evaporation from surface water (Table 6.4). Overall, irrigation increased the total evapotranspiration by 0.2 mm d^{-1} and increased the evaporation to evapotranspiration ratio from 0.06 to 0.30.

The sharp reduction in transpiration in the irrigated scenario occurred from 14:00 to 15:59 local time (Fig. 6.9c) and coincided with the modelled increase in intercepted water on leaf surfaces (Fig. 6.10a). Apart from this period, irrigation also slightly reduced transpiration in other times of the day, which is caused by a smaller leaf-to-air vapour pressure deficit (Fig. 6.10b) due to a lower modelled leaf temperature (=turf surface temperature in UT&C) (Fig. 6.10c).

Table 6.4. Modelled mean daily total evaporation from canopy interception, evaporation from soil surface, evaporation from ponding surface water, transpiration and total evapotranspiration of the unirrigated and irrigated scenarios, and the difference between them. The data from the model evaluation period (2022-01-28 to 2022-03-06) were used.

	Daily total (mm)		
Process	Unirrigated scenario	Irrigated scenario	Irrigated–Unirrigated
Evaporation from canopy interception	0.1	0.3	0.2
Evaporation from soil surface	0.1	0.7	0.6
Evaporation from ponding surface water	0.0	0.0	0.0
Transpiration	2.9	2.3	–0.6
Total evapotranspiration	3.1	3.3	0.2

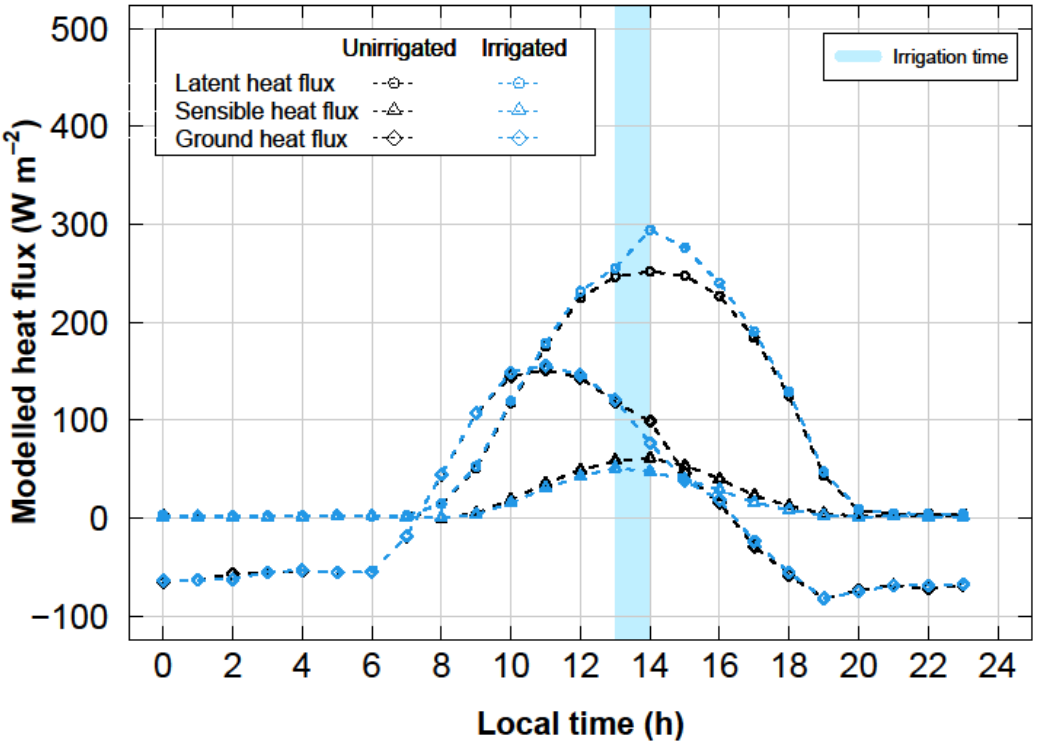

Fig. 6.8. The average diurnal cycle of modelled latent heat flux, sensible heat flux and ground heat flux of the irrigated and unirrigated scenarios. Irrigation was applied at 13:00, which increased latent heat flux and ground heat flux from 14:00 to 15:59. The data from the model evaluation period (2022-01-28 to 2022-03-06) were used.

6.3.3. Modelling the impacts of different daily irrigation amounts on cooling benefits

UT&C predicted that irrigation of the simulated amounts (2 to 30 mm d^{-1}) would all significantly reduce daytime (10:00–16:59) mean air temperature ($p < 0.05$) (Fig. 6.11a). Irrigating 2, 4, 6, 8, 15 and, 30 mm d^{-1} at 13:00 local time would reduce daytime mean air temperature by –0.2±0.0, –0.4±0.1, –0.5±0.1, –0.5±0.1, –0.6±0.1, and –0.7±0.1°C, respectively. Irrigation would significantly increase night-time (21:00–05:59) mean air temperature if the irrigation amounts were ≥8 mm d^{-1}. Irrigation of these amounts would also significantly increase daily, daytime and night-time mean vapour pressure by a small amount (<0.1 kPa) ($p < 0.05$) (Fig. 6.11b). UT&C predicted that irrigation of these amounts would significantly reduce daily and daytime mean turf surface temperature ($p < 0.05$) (Fig. 6.11c). Irrigation of these amounts would also significantly reduce daily, daytime, and night-time mean soil temperature (Fig. 6.11d). Overall, an increasing daily irrigation amount would

lead to a stronger daytime cooling benefit, but the additional cooling benefits would greatly reduce when the daily irrigation amounts increase beyond 4 mm d^{-1}.

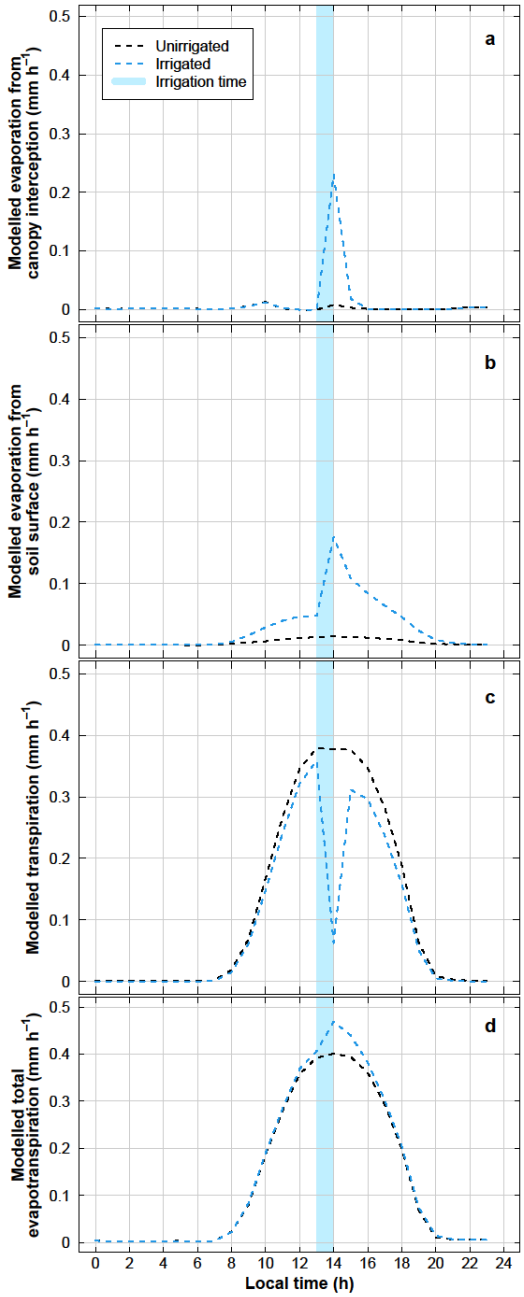

Fig. 6.9. The average diurnal cycle of modelled mean (a) evaporation from canopy interception, (b) evaporation from soil surface, (c) transpiration, and (d) total evapotranspiration. The evaporation from surface water was not plotted because it was always closed to zero. The data from the model evaluation period (2022-01-28 to 2022-03-06) were used.

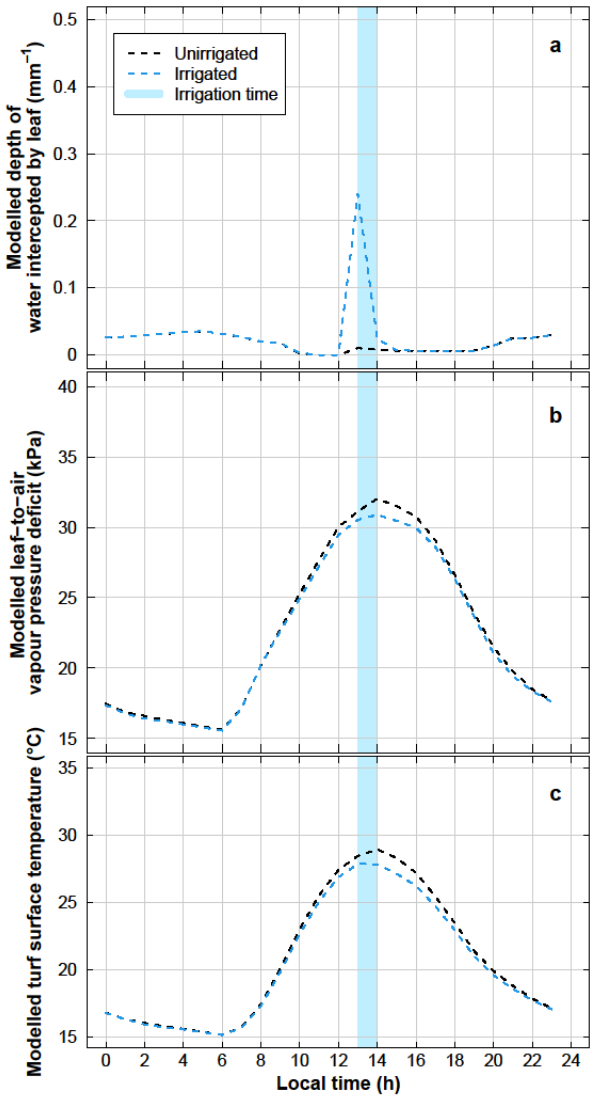

Fig. 6.10. The average diurnal cycle of modelled (a) depth of water intercepted by leaf, (b) leaf-to-air vapour pressure deficit, and (c) turf surface temperature of the irrigated and unirrigated scenarios. Irrigation was applied at 13:00, which reduced transpiration from 14:00 to 15:59 because transpiration did not occur on the leaf surface with intercepted water in UT&C. Irrigation also reduced transpiration in other times of the day because it reduced leaf-to-air vapour pressure deficit due to reduced leaf temperature (=turf surface temperature in UT&C). The data from the model evaluation period (2022-01-28 to 2022-03-06) were used.

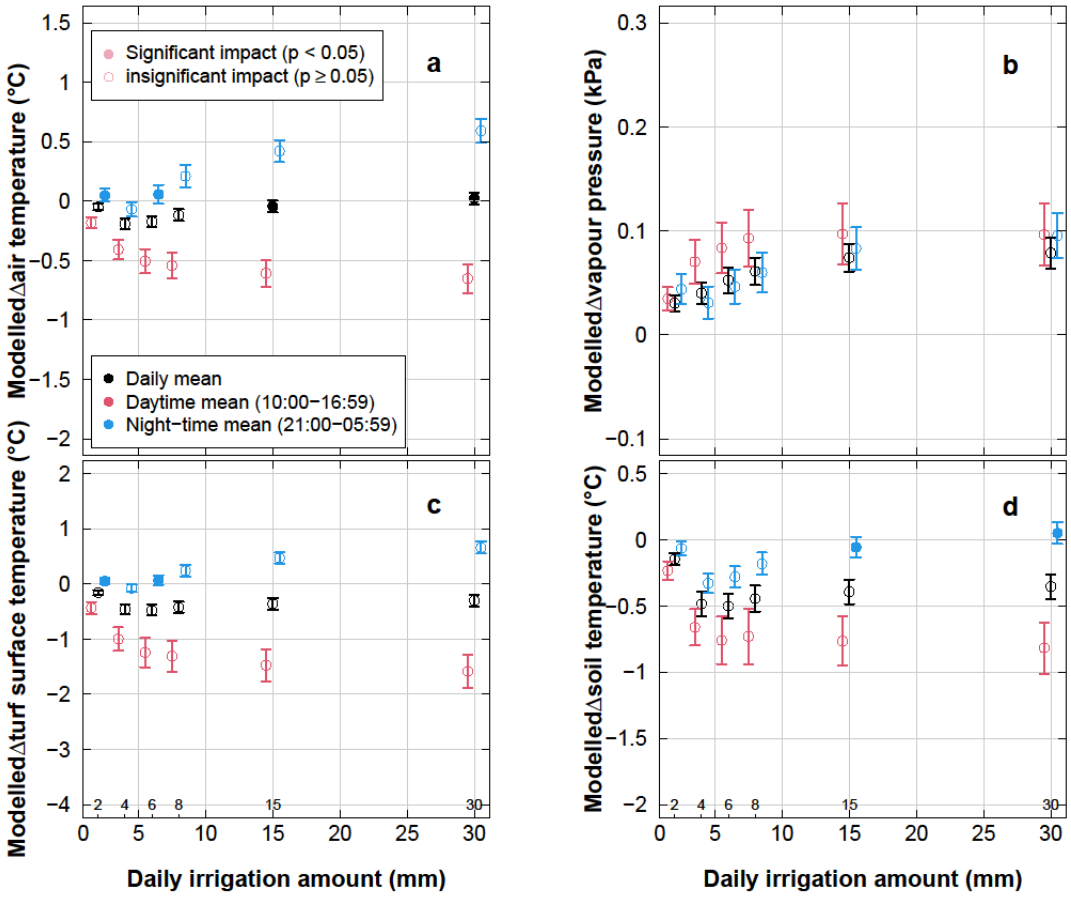

Fig. 6.11. Modelled impacts of different daily irrigation amount (2, 4, 6, 8, 15 and 30 mm) on (a) air temperature, (b) vapour pressure, (c) turf surface temperature, and (d) soil temperature. The impacts were calculated as the difference between the irrigated and unirrigated scenarios (Δ = irrigated – unirrigated). The circles represented the mean impacts in the simulation period. An open circle represented a significant impact ($p < 0.05$, *t*-test) while a closed circle an insignificant impact ($p \geq 0.05$, t-test). The error bars represent the 95% confident intervals. The overlapping of two error bars is indicative of an insignificant difference ($p \geq 0.05$) between the two means. The forcing data of the model evaluation period (2022-01-28 to 2022-03-06, 38 days) was used in this simulation.

6.4. Discussion

6.4.1. Impacts of irrigating turf on surface energy balance and evapotranspiration processes

In this study, both the measurements and the UT&C model agreed that irrigating turf can reduce daytime air and turf surface temperatures. This daytime cooling effect was attributed to an increase in total daytime evapotranspiration. The model predicted that the increase in daytime evapotranspiration was primarily driven by the increase in evaporation from soil surface and from intercepted water on the plant canopy. Other studies have also concluded that irrigating urban vegetated surfaces would increase evapotranspiration (Broadbent et al., 2018a; Daniel et al., 2018;

Gao et al., 2020). Using the Town Energy Balance model, Daniel et al. (2018) predicted that the increase in daytime evapotranspiration from sprinkler irrigation was primarily driven by an increase in the transpiration of plant (up to 0.2 mm h^{-1}), which was different from the prediction of the UT&C model in the current study. The UT&C model predicted that sprinkler irrigation would reduce the transpiration of turf for two reasons. First, a fraction of the turf canopy would intercept the water and stop transpiring until the intercepted water is evaporated (Meili et al., 2020). In the UT&C model, the plant canopy is divided into a wet and a dry fraction after rainfall or irrigation (Deardorff, 1978). Transpiration only occurs on the dry fraction while evaporation occurs on the wet fraction. The wet fraction may be overestimated in UT&C at the 13:00 timestep when irrigation is applied because part of the water is likely to evaporate when passing through the air (droplet evaporation) and may not reach the plant canopy as simulated in the model (Fig. 6.10a). Second, the vegetated ground surface and grass vegetation canopy is modelled with one temperature, which might lead to a larger decrease in modelled vegetation canopy temperature (and leaf-to-air vapor pressure deficit) due to ground evaporation than occurring in reality. Transpiration is reduced with a smaller leaf-to-air vapour pressure deficit (Grossiord et al., 2020). The modelled transpiration rate of the irrigated turf was lower than that of the unirrigated most of the time (Fig. 6.9c) although the soil moisture content of the irrigated turf was higher throughout the simulation period (Fig. 6.4), indicating that soil moisture was not limiting transpiration in the simulations of the unirrigated plot.

We measured a strong, instantaneous cooling effect from 13:00 to 13:59 which coincided with the irrigation time (13:00–13:23) (Fig. 6.6a and Fig. 6.6g). The measured instantaneous cooling effect was induced by droplet evaporation when the water streams passed through the air and by evaporation of water intercepted by the turf canopy. Droplet evaporation can contribute to 10% of water loss in sprinkler irrigation (Molle et al., 2012). The droplet evaporation in this study was likely to be smaller than traditional sprinkler irrigation because the nozzles used in this study were designed to produce water streams that were less conducive to droplet evaporation. Yet, we measured sharp reductions in air and turf surface temperatures during and immediately after irrigation, suggesting that droplet evaporation could greatly influence microclimate for a short period of time.

The UT&C model predicted the same instantaneous cooling effect once irrigation had ceased from 14:00 to 14:59 and to a smaller magnitude. The modelled instantaneous cooling effect was not induced by droplet evaporation because the UT&C model does not include this. The modelled instantaneous cooling effect was driven by the evaporation from canopy interception (Fig. 6.9a) and the soil surface (Fig. 6.9b). There have been numerous models developed to predict the direction evaporation during irrigation under different weather conditions for different irrigation methods

(Playán et al., 2005). Our experiments suggested that it is necessary to account for droplet evaporation in the climate model to predict the cooling effect of sprinkler irrigation accurately. Moreover, there was a delayed cooling response of one hour because the UT&C model first solved the energy budget then the water budget. Finer time steps, e.g. minutes not hours, are required to run the model if the instantaneous cooling effect of irrigation needs to be resolved.

In this study, UT&C predicted that irrigation would reduce ground heat flux (less energy flowing into the ground) from 14:00 to 16:59 due to decreased turf surface temperature (Fig. 6.8). Furthermore, UT&C predicted that irrigation would have almost no impact on night-time ground heat flux and would not induce night-time warming of air temperature (Fig. 6.7). However, this is contrary to most modelling studies that have predicted that irrigation would increase ground heat flux (more energy flowing into the ground) during the day because wet soils have a higher thermal conductivity (Kanamaru and Kanamitsu, 2008; Vahmani and Ban-Weiss, 2016; Wang et al., 2019). These studies also predicted that wet soils would store more heat during the day and increase night-time air temperature because more heat is released from the soils at night. Experiment studies confirmed the findings of these modelling studies (Cheung et al., 2022a; Horton and Wierenga, 1983). Ground heat flux is difficult to model because of the lack of detailed observational data and the high diversity of soil composition (Kanamaru and Kanamitsu, 2008). Modelling ground heat flux accurately is important to predict the impacts of irrigation on night-time microclimate because ground heat flux strongly influences the night-time microclimate when latent and sensible heat fluxes are close to zero (Fig. 6.10).

UT&C predicted that irrigation would increase night-time air temperature only when irrigation amount was $\geq$ 8 mm d^{-1}. At a lower irrigation amount, e.g., 4 mm d^{-1}, irrigation would reduce ground heat flux (less heat flowing into the soils) during the day due to increased latent heat flux (Fig. 6.8), causing no night-time warming. As irrigation amount increases to $\geq$ 8 mm d^{-1}, both the ground heat flux and the latent heat flux during the day should increase because of increased thermal conductivity and increased evapotranspiration, respectively. The increase in evapotranspiration should be small because atmospheric demand would be the limiting factor of evapotranspiration but not soil moisture content. The increase in ground heat flux is likely to be higher than the increase in latent heat flux during the day, causing a significant release of soil heat and an increase in air temperature at night. More research is required to disentangle the dynamics between soil moisture content, soil heat flux and air temperature.

Overall, the edge effect of the experimental plots may contribute to the discrepancy between the modelled and measured surface energy balance, evapotranspiration, microclimate and soil

temperature. Given that the plots were relatively small (6 m × 6 m), the landscape elements such as trees in the site might change the microclimate of the plots through modifying the wind profile and shading and change the soil moisture content through roots. UT&C, in contrast, assumes an idealised canyon with infinite length and homogenous surfaces. The permeability of the fences in the experiments may contribute to some turbulent mixing between the plots and the surrounding which represented an additional source of errors.

6.4.2. Impacts of different daily irrigation amount on cooling benefits

UT&C predicted that the daily mean air temperature reductions from irrigation would not increase greatly beyond a daily irrigation amount of 4 mm. This amount is reasonable because the mean reference crop evapotranspiration in Melbourne's summer is approximately 4 mm d^{-1} (Bureau of Meteorology, 2023b). The reference crop evapotranspiration is the evapotranspiration rate of a grass-covered surface that is not short of water (Allen et al., 1998). The reference crop evapotranspiration is a function of available energy (net radiation – ground heat flux) at the ground surface, wind speed, air temperature and vapour pressure deficit. If extreme weather conditions occur such as heatwaves, the reference crop evapotranspiration in Melbourne will increase to >4 mm d^{-1} and a daily irrigation amount >4 mm d^{-1} will induce extra cooling benefits. Broadbent et al. (2018a) used the SURFEX model to predict that the daily mean air temperature reductions would increase almost linearly from 0.5 to 1.8°C during a heatwave in Adelaide, Australia as irrigation amount increased from 5 to 15 mm d^{-1}. The maximum and mean air temperatures during the heatwave were 45°C and 30°C, respectively. The high air temperature during the heatwave have allowed more evapotranspiration to occur, inducing a stronger cooling effect of irrigation.

For the urban green spaces in heavily built-up urban areas, daily evapotranspiration may be greatly increased by the advective sensible heat from surrounding dry surfaces (Oke, 1979). The daily total evapotranspiration of an well-irrigated park in Sacramento, USA was 130% higher than that of a rural irrigated grass site (Spronken-Smith et al., 2000). The air temperature of the park was approximately 2°C lower than a nearby paved surface for most of the time during the day. Therefore, the actual daily total evapotranspiration can be higher than the reference crop evapotranspiration in certain urban green spaces. The daily irrigation amount for these urban green spaces needs to be higher than the reference crop evapotranspiration to induce the strongest possible cooling effect. Some of the irrigation water will be directly evaporated whilst passing through the air, as well as evaporated from leaf surfaces when intercepted – none of these processes are considered in the reference evapotranspiration calculations but should be maximised for optimal cooling benefit.

6.4.3. Implications for using irrigation to cool urban green spaces

This study has demonstrated that irrigating a small urban green space can significantly reduce daytime air temperature, turf surface temperature and soil temperature under non-heatwave summer conditions in a temperate region. The cooling effect of irrigation is highly dependent on background climate (Cook et al., 2015; Thiery et al., 2017). The cooling effect of irrigation is stronger in regions with a higher air temperature and lower rainfall in summer (Cheung et al., 2021). Irrigating urban green spaces was estimated to reduce mean summer air temperature by 2.3°C in arid hot desert climate (Köppen climate classification: BWh), whereas irrigating urban green spaces might increase mean summer air temperature by 0.3°C in Mediterranean dry–warm summer climate (Köppen climate classification: Csb) (Cheung et al., 2021). It is necessary to take background climate into account when assessing the potential of using irrigation to cool urban green spaces.

Water supply is another important consideration when using irrigation to cool urban green spaces. Through water sensitive urban design, non-potable water can be collected and stored in the city to support irrigation. Water sensitive urban designs are the approaches and technologies that aim to retain water in the urban landscapes to meet different purposes such as irrigation (Coutts et al., 2013). For example, housing estates can collect and treat their sewage in a centralised system to provide a collective supply of fit-for-purpose water for irrigation (Gil-Meseguer et al., 2019; South East Water, 2021). De-centralised stormwater storage is also possible for individual households. Individual households can collect stormwater runoff from their roofs through gutters and pipes, and store the water in rainwater tanks for future uses (Mitchell et al., 2007). As stormwater harvesting systems become more affordable and accessible, it is estimated that the new housing projects in Melbourne will increase the city's non-potable water supply by seven times by 2050 (9.8% of the city's water consumption) (Environment and Natural Resources Committee, 2009).

6.5. Conclusion

The impacts of irrigating an urban green space on microclimate were measured and modelled in this study. The UT&C model can predict the impacts of irrigating a small, turfed urban green space on air temperature well. Daytime irrigation is predicted to increase the daytime evaporation from the canopy of plant and the daytime evaporation from soil surface, leading to an increase in total evapotranspiration. Daytime sensible heat is therefore reduced, causing significant reductions in daytime air temperature, turf surface temperature and soil temperature. The impacts of irrigation on night-time microclimate, surface energy balance and evapotranspiration are small.

Incorporating all evapotranspiration processes into an urban canopy model is crucial for the model to predict the impacts of irrigating urban green spaces on microclimate and surface energy balance. The droplet evaporation during sprinkler or nozzle irrigation needs to be included in urban canopy models because its contribution to total evapotranspiration is sizeable, particular for daytime irrigation. For a turfed urban green space, the daily irrigation amount that can generate the strongest possible cooling effect on an average summer day is approximately equivalent to the reference crop evapotranspiration of the background climate in question.

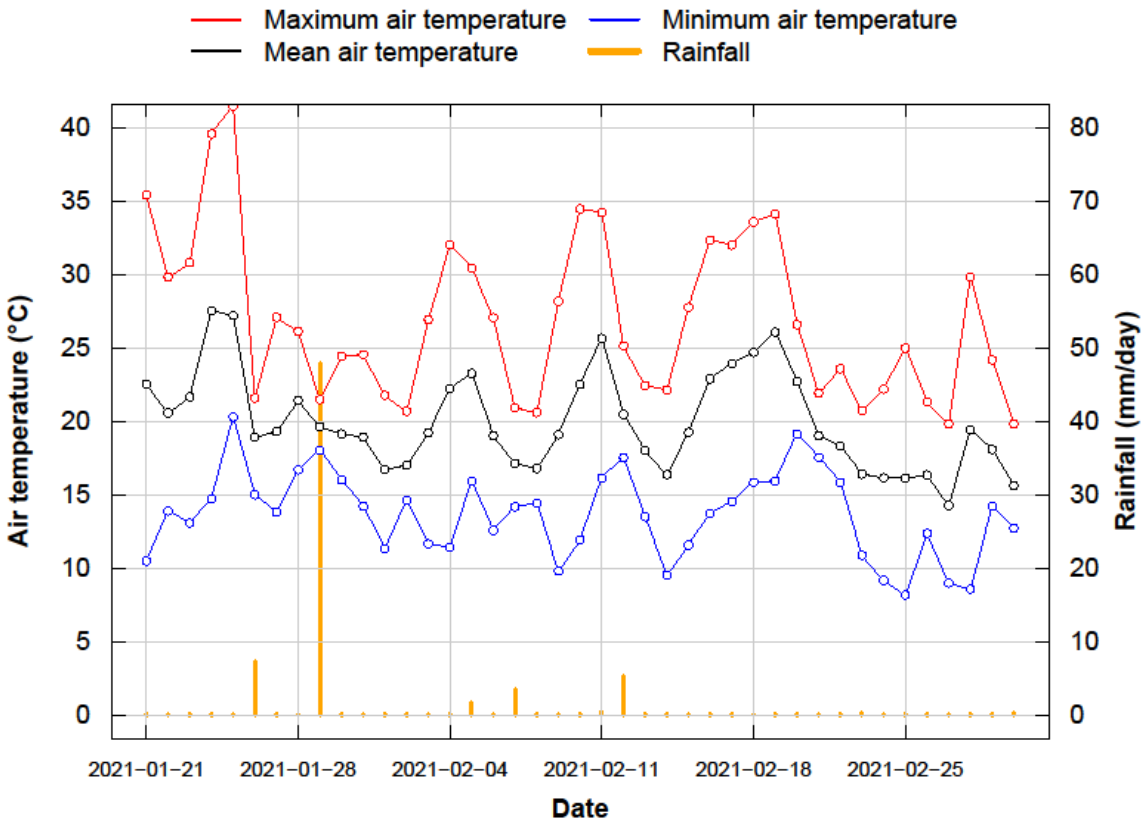

Fig. S6.1. Daily minimum, mean and maximum air temperatures and total rainfall of the model testing period (2021-01-21 to 2021-03-02, 41 days).

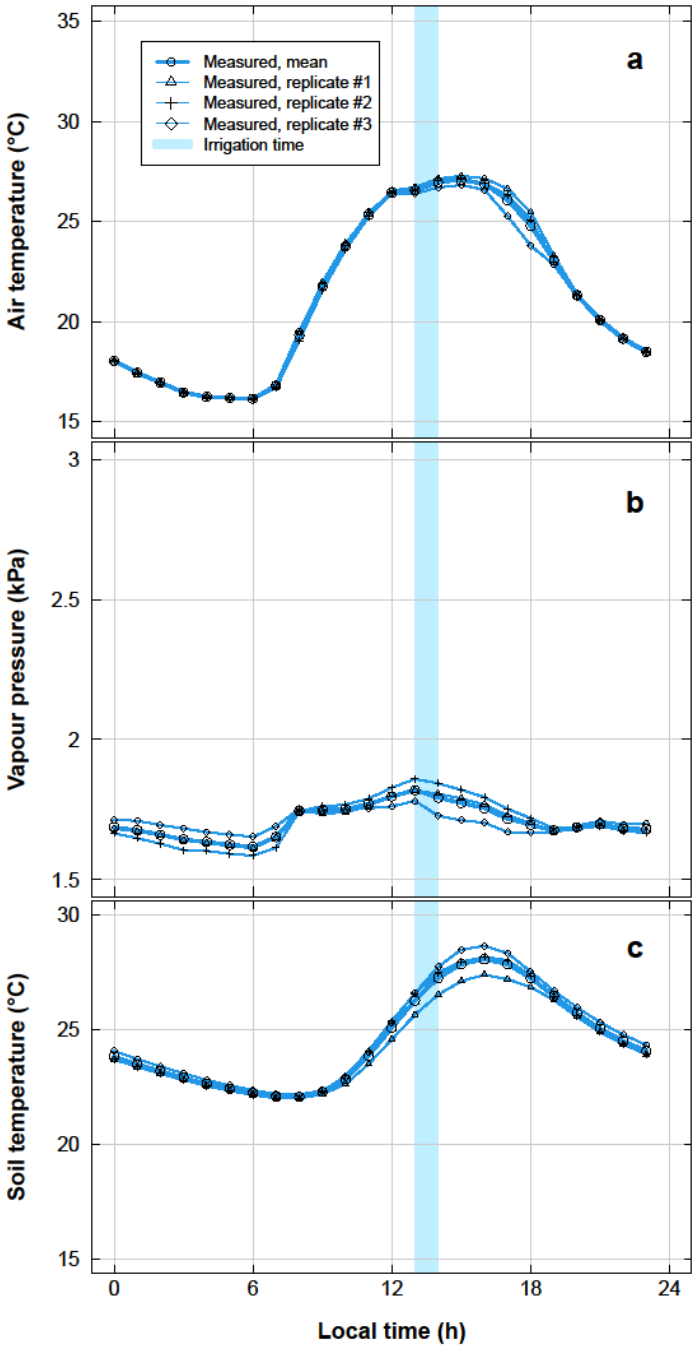

Fig. S6.2. The average diurnal cycle of measured (a) air temperature, (b) vapour pressure, and (c) soil temperature of the three replicated plots with irrigation. The measurement period was from 2022-01-28 to 2022-03-06 (38 days).

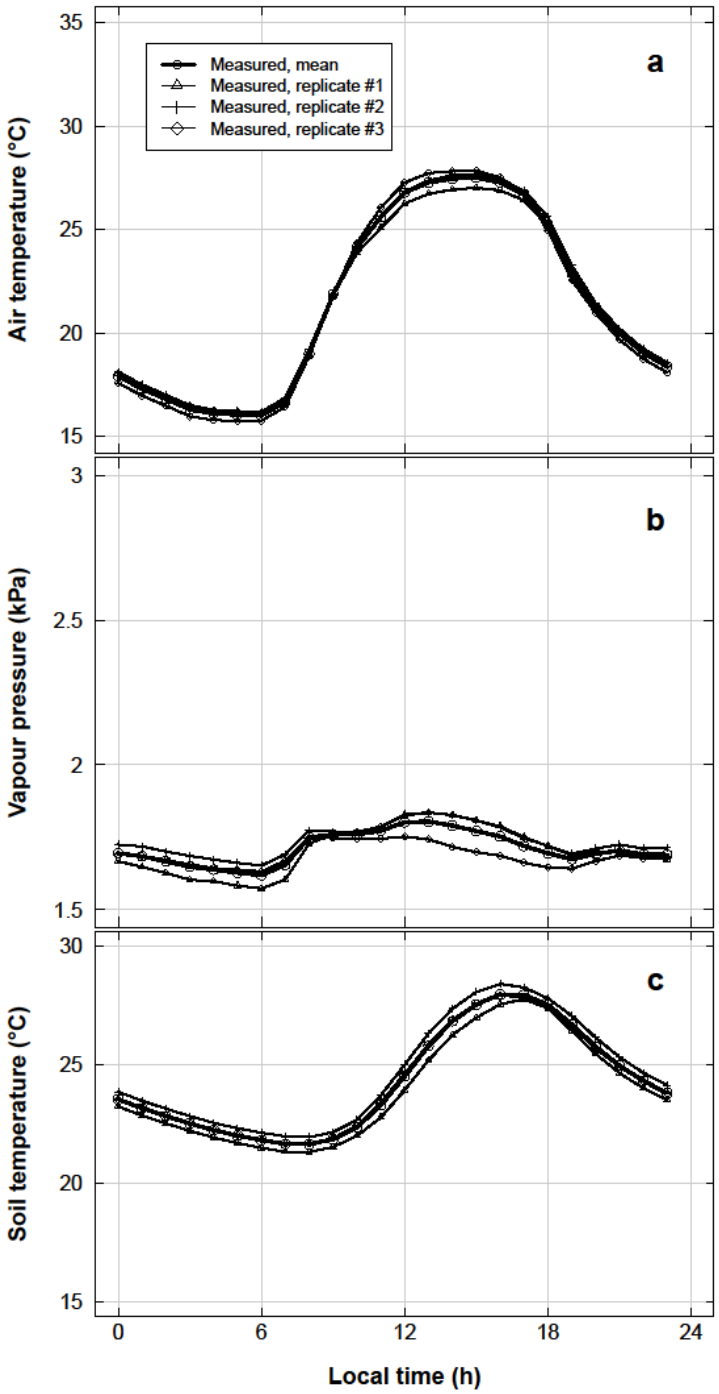

Fig. S6.3. The average diurnal cycle of measured (a) air temperature, (b) vapour pressure, and (c) soil temperature of the three replicated plots without irrigation. The measurement period was from 2022-01-28 to 2022-03-06 (38 days).

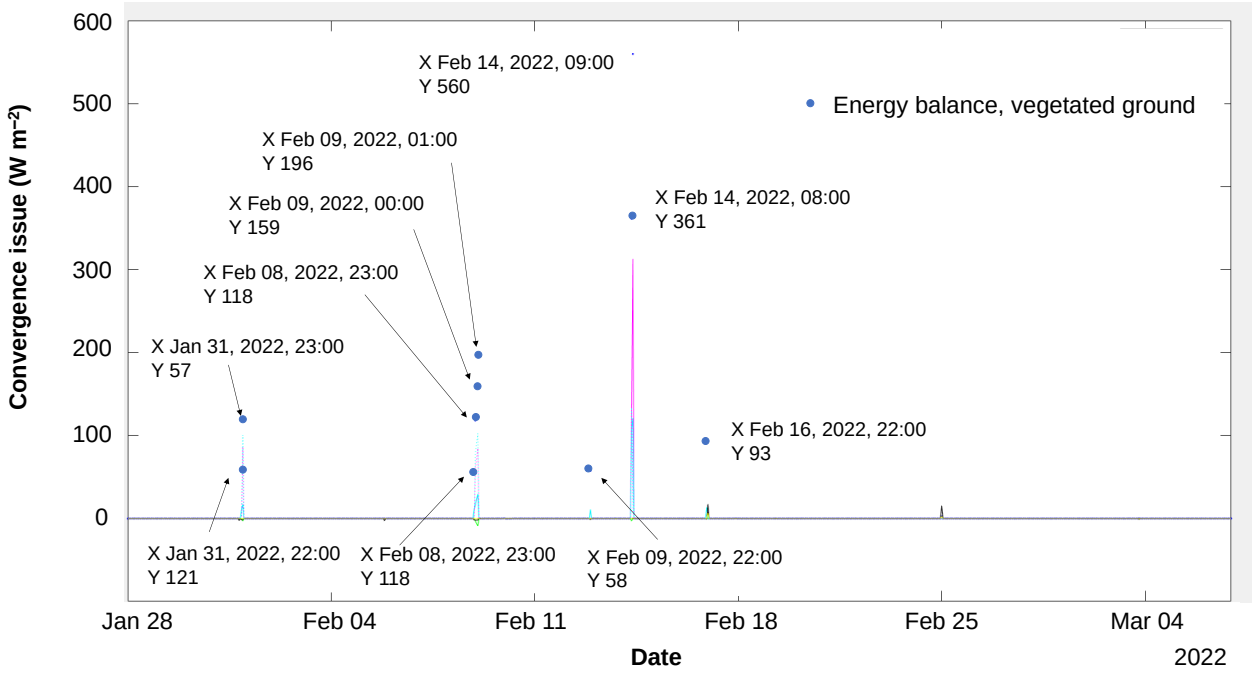

Fig. S6.4. Convergence issues of the unirrigated scenario. The energy balance of ground vegetated surface (EBGroundVeg) failed to converge in a number of time steps in the simulation. Those time steps were removed from the analysis.

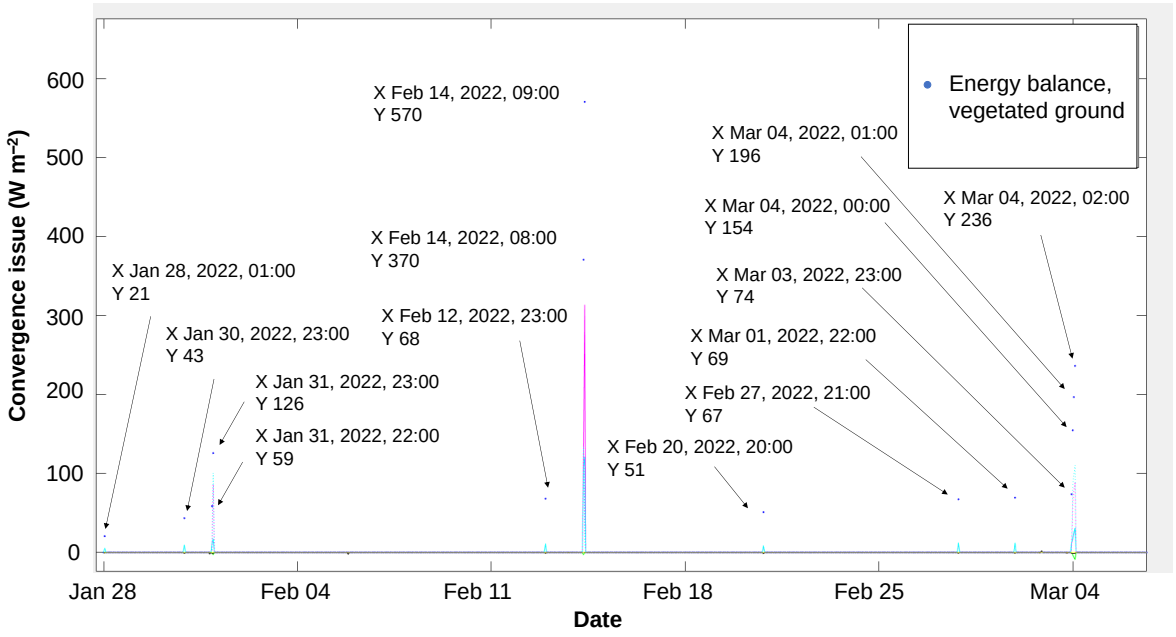

Fig. S6.5. Convergence issues of the irrigated scenario. The energy balance of ground vegetated surface (EBGroundVeg) failed to converge in a number of time steps in the simulation. Those time steps were removed from the analysis.

Table S6.1. Urban Geometry, radiation, and conductive heat flux parameters used for simulation.

Parameter	Description	Unit	Value	Reference
H_{can}	Average height of urban canyon	m	5	Site condition
W_{can}	Ground width of urban canyon	m	50	Site condition
W_{roof}	Roof width of urban canyon	m	5	Site condition
N_{tree}	Absence (0) or presence (1) of trees	–	0	Site condition
$f_{r,imp}$	Fraction of impervious roof	–	0	Site condition
$f_{r,veg}$	Fraction of vegetated roof	–	0	Site condition
$f_{g,imp}$	Fraction of impervious ground	–	1	Site condition
$f_{g,bare}$	Fraction of bare ground	–	0	Site condition
$f_{g,veg}$	Fraction of vegetated ground	–	1	Site condition
α_r	Albedo roof [imp, veg]	–	[0.15,–]	(Nice et al., 2018)
α_g	Albedo ground [imp, bare, veg]	–	[–,–,0.22]	Measured
α_w	Albedo wall	–	0.3	(Nice et al., 2018)
ε_r	Emissivity roof [imp, veg]	–	[0.92,–]	(Nice et al., 2018)
ε_g	Emissivity ground [imp, bare, veg]	–	[–,–,0.97]	(Harshan et al., 2018)
ε_w	Emissivity wall	–	[0.88]	(Nice et al., 2018)
$\lambda_{r,imp}$	Thermal conductivity of impervious roof	W K^{-1} m^{-1}	0.773	(Meili et al. 2020)
λ_w	Thermal conductivity of wall	W K^{-1} m^{-1}	0.342	(Meili et al. 2020)
$Cv_{r,imp}$	Volumetric heat capacity of impervious roof	MJ K^{-1} m^{-3}	0.813	(Meili et al. 2020)
Cv_w	Volumetric heat capacity of wall	MJ K^{-1} m^{-3}	0.9035	(Meili et al. 2020)
dz_r	Thickness of roof layers [1, 2]	m	[0.057, 0.057]	(Meili et al. 2020)
dz_w	Thickness of wall layers [1, 2]	m	[0.074, 0.074]	(Meili et al. 2020)

Table S6.2. Vegetation parameters used for the simulation. Separate parameters for roof vegetation [r_{veg}], ground vegetation [g_{veg}], and trees [$_{tree}$] are specified in this order.

Parameter	Description	Unit/code	Value [r_{veg}, g_{veg}, $_{tree}$]	Reference
h_c	Ground vegetation canopy height	m	[–, 0.1, –]	Site condition
d_{leaf}	Leaf dimension	cm	[–, 2, –]	(Fatichi and Pappas, 2017)
LAI	Leaf area index	–	[–, 3, –]	(Fatichi and Pappas, 2017)
SAI	Stem area index	–	[–, 0.001, –]	(Fatichi and Pappas, 2017)
S_{LAI}	Specific leaf area	m^2 LAI g C^{-1}	[–, 0.016, –]	(Fatichi and Pappas, 2017)
K_{opt}	Canopy light extinction coefficient	–	[–, 0.5, –]	(Fatichi and Pappas, 2017)
$VCASE_{root}$	Vertical root profile (1, 2, 3, 4)	–	[–, 1, –]	(Fatichi and Pappas, 2017)
ZR_{95}	Root depth, 95th percentile of vegetation	mm	[–, 250, –]	Tested
RI_{root}	Root length index	m root m^{-2} PFT	[–, 4500, –]	(Fatichi and Pappas, 2017)
ψ_{Sto00}	Soil water potential at the beginning of stomatal closure	MPa	[–, –0.6, –]	(Fatichi and Pappas, 2017)
ψ_{Sto50}	Soil water potential at 50% stomatal closure	MPa	[–, –2, –]	(Fatichi and Pappas, 2017)
ψ_{L50}	Water potential at 50% leaf hydraulic conductivity	MPa	[–, –2.5, –]	(Fatichi and Pappas, 2017)
ψ_{X50}	Water potential at 50% of xylem hydraulic conductivity and limit for water extraction from soil	MPa	[–, –0.95, –]	(Fatichi and Pappas, 2017)
ϕ_P	Photosynthesis pathway	3:C3, 4:C4, or 5:CAM	[–, 3, –]	(Fatichi and Pappas, 2017)
K_N	Canopy nitrogen decay coefficient	–	[–, 0.3, –]	(Fatichi and Pappas, 2017)
$V_{c,max}$	Maximum Rubisco capacity at 25°C leaf scale	µmol CO_2 m^{-2} s^{-1}	[–, 64, –]	Tested
$g_{0,CO2}$	Minimum/cuticular stomatal conductance	mol CO_2 m^{-2} leaf s^{-1}	[–, 0.01, –]	(Fatichi and Pappas, 2017)
a_1	Empirical parameter linking net assimilation AnC to stomatal conductance $g_{s,CO2}$	–	[–, 7, –]	(Fatichi and Pappas, 2017)
r_{jv}	Scaling factor between J_{max} and $V_{c,max}$	µmol equivalent μmol^{-1} CO_2	[–, 2.1, –]	(Fatichi and Pappas, 2017)
ε_{FI}	Intrinsic quantum efficiency	µmol CO_2 μmol^{-1} photons	[–, 0.081, –]	(Fatichi and Pappas, 2017)
$\Delta_{0,r}$	Empirical coefficient that expresses the value of vapour pressure deficit at which f(Δe) = 0.5	Pa	[–, 2000, –]	Tested

Table S6.3. Soil, interception, and runoff parameters used for the simulation.

Parameter	Description	Unit/code	Value/code	Reference
$Z_{s,g}$	Ground soil layer discretisation	mm	[0 … 2000]	(Meili et al., 2020)
$F_{g,soil}$	Ground soil composition [f_{clay}, f_{sand}, $f_{organic}$]	–	[0.2, 0.4, 0.06]	Tested
K_{imp}	Hydralic conductivity of impervious surface [$_{roof,\ ground}$]	mm h^{-1}	[0, –]	(Meili et al., 2020)
K_{bot}	Hydralic conductivity at the bottom of the last soil layer [$_{roof,\ ground}$]	mm h^{-1}	[–, free drainage]	(Meili et al., 2020)
SPAR	Soil parameter type [$_{roof,\ ground}$]	1: VanGenuchten or 2: Saxton–Rawls	[, 2]	(Meili et al., 2020)
In^{max}_{imp}	Maximum interception capacity of impervious surfaces [$_{roof,\ ground}$]	mm	[0.25, 0.5]	(Meili et al., 2020)
In^{max}_{soil}	Maximum interception capacity on top of soil [$_{r,veg,\ g,bare,\ g,veg}$]	mm	[–, –, 10]	(Meili et al., 2020)
$S^{max}_{P,In}$	Specific water retained by vegetation surface [$_{r,veg,\ g,bare,\ g,veg}$]	mm m^2 PFT area m^{-2} leaf area	[–, –, 0.1]	(Meili et al., 2020)
λ_r	Percentage of runoff that leaves the system [$_{roof,\ ground}$]	–	[1, 0.5]	(Meili et al., 2020)
Z_{ifc}	Depth from which initial soil moisture content is at field capacity	mm	100	Tested
Z_{fc}	Depth from which soil moisture content is at field capacity	mm	400	Tested

Table S6.4. Location and measurement parameters, and anthropogenic heat used for the simulation.

Parameter	Description	Unit	Value	Reference
ϕ_{data}	Latitude (positive north)	°	–37.83	Site condition
λ_{data}	Longitude (positive east)	°	145.02	Site condition
θ_{canyon}	Canyon orientation [direction 1, direction 2]	°	25	Site condition
Δ_{GMT}	Difference between local time and Greenwich Meridian Time	h	10	Site condition
Z_{atm}	Atmospheric forcing/reference height	m	80	Data
$T_{b,min}$	Minimum interior building temperature	°C	18	(Meili et al., 2020)
$T_{b,max}$	Maximum interior building temperature	°C	27	(Meili et al., 2020)
$Q_{f,roof}$	Anthropogenic heat input on top of roof	W m^{-1}	0	Site condition
$Q_{f,can}$	Anthropogenic heat input within canyon	W m^{-1}	0	Site condition

Table S6.5. Root mean square errors of modelled air temperature difference between the irrigated and unirrigated scenarios for six model parameters at four different levels. These six parameters are site-specific and therefore a testing is conducted to find out the level that generate the lowest root mean square errors for each parameter using 2021's data. The level with the smallest root mean square error of each parameter is in bold.

Depth below which initial soil moisture is at field capacity (mm)	**0**	*100*	200	400
Root mean square error (°C)	0.490	0.515	0.601	0.837
Depth below which soil moisture is kept at field capacity (mm)	100	200	*400*	**800**
Root mean square error (°C)	0.459	0.493	0.489	0.515
Ground soil composition [f_{clay}, f_{sand}, $f_{organic}$]	***0.2, 0.4, 0.025***	0.2, 0.4, 0.06	0.05, 0.75, 0.06	0.1, 0.7, 0.06
Root mean square error (°C)	0.489	0.558	1.095	1.102
Empirical coefficient that expresses the value of vapour pressure deficit at which f(Δe) = 0.5 (Pa)	500	**1000**	*2000*	4000
Root mean square error (°C)	0.549	0.489	0.452	0.461
Root depth, 95th percentile of vegetation (mm)	***250***	300	350	400
Root mean square error (°C)	0.452	0.457	0.456	0.455
Maximum Rubisco capacity at 25°C leaf scale (μmol CO_2 m^{-2} s^{-1})	***54***	64	74	84
Root mean square error (°C)	0.452	0.456	0.533	0.474

Chapter 7 – Synthesis

Heatwaves are periods of abnormally hot weather. The frequency of heatwaves across the globe have increased in the past few decades (Perkins-Kirkpatrick and Lewis, 2020) and is expected to increase in the future (Domeisen et al., 2022). Heatwaves can severely affect the users and fauna of urban green spaces. Although governments and health agencies generally recommend people to stay in air-conditioned facilities such as libraries and shopping malls during heatwaves, outdoor workers may be present in urban green spaces during heatwaves. Urban fauna will have no option but to continue using urban green spaces as habitats. It is worth exploring the potentials of using irrigation as a heat mitigation strategy for urban green spaces during heatwaves because heat-related mortality rate is strongly associated with high air temperature (Basu and Samet, 2002). As management decisions can impact human health and mortality, any management decision that uses irrigation as a heat mitigation strategy needs to be based on scientific evidence, both empirical and modelled. It is also important that the limits of cooling benefit from UGS irrigation are explored and recognised. To understand the potentials of using irrigation as a heat mitigation strategy for urban green spaces during heatwaves, I will use the experimental data in Chapter 5 to develop an empirical model to predict the air temperature reductions from irrigation for three past heatwave events (2009, 2013 and 2014) in Melbourne, Australia with historic weather data.

7.1. Predicting the potential air temperature reductions from irrigating urban green spaces during heatwaves in Melbourne

7.1.1. Multiple linear regression model

With the data from Chapter 5, I established a multiple linear regression model to predict the afternoon (12:00–15:59) mean air temperature reduction from irrigating urban green spaces using background weather data. I used the cooling effect data from the multiple daytime irrigation treatment (irrigating 1 mm at 12:00, 13:24, 14:00 and 15:00 = 4 mm d^{-1}) and the background weather data. The explanatory weather variables included daily mean air temperature, daily mean vapour pressure deficit and daily total incoming shortwave radiation. Wind speed was excluded from the analysis because it did not have a linear relationship with the afternoon (12:00–15:59) mean cooling effect (c.f. Chapter 5). I used a stepwise multiple linear regression to construct a model with the smallest Akaike information criterion. The regression started with a full model that included the full set of explanatory weather variables. One explanatory weather variable was then added or removed at one time to give one variant of the full model. The full model and each of its variants had an Akaike information criterion that represented the quality of the model relative to others. The best and final

model has the minimum Akaike information criterion (Hastie and Pregibon, 1992). The model with the minimum Akaike information criterion was as follows:

$$\Delta T_a = -0.022 T_a - 0.029 SW_{in}\ ,\ R^2 = 0.42 \quad (7.1)$$

where ΔT_a is the afternoon (12:00–15:59) mean air temperature reduction from irrigation (°C), T_a the daily mean air temperature (°C), SW_{in} the daily total incoming shortwave radiation (MJ m^{-2}). The afternoon (12:00–15:59) mean air temperature reduced would strengthen by –0.022 and –0.029°C as daily mean air temperature and daily total incoming solar radiation increase by 1°C and 1 MJ m^{-2}, respectively.

7.1.2. Air temperature reductions during heatwaves

I used the model to predict the afternoon (12:00–15:59) mean air temperature reductions from irrigating urban green spaces in the three most recent heatwave periods in Melbourne, namely 2009 (27th January to 1st February), 2013 (4th to 9th March) and 2014 (13th to 17th January). The weather data for these three heatwave periods were collected from the Bureau of Meteorology (2023c). The daily mean air temperatures of the three heatwave periods were 28.6, 26.2 and 30.1°C, respectively. The daily total incoming shortwave radiation of the three heatwave periods were 29.7, 20.6 and 27.6 MJ m^{-2}, respectively.

The potential afternoon (12:00–15:59) mean air temperature reductions from irrigating urban green spaces were –1.3°C in 2009, –1.0°C in 2013 and –1.3°C in 2014 (Fig. 7.1). The strongest potential afternoon (12:00–15:59) mean air temperature reduction (–1.4°C) occurred on 28–30 January 2009 and 14 January 2014 when the daily mean air temperature and the daily total incoming shortwave radiation exceeded 31°C and 29 MJ m^{-2}, respectively.

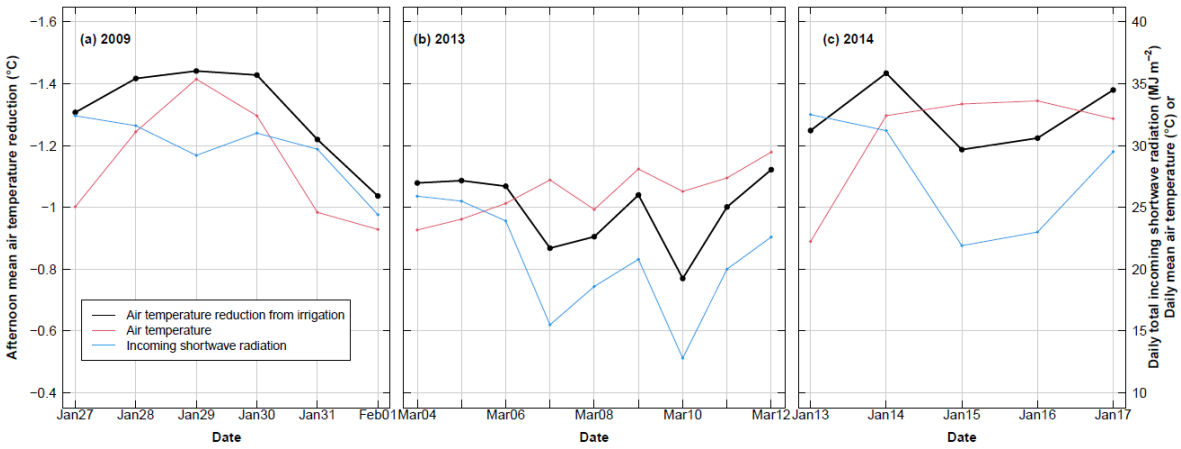

Fig. 7.1. The daily mean air temperature, daily total incoming shortwave radiation and potential afternoon (12:00–15:59) mean air temperature reductions from irrigating urban green spaces on air temperature during the heatwave periods in Melbourne in (a) 2009, (b) 2013 and (c) 2014. The potential cooling effects were predicted by a multiple linear regression model using daily mean air temperature and daily total incoming shortwave radiation as the explanatory variables.

The potential afternoon (12:00–15:59) mean air temperature reductions irrigating urban green spaces during heatwaves in Melbourne were stronger than the afternoon (12:00–15:59) mean air temperature reduction (–0.9°C) that we observed in a normal summer without heatwave in 2022 (c.f. Chapter 5). The finding corroborated with that of a modelling study which reported that the maximum air temperature reduction from irrigation during heatwaves (–1.3°C) was stronger than that during non-heatwave period (–0.6°C) (Gao et al., 2020). The finding was also in line with that in the literature review in Chapter 2 which proposed that weather was one of the important factors that influenced the cooling effect of irrigation. The limitation of the multiple regression model is that it assumes the difference in soil moisture content between the irrigated and unirrigated scenarios in the heatwaves is similar to that between the irrigated and unirrigated plots in the field experiments. The model also assumes that the irrigation scheduling is the same as that of the multiple daytime irrigation treatment in the field experiment at Burnley. The model is only applicable to regions that have a similar background climate and soil type to Melbourne, Australia. Despite the assumptions and restrictions, the model provides a good estimation of the cooling benefits of irrigating urban green spaces in Melbourne using only two commonly available weather variables.

7.2. Contributions of the thesis to the advances in knowledge

7.2.1. Impacts of irrigating urban green spaces on surface energy balance, microclimate and human heat stress

In Chapter 2, I constructed a theoretical framework about the impacts of irrigating urban green spaces on daytime and night-time microclimate (Fig. 2.1), human heat stress and surface energy balance in summer. The theoretical framework was based on a literature review which consisted mainly of city- or regional-scale modelling studies. In Chapters 4–6, the impacts of irrigating a small urban green space on daytime and night-time microclimate, human heat stress and surface energy balance were measured and modelled. The theoretical framework is revised according to the findings from Chapters 4–6 contributed to reflect the advances in knowledge (Fig. 7.2).

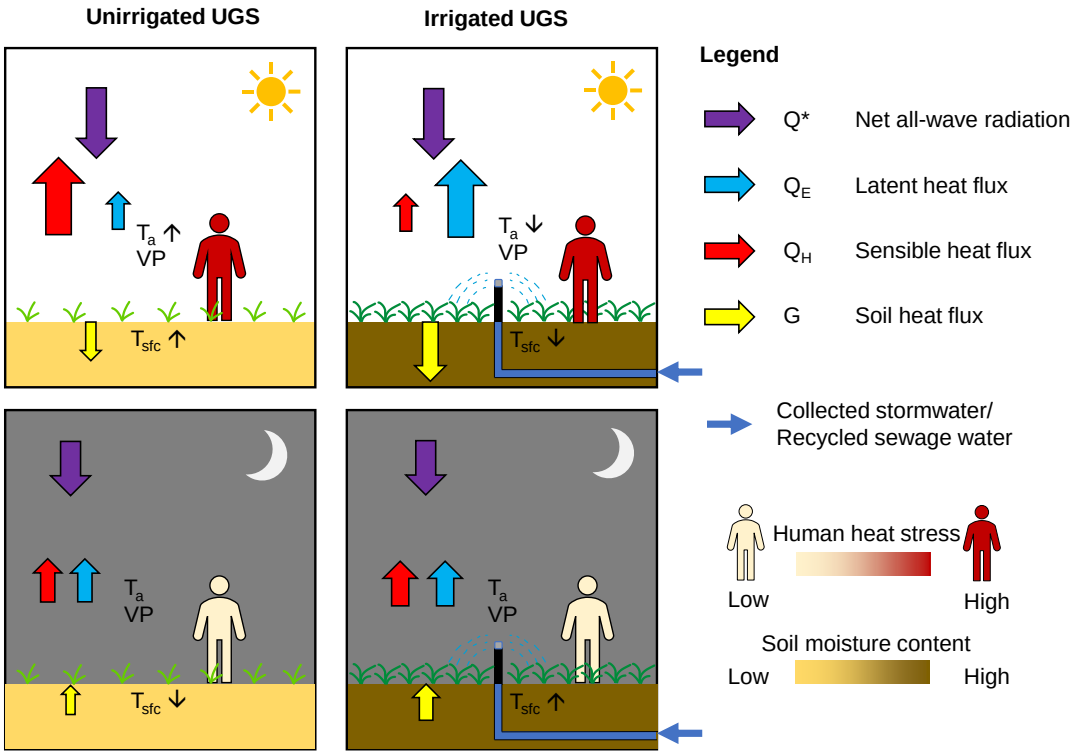

Fig. 7.2. Revised theoretical framework about the daytime and nigh-time impacts of irrigating urban green spaces on surface energy balance, microclimate and human heat stress. This theoretical framework was revised from the original framework (Fig. 2.1) based on the findings from the field experiments and microclimate simulations in Chapters 4–6.

In the theoretical framework, I hypothesised that irrigating urban green spaces would increase daytime latent heat flux and downward ground heat flux and reduce sensible heat flux (Table 7.1). The findings from the field experiment and microclimate simulations supported this. I also hypothesised that irrigating urban green spaces would reduce daytime air temperature, turf surface

temperature and human heat stress and increase vapour pressure. The findings from the field experiment and microclimate simulations supported the first two, but the findings showed that irrigation had no significant impacts on vapour pressure and human heat stress (measured by universal thermal climate index). The lack of significant impacts on vapour pressure were probably due to the scale of irrigation being small, which limited the measurable increase in vapour pressure after some mixing and dispersion.

Table 7.1

Comparison of the original and revised theoretical frameworks about the impacts of irrigating urban green spaces on surface energy balance, microclimate and human thermal stress in summer.

		Daytime		Night-time	
	Variable	Original framework	Revised framework	Original framework	Revised framework
Surface energy balance	Latent heat flux	↑	↑	↑	-
	Sensible heat flux	↓	↓	↓	-
	Downward ground heat flux (daytime)/ Upward ground heat flux (night-time)	↑	↑	↑	↑
Microclimate	Air temperature	↓	↓	↑/↓	-
	Vapour pressure	↑	-	↑	-
	Turf surface temperature	↓	↓	↑	↑
Human heat stress	Universal thermal climate index	↓	-	-	-

"↑". "↓" and "-" represent increase, decrease and no impact, respectively.

In this conceptual framework, I also hypothesised that irrigating urban green spaces would increase night-time latent heat flux and upward ground heat flux and reduce sensible heat flux (Table 7.1). The findings from the field experiment and microclimate simulations partly supported this because irrigation increased upward ground heat flux but it did not change latent heat flux and sensible heat flux. I also hypothesised that irrigating urban green spaces would increase night-time vapour pressure and turf surface temperature and have unclear or no impact on night-time air temperature and human heat stress. The findings from the field experiment and microclimate simulations partly supported this because irrigation had no impact on vapour pressure.

7.2.2. Environmental and management factors that influence the cooling effect of irrigating urban green spaces

In Chapter 2, I identified the key environmental and management factors that influence the cooling effect of irrigating urban green spaces, which included background climate, weather, daily

irrigation amount, irrigation scheduling and vegetation type (Fig. 7.3). I identified these factors based on a literature review which consisted mainly of city- and regional-scale modelling studies. In Chapters 3, 4, 5 and 6, I investigated how these factors influence the cooling effect of irrigating urban green spaces using a meta-analysis, field experiments and microclimate simulations. The findings from Chapters 3, 4, 5 and 6 confirmed the importance of these environmental and managements factors and quantified their influences on the irrigation cooling effect in turf grass green spaces.

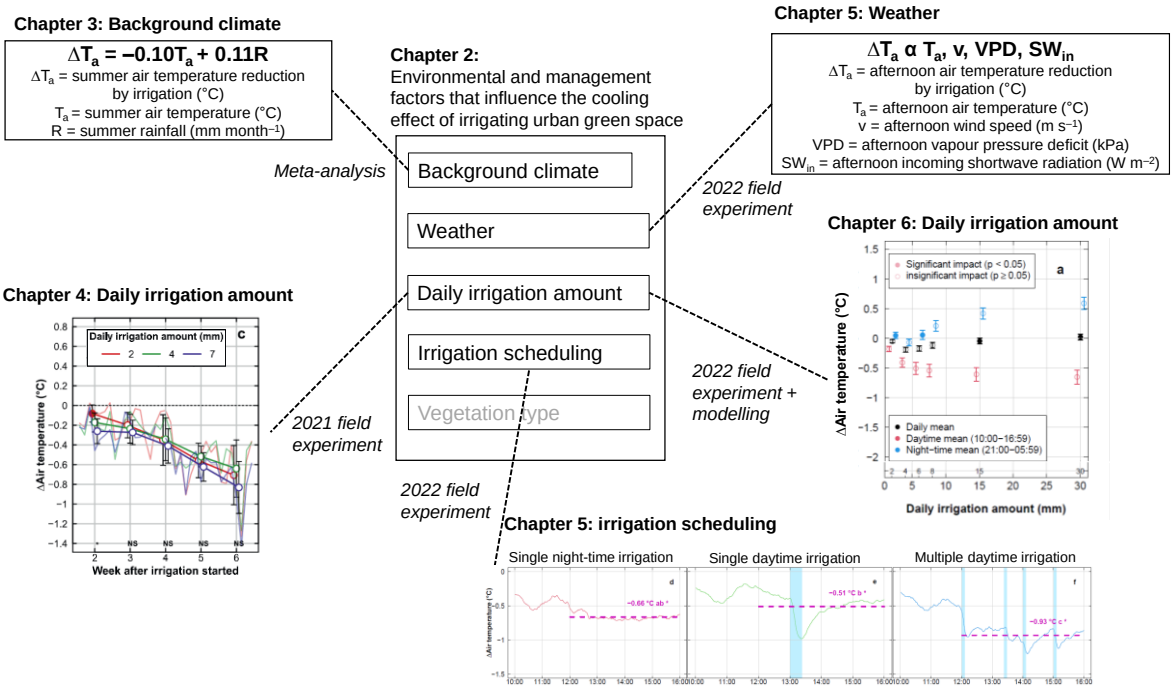

Fig. 7.3. Summary of the findings from Chapter 2 to Chapter 6. Chapter 2 identified the factors that influence the cooling effects of irrigating urban green spaces. In Chapters 3, 4, 5 and 6, the influences of those factors were investigated using a meta-analysis, field experiments and microclimate simulations.

Background climate is the most important factor to consider when it comes to using irrigation to cool urban green spaces in summer. The background climate of a city determines whether irrigating urban green spaces could be an effective cooling strategy for that city in summer. In Chapter 3, I used a meta-analysis of the literature and a stepwise regression model to identify the two most important climate variables that influenced the cooling effect of irrigating urban green spaces in summer – air temperature and rainfall. The mean cooling effect of irrigating urban green spaces in summer on air temperature would strengthen by 0.10°C as the mean background air temperature increases by 1°C. Conversely, the mean cooling effect of irrigating urban green spaces would weaken by 0.11°C as the

monthly total rainfall increases by 10 mm. The stepwise regression model in this synthesis chapter provides an estimate of the cooling effectiveness of irrigating urban green spaces in a Melbourne summer using two commonly available climate variables, daily solar radiation and mean air temperature.

Weather can change substantially from day to day within the summer season. It is important to understand under what weather conditions irrigation is an effective cooling strategy. In Chapter 5, I showed that the afternoon mean cooling effects of irrigating turfgrass in a small green space on air temperature and turf surface temperature strengthened linearly with increasing background air temperature, vapour pressure deficit and incoming shortwave radiation. The findings suggest that irrigating urban green spaces is a more effective cooling strategy when the weather is warmer and drier. When irrigation water supply is limited, irrigation can be prioritised to warmer and drier days to obtain a stronger cooling benefit. Smart irrigation control systems can be installed to initiate irrigation with meteorological predictions or temperature thresholds.

Daily irrigation amount has been reported to relate almost linearly with the cooling effect of irrigating urban green spaces in Adelaide, Australia within the range of 0 to 15 mm under heatwave conditions without advection (Broadbent et al., 2018a). A similar finding was reported for irrigating vegetation in the contiguous US under non-heatwave conditions with advection (Wang et al., 2019). However, in Chapter 4, the measured daytime cooling effect of irrigating turfgrass under non-heatwave conditions in Melbourne did not strengthen as the daily irrigation amount increased from 2 to 4, and to 7 mm. The impact of large rainfall event masked the potential differences of three irrigation treatments. In Chapter 6, the UT&C model predicted that the daytime cooling effect of irrigating turfgrass under non-heatwave conditions in Melbourne would strengthen significantly as the daily irrigation amount increased from 0 to 4 mm. However, this daytime cooling effect was not predicted to strengthen linearly as the daily irrigation amount increased beyond 4 mm. The findings suggested that irrigating 4 mm d^{-1} under non-heatwave and non-advective conditions is the most reasonable irrigation amount to achieve the strongest cooling effect in summer in Melbourne. The mean reference crop evapotranspiration rate in summer in Melbourne is approximately 4 mm d^{-1} (Bureau of Meteorology, 2023b), suggesting that irrigating 4 mm d^{-1} can fully meet the evapotranspirative demand of turfgrass and further increase in irrigation amount will not lead to a substantial increase in evapotranspiration and cooling effect.

Irrigation scheduling provides an opportunity to strengthen the cooling effect of irrigating urban green spaces without using more water (Broadbent et al., 2018a). In Chapter 5, I measured that the afternoon mean cooling effect of multiple daytime irrigation was significantly stronger than those

of a single night-time and a single daytime irrigation, given that the total irrigation amount was the same for all three irrigation schedules. The reasons for the stronger afternoon cooling effect were likely attributed to an increase in total evapotranspiration due to an increase in droplet evaporation in the air, evaporation on soil surface and evaporation of water intercepted by the turfgrass canopy.

7.3. Future research directions

7.3.1. Cooling effect of irrigating urban green spaces on the neighbourhood scale

The field experiments and microclimate simulations in this thesis have focused on the cooling effect of irrigating urban green spaces on the plot or local scale, where the entire urban green space is irrigated. The beneficiaries of urban green space irrigation are restricted to their users and the spatial extent of the cooling effect is likely to be restricted to the footprint of the urban green spaces for small urban green spaces such as private backyards. Since the cooling effect of irrigating small urban green spaces is strong and significant, it is worth investigating how irrigation can be used to cool the environment at a larger spatial scale. The spatial scale that is immediately larger than the street scale is the neighbourhood scale (0.5 km × 0.5 km) which can consist of tens of single-level houses (Oke, 2006).

Fig. 7.4. An example of an older (left) and a newer (right) suburb in Melbourne. In an older suburb, the houses typically have large, vegetated backyards and front yards relative to the building footprint. In a newer suburb, the houses typically have small, vegetated backyards and front yards relative to the building footprint.

The neighbourhoods in older and newer suburbs in Melbourne have different types and spatial distribution of urban green spaces. In older suburbs, the houses typically have large, vegetated

backyards and front yards relative to the building footprint (Fig. 7.4). Irrigating all backyards and front yards in the neighbourhood may induce a collective and evenly distributed cooling effect that benefits the whole neighbourhood. In newer suburbs, the houses typically have small, vegetated backyards and front yards relative to the building footprint (Fig. 7.4). The collective cooling effect of irrigating small backyards and front yards may be limited in this case. Yet, there is some evidence that irrigating larger urban green spaces can cool the surrounding built-up environment through local scale advection (Spronken-Smith et al., 2000; Vivoni et al., 2020). Irrigating the large public urban green space may provide a strong cooling effect to the residents closer to it and a weaker cooling effect to those further away from it. Since large-scale agricultural irrigation has been confirmed to influence regional and global climate (Lobell et al., 2008a), irrigating urban green spaces on the neighbourhood scale is a promising cooling strategies and is worth investigating. Spatially-resolved climate models such as ENVI-met (Bruse and Fleer, 1998) and PALM-4U (Maronga et al., 2020) are ideal for investigating the cooling effect of irrigating urban green spaces with different spatial arrangements. Alternatively, urban surface models that simulate urban energy and water balances such as SUEWS (Järvi et al., 2011; Ward et al., 2016) are suitable for investigating the average cooling effect of irrigating urban green spaces for the whole neighbourhood.

7.3.2. Contribution of the increase in leaf area index to irrigation cooling effect

Irrigating vegetation can lead to a cooling effect on air temperature through wetting the soil and increasing leaf area index of the vegetation. Most modelling studies that investigated the cooling effect of irrigation only focused on the cooling effect from wetting the soil (Liu and Wang, 2023). The cooling effect from increasing leaf area index due to irrigation received less attention, as has a cooling effect from irrigating vegetation (such as turfgrass) that is allowed to achieve greater leaf area index through less-frequent mowing. The leaf area index of irrigated vegetation can increase substantially over time, which in turn can lead to greater evapotranspiration. The leaf area index of turf grass has been shown to explain 78% of the variance in evapotranspiration (Barton et al., 2009). Such increase in evapotranspiration will change the surface energy balance and strengthen the cooling effect of irrigation. It was estimated that the increase in leaf area index in crops due to irrigation accounted for 34.5% and 14.0% of the irrigation cooling effects in spring and summer, respectively (Liu and Wang, 2023). Although the increase in leaf area index in the lawns in urban green spaces may be limited because they are mowed regularly, irrigating other vegetation such as shrubs and trees may enhance their cooling effect through increasing their leaf area index over time.

Irrigation is particularly important to maintain the health and cooling benefits of urban vegetation during droughts and heatwaves. It was estimated that the water stress due to climate change

can suppress the evapotranspiration of turfgrass for 3–5 months in a year by the 2080s in the UK, which increases the turf surface temperature by up to 15°C (Gill et al., 2013). Heatwaves can cause street trees to lose up to 50% of the their leaves, which greatly reduces their cooling benefits through shading and evapotranspiration (Sanusi and Livesley, 2020). The high air temperature during heatwaves directly causes the canopy loss and the water stress before and during the heatwaves may aggravate this canopy loss. Future studies are recommended to account for the changes in leaf area index due to irrigation, droughts and heatwaves when investigating the cooling effect of irrigating urban green spaces.

The benefits of irrigation on increasing and maintaining the leaf area index of urban surfaces are particularly important in arid regions. In many arid regions, urban ground vegetation cannot survive through the hot and dry summer without irrigation. This means that irrigation can prevent the green and cool vegetated surfaces from turning into dark and warm bare soil surfaces, which implies an extra cooling benefit from keeping the surface temperature lower by reflecting more solar radiation. The resultant cooling benefit of irrigating urban green spaces in arid regions require a dedicated experiment that compares the microclimate and surface energy balance of irrigated turf and unirrigated bare soil.

7.4. Conclusion

Irrigating turfgrass is an effective strategy to reduce the daytime air temperature and turf surface temperature in urban green spaces in temperate summers. The cooling effects are induced by an increase in total evapotranspiration, which reduces sensible heat flux. The increase in total evapotranspiration is attributed to the increase in droplet evaporation in the air, evaporation on soil surface and evaporation of water intercepted by the turfgrass canopy due to overhead irrigation. In comparison to a single night-time irrigation and a single daytime irrigation, separating irrigation into multiple smaller daytime applications can increase the cooling effects on afternoon air temperature and turf surface temperature without using more water. This multiple daytime irrigation approach is able to further increase canopy evaporation and droplet evaporation in the air. When daily irrigation is applied, the most reasonable daily total irrigation amount that can maximise the daytime cooling effect of irrigating turfgrass is approximately equivalent to reference crop evapotranspiration of the site. Increasing the daily total irrigation amount beyond the reference crop evapotranspiration will only strengthen the daytime cooling effect by a small amount. Irrigating small urban green spaces does not increase vapour pressure during the daytime because the moisture disperses quickly into the surrounding unirrigated environment. However, irrigating larger urban green spaces may increase vapour pressure noticeably, but was not studied in this thesis. Importantly, irrigating urban green

spaces does not appear to reduce human heat stress in summer because it cannot reduce mean radiant temperature. Tree shade and artificial shading are still necessary to reduce human heat stress in summer.

Apart from irrigation scheduling and irrigation amount, background climate and weather are important factors that influence the cooling effect of irrigating urban green spaces. The cooling effect of irrigating urban green spaces on air temperature in summer is stronger in regions with higher air temperatures and lower rainfalls in summer. Except the tropical and polar climates, the cooling effect of irrigating urban green spaces in summer is the strongest in arid hot desert (BWh) and arid cold desert (BWk) regions, and weakest in Mediterranean dry-cold summer (Csc) Mediterranean dry-warm summer (Csb) regions. The afternoon cooling effects of irrigating urban green spaces on air temperature and turf surface temperature strengthen significantly with increasing afternoon air temperature, vapour pressure deficit and incoming shortwave radiation. For a small urban green space, the cooling effect of irrigation on air temperature first strengthens with increasing wind speed but weakens as wind speed increases further.

The findings in this thesis are only representative of how irrigating small turfgrass green spaces in temperate summer impacts the surface energy balance and microclimate of that urban green space. It is worth investigating how irrigating larger green spaces, or irrigating a network of small urban green spaces in the same neighbourhood, impacts the surface energy balance and microclimate, while accounting for the changes in leaf area index due to irrigation, droughts and heatwaves.

References

Adegoke, J.O., Pielke, R.A., Eastman, J., Mahmood, R., Hubbard, K.G., 2003. Impact of irrigation on midsummer surface fluxes and temperature under dry synoptic conditions: A regional atmospheric model study of the U.S. high plains. Mon. Weather Rev. 131, 556–564. https://doi.org/10.1175/1520-0493(2003)131<0556:IOIOMS>2.0.CO;2

Akaike, H., 1974. A New Look at the Statistical Model Identification. IEEE Trans. Automat. Contr. 19, 716–723. https://doi.org/10.1109/TAC.1974.1100705

Akbari, H., Damon Matthews, H., Seto, D., 2012. The long-term effect of increasing the albedo of urban areas. Environ. Res. Lett. 7. https://doi.org/10.1088/1748-9326/7/2/024004

Al-Obaidi, K.M., Ismail, M., Abdul Rahman, A.M., 2014. Passive cooling techniques through reflective and radiative roofs in tropical houses in Southeast Asia: A literature review. Front. Archit. Res. 3, 283–297. https://doi.org/10.1016/j.foar.2014.06.002

Allen, R.G., Pereira, L.S., Raes, D., Smith, M., 1998. Crop evapotranspiration - Guidelines for computing crop water requirements - FAO Irrigation and drainage paper 56. Rome, Italy.

Allen, R.G., Pereira, L.S., Smith, M., Raes, D., Wright, J.L., 2005. FAO-56 Dual Crop Coefficient Method for Estimating Evaporation from Soil and Application Extensions. J. Irrig. Drain. Eng. 131, 2–13. https://doi.org/10.1061/(ASCE)0733-9437(2005)131:1(2)

Alter, R.E., Im, E.S., Eltahir, E.A.B., 2015. Rainfall consistently enhanced around the Gezira Scheme in East Africa due to irrigation. Nat. Geosci. 8, 763–767. https://doi.org/10.1038/ngeo2514

Anenberg, S.C., Haines, S., Wang, E., Nassikas, N., Kinney, P.L., 2020. Synergistic health effects of air pollution, temperature, and pollen exposure: a systematic review of epidemiological evidence. Environ. Heal. 19, 130. https://doi.org/10.1186/s12940-020-00681-z

Angold, P.G., Sadler, J.P., Hill, M.O., Pullin, A., Rushton, S., Austin, K., Small, E., Wood, B., Wadsworth, R., Sanderson, R., Thompson, K., 2006. Biodiversity in urban habitat patches. Sci. Total Environ. 360, 196–204. https://doi.org/10.1016/j.scitotenv.2005.08.035

Argüeso, D., Evans, J.P., Fita, L., Bormann, K.J., 2014. Temperature response to future urbanization and climate change. Clim. Dyn. 42, 2183–2199. https://doi.org/10.1007/s00382-013-1789-6

Arnfield, A.J., 1990. Street design and urban canyon solar access. Energy Build. 14, 117–131. https://doi.org/10.1016/0378-7788(90)90031-D

Ashley, R., Lundy, L., Ward, S., Shaffer, P., Walker, L., Morgan, C., Saul, A., Wong, T., Moore, S., 2013. Water-sensitive urban design: Opportunities for the UK. Proc. Inst. Civ. Eng. Munic. Eng. 166, 65–76. https://doi.org/10.1680/muen.12.00046

Awal, R., Fares, A., Habibi, H., 2019. Optimum turf grass irrigation requirements and corresponding water- energy-CO2 Nexus across Harris County, Texas. Sustain. 11, 1–12. https://doi.org/10.3390/su11051440

Barton, L., Wan, G.G.Y., Buck, R.P., Colmer, T.D., 2009. Nitrogen increases evapotranspiration and growth of a warm-season turfgrass. Agron. J. 101, 17–24. https://doi.org/10.2134/agronj2008.0078

Basu, R., Samet, J.M., 2002. Relation between elevated ambient temperature and mortality: A review of the epidemiologic evidence. Epidemiol. Rev. 24, 190–202. https://doi.org/10.1093/epirev/mxf007

Bonfils, C., Lobell, D., 2007. Empirical evidence for a recent slowdown in irrigation-induced cooling. Proc. Natl. Acad. Sci. U. S. A. 104, 13582–13587. https://doi.org/10.1073/pnas.0700144104

Boucher, O., Myhre, G., Myhre, A., 2004. Direct human influence of irrigation on atmospheric water vapour and climate. Clim. Dyn. 22, 597–603. https://doi.org/10.1007/s00382-004-0402-4

Bowler, D.E., Buyung-Ali, L., Knight, T.M., Pullin, A.S., 2010. Urban greening to cool towns and cities: A systematic review of the empirical evidence. Landsc. Urban Plan. 97, 147–155. https://doi.org/10.1016/j.landurbplan.2010.05.006

Broadbent, A.M., Coutts, A.M., Nice, K.A., Demuzere, M., Krayenhoff, E.S., Tapper, N.J., Wouters, H., 2019. The Air-temperature Response to Green/blue-infrastructure Evaluation Tool (TARGET v1.0): an efficient and user-friendly model of city cooling. Geosci. Model Dev. 12, 785–803. https://doi.org/10.5194/gmd-12-785-2019

Broadbent, A.M., Coutts, A.M., Tapper, N.J., Demuzere, M., 2018a. The cooling effect of irrigation on urban microclimate during heatwave conditions. Urban Clim. 23, 309–329. https://doi.org/10.1016/j.uclim.2017.05.002

Broadbent, A.M., Coutts, A.M., Tapper, N.J., Demuzere, M., Beringer, J., 2018b. The microscale cooling effects of water sensitive urban design and irrigation in a suburban environment. Theor. Appl. Climatol. 134, 1–23. https://doi.org/10.1007/s00704-017-2241-3

Bröde, P., Fiala, D., Blazejczyk, K., Holmér, I., Jendritzky, G., Kampmann, B., Tinz, B., Havenith,

G., 2012. Deriving the operational procedure for the Universal Thermal Climate Index (UTCI). Int. J. Biometeorol. 56, 481–494. https://doi.org/10.1007/s00484-011-0454-1

Brown, R.D., Vanos, J., Kenny, N., Lenzholzer, S., 2015. Designing urban parks that ameliorate the effects of climate change. Landsc. Urban Plan. 138, 118–131. https://doi.org/10.1016/j.landurbplan.2015.02.006

Bruse, M., Fleer, H., 1998. Simulating surface–plant–air interactions inside urban environments with a three dimensional numerical model. Environ. Model. Softw. 13, 373–384. https://doi.org/10.1016/S1364-8152(98)00042-5

Budyko, M.I., 1974. Climate and Life. Academic Press.

Bunker, A., Wildenhain, J., Vandenbergh, A., Henschke, N., Rocklöv, J., Hajat, S., Sauerborn, R., 2016. Effects of Air Temperature on Climate-Sensitive Mortality and Morbidity Outcomes in the Elderly; a Systematic Review and Meta-analysis of Epidemiological Evidence. EBioMedicine 6, 258–268. https://doi.org/10.1016/j.ebiom.2016.02.034

Bureau of Meteorology, 2023a. Climate statistics for Australian locations: summary statistics [WWW Document]. URL http://www.bom.gov.au/jsp/ncc/cdio/cvg/av?p_stn_num=086071&p_prim_element_index=0&p_comp_element_index=0&redraw=null&p_display_type=statistics_summary&normals_years=1991-2020&tablesizebutt=normal (accessed 6.2.23).

Bureau of Meteorology, 2023b. Recent Evapotranspiration [WWW Document]. URL http://www.bom.gov.au/watl/eto/ (accessed 7.13.23).

Bureau of Meteorology, 2023c. Climate Data Online [WWW Document]. https://doi.org/http://www.bom.gov.au/climate/data/index.shtml

Bureau of Meteorology, 2009. The exceptional January-February 2009 heatwave in south-eastern Australia.

Burt, C.M., Mutziger, A.J., Allen, R.G., Howell, T.A., 2005. Evaporation Research: Review and Interpretation. J. Irrig. Drain. Eng. 131, 37–58. https://doi.org/10.1061/(ASCE)0733-9437(2005)131:1(37)

Cellier, P., Olioso, A., 1993. A simple system for automated long-term Bowen ratio measurement. Agric. For. Meteorol. 66, 81–92. https://doi.org/10.1016/0168-1923(93)90083-T

Chang, C.R., Li, M.H., Chang, S.D., 2007. A preliminary study on the local cool-island intensity of Taipei city parks. Landsc. Urban Plan. 80, 386–395. https://doi.org/10.1016/j.landurbplan.2006.09.005

Chen, F., Xu, X., Barlage, M., Rasmussen, R., Shen, S., Miao, S., Zhou, G., 2018. Memory of irrigation effects on hydroclimate and its modeling challenge. Environ. Res. Lett. 13. https://doi.org/10.1088/1748-9326/aab9df

Chen, L., Ma, Z.-G., Zhao, T.-B., Li, Z.-H., Li, Y.-P., 2017. Simulation of the regional climatic effect of irrigation over the Yellow River Basin. Atmos. Ocean. Sci. Lett. 10, 291–297. https://doi.org/10.1080/16742834.2017.1313681

Cheung, P.K., Jim, C.Y., 2019a. Differential cooling effects of landscape parameters in humid-subtropical urban parks. Landsc. Urban Plan. 192, 103651. https://doi.org/10.1016/j.landurbplan.2019.103651

Cheung, P.K., Jim, C.Y., 2019b. Effects of urban and landscape elements on air temperature in a high-density subtropical city. Build. Environ. 164, 106362. https://doi.org/10.1016/j.buildenv.2019.106362

Cheung, P.K., Jim, C.Y., 2019c. Improved assessment of outdoor thermal comfort: 1-hour acceptable temperature range. Build. Environ. 151, 303–317. https://doi.org/10.1016/j.buildenv.2019.01.057

Cheung, P.K., Jim, C.Y., 2018a. Subjective outdoor thermal comfort and urban green space usage in humid-subtropical Hong Kong. Energy Build. 173, 150–162. https://doi.org/10.1016/j.enbuild.2018.05.029

Cheung, P.K., Jim, C.Y., 2018b. Comparing the cooling effects of a tree and a concrete shelter using PET and UTCI. Build. Environ. 130, 49–61. https://doi.org/10.1016/j.buildenv.2017.12.013

Cheung, P.K., Jim, C.Y., Tapper, N., Nice, K.A., Livesley, S.J., 2022a. Daytime irrigation leads to significantly cooler private backyards in summer. Urban Clim. 46, 101310. https://doi.org/10.1016/j.uclim.2022.101310

Cheung, P.K., Livesley, S.J., Nice, K.A., 2021. Estimating the cooling potential of irrigating green spaces in 100 global cities with arid, temperate or continental climates. Sustain. Cities Soc. 71, 102974. https://doi.org/10.1016/j.scs.2021.102974

Cheung, P.K., Nice, K.A., Livesley, S.J., 2022b. Irrigating urban green space for cooling benefits: the

mechanisms and management considerations. Environ. Res. Clim. 1, 015001. https://doi.org/10.1088/2752-5295/ac6e7c

City of Melbourne, 2022. Climate change impacts on Melbourne [WWW Document]. URL https://www.melbourne.vic.gov.au/about-council/vision-goals/eco-city/Pages/adapting-to-climate-change.aspx (accessed 1.25.22).

Coccolo, S., Kämpf, J., Mauree, D., Scartezzini, J.L., 2018. Cooling potential of greening in the urban environment, a step further towards practice. Sustain. Cities Soc. 38, 543–559. https://doi.org/10.1016/j.scs.2018.01.019

Connellan, G., 2002. Efficient irrigation: A reference manual for turf and landscape. Melbourne.

Cook, B.I., Puma, M.J., Krakauer, N.Y., 2011. Irrigation induced surface cooling in the context of modern and increased greenhouse gas forcing. Clim. Dyn. 37, 1587–1600. https://doi.org/10.1007/s00382-010-0932-x

Cook, B.I., Shukla, S.P., Puma, M.J., Nazarenko, L.S., 2015. Irrigation as an historical climate forcing. Clim. Dyn. 44, 1715–1730. https://doi.org/10.1007/s00382-014-2204-7

Coutts, A.M., Tapper, N.J., Beringer, J., Loughnan, M., Demuzere, M., 2013. Watering our cities: The capacity for Water Sensitive Urban Design to support urban cooling and improve human thermal comfort in the Australian context. Prog. Phys. Geogr. Earth Environ. 37, 2–28. https://doi.org/10.1177/0309133312461032

Coutts, A.M., White, E.C., Tapper, N.J., Beringer, J., Livesley, S.J., 2016. Temperature and human thermal comfort effects of street trees across three contrasting street canyon environments. Theor. Appl. Climatol. 124, 55–68. https://doi.org/10.1007/s00704-015-1409-y

Crum, S.M., Jenerette, G.D., 2017. Microclimate Variation among Urban Land Covers: The Importance of Vertical and Horizontal Structure in Air and Land Surface Temperature Relationships. J. Appl. Meteorol. Climatol. 56, 2531–2543. https://doi.org/10.1175/JAMC-D-17-0054.1

Daniel, M., Lemonsu, A., Viguié, V., 2018. Role of watering practices in large-scale urban planning strategies to face the heat-wave risk in future climate. Urban Clim. 23, 287–308. https://doi.org/10.1016/j.uclim.2016.11.001

Darmanto, N.S., Varquez, A.C.G., Kawano, N., Kanda, M., 2019. Future urban climate projection in a tropical megacity based on global climate change and local urbanization scenarios. Urban

Clim. 29, 100482. https://doi.org/10.1016/j.uclim.2019.100482

de Abreu-Harbich, L.V., Labaki, L.C., Matzarakis, A., 2015. Effect of tree planting design and tree species on human thermal comfort in the tropics. Landsc. Urban Plan. 138, 99–109. https://doi.org/10.1016/j.landurbplan.2015.02.008

Deardorff, J.W., 1978. Efficient prediction of ground surface temperature and moisture, with inclusion of a layer of vegetation. J. Geophys. Res. 83, 1889. https://doi.org/10.1029/JC083iC04p01889

Demographia, 2020. Demographia World Urban Areas 16th Annual Edition.

Demuzere, M., Kittner, J., Martilli, A., Mills, G., Moede, C., Stewart, I.D., van Vliet, J., Bechtel, B., 2022. A global map of local climate zones to support earth system modelling and urban-scale environmental science. Earth Syst. Sci. Data 14, 3835–3873. https://doi.org/10.5194/essd-14-3835-2022

Derkzen, M.L., van Teeffelen, A.J.A., Verburg, P.H., 2015. REVIEW: Quantifying urban ecosystem services based on high-resolution data of urban green space: An assessment for Rotterdam, the Netherlands. J. Appl. Ecol. 52, 1020–1032. https://doi.org/10.1111/1365-2664.12469

Dewaelheyns, V., Jakobsson, A., Saltzman, K., 2018. Strategic gardens and gardening: Inviting a widened perspective on the values of private green space. Urban For. Urban Green. 30, 207–209. https://doi.org/10.1016/j.ufug.2017.12.009

Doick, K.J., Peace, A., Hutchings, T.R., 2014. The role of one large greenspace in mitigating London's nocturnal urban heat island. Sci. Total Environ. 493, 662–671. https://doi.org/10.1016/j.scitotenv.2014.06.048

Domeisen, D.I. V, Eltahir, E.A.B., Fischer, E.M., Knutti, R., Perkins-Kirkpatrick, S.E., Schär, C., Seneviratne, S.I., Weisheimer, A., Wernli, H., 2022. Prediction and projection of heatwaves. Nat. Rev. Earth Environ. 4, 36–50. https://doi.org/10.1038/s43017-022-00371-z

Doorenbos, J., Pruitt, W.O., 1977. Guidelines for predicting crop water requirements, FAO Irrigation and Drainage Paper No. 24, 2nd Edition. Rome, Italy.

Emmanuel, R., Rosenlund, H., Johansson, E., 2007. Urban shading—a design option for the tropics? A study in Colombo, Sri Lanka. Int. J. Climatol. 27, 1995–2004. https://doi.org/10.1002/joc.1609

Environment and Natural Resources Committee, 2009. Inquiry into Melbourne's Future Water Supply. Melbourne, Australia.

Fanger, P.O., 1970. Thermal Comfort: Analysis and applications in environmental engineering. Copenhagen: Danish Technical Press., New York.

Fatichi, S., Ivanov, V.Y., Caporali, E., 2012. A mechanistic ecohydrological model to investigate complex interactions in cold and warm water-controlled environments: 1. Theoretical framework and plot-scale analysis. J. Adv. Model. Earth Syst. 4, 1–31. https://doi.org/10.1029/2011MS000086

Fatichi, S., Pappas, C., 2017. Constrained variability of modeled T : ET ratio across biomes. Geophys. Res. Lett. 44, 6795–6803. https://doi.org/10.1002/2017GL074041

Fay, P.A., Schultz, M.J., 2009. Germination, survival, and growth of grass and forb seedlings: Effects of soil moisture variability. Acta Oecologica 35, 679–684. https://doi.org/10.1016/j.actao.2009.06.007

Fuller, R.A., Gaston, K.J., 2009. The scaling of green space coverage in European cities. Biol. Lett. 5, 352–355. https://doi.org/10.1098/rsbl.2009.0010

Gao, K., Santamouris, M., 2019. The use of water irrigation to mitigate ambient overheating in the built environment: Recent progress. Build. Environ. 164, 106346. https://doi.org/10.1016/j.buildenv.2019.106346

Gao, K., Santamouris, M., Feng, J., 2020. On the cooling potential of irrigation to mitigate urban heat island. Sci. Total Environ. 740, 139754. https://doi.org/10.1016/j.scitotenv.2020.139754

Geerts, B., 2002. On the effects of irrigation and urbanisation on the annual range of monthly-mean temperatures. Theor. Appl. Climatol. 72, 157–163. https://doi.org/10.1007/s00704-002-0683-7

Gil-Meseguer, E., Bernabé-Crespo, M.B., Gómez-Espín, J.M., 2019. Recycled Sewage - A Water Resource for Dry Regions of Southeastern Spain. Water Resour. Manag. 33, 725–737. https://doi.org/10.1007/s11269-018-2136-9

Giles-Corti, B., Broomhall, M.H., Knuiman, M., Collins, C., Douglas, K., Ng, K., Lange, A., Donovan, R.J., 2005. Increasing walking: How important is distance to, attractiveness, and size of public open space? Am. J. Prev. Med. 28, 169–176. https://doi.org/10.1016/j.amepre.2004.10.018

Gill, S.E., Rahman, M.A., Handley, J.F., Ennos, A.R., 2013. Modelling water stress to urban amenity grass in Manchester UK under climate change and its potential impacts in reducing urban cooling. Urban For. Urban Green. 12, 350–358. https://doi.org/10.1016/j.ufug.2013.03.005

Givoni, B., 1963. Estimation of the effect of climate on man: development of a new thermal index. Israel Institute of Technology.

Gober, P., Brazel, A., Quay, R., Myint, S., Grossman-Clarke, S., Miller, A., Rossi, S., 2010. Using watered landscapes to manipulate urban heat island effects: How much water will it take to cool phoenix? J. Am. Plan. Assoc. 76, 109–121. https://doi.org/10.1080/01944360903433113

González-Muñoz, N., Castro-Díez, P., Fierro-Brunnenmeister, N., 2011. Establishment success of coexisting native and exotic trees under an experimental gradient of irradiance and soil moisture. Environ. Manage. 48, 764–773. https://doi.org/10.1007/s00267-011-9731-3

Google Scholar, 2020. Google Scholar [WWW Document]. URL https://scholar.google.com.hk/ (accessed 4.25.20).

Grant, S.B., Saphores, J.D., Feldman, D.L., Hamilton, A.J., Fletcher, T.D., Cook, P.L.M., Stewardson, M., Sanders, B.F., Levin, L.A., Ambrose, R.F., Deletic, A., Brown, R., Jiang, S.C., Rosso, D., Cooper, W.J., Marusic, I., 2012. Taking the "waste" out of "wastewater" for human water security and ecosystem sustainability. Science (80-.). 337, 681–686. https://doi.org/10.1126/science.1216852

Griggs, D., 2013. Sustainable developmnet goals for people and planet. Nature 495, 305–307.

Groenewegen, P.P., den Berg, A.E., de Vries, S., Verheij, R.A., 2006. Vitamin G: effects of green space on health, well-being, and social safety. BMC Public Health 6, 1–9. https://doi.org/10.1186/1471-2458-6-149

Grossiord, C., Buckley, T.N., Cernusak, L.A., Novick, K.A., Poulter, B., Siegwolf, R.T.W., Sperry, J.S., McDowell, N.G., 2020. Plant responses to rising vapor pressure deficit. New Phytol. 226, 1550–1566. https://doi.org/10.1111/nph.16485

Gunawardena, K.R., Wells, M.J., Kershaw, T., 2017. Utilising green and bluespace to mitigate urban heat island intensity. Sci. Total Environ. 584–585, 1040–1055. https://doi.org/10.1016/j.scitotenv.2017.01.158

Guo, H., Aviv, D., Loyola, M., Teitelbaum, E., Houchois, N., Meggers, F., 2020. On the understanding of the mean radiant temperature within both the indoor and outdoor environment,

a critical review. Renew. Sustain. Energy Rev. 117, 109207. https://doi.org/10.1016/j.rser.2019.06.014

Haley, M.B., Dukes, M.D., 2012. Validation of Landscape Irrigation Reduction with Soil Moisture Sensor Irrigation Controllers. J. Irrig. Drain. Eng. 138, 135–144. https://doi.org/10.1061/(asce)ir.1943-4774.0000391

Hall, T., 2015. What has happened to the Australian backyard? Aust. Gard. Hist. 27, 12–15. https://doi.org/01601009

Hamlyn-Harris, D., McAlister, T., Dillon, P., 2018. Water Harvesting Potential of WSUD Approaches, Approaches to Water Sensitive Urban Design: Potential, Design, Ecological Health, Urban Greening, Economics, Policies, and Community Perceptions. Elsevier Inc. https://doi.org/10.1016/B978-0-12-812843-5.00009-5

Hancock, N.H., Uddin, J.M., Smith, R.J., Foley, J.P., 2015. Micrometeorology of sprinkler irrigation. Agric. For. Meteorol. 200, 293–301. https://doi.org/10.1016/j.agrformet.2014.10.010

Handreck, K.A., Black, N.D., 2001. Growing media for ornamental plants and turf, 3rd ed. New South Wales University Press, Kensington, Australia.

Hao, T., Chang, H., Liang, S., Jones, P., Chan, P.W., Li, L., Huang, J., 2023. Heat and park attendance: Evidence from “small data” and “big data” in Hong Kong. Build. Environ. 234, 110123. https://doi.org/10.1016/j.buildenv.2023.110123

Harding, K.J., Snyder, P.K., 2012. Modeling the atmospheric response to irrigation in the great plains. Part I: General impacts on precipitation and the energy budget. J. Hydrometeorol. 13, 1667–1686. https://doi.org/10.1175/JHM-D-11-098.1

Harshan, S., Roth, M., Velasco, E., Demuzere, M., 2018. Evaluation of an urban land surface scheme over a tropical suburban neighborhood. Theor. Appl. Climatol. 133, 867–886. https://doi.org/10.1007/s00704-017-2221-7

Hastie, T.J., Pregibon, D., 1992. Generalised linear models, in: Chambers, J., Hastie, T. (Eds.), Statistical Models in S. Wadsworth & Brooks/Cole, p. 53.

He, B.J., Ding, L., Prasad, D., 2020. Relationships among local-scale urban morphology, urban ventilation, urban heat island and outdoor thermal comfort under sea breeze influence. Sustain. Cities Soc. 60, 102289. https://doi.org/10.1016/j.scs.2020.102289

He, B.J., Wang, J., Liu, H., Ulpiani, G., 2021. Localized synergies between heat waves and urban heat islands: Implications on human thermal comfort and urban heat management. Environ. Res. 193, 110584. https://doi.org/10.1016/j.envres.2020.110584

Hersbach, H., Bell, B., Berrisford, P., Hirahara, S., Horányi, A., Muñoz-Sabater, J., Nicolas, J., Peubey, C., Radu, R., Schepers, D., Simmons, A., Soci, C., Abdalla, S., Abellan, X., Balsamo, G., Bechtold, P., Biavati, G., Bidlot, J., Bonavita, M., Chiara, G., Dahlgren, P., Dee, D., Diamantakis, M., Dragani, R., Flemming, J., Forbes, R., Fuentes, M., Geer, A., Haimberger, L., Healy, S., Hogan, R.J., Hólm, E., Janisková, M., Keeley, S., Laloyaux, P., Lopez, P., Lupu, C., Radnoti, G., Rosnay, P., Rozum, I., Vamborg, F., Villaume, S., Thépaut, J., 2020. The ERA5 global reanalysis. Q. J. R. Meteorol. Soc. 146, 1999–2049. https://doi.org/10.1002/qj.3803

Höppe, P., 1999. The physiological equivalent temperature - a universal index for the biometeorological assessment of the thermal environment. Int. J. Biometeorol. 43, 71–75. https://doi.org/10.1007/s004840050118

Horton, R., Wierenga, P.J., 1983. Estimating the Soil Heat Flux from Observations of Soil Temperature Near the Surface. Soil Sci. Soc. Am. J. 47, 14–20. https://doi.org/10.2136/sssaj1983.03615995004700010003x

Howells, M., Hermann, S., Welsch, M., Bazilian, M., Segerström, R., Alfstad, T., Gielen, D., Rogner, H., Fischer, G., Van Velthuizen, H., Wiberg, D., Young, C., Alexander Roehrl, R., Mueller, A., Steduto, P., Ramma, I., 2013. Integrated analysis of climate change, land-use, energy and water strategies. Nat. Clim. Chang. 3, 621–626. https://doi.org/10.1038/nclimate1789

Huber, D.B., Mechem, D.B., Brunsell, N.A., 2014. The effects of great plains irrigation on the surface energy balance, regional circulation, and precipitation. Climate 2, 103–128. https://doi.org/10.3390/cli2020103

Hunter, 2023. MP ROTATOR [WWW Document]. URL https://www.hunterindustries.com/product-line/MP Rotator (accessed 6.2.23).

ISO 7726, 1998. Ergonomics of the thermal environment - Instruments for measuring physical quantities. Geneva.

Järvi, L., Grimmond, C.S.B., Christen, A., 2011. The Surface Urban Energy and Water Balance Scheme (SUEWS): Evaluation in Los Angeles and Vancouver. J. Hydrol. 411, 219–237. https://doi.org/10.1016/j.jhydrol.2011.10.001

Jauregui, E., 1990. Influence of a large urban park on temperature and convective precipitation in a tropical city. Energy Build. 15, 457–463. https://doi.org/10.1016/0378-7788(90)90021-A

Jennings, V., Bamkole, O., 2019. The relationship between social cohesion and urban green space: An avenue for health promotion. Int. J. Environ. Res. Public Health 16. https://doi.org/10.3390/ijerph16030452

Jiang, Y., Liu, J., Li, H., Hua, L., Yong, Y., 2021. Droplet distribution characteristics of impact sprinklers with circular and noncircular nozzles: Effect of nozzle aspect ratios and equivalent diameters. Biosyst. Eng. 212, 200–214. https://doi.org/10.1016/j.biosystemseng.2021.10.013

Jim, C.Y., 2019. Resolving intractable soil constraints in urban forestry through research–practice synergy. Socio-Ecological Pract. Res. 1, 41–53. https://doi.org/10.1007/s42532-018-00005-z

Jim, C.Y., Chan, M.W.H., 2016. Urban greenspace delivery in Hong Kong: Spatial-institutional limitations and solutions. Urban For. Urban Green. 18, 65–85. https://doi.org/10.1016/j.ufug.2016.03.015

Jung, M., Reichstein, M., Ciais, P., Seneviratne, S.I., Sheffield, J., Goulden, M.L., Bonan, G., Cescatti, A., Chen, J., De Jeu, R., Dolman, A.J., Eugster, W., Gerten, D., Gianelle, D., Gobron, N., Heinke, J., Kimball, J., Law, B.E., Montagnani, L., Mu, Q., Mueller, B., Oleson, K., Papale, D., Richardson, A.D., Roupsard, O., Running, S., Tomelleri, E., Viovy, N., Weber, U., Williams, C., Wood, E., Zaehle, S., Zhang, K., 2010. Recent decline in the global land evapotranspiration trend due to limited moisture supply. Nature 467, 951–954. https://doi.org/10.1038/nature09396

Kanamaru, H., Kanamitsu, M., 2008. Model diagnosis of nighttime minimum temperature warming during summer due to irrigation in the California Central Valley. J. Hydrometeorol. 9, 1061–1072. https://doi.org/10.1175/2008JHM967.1

Kent, C.W., Grimmond, S., Gatey, D., 2017. Aerodynamic roughness parameters in cities: Inclusion of vegetation. J. Wind Eng. Ind. Aerodyn. 169, 168–176. https://doi.org/10.1016/j.jweia.2017.07.016

Kolka, R., Steber, A., Brooks, K., Perry, C.H., Powers, M., 2012. Relationships between Soil Compaction and Harvest Season, Soil Texture, and Landscape Position for Aspen Forests. North. J. Appl. For. 29, 21–25. https://doi.org/10.5849/njaf.10-039

Konarska, J., Lindberg, F., Larsson, A., Thorsson, S., Holmer, B., 2014. Transmissivity of solar radiation through crowns of single urban trees-application for outdoor thermal comfort

modelling. Theor. Appl. Climatol. 117, 363–376. https://doi.org/10.1007/s00704-013-1000-3

Kool, D., Agam, N., Lazarovitch, N., Heitman, J.L., Sauer, T.J., Ben-Gal, A., 2014. A review of approaches for evapotranspiration partitioning. Agric. For. Meteorol. 184, 56–70. https://doi.org/10.1016/j.agrformet.2013.09.003

Koprowska, K., Łaszkiewicz, E., Kronenberg, J., Marcińczak, S., 2018. Subjective perception of noise exposure in relation to urban green space availability. Urban For. Urban Green. 31, 93–102. https://doi.org/10.1016/j.ufug.2018.01.018

Koster, R.D., Guo, Z., Dirmeyer, P.A., Bonan, G., Chan, E., Cox, P., Davies, H., Gordon, C.T., Kanae, S., Kowalczyk, E., Lawrence, D., Liu, P., Lu, C.H., Malyshev, S., McAvaney, B., Mitchell, K., Mocko, D., Oki, T., Oleson, K.W., Pitman, A., Sud, Y.C., Taylor, C.M., Verseghy, D., Vasic, R., Xue, Y., Yamada, T., 2006. GLACE: The Global Land-Atmosphere Coupling Experiment. Part I: Overview. J. Hydrometeorol. 7, 590–610. https://doi.org/10.1175/JHM510.1

Koster, R.D., Schubert, S.D., Suarez, M.J., 2009. Analyzing the Concurrence of Meteorological Droughts and Warm Periods, with Implications for the Determination of Evaporative Regime. J. Clim. 22, 3331–3341. https://doi.org/10.1175/2008JCLI2718.1

Krüger, E.L., Minella, F.O., Matzarakis, A., 2014. Comparison of different methods of estimating the mean radiant temperature in outdoor thermal comfort studies. Int. J. Biometeorol. 58, 1727–1737. https://doi.org/10.1007/s00484-013-0777-1

Kueppers, L.M., Snyder, M.A., Sloan, L.C., 2007. Irrigation cooling effect: Regional climate forcing by land-use change. Geophys. Res. Lett. 34, 1–5. https://doi.org/10.1029/2006GL028679

Kustas, W.P., Stannard, D.I., Allwine, K.J., 1996. Variability in surface energy flux partitioning during Washita ’92: Resulting effects on Penman-Monteith and Priestley-Taylor parameters. Agric. For. Meteorol. 82, 171–193. https://doi.org/10.1016/0168-1923(96)02334-9

Kvålseth, T.O., 1985. Cautionary Note about R 2. Am. Stat. 39, 279–285. https://doi.org/10.1080/00031305.1985.10479448

Lachowycz, K., Jones, A.P., 2013. Towards A Better Understanding Of The Relationship Between Greenspace And Health: Development Of A Theoretical Framework. Landsc. Urban Plan. 118, 62–69. https://doi.org/10.1016/j.landurbplan.2012.10.012

Lai, D., Liu, W., Gan, T., Liu, K., Chen, Q., 2019. A review of mitigating strategies to improve the thermal environment and thermal comfort in urban outdoor spaces. Sci. Total Environ.

#pagerange#. https://doi.org/10.1016/j.scitotenv.2019.01.062

Lam, C.K.C., Gallant, A.J.E., Tapper, N.J., 2020. Does irrigation cooling effect intensify during heatwaves? A case study in the Melbourne botanic gardens. Urban For. Urban Green. 55, 126815. https://doi.org/10.1016/j.ufug.2020.126815

Lam, C.K.C., Lau, K.K.-L., 2018. Effect of long-term acclimatization on summer thermal comfort in outdoor spaces: a comparative study between Melbourne and Hong Kong. Int. J. Biometeorol. 62, 1311–1324. https://doi.org/10.1007/s00484-018-1535-1

Lee, A.C.K., Maheswaran, R., 2011. The health benefits of urban green spaces: a review of the evidence. J. Public Health (Bangkok). 33, 212–222. https://doi.org/10.1093/pubmed/fdq068

Leverenz, H.L., Tchobanoglous, G., Asano, T., 2011. Direct potable reuse: A future imperative. J. Water Reuse Desalin. 1, 2–10. https://doi.org/10.2166/wrd.2011.000

Li, D., Sun, T., Liu, M., Yang, L., Wang, L., Gao, Z., 2015. Contrasting responses of urban and rural surface energy budgets to heat waves explain synergies between urban heat islands and heat waves. Environ. Res. Lett. 10. https://doi.org/10.1088/1748-9326/10/5/054009

Li, Y., Fan, S., Li, K., Zhang, Y., Dong, L., 2021. Microclimate in an urban park and its influencing factors: a case study of Tiantan Park in Beijing, China. Urban Ecosyst. 24, 767–778. https://doi.org/10.1007/s11252-020-01073-4

Li, Y., Guan, K., Peng, B., Franz, T.E., Wardlow, B., Pan, M., 2020. Quantifying irrigation cooling benefits to maize yield in the US Midwest. Glob. Chang. Biol. 26, 3065–3078. https://doi.org/10.1111/gcb.15002

Lin, B.B., Meyers, J., Beaty, R.M., Barnett, G.B., 2016. Urban green infrastructure impacts on climate regulation services in Sydney, Australia. Sustain. 8. https://doi.org/10.3390/su8080788

Lin, T.-P., Yang, S.-R., Chen, Y.-C., Matzarakis, A., 2019. The potential of a modified physiologically equivalent temperature (mPET) based on local thermal comfort perception in hot and humid regions. Theor. Appl. Climatol. 135, 873–876. https://doi.org/10.1007/s00704-018-2419-3

Lin, T.P., Matzarakis, A., Hwang, R.L., 2010. Shading effect on long-term outdoor thermal comfort. Build. Environ. 45, 213–221. https://doi.org/10.1016/j.buildenv.2009.06.002

Lin, T.P., Tsai, K.T., Liao, C.C., Huang, Y.C., 2013. Effects of thermal comfort and adaptation on

park attendance regarding different shading levels and activity types. Build. Environ. 59, 599–611. https://doi.org/10.1016/j.buildenv.2012.10.005

Litvak, E., Pataki, D.E., 2016. Evapotranspiration of urban lawns in a semi-arid environment: An in situ evaluation of microclimatic conditions and watering recommendations. J. Arid Environ. 134, 87–96. https://doi.org/10.1016/j.jaridenv.2016.06.016

Liu, G., Wang, W., 2023. Irrigation-Induced Crop Growth Enhances Irrigation Cooling Effect Over the North China Plain by Increasing Transpiration. Water Resour. Res. 59, 1–22. https://doi.org/10.1029/2022WR034142

Livesley, S.J., Marchionni, V., Cheung, P.K., Daly, E., Pataki, D.E., 2021. Water smart cities increase irrigation to provide cool refuge in a climate crisis. Earth's Futur. 9, 1–6. https://doi.org/10.1029/2020EF001806

Livesley, S.J., McPherson, E.G., Calfapietra, C., 2016. The Urban Forest and Ecosystem Services: Impacts on Urban Water, Heat, and Pollution Cycles at the Tree, Street, and City Scale. J. Environ. Qual. 45, 119–124. https://doi.org/10.2134/jeq2015.11.0567

Lobell, D., Bala, G., Mirin, A., Phillips, T., Maxwell, R., Rotman, D., 2009. Regional differences in the influence of irrigation on climate. J. Clim. 22, 2248–2255. https://doi.org/10.1175/2008JCLI2703.1

Lobell, D.B., Bonfils, C., 2008. The effect of irrigation on regional temperatures: A spatial and temporal analysis of trends in California, 1934-2002. J. Clim. 21, 2063–2071. https://doi.org/10.1175/2007JCLI1755.1

Lobell, D.B., Bonfils, C., Faurès, J.M., 2008a. The role of irrigation expansion in past and future temperature trends. Earth Interact. 12, 1–11. https://doi.org/10.1175/2007EI241.1

Lobell, D.B., Bonfils, C.J., Kueppers, L.M., Snyder, M.A., 2008b. Irrigation cooling effect on temperature and heat index extremes. Geophys. Res. Lett. 35, 1–5. https://doi.org/10.1029/2008GL034145

Loram, A., Tratalos, J., Warren, P.H., Gaston, K.J., 2007. Urban domestic gardens (X): The extent & structure of the resource in five major cities. Landsc. Ecol. 22, 601–615. https://doi.org/10.1007/s10980-006-9051-9

Ma, S., Pitman, A., Yang, J., Carouge, C., Evans, J.P., Hart, M., Green, D., 2018. Evaluating the effectiveness of mitigation options on heat stress for Sydney, Australia. J. Appl. Meteorol.

Climatol. 57, 209–220. https://doi.org/10.1175/JAMC-D-17-0061.1

Maas, J., Verheij, R.A., Groenewegen, P.P., de Vries, S., Spreeuwenberg, P., 2006a. Green space, urbanity, and health: how strong is the relation? J. Epidemiol. Community Health 60, 587–592. https://doi.org/10.1136/jech.2005.043125

Maas, J., Verheij, R.A., Groenewegen, P.P., Vries, S. De, Spreeuwenberg, P., 2006b. Green space, urbanity, and health: how strong is the relation ? 587–592. https://doi.org/10.1136/jech.2005.043125

Macdonald, R.W., Griffiths, R.F., Hall, D.J., 1998. An improved method for the estimation of surface roughness of obstacle arrays. Atmos. Environ. 32, 1857–1864. https://doi.org/10.1016/S1352-2310(97)00403-2

Mahat, V., Tarboton, D.G., Molotch, N.P., 2013. Testing above- and below-canopy representations of turbulent fluxes in an energy balance snowmelt model. Water Resour. Res. 49, 1107–1122. https://doi.org/10.1002/wrcr.20073

Markevych, I., Schoierer, J., Hartig, T., Chudnovsky, A., Hystad, P., Dzhambov, A.M., Vries, S. De, Triguero-mas, M., Brauer, M., Nieuwenhuijsen, M.J., Lupp, G., Richardson, E.A., Astell-burt, T., Dimitrova, D., Feng, X., Sadeh, M., Standl, M., Heinrich, J., Fuertes, E., 2017. Exploring pathways linking greenspace to health : Theoretical and methodological guidance. Environ. Res. 158, 301–317. https://doi.org/10.1016/j.envres.2017.06.028

Maronga, B., Banzhaf, S., Burmeister, C., Esch, T., Forkel, R., Fröhlich, D., Fuka, V., Gehrke, K.F., Geletič, J., Giersch, S., Gronemeier, T., Groß, G., Heldens, W., Hellsten, A., Hoffmann, F., Inagaki, A., Kadasch, E., Kanani-Sühring, F., Ketelsen, K., Khan, B.A., Knigge, C., Knoop, H., Krč, P., Kurppa, M., Maamari, H., Matzarakis, A., Mauder, M., Pallasch, M., Pavlik, D., Pfafferott, J., Resler, J., Rissmann, S., Russo, E., Salim, M., Schrempf, M., Schwenkel, J., Seckmeyer, G., Schubert, S., Sühring, M., von Tils, R., Vollmer, L., Ward, S., Witha, B., Wurps, H., Zeidler, J., Raasch, S., 2020. Overview of the PALM model system 6.0. Geosci. Model Dev. 13, 1335–1372. https://doi.org/10.5194/gmd-13-1335-2020

Masoudi, M., Tan, P.Y., Fadaei, M., 2021. The effects of land use on spatial pattern of urban green spaces and their cooling ability. Urban Clim. 35, 100743. https://doi.org/10.1016/j.uclim.2020.100743

Masterton, J., Richardson, F., 1979. Humidex: A Method of Quantifying Human Discomfort due to Excessive Heat and Humidity. Downsview, Ont. : Environment Canada, Atmospheric

Environment.

Mathieu, R., Freeman, C., Aryal, J., 2007. Mapping private gardens in urban areas using object-oriented techniques and very high-resolution satellite imagery. Landsc. Urban Plan. 81, 179–192. https://doi.org/10.1016/j.landurbplan.2006.11.009

Matzarakis, A., Amelung, B., 2008. Physiological Equivalent Temperature as Indicator for Impacts of Climate Change on Thermal Comfort of Humans, in: Seasonal Forecasts, Climatic Change and Human Health. Springer Netherlands, Dordrecht, pp. 161–172. https://doi.org/10.1007/978-1-4020-6877-5_10

Matzarakis, A., Mayer, H., Iziomon, M.G., 1999. Applications of a universal thermal index: physiological equivalent temperature. Int. J. Biometeorol. 43, 76–84. https://doi.org/10.1007/s004840050119

McAdam, S.A.M., Brodribb, T.J., 2015. The Evolution of Mechanisms Driving the Stomatal Response to Vapor Pressure Deficit. Plant Physiol. 167, 833–843. https://doi.org/10.1104/pp.114.252940

McCarthy, H.R., Pataki, D.E., 2010. Drivers of variability in water use of native and non-native urban trees in the greater Los Angeles area. Urban Ecosyst. 13, 393–414. https://doi.org/10.1007/s11252-010-0127-6

McCarthy, M.P., Best, M.J., Betts, R.A., 2010. Climate change in cities due to global warming and urban effects. Geophys. Res. Lett. 37, 1–6. https://doi.org/10.1029/2010GL042845

Meili, N., Manoli, G., Burlando, P., Bou-Zeid, E., Chow, W.T.L., Coutts, A.M., Daly, E., Nice, K.A., Roth, M., Tapper, N.J., Velasco, E., Vivoni, E.R., Fatichi, S., 2020. An urban ecohydrological model to quantify the effect of vegetation on urban climate and hydrology (UT&C v1.0). Geosci. Model Dev. 13, 335–362. https://doi.org/10.5194/gmd-13-335-2020

Meili, N., Manoli, G., Burlando, P., Carmeliet, J., Chow, W.T.L., Coutts, A.M., Roth, M., Velasco, E., Vivoni, E.R., Fatichi, S., 2021. Tree effects on urban microclimate: Diurnal, seasonal, and climatic temperature differences explained by separating radiation, evapotranspiration, and roughness effects. Urban For. Urban Green. 58, 126970. https://doi.org/10.1016/j.ufug.2020.126970

Middel, A., Krayenhoff, E.S., 2019. Micrometeorological determinants of pedestrian thermal exposure during record-breaking heat in Tempe, Arizona: Introducing the MaRTy observational

platform. Sci. Total Environ. 687, 137–151. https://doi.org/10.1016/j.scitotenv.2019.06.085

Mitchell, V.G., Deletic, A., Fletcher, T.D., Hatt, B.E., McCarthy, D.T., 2007. Achieving multiple benefits from stormwater harvesting. Water Sci. Technol. 55, 135–144. https://doi.org/10.2166/wst.2007.103

Molle, B., Tomas, S., Hendawi, M., Granier, J., 2012. EVAPORATION AND WIND DRIFT LOSSES DURING SPRINKLER IRRIGATION INFLUENCED BY DROPLET SIZE DISTRIBUTION. Irrig. Drain. 61, 240–250. https://doi.org/10.1002/ird.648

Mosaddeghi, M.R., Hajabbasi, M.A., Hemmat, A., Afyuni, M., 2000. Soil compactibility as affected by soil moisture content and farmyard manure in central Iran. Soil Tillage Res. 55, 87–97. https://doi.org/10.1016/S0167-1987(00)00102-1

Nagelkerke, N.J.D., 1991. A note on a general definition of the coefficient of determination. Biometrika 78, 691–692. https://doi.org/10.1093/biomet/78.3.691

Nice, K.A., Coutts, A.M., Tapper, N.J., 2018. Development of the VTUF-3D v1.0 urban micro-climate model to support assessment of urban vegetation influences on human thermal comfort. Urban Clim. 24, 1052–1076. https://doi.org/10.1016/j.uclim.2017.12.008

Nocco, M.A., Smail, R.A., Kucharik, C.J., 2019. Observation of irrigation-induced climate change in the Midwest United States. Glob. Chang. Biol. 25, 3472–3484. https://doi.org/10.1111/gcb.14725

Norton, B.A., Coutts, A.M., Livesley, S.J., Harris, R.J., Hunter, A.M., Williams, N.S.G., 2015. Planning for cooler cities: A framework to prioritise green infrastructure to mitigate high temperatures in urban landscapes. Landsc. Urban Plan. 134, 127–138. https://doi.org/10.1016/j.landurbplan.2014.10.018

Nouri, H., Beecham, S., Hassanli, A.M., Kazemi, F., 2013. Water requirements of urban landscape plants: A comparison of three factor-based approaches. Ecol. Eng. 57, 276–284. https://doi.org/10.1016/j.ecoleng.2013.04.025

Nowakowski, A.J., Watling, J.I., Thompson, M.E., Brusch, G.A., Catenazzi, A., Whitfield, S.M., Kurz, D.J., Suárez-Mayorga, Á., Aponte-Gutiérrez, A., Donnelly, M.A., Todd, B.D., 2018. Thermal biology mediates responses of amphibians and reptiles to habitat modification. Ecol. Lett. 21, 345–355. https://doi.org/10.1111/ele.12901

Oke, T.R., 2006. Towards better scientific communication in urban climate. Theor. Appl. Climatol.

84, 179–190. https://doi.org/10.1007/s00704-005-0153-0

Oke, T.R., 1988. The urban energy balance. Prog. Phys. Geogr. 12, 471–508. https://doi.org/10.1177/030913338801200401

Oke, T.R., 1982. The energetic basis of the urban heat island. Q. J. R. Meteorol. Soc. 108, 1–24. https://doi.org/10.1002/qj.49710845502

Oke, T.R., 1979. Advectively-assisted evapotranspiration from irrigated urban vegetation. Boundary-Layer Meteorol. 17, 167–173. https://doi.org/10.1007/BF00117976

Oke, T.R., Crowther, J.M., McNaughton, K.G., Monteith, J.L., Gardiner, B., 1989. The Micrometeorology of the Urban Forest [and Discussion]. Philos. Trans. R. Soc. B Biol. Sci. 324, 335–349. https://doi.org/10.1098/rstb.1989.0051

Oke, T.R., Mills, G., Christen, A., Voogt, J.A., 2017. Urban Climates. Cambridge University Press, Cambridge. https://doi.org/10.1017/9781139016476

Ozdogan, M., Rodell, M., Beaudoing, H.K., Toll, D.L., 2010. Simulating the effects of irrigation over the united states in a land surface model based on satellite-derived agricultural data. J. Hydrometeorol. 11, 171–184. https://doi.org/10.1175/2009JHM1116.1

Pearlmutter, D., Berliner, P., Shaviv, E., 2007. Urban climatology in arid regions: current research in the Negev desert. Int. J. Climatol. 27, 1875–1885. https://doi.org/10.1002/joc.1523

Peck, A., Prodanovic, P., Simonovic, S.P., 2012. Rainfall intensity duration frequency curves under climate change: City of London, Ontario, Canada. Can. Water Resour. J. 37, 177–189. https://doi.org/10.4296/cwrj2011-935

Peel, M.C., Finlayson, B.L., McMahon, T.A., 2007. Updated world map of the Köppen-Geiger climate classification. Hydrol. Earth Syst. Sci. 11, 1633–1644. https://doi.org/10.5194/hess-11-1633-2007

Perez, P.J., Castellvi, F., Ibañez, M., Rosell, J.I., 1999. Assessment of reliability of Bowen ratio method for partitioning fluxes. Agric. For. Meteorol. 97, 141–150. https://doi.org/10.1016/S0168-1923(99)00080-5

Perkins-Kirkpatrick, S.E., Lewis, S.C., 2020. Increasing trends in regional heatwaves. Nat. Commun. 11, 3357. https://doi.org/10.1038/s41467-020-16970-7

Playán, E., Salvador, R., Faci, J.M., Zapata, N., Martínez-Cob, A., Sánchez, I., 2005. Day and night

wind drift and evaporation losses in sprinkler solid-sets and moving laterals. Agric. Water Manag. 76, 139–159. https://doi.org/10.1016/j.agwat.2005.01.015

Portland State Aerospace Society, 2004. A quick derivation relating altitude to air pressure.

Potchter, O., Cohen, P., Bitan, A., 2006. Climatic behavior of various urban parks during hot and humid summer in the mediterranean city of Tel Aviv, Israel. Int. J. Climatol. 26, 1695–1711. https://doi.org/10.1002/joc.1330

Puma, M.J., Cook, B.I., 2010. Effects of irrigation on global climate during the 20th century. J. Geophys. Res. Atmos. 115, 1–15. https://doi.org/10.1029/2010JD014122

Qian, Y., Huang, M., Yang, B., Berg, L.K., 2013. A modeling study of irrigation effects on surface fluxes and land-air-cloud interactions in the southern great plains. J. Hydrometeorol. 14, 700–721. https://doi.org/10.1175/JHM-D-12-0134.1

Qiu, G.Y., Zou, Z., Li, X., Li, H., Guo, Q., Yan, C., Tan, S., 2017. Experimental studies on the effects of green space and evapotranspiration on urban heat island in a subtropical megacity in China. Habitat Int. 68, 30–42. https://doi.org/10.1016/j.habitatint.2017.07.009

Qiu, K., Jia, B., 2020. The roles of landscape both inside the park and the surroundings in park cooling effect. Sustain. Cities Soc. 52, 101864. https://doi.org/10.1016/j.scs.2019.101864

R Core Team, 2023. R: A language and environment for statistical computing. Vienna, Austria. URL https://www.R-project.org/.

Rahman, M.A., Moser, A., Rötzer, T., Pauleit, S., 2019. Comparing the transpirational and shading effects of two contrasting urban tree species. Urban Ecosyst. https://doi.org/10.1007/s11252-019-00853-x

Rahman, M.A., Stratopoulos, L.M.F., Moser-Reischl, A., Zölch, T., Häberle, K.H., Rötzer, T., Pretzsch, H., Pauleit, S., 2020. Traits of trees for cooling urban heat islands: A meta-analysis. Build. Environ. 170. https://doi.org/10.1016/j.buildenv.2019.106606

Rodell, M., Famiglietti, J.S., Wiese, D.N., Reager, J.T., Beaudoing, H.K., Landerer, F.W., Lo, M.H., 2018. Emerging trends in global freshwater availability. Nature 557, 651–659. https://doi.org/10.1038/s41586-018-0123-1

Rodell, M., Houser, P.R., Jambor, U., Gottschalck, J., Mitchell, K., Meng, C.J., Arsenault, K., Cosgrove, B., Radakovich, J., Bosilovich, M., Entin, J.K., Walker, J.P., Lohmann, D., Toll, D.,

2004. The Global Land Data Assimilation System. Bull. Am. Meteorol. Soc. 85, 381–394. https://doi.org/10.1175/BAMS-85-3-381

Ronchi, S., Salata, S., Arcidiacono, A., 2020. Which urban design parameters provide climate-proof cities ? An application of the Urban Cooling InVEST Model in the city of Milan comparing historical planning morphologies. Sustain. Cities Soc. 63, 102459. https://doi.org/10.1016/j.scs.2020.102459

Roxy, M.S., Sumithranand, V.B., Renuka, G., 2010. Variability of soil moisture and its relationship with surface albedo and soil thermal diffusivity at Astronomical Observatory, Thiruvananthapuram, South Kerala. J. Earth Syst. Sci. 119, 507–517. https://doi.org/10.1007/s12040-010-0038-1

Rupprecht, C.D.D., Byrne, J.A., 2014. Informal urban green-space: Comparison of quantity and characteristics in Brisbane, Australia and Sapporo, Japan. PLoS One 9. https://doi.org/10.1371/journal.pone.0099784

Rutter, A.J., Kershaw, K.A., Robins, P.C., Morton, A.J., 1971. A predictive model of rainfall interception in forests, 1. Derivation of the model from observations in a plantation of Corsican pine. Agric. Meteorol. 9, 367–384. https://doi.org/10.1016/0002-1571(71)90034-3

Sacks, W.J., Cook, B.I., Buenning, N., Levis, S., Helkowski, J.H., 2009. Effects of global irrigation on the near-surface climate. Clim. Dyn. 33, 159–175. https://doi.org/10.1007/s00382-008-0445-z

Santamouris, M., Ban-weiss, G., Osmond, P., Paolini, R., Synnefa, A., Cartalis, C., Muscio, A., Zinzi, M., Morakinyo, T.E., Ng, E., Tan, Z., Takebayashi, H., Sailor, D., Crank, P., Taha, H., Pisello, A.L., Rossi, F., 2018. PROGRESS IN URBAN GREENERY MITIGATION SCIENCE – ASSESSMENT METHODOLOGIES ADVANCED TECHNOLOGIES AND IMPACT ON CITIES. J. Civ. Eng. Manag. 24, 638–671. https://doi.org/10.3846/jcem.2018.6604

Santamouris, M., Cartalis, C., Synnefa, A., Kolokotsa, D., 2015. On the impact of urban heat island and global warming on the power demand and electricity consumption of buildings — A review. Energy Build. 98, 119–124. https://doi.org/10.1016/j.enbuild.2014.09.052

Santamouris, M., Ding, L., Fiorito, F., Oldfield, P., Osmond, P., Paolini, R., Prasad, D., Synnefa, A., 2017. Passive and active cooling for the outdoor built environment – Analysis and assessment of the cooling potential of mitigation technologies using performance data from 220 large scale projects. Sol. Energy 154, 14–33. https://doi.org/10.1016/j.solener.2016.12.006

Sanusi, R., Johnstone, D., May, P., Livesley, S.J., 2017. Microclimate benefits that different street tree species provide to sidewalk pedestrians relate to differences in Plant Area Index. Landsc. Urban Plan. 157, 502–511. https://doi.org/10.1016/j.landurbplan.2016.08.010

Sanusi, R., Livesley, S.J., 2020. London Plane trees (Platanus x acerifolia) before, during and after a heatwave: Losing leaves means less cooling benefit. Urban For. Urban Green. 54, 126746. https://doi.org/10.1016/j.ufug.2020.126746

Sauer, T.J., Horton, R., 2005. Soil Heat Flux, in: Micrometeorology in Agricultural Systems. American Society of Agronomy, Crop Science Society of America, Soil Science Society of America, Madison, WI, pp. 131–154. https://doi.org/10.2134/agronmonogr47.c7

Schneider, C.A., Rasband, W.S., Eliceiri, K.W., 2012. NIH Image to ImageJ: 25 years of image analysis. Nat. Methods 9, 671–675. https://doi.org/10.1038/nmeth.2089

Seneviratne, S.I., Corti, T., Davin, E.L., Hirschi, M., Jaeger, E.B., Lehner, I., Orlowsky, B., Teuling, A.J., 2010. Investigating soil moisture-climate interactions in a changing climate: A review. Earth-Science Rev. 99, 125–161. https://doi.org/10.1016/j.earscirev.2010.02.004

Shah, A., Garg, A., Mishra, V., 2021. Quantifying the local cooling effects of urban green spaces: Evidence from Bengaluru, India. Landsc. Urban Plan. 209, 104043. https://doi.org/10.1016/j.landurbplan.2021.104043

Shashua-Bar, L., Hoffman, M.E., 2000. Vegetation as a climatic component in the design of an urban street. Energy Build. 31, 221–235. https://doi.org/10.1016/S0378-7788(99)00018-3

Shashua-Bar, L., Pearlmutter, D., Erell, E., 2011. The influence of trees and grass on outdoor thermal comfort in a hot-arid environment. Int. J. Climatol. 31, 1498–1506. https://doi.org/10.1002/joc.2177

Shashua-Bar, L., Pearlmutter, D., Erell, E., 2009. The cooling efficiency of urban landscape strategies in a hot dry climate. Landsc. Urban Plan. 92, 179–186. https://doi.org/10.1016/j.landurbplan.2009.04.005

Shi, W., Tao, F., Liu, J., 2014. Regional temperature change over the Huang-Huai-Hai Plain of China: The roles of irrigation versus urbanization. Int. J. Climatol. 34, 1181–1195. https://doi.org/10.1002/joc.3755

Shiflett, S.A., Liang, L.L., Crum, S.M., Feyisa, G.L., Wang, J., Jenerette, G.D., 2017. Variation in the urban vegetation, surface temperature, air temperature nexus. Sci. Total Environ. 579, 495–

505. https://doi.org/10.1016/j.scitotenv.2016.11.069

Shih, W., 2017. Greenspace patterns and the mitigation of land surface temperature in Taipei metropolis. Habitat Int. 60, 69–80. https://doi.org/10.1016/j.habitatint.2016.12.006

Sorooshian, S., Li, J., Hsu, K.L., Gao, X., 2011. How significant is the impact of irrigation on the local hydroclimate in Californias Central Valley? Comparison of model results with ground and remote-sensing data. J. Geophys. Res. Atmos. 116, 1–11. https://doi.org/10.1029/2010JD014775

South East Water, 2021. Aquarevo - A new way of living [WWW Document]. URL https://southeastwater.com.au/residential/upgrades-and-projects/projects/aquarevo/ (accessed 2.21.22).

Speak, A.F., Rothwell, J.J., Lindley, S.J., Smith, C.L., 2013. Reduction of the urban cooling effects of an intensive green roof due to vegetation damage. Urban Clim. 3, 40–55. https://doi.org/10.1016/j.uclim.2013.01.001

Spronken-Smith, R.A., Oke, T.R., 1998. The thermal regime of urban parks in two cities with different summer climates. Int. J. Remote Sens. 19, 2085–2104. https://doi.org/10.1080/014311698214884

Spronken-Smith, R.A., Oke, T.R., Lowry, W.P., 2000. Advection and the surface energy balance across an irrigated urban park. Int. J. Climatol. 20, 1033–1047. https://doi.org/10.1002/1097-0088(200007)20:9<1033::AID-JOC508>3.0.CO;2-U

Stewart, I.D., Oke, T.R., 2012. Local climate zones for urban temperature studies. Bull. Am. Meteorol. Soc. 93, 1879–1900. https://doi.org/10.1175/BAMS-D-11-00019.1

Sugawara, H., Shimizu, S., Takahashi, H., Hagiwara, S., Narita, K., Mikami, T., Hirano, T., 2016. Thermal Influence of a Large Green Space on a Hot Urban Environment. J. Environ. Qual. 45, 125–133. https://doi.org/10.2134/jeq2015.01.0049

Sugimoto, S., Takahashi, H.G., Sekiyama, H., 2019. Modification of Near-Surface Temperature Over East Asia Associated With Local-Scale Paddy Irrigation. J. Geophys. Res. Atmos. 124, 2665–2676. https://doi.org/10.1029/2018JD029434

Tal, A., 2006. Seeking Sustainability: Israel's Evolving Water Management Strategy. Science (80-.). 313, 1081–1084. https://doi.org/10.1126/science.1126011

Tan, J., Zheng, Y., Tang, X., Guo, C., Li, L., Song, G., Zhen, X., Yuan, D., Kalkstein, A.J., Li, F., Chen, H., 2010. The urban heat island and its impact on heat waves and human health in Shanghai. Int. J. Biometeorol. 54, 75–84. https://doi.org/10.1007/s00484-009-0256-x

Tan, P.Y., Wong, N.H., Tan, C.L., Jusuf, S.K., Chang, M.F., Chiam, Z.Q., 2018. A method to partition the relative effects of evaporative cooling and shading on air temperature within vegetation canopy. J. Urban Ecol. 4, 1–11. https://doi.org/10.1093/jue/juy012

Tan, Z., Lau, K.K.L., Ng, E., 2017. Planning strategies for roadside tree planting and outdoor comfort enhancement in subtropical high-density urban areas. Build. Environ. 120, 93–109. https://doi.org/10.1016/j.buildenv.2017.05.017

Tanner, E.P., Elmore, R.D., Fuhlendorf, S.D., Davis, C.A., Dahlgren, D.K., Orange, J.P., 2017. Extreme climatic events constrain space use and survival of a ground-nesting bird. Glob. Chang. Biol. 23, 1832–1846. https://doi.org/10.1111/gcb.13505

Tapper, N., 2021. Creating cooler, healthier and more liveable Australian cities using irrigated green infrastructure, in: Urban Climate Science for Planning Healthy Cities. Springer International Publishing, Cham, pp. 219–237. https://doi.org/10.1007/978-3-030-87598-5_10

Teitelbaum, E., Chen, K.W., Meggers, F., Guo, H., Houchois, N., Pantelic, J., Rysanek, A., 2020. Globe thermometer free convection error potentials. Sci. Rep. 10, 2652. https://doi.org/10.1038/s41598-020-59441-1

The World Bank, 2023. Urban population (% of total population) [WWW Document]. URL https://data.worldbank.org/indicator/SP.URB.TOTL.IN.ZS (accessed 7.6.23).

Thiery, W., Davin, E.L., Lawrence, D.M., Hirsch, A.L., Hauser, M., Seneviratne, S.I., 2017. Present-day irrigation mitigates heat extremes. J. Geophys. Res. Atmos. 122, 1403–1422. https://doi.org/10.1002/2016JD025740

Thiery, W., Visser, A.J., Fischer, E.M., Hauser, M., Hirsch, A.L., Lawrence, D.M., Lejeune, Q., Davin, E.L., Seneviratne, S.I., 2020. Warming of hot extremes alleviated by expanding irrigation. Nat. Commun. 11, 1–7. https://doi.org/10.1038/s41467-019-14075-4

Thompson, A.L., Gilley, J.R., Norman, J.M., 1993. A sprinkler water droplet evaporation and plant canopy model: II. Model application. Trans. - Am. Soc. Agric. Eng. Gen. Ed. 36, 743–750. https://doi.org/10.13031/2013.28393

Thompson, A.L., Martin, D.L., Norman, J.M., Tolk, J.A., Howell, T.A., Gilleym, J.R., A. D.

Schneider, 1997. TESTING OF A WATER LOSS DISTRIBUTION MODEL FOR MOVING SPRINKLER SYSTEMS. Trans. ASAE 40, 81–88. https://doi.org/10.13031/2013.21251

Thorsson, S., Lindberg, F., Eliasson, I., Holmer, B., 2007. Different methods for estimating the mean radiant temperature in an outdoor urban setting. Int. J. Climatol. 27, 1983–1993. https://doi.org/10.1002/joc.1537

Todd, R., Evett, S.R., Howell, T.A., 2000. The Bowen ratio-energy balance method for estimating latent heat flux of irrigated aflalfa. Agric. For. Meteorol. 103, 335–348.

Tolk, J.A., Howell, T.A., Steiner, J.L., Krieg, D.R., Schneider, A.D., 1995. Role of transpiration suppression by evaporation of intercepted water in improving irrigation efficiency. Irrig. Sci. 16, 89–95. https://doi.org/10.1007/BF00189165

Trancoso, R., Syktus, J., Toombs, N., Ahrens, D., Wong, K.K.H., Pozza, R.D., 2020. Heatwaves intensification in Australia: A consistent trajectory across past, present and future. Sci. Total Environ. 742, 140521. https://doi.org/10.1016/j.scitotenv.2020.140521

Twohig-Bennett, C., Jones, A., 2018. The health benefits of the great outdoors: A systematic review and meta-analysis of greenspace exposure and health outcomes. Environ. Res. 166, 628–637. https://doi.org/10.1016/j.envres.2018.06.030

Tyree, M.T., Cochard, H., Cruiziat, P., Sinclair, B., Ameglio, T., 1993. Drought-induced leaf shedding in walnut: evidence for vulnerability segmentation. Plant, Cell Environ. 16, 879–882. https://doi.org/10.1111/j.1365-3040.1993.tb00511.x

Unal Cilek, M., Cilek, A., 2021. Analyses of land surface temperature (LST) variability among local climate zones (LCZs) comparing Landsat-8 and ENVI-met model data. Sustain. Cities Soc. 102877. https://doi.org/10.1016/j.scs.2021.102877

Urrego-Pereira, Y.F., Martínez-Cob, A., Cavero, J., 2013. Relevance of Sprinkler Irrigation Time and Water Losses on Maize Yield. Agron. J. 105, 845–853. https://doi.org/10.2134/agronj2012.0488

Usowicz, B., Kossowski, J., Baranowski, P., 1996. Spatial variability of soil thermal properties in cultivated fields. Soil Tillage Res. 39, 85–100. https://doi.org/10.1016/S0167-1987(96)01038-0

Vahmani, P., Ban-Weiss, G., 2016. Climatic consequences of adopting drought-tolerant vegetation over Los Angeles as a response to California drought. Geophys. Res. Lett. 43, 8240–8249.

https://doi.org/10.1002/2016GL069658

Vahmani, P., Hogue, T.S., 2015. Urban irrigation effects on <scp>WRF-UCM</scp> summertime forecast skill over the Los Angeles metropolitan area. J. Geophys. Res. Atmos. 120, 9869–9881. https://doi.org/10.1002/2015JD023239

Valmassoi, A., Dudhia, J., Di Sabatino, S., Pilla, F., 2020. Evaluation of three new surface irrigation parameterizations in the WRF-ARW v3.8.1 model: the Po Valley (Italy) case study. Geosci. Model Dev. 13, 3179–3201. https://doi.org/10.5194/gmd-13-3179-2020

Van den Berg, M., Van Poppel, M., Van Kamp, I., Andrusaityte, S., Balseviciene, B., Cirach, M., Danileviciute, A., Ellis, N., Hurst, G., Masterson, D., Smith, G., Triguero-Mas, M., Uzdanaviciute, I., Wit, P. de, Van Mechelen, W., Gidlow, C., Grazuleviciene, R., Nieuwenhuijsen, M.J., Kruize, H., Maas, J., 2016. Visiting green space is associated with mental health and vitality: A cross-sectional study in four european cities. Heal. Place 38, 8–15. https://doi.org/10.1016/j.healthplace.2016.01.003

van den Berg, M., Wendel-Vos, W., van Poppel, M., Kemper, H., van Mechelen, W., Maas, J., 2015. Health benefits of green spaces in the living environment: A systematic review of epidemiological studies. Urban For. Urban Green. 14, 806–816. https://doi.org/10.1016/j.ufug.2015.07.008

Vivoni, E.R., Kindler, M., Wang, Z., Pérez-Ruiz, E.R., 2020. Abiotic Mechanisms Drive Enhanced Evaporative Losses under Urban Oasis Conditions. Geophys. Res. Lett. 47. https://doi.org/10.1029/2020GL090123

Wang, C., Wang, Z.H., Yang, J., 2019. Urban water capacity: Irrigation for heat mitigation. Comput. Environ. Urban Syst. 78, 101397. https://doi.org/10.1016/j.compenvurbsys.2019.101397

Ward, H.C., Kotthaus, S., Järvi, L., Grimmond, C.S.B., 2016. Surface Urban Energy and Water Balance Scheme (SUEWS): Development and evaluation at two UK sites. Urban Clim. 18, 1–32. https://doi.org/10.1016/j.uclim.2016.05.001

Wen, L., Jin, J., 2012. Modelling and analysis of the impact of irrigation on local arid climate over northwest China. Hydrol. Process. 26, 445–453. https://doi.org/10.1002/hyp.8142

Williams, I.N., Torn, M.S., 2015. Vegetation controls on surface heat flux partitioning, and land-atmosphere coupling. Geophys. Res. Lett. 42, 9416–9424. https://doi.org/10.1002/2015GL066305

Wong, T.H.F., 2006. An Overview of Water Sensitive Urban Design Practices in Australia. Water Pract. Technol. 1. https://doi.org/10.2166/wpt.2006018

Wong, T.H.F., Brown, R.R., 2009. The water sensitive city: Principles for practice. Water Sci. Technol. 60, 673–682. https://doi.org/10.2166/wst.2009.436

Wu, L., Chen, C., 2023. Does pattern matter? Exploring the pathways and effects of urban green space on promoting life satisfaction through reducing air pollution. Urban For. Urban Green. 82, 127890. https://doi.org/10.1016/j.ufug.2023.127890

Wu, Z., Dou, P., Chen, L., 2019. Comparative and combinative cooling effects of different spatial arrangements of buildings and trees on microclimate. Sustain. Cities Soc. 51, 101711. https://doi.org/10.1016/j.scs.2019.101711

Xiao, X.D., Dong, L., Yan, H., Yang, N., Xiong, Y., 2018. The influence of the spatial characteristics of urban green space on the urban heat island effect in Suzhou Industrial Park. Sustain. Cities Soc. 40, 428–439. https://doi.org/10.1016/j.scs.2018.04.002

Xing, Y., Brimblecombe, P., Wang, S., Zhang, H., 2019. Tree distribution, morphology and modelled air pollution in urban parks of Hong Kong. J. Environ. Manage. 248, 109304. https://doi.org/10.1016/j.jenvman.2019.109304

Yang, B., Zhang, Y., Qian, Y., Tang, J., Liu, D., 2016. Climatic effects of irrigation over the Huang-Huai-Hai plain in China simulated by the weather research and forecasting model. J. Geophys. Res. 121, 2246–2264. https://doi.org/10.1002/2015JD023736

Yang, J., Ren, J., Sun, D., Xiao, X., Xia, J. (Cecilia), Jin, C., Li, X., 2021. Understanding land surface temperature impact factors based on local climate zones. Sustain. Cities Soc. 69, 102818. https://doi.org/10.1016/j.scs.2021.102818

Yang, J., Wang, Z.H., 2015. Optimizing urban irrigation schemes for the trade-off between energy and water consumption. Energy Build. 107, 335–344. https://doi.org/10.1016/j.enbuild.2015.08.045

Yang, L., Zhang, L., Li, Y., Wu, S., 2015. Water-related ecosystem services provided by urban green space: A case study in yixing city (china). Landsc. Urban Plan. 136, 40–51. https://doi.org/10.1016/j.landurbplan.2014.11.016

Yang, Z., Dominguez, F., Zeng, X., Hu, H., Gupta, H., Yang, B., 2017. Impact of irrigation over the California Central Valley on regional climate. J. Hydrometeorol. 18, 1341–1357.

https://doi.org/10.1175/JHM-D-16-0158.1

Yao, L., Chen, L., Wei, W., Sun, R., 2015. Potential reduction in urban runoff by green spaces in Beijing: A scenario analysis. Urban For. Urban Green. 14, 300–308. https://doi.org/10.1016/j.ufug.2015.02.014

Yoshida, R., Iizumi, T., Nishimori, M., Yokozawa, M., 2012. Impacts of land-use changes on surface warming rates and rice yield in Shikoku, western Japan. Geophys. Res. Lett. 39, 1–5. https://doi.org/10.1029/2012GL053711

Yu, Z., Xu, S., Zhang, Y., Jørgensen, G., Vejre, H., 2018. Strong contributions of local background climate to the cooling effect of urban green vegetation. Sci. Rep. 8, 1–9. https://doi.org/10.1038/s41598-018-25296-w

Zhang, G., Shen, D., Ming, B., Xie, R., Hou, P., Xue, J., Wang, K., Li, S., 2022. Optimizing Planting Density to Increase Maize Yield and Water Use Efficiency and Economic Return in the Arid Region of Northwest China. Agric. 12. https://doi.org/10.3390/agriculture12091322

Zhang, Z., Dobson, B., Moustakis, Y., Meili, N., Mijic, A., Butler, A., Athanasios, P., 2023. Assessing the co-benefits of urban greening coupled with rainwater harvesting management under current and future climates across USA cities. Environ. Res. Lett. 18. https://doi.org/10.1088/1748-9326/acbc90

Zheng, S., Guldmann, J.M., Wang, Z., Qiu, Z., He, C., Wang, K., 2021. Experimental and theoretical study of urban tree instantaneous and hourly transpiration rates and their cooling effect in hot and humid area. Sustain. Cities Soc. 68, 102808. https://doi.org/10.1016/j.scs.2021.102808

Ziter, C.D., Pedersen, E.J., Kucharik, C.J., Turner, M.G., 2019. Scale-dependent interactions between tree canopy cover and impervious surfaces reduce daytime urban heat during summer. Proc. Natl. Acad. Sci. U. S. A. 116, 7575–7580. https://doi.org/10.1073/pnas.1817561116

Zou, J., Xie, Z., Yu, Y., Zhan, C., Sun, Q., 2014. Climatic responses to anthropogenic groundwater exploitation: A case study of the Haihe River Basin, Northern China. Clim. Dyn. 42, 2125–2145. https://doi.org/10.1007/s00382-013-1995-2